# An Exploration of the Effect of the Mesenchymal Stem Cell Secretome on Pancreatic Beta Cells

Maximilian Wood

Submitted in fulfilment of the requirements of the degree Master of Philosophy

Date of submission: October 2017

Institute for Science and Technology in Medicine

Keele University

Keele University

# PGR STUDENT: ACADEMIC HONESTY DECLARATION FORM

**To be completed by the student:**

| Section A: Student Details | | | |
|---|---|---|---|
| Name of student | Maximilian Wood | Student No. | |
| Research Home: | ISTM ☒ PCHS ☐ IACS ☐ HUMSS ☐ NATSCI ☐ | | |
| Lead supervisor: | Professor Nicholas R Forsyth | | |
| Degree for which thesis being submitted: | MPhil | Submission Date: *Must comply with Regulation 2D* | 14th August 2017 |
| Title of Thesis: | An Exploration of the Effect of the Mesenchymal Stem Cell Secretome on Pancreatic Beta Cells | | |
| This thesis contains confidential information and is subject to the protocol set down for the submission and examination of such a thesis: *(if yes please complete the relevant section in Declaration for a Research Degree Form)* | | | Yes ☐ No ☒ |

| Section B: Thesis Details | |
|---|---|
| **I certify that:** | |
| The thesis being submitted for examination is my own account of my own research | Yes ☒ No ☐ |
| My research has been conducted ethically. Where relevant a letter from the approving body confirming that ethical approval has been given has been bound into the thesis as an Annex | Yes ☒ No ☐ |
| The data and results presented are the genuine data and results actually obtained by me during the conduct of the research | Yes ☒ No ☐ |
| Where I have drawn on the work, ideas and results of others this has been appropriately acknowledged in the thesis | Yes ☒ No ☐ |
| Where any collaboration has taken place with one or more other researchers, I have included within an 'Acknowledgements' section in the thesis a clear statement of their contributions, in line with the relevant guidance document *(see note*)* | Yes ☒ No ☐ |
| The greater portion of the work described in the thesis has been undertaken subsequent to my registration for the higher degree for which I am submitting for examination | Yes ☒ No ☐ |
| Where part of the work described in the thesis has previously been incorporated in another thesis submitted by me for a higher degree (if any), this has been identified and acknowledged in the thesis | Yes ☒ No ☐ |
| The thesis submitted is within the required word limit as specified in the Regulations | Yes ☒ No ☐ |
| Total words in submitted thesis (including text and footnotes, but excluding references and appendices) | 35 642 |

| Student Signature: | | Date: | |
|---|---|---|---|

# Abstract

Type 1 diabetes is a challenging condition to manage effectively. Utilising the mesenchymal stem cell (MSC) secretome is an avenue being researched in regenerative medicine which could potentially ameliorate the condition. Previous studies have identified potential anti-apoptotic, trophic and immunomodulatory factors that may be implicated in its therapeutic effect. We theorise that IL-10 may play an important role in disease modulation. This study aims to explore the effects of MSC-conditioned medium (MSC-CM) on *in vitro* and *in vivo* models of diabetes as well as to characterise the presence of IL-10 receptors on beta cell lines.

BRIN-bd11 and TC6 cells were exposed to increasing concentrations of pro-inflammatory cytokines (TNF$\alpha$, IFN$\gamma$, IL-1$\beta$) implicated in the pathogenesis of type 1 diabetes for 24 hours, both in the presence and absence of MSC-CM. MTT assays were used to determine falls in viability. To determine the effect of MSC-CM on an *in vivo* model of diabetes, diabetes was induced in mice via intraperitoneal injections of STZ. Mice treated with Intraperitoneal MSC-CM were compared to untreated diabetic mice and a non-diabetic control. A plasma insulin ELISA, DEXA scans and pancreatic histology were used for

analysis. Characterisation of IL-10 on BRIN-bd11 and TC6 cells was performed using electrophoresis and immunofluorescence techniques.

This thesis demonstrates that the MSC-CM ameliorates falls in viability of BRIN-bd11 and TC6 cell lines in the presence of pro-inflammatory cytokines implicated in the pathogenesis of diabetes in an *in vitro* model. It also demonstrates that MSC-CM potentially improves the histology and biochemistry of diabetic mice *in vivo*. We also demonstrated the presence of IL-10 receptors on beta cell lines.

Thus, MSC-CM appears to be a potential therapeutic tool for use in type 1 diabetes. Further research needs to be conducted to determine the mechanisms through which paracrine factors including IL-10 exert their therapeutic effect.

# Contents

# Index of Figures

**Chapter 1**

**Chapter 2**



**Chapter 3**

**Chapter 5**

# Index of Tables

# Acknowledgements

I would like to express my gratitude to my Lead Supervisor Professor Nicholas R Forsyth for his guidance and unending patience through my learning process. I would also like to thank Dr. Buthainah Al-Azzawi and Mr. Marwan Merkan for their guidance and support in times of difficulty.

I would like to thank Dr. Catriona Kelly for the chance to collaborate with her lab in Ulster to conduct the *in vivo* experiments during my MPhil. I would also like to thank Dr. Dawood Khan for all his help and support in conducting the *in vivo* work. I would also like to thank Mr. Ryan Kelsey and Dr. Annie Hasib for their help with the project.

I would like to extend my thanks to Keele Medical School who have allowed me to take a year out of my medical studies to further my interest in research. This has allowed me to gain invaluable research skills for the future.

I would also like to thank my family who have always supported and encouraged me throughout my studies. Finally, I would like to thank all my friends and colleagues at the Guy Hilton Research centre who have made me very welcome during my time there.


# Chapter 1: Introduction

# 1.1 Islet Transplantation and Stem Cell Therapies

## 1.1.1 Islet Cell Transplantation

The discovery of insulin and its extraction from animal pancreas by Banting *et al.* resulted in dramatic improvements in the quality of life of patients with diabetes.[1] Treatments before this had largely consisted of strict diets which were not very successful, and diabetes was a fatal condition.[2] However, the use of exogenous insulin is not a cure, and it poorly mirrors the normal physiological response to changes in blood glucose. Poor glucose control increases the risk of complications including microvascular complications such as diabetic neuropathy and retinopathy and macrovascular complications such as stroke and ischaemic heart disease.[3]The Diabetes Control and Complications Trial showed that intense insulin therapy reduced secondary complication rates in patients at the cost of severe episodes of hypoglycaemia in the majority of patients.[4] Treatments have improved over the years with the advent of new insulin analogues, blood glucose monitoring and insulin pumps, but adequate glucose control still requires diligence on the part of the patient and their care team.

The idea of transplanting islets to obtain a physiological insulin response predates the advent of insulin therapies for type 1 diabetes. Early attempts included that of Watson-Williams *et al*., who performed a subcutaneous xenotransplant of minced sheep pancreas into the thigh of a child who was ketoacidotic.[5] The child's condition improved initially, but the graft subsequently failed, most likely due to rejection and ischaemia at the poorly vascularised site. In the 1960s islet isolation and transplantation was pioneered by Lay *et al.,* who successfully demonstrated restoration of normoglycaemia in diabetic Lewis rats that received transplantation of healthy islets isolated from non-diabetic Lewis rats.[6] These results were not duplicated in human patients however. Ricordi *et al*. developed an automated method of isolating human cadaveric pancreatic islets in 1988, making obtaining therapeutic quantities of islets for transplantation easier.[7]

In 2000 the Edmonton group published a landmark study in which all seven patients who received islet transplantations from cadaveric donors became insulin independent after the procedure, as measured by normalised glycosylated haemoglobin (HbA1C) levels following a median follow up of one year.[8] The procedure involved isolation of pancreatic islets via controlled

ductal perfusion of liberase human islet enzyme and subsequent digestion of the pancreas in a Ricordi chamber and purification by Ficoll density-gradient centrifugation. Islet preparations were matched for blood type and matched for lymphocytic antibodies[8] The freshly purified islets were subsequently infused into the portal vein of the recipient immediately, removing the need for islet culture[8] A cumulative >11,000 islets equivalent (IE) per kilogram body weight was delivered on average to each patient to achieve insulin independence. (Figure 1.1).[8] One islet equivalent (IE) is considered equal to a pancreatic islet with a diameter of 150μm.[8]

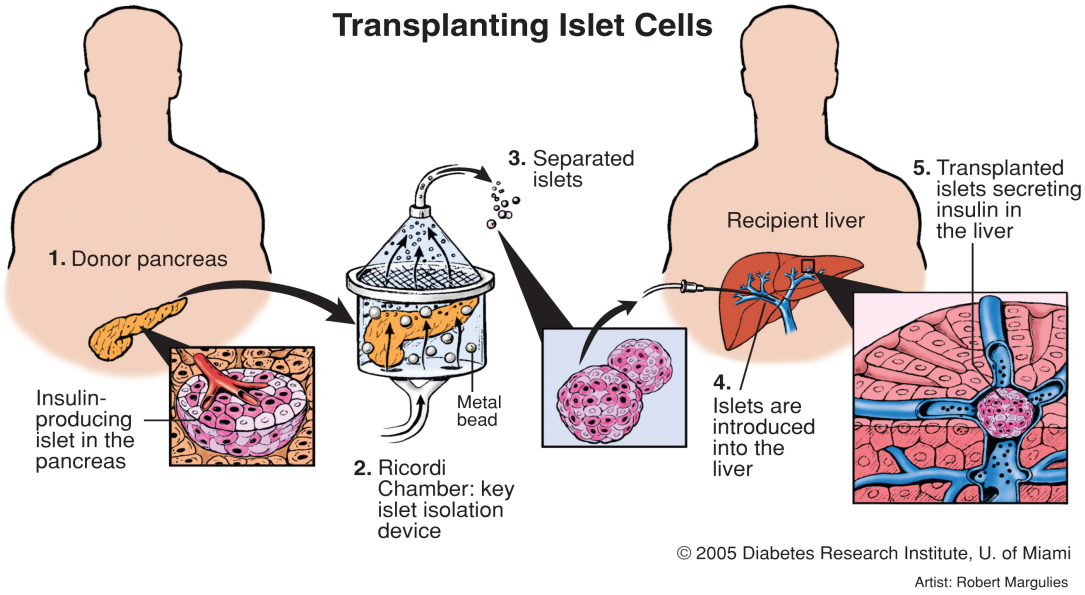


*Figure 1.1 : Depiction of the islet transplantation process. Islets are isolated from the donor and purified before being introduced in to the hepatic vasculature via the hepatic portal vein. Islets engraft in the liver and secrete insulin. (Image adapted from: Diabetes Research Institute, Miami)* [9]

The cumulative transplantation of >11,000 islets equivalent (IE) /kg (weight of recipient) was one of the key modifications of the islet transplantation procedure introduced by the Edmonton protocol that contributed to it's success.[8] This was achieved by transplanting a large islet mass from at least two donors over multiple transfusions.[8,10] Early islet transplantations failed partly due to insufficient transfusion and subsequent engraftment of islets and immediate loss of islets through non immune-mediated inflammatory pathways, resulting in an inadequate working islet mass.[8] Indeed, Shapiro *et al.* fond that infusion of islets from a single donor was insufficient to achieve insulin independence.[8] The study found that a cumulative transplantation of (>11,000 islets/kg) from at least two cadaveric donors administered over at least two transfusions within 3 months could reliably achieve insulin independence.[8]

A glucocorticoid sparring immunosuppressive regime was subsequently used to prevent graft rejection, consisting initially of induction with Daclizumab followed by maintenance therapy with Tacrolimus and Sirolimus. [8] As discussed later, the omission of glucocorticoids is another important modification key to the Edmonton Protocol's success.

A long-term follow-up of the Edmonton Protocol for islet transplantation was published in 2016.[11] The study followed up seven patients enrolled in the NIS01 clinical trial who received multiple islet transplants in accordance with the Edmonton protocol.[11] These patients were subsequently enrolled in the EXIIST extension study which demonstrated that all seven subjects had continued islet function for over a decade after initial transplantation.[11] By the end of the study one subject remained insulin independent without the need for supplemental transplant and six demonstrated continued islet function. Three of the subjects however required a supplementary islet transplant each, which involved a further islet transplant outside of the NIS01 clinical trail four years after the trials completion.[11]

The initial results of the Edmonton Protocol sparked renewed interest in research into the transplantation of islets, with many groups trying to reproduce the results. In 2006 an international trial involving nine international centres (six in North America and three in Europe) was carried out to determine if the results of the Edmonton Protocol were reproducible.[10] 2000 prospective subjects were screened to determine eligibility for enrolment in the trial. 149 of these fulfilled the screening criteria

and were referred to the nine centres. All nine sites enrolled subjects and a total of 36 subjects were enrolled in the study.[10] The 36 subjects received up to three islet transplantations in accordance with the Edmonton protocol to achieve insulin independence.[10] The results showed that 44% (16 of 36) of the subjects reached the primary endpoint, which was defined as insulin independence with adequate glycaemic control one year after final transplantation.[10] 28% (10 of 36) of subjects had partial graft function after one year, which was defined as a C-Peptide level of at least 0.3ng per millilitre and a requirement for insulin or inadequate glycaemic control.[10] and 28% (10 of 36) had complete graft loss, defined as an initial C-peptide level of <0.3ng per millilitre either immediately after transplantation (non-functioning graft) or within 2 months of transplantation (early loss of graft).[10] The study concluded that islet transplantation may successfully restore long term endogenous insulin production and glycaemic stability in patients with type 1 diabetes who had initially unstable baseline controls.[10]

The Collaborative Islet Transplant Registry has collected islet transplant data since 1999 from allogenic transplant programs from several countries in North America, Europe and Asia.[12] A report by Barton *et al.* analysed 677 islet alone

or islet after kidney recipients in the Collaborative Islet Transplant Registry between 1999 and 2010. The study showed gradual improvements in insulin independence rates post islet transplant from 27% three years post-transplant in the early era of islet transplantation (1999-2002) to 44% in the years 2007-2010.[13] Improvements in islet isolation, peritransplant handling to reduce cold ischaemia loss of islets, as well as improvements in the immunosuppression regimen to reduce toxicity to transplanted islets contributed to the gradual improvement in retention of graft function in transplant patients.[13]

Although the results are promising, there are currently many limitations to islet transplant procedures. Since transplantable islets can only be sourced from brain-dead donors, the number of cadaveric pancreata available for islet transplantation is limited.[14] In studies like the Edmonton Protocol multiple donors were required to obtain sufficient islets to carry out one procedure. Furthermore, multiple islet transplantations are often needed to obtain a sufficient working islet mass to achieve insulin independence, compounding the issue with islet shortage for transplantation.[8]

The viability of the islets depends very much on handling, from the time taken to harvest the islets to processing and purifying of the cells.[15] The cells are highly susceptible to ischaemia, although methods of prolonging the cold ischaemic time, including the use of continuously oxygenated perfluorocarbons, have recently been used to good effect.[16] The Edmonton protocol limits cold storage time to less than 13 hours , including islet isolation time, which could be another factor contributing to it's success.[17]

Due to the limited supply of islets, criteria for inclusion in the trials are relatively stringent. Ideal candidates for trials as described by Srinivan *et al.* are insulin-sensitive individuals with type 1 diabetes who have poor hypoglycaemia awareness and recurrent severe hypoglycaemic episodes despite optimal medical therapy.[14] Progressive secondary complications of diabetes such as diabetic retinopathy, diabetic nephropathy and diabetic neuropathy is another criterion cited.[14]

In addition to problems in the supply of islets, complications associated with the procedures also need to be contended with. Some of the complications

include portal vein thrombosis, which can have a fatal outcome, as well as portal hypertention.[18] Islets tend to cause blood to clot, affecting their viability in a process termed the 'instant blood-mediated inflammatory reaction'.[19] This process is cited as one of the reasons for the poor success rates before the Edmonton Protocol.[14] Addition of heparin to prevent blood coagulation in the suspension of islets for infusion in the Edmonton Protocol to address this issue probably contributed to the success of the transplants.[14] Because of the complexities and risks involved, treatment requires the input of a multidisciplinary team. The team includes specialists from a wide range of fields including endocrinologists, transplant surgeons and interventional radiologists.[20] Psychologists are also involved who determine the patients motivation to adhere to treatment and mental fitness to undergo the procedure.[20]

Immunosuppressants are required after transplant to prevent rejection of the transplanted grafts. Ironically, the immunosuppressants used in these trials were toxic to the transplanted grafts and impaired their function.[21] Glucocorticoids were recognised to be cytotoxic to transplanted islets and their omission from the maintenance regimen in trials like the Edmonton

Protocol contributed to their success.[21] Calcineurin inhibitors are nephrotoxic and have been shown to result in the progression of diabetic nephropathy.[22] Kidney function has been found independently to predict mortality of patients with diabetes.[23] Use of these drugs in patients with diabetes-related kidney disease may increase mortality in these patients.

Immunosuppressants also have many side effects. Immunosuppressed transplant patients are known to be at greater risk of opportunistic infections and certain cancers, including lymphomas, Kaposi sarcomas and other forms of sarcoma.[10] Other noted side effects include mouth ulcers, GI symptoms, fever and chest pains.[10]

Research currently underway to address these issues includes finding alternative sources of islet cells. Avenues being explored include xenogenic islet transplants, as well as deriving insulin-producing cells from stem cells The next section will review research into utilising the differentiating potential of stem cells to replace islet cells lost in autoimmune diabetes.

### 1.1.2 Generation of Insulin-Producing Cells from Human Embryonic Stem Cells (hESCs)

A shortage of suitable islet donors to meet the demand for pancreatic transplantation has led to research into ways to generate supplies of insulin-secreting cells. The use of stem cells is one avenue that has been extensively researched and could potentially provide a limitless source of insulin secreting cells for transplant.

Human embryonic stem cells (hESCs) are pluripotent stem cells that are capable of differentiating into all three germ layers of embryonic development (ectoderm, mesoderm and endoderm). [24] These cells exhibit characteristics of pluripotency, including forming tumours containing tissue of more than one germ layer (teratomas) when injected into immunocompromised murine models, as well as the ability to integrate into developing embryos to form a chimeric organism.[25,26] This has led to research aimed at exploiting the capacity of pluripotent stem cells to differentiate into other cell types for use in medical therapy (Figure 1.2).

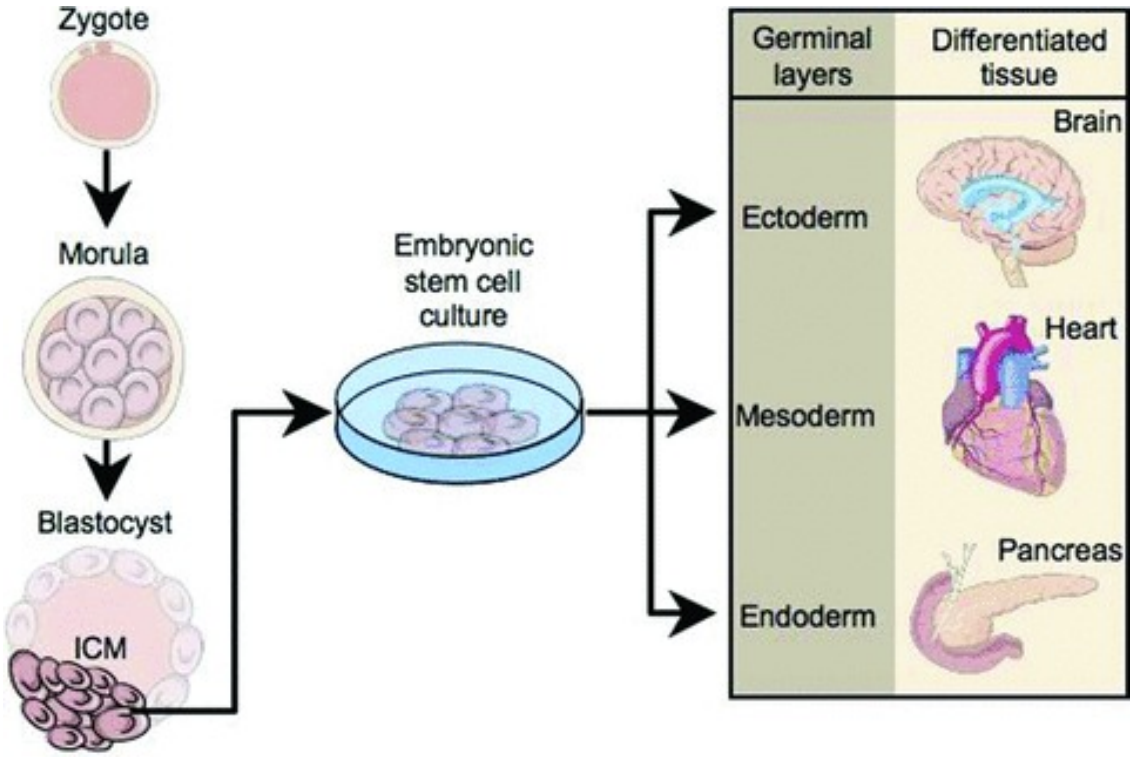


*Figure 1.2 : Depiction of the derivation of Embryonic stem cells (ESCs) from the inner cell mass (ICM) of pre-implantation blastocysts. ESCs cultured in vitro have the capacity to differentiate into cells of all three germ layers for therapeutic use in patients. (Image adapted from Nelson et al, 2009).* [27]

hESCs were first successfully isolated and cultured from mice in 1981, when the cells were isolated from the inner cell mass of pre-implantation embryos and placed on mitotically inactivated murine feeder cells.[28] The isolation of human embryonic stem cells followed in 1998.[29] The ability of hESCs to differentiate into many different cell types has been extensively researched for use in many diseases, including type 1 diabetes. The first study to demonstrate functional insulin-secreting cells generated from hESCs was

published in 2008.[30] Since then many groups have published protocols for the production of beta cells from hESCs.

Cells are cultured on feeder cells which are cells used in co-culture techniques that support the growth of other cells in the culture.[31] Commonly used feeder cells for hESC cultures include mouse embryonic fibroblasts.[32] These cells support hESCs attachment through secretion of extracellular matrix and expression of adhesion molecules, promote growth and survival of ESCs and secrete factors that help maintain the stem cells in a pluripotent state.[32] When removed from the feeder cells, ESCs quickly form embryoid bodies and start differentiating into cells of the three germ layers.[33] Several feeder-free culture systems have been developed, including growing cells on matrigels and synthetic polymers.[34] One approach for producing insulin-producing cells from ESCs starts with the production of definitive endoderm via the introduction of factors such as Activin A, WNT3A and bone morphogenic proteins into hESCs.[35] Subsequent steps involve the addition of factors to mimic the conditions seen in the embryological development of the pancreas. The differentiation process involves several stages as depicted in Figure 1.3.

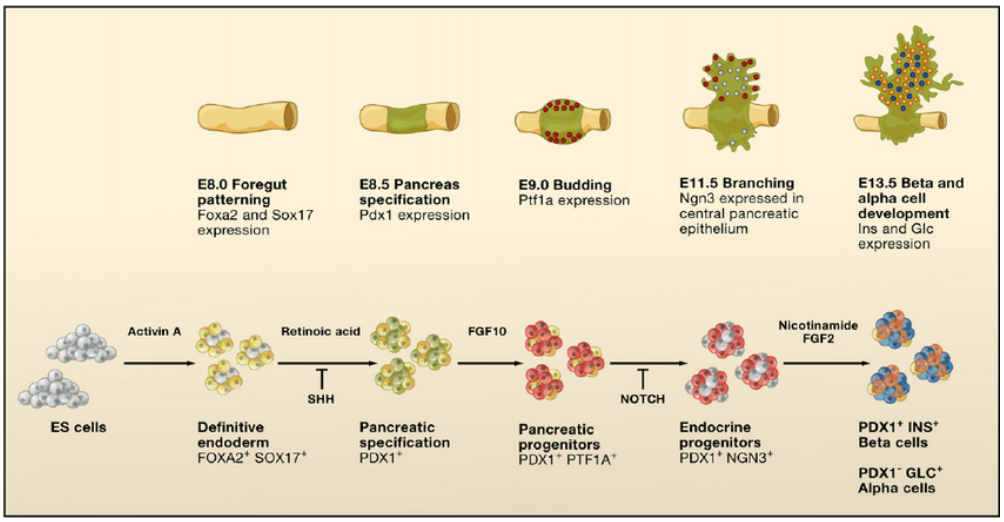


*Figure 1.3 : (Top) Depiction of the embryological stages and key transcription factors of pancreatic development in mice. (Bottom) Differentiation scheme for deriving insulin-producing cells for ESCs. (Image adapted from Murry et al, 2008).*[36]

There are several issues surrounding the use of insulin-secreting cells derived from hESCs for therapeutic purposes. One of these is the rejection of the graft post-transplant. The implanted cells are susceptible to immune-mediated apoptosis.[37] Indeed, transplant of beta cells does not remove the underlying cause of type 1 diabetes, which is an immune-mediated destruction of beta cells. One way to address this issue currently being researched is the use of cell encapsulation technologies. This involves the encapsulation of cells within gels which protect them from the immune system while allowing oxygen, nutrients and insulin to pass freely across the barrier. Viacyte has obtained FDA approval and initiated phase I/II trials of cell encapsulation of progenitor

cells from the hESC/VC-01 cell line.[30] There are also ethical issues surrounding the sourcing of stem cells from embryos for use in medical therapies.[38]

### 1.1.3 Induced Pluripotent Stem Cells (IPSCs): A New Approach to Stem Cell Therapy

The use of induced pluripotent stem cells (IPSCs) is a relatively new technology that involves the reprogramming of mature adult cells into a pluripotent state.[39,40] This is done by introducing genes associated with pluripotency to mature cells and repressing genes associated with pluripotency.[39,40] The IPSCs thus generated can subsequently be reprogrammed to differentiate into cells of any of the germ layers.[39,40] One of the advantages of this approach is the capacity to generate beta cells from the patient's own cells, thus eliminating the risk of graft rejection. In theory, any cell can be harvested and reverted to a pluripotent state. Previous studies have utilised fibroblasts obtained from skin biopsies making harvesting cells to generate iPSCs a simple and non-invasive process.[40] It is also not subject to the same ethical issues surrounding the use of ESCs, making it an attractive source of insulin-producing cells.

The formation of IPS cells from differentiated cells was first demonstrated by Takahashi and Yamanaka.[41] They found that by transfecting fibroblasts with plasmids containing the transcription factors OCT4, SOX2, c-Myc and Klf4 via the use of retroviral vectors, cells returned to a pluripotent state.[41] The extent to which IPS cells are similar to ESCs is an area of much debate. IPS cells have been shown to express many of the surface markers associated with ESCs including SSEA-3, SSEA-4, TRA-1-60 and TRA-1-81.[41] Like ESCs they have also been shown to be capable of forming teratomas when introduced to immune-compromised mice, as well as the capacity to be incorporated into the cell mass of developing embryos to form viable organisms.[42] Indeed, many genomic studies have shown that IPSCs and ESCs are very similar in their gene expression. Other studies have shown differences in gene expression.[39]

IPSCs have also attracted attention as a potential source of insulin-secreting cells for transplantation. Numerous studies have been published demonstrating the formation of insulin-secreting cells from IPSCs involving stage-wise protocols similar to those seen in ESCs.[42] As a proof of concept for the viability of using insulin-secreting cells derived from IPSCs, animal models have shown that implanted cells improve the animals' glycaemic control. A

study by Alipo et al. has shown that engraftment of IPS-derived insulin cells into the liver of a murine model of diabetes resulted in normalisation of glucose levels for at least three months as well as improved HbA1C levels, indicating better glycaemic control.[43]

Despite promising results, these cells currently present a number of limitations. One of these is the safety of the cells for transplantation. Expression of proto-oncogenes such as c-Myc in cells has been shown to result in tumour formation when these cells are transplanted into nude mice. [44] The use of a viral vector results in integration of the transfected genetic material into the host genome. This also increases the risk of tumorgenicity.[45] Proposed ways around this include ensuring all genes introduced are non-oncogenic in nature. A study by Yu *et al.* has shown that the genes OCT4, SOX2 NANOG and LIN28 are sufficient to induce pluripotency without the need for proto-oncogenes like c-Myc.[46] Another area being studied is new vectors to transfer desired genes into the host cells. Studies by Fusaki *et al.* have shown the use of a non-integrating Sendai viral vector that avoids integration of genetic material into the host genome, thus reducing the risk of cancerous cells developing.[47] Another issue that has been highlighted is the inefficiency of programming of the cells. Quoted figures range from 0.01-0.1% of cells

achieving pluripotency depending on the method of gene transfer and the host cells used.[42] Engrafted cells are also still susceptible to autoimmune destruction by the body.

### 1.1.4 Mesenchymal Stem Cells for the Treatment of Diabetes

Mesenchymal stem cells (MSCs) were first discovered by Friedenstein.[48] He described adherent fibroblast populations isolated from rat bone marrow that could undergo osteogenic differentiation.[48] Since then MSCs have also been isolated from adipose tissue, cord blood, placental tissue and dental pulp, among other sources.[49]

MSCs are multipotent stem cells with the ability to differentiate into different mesenchymal cell lineages.[50] They have the advantage of being hypoallergenic, as they express low levels of MHC class I and have no MHC class II receptors and are devoid of costimulatory receptors such as B7-1 and B7-2.[51] MHC class II presents alloantigens of transplanted cells to the host's immune system, resulting in an immune response and graft rejection. The absence of MHC class II expression by transplanted MSCs could allow them to escape recognition by alloreactive CD4+ T cells.[51] Furthermore, the lack of co-

stimulatory molecules like B7-1 and B7-2 which could render T-cells anergic when they interact with MSCs.[51] Peripheral control of T-cell activation is described in more detail in Section 1.2.3. They can readily be obtained from donors, grown, and expanded in culture. They can maintain their pluripotency even after prolonged periods in culture.[52] These factors make MSCs an attractive option for cellular therapy. The International Society for Cellular Therapy has offered criteria for identifying MSCs in culture. These are (1) expression of certain surface markers (CD73, CD90, and CD105) and the absence of other surface markers (CD34, CD45, CD14, CD11B, CD19 and HLA markers); (2) the ability to differentiate into adipogenic, chondrogenic and osteogenic lineages; and (3) plastic adherence seen while maintaining cells in standard culture conditions.[53]

MSCs have been shown to be capable of differentiating into cells derived from all three germ layers.[50] Consequently, the value of these cells in generating insulin-producing cells *in vitro* has been explored. Many studies describe the differentiation of MSCs in culture in a similar manner to that described for ESCs and IPCs. Wu *et al.* described the use of a high glucose culture containing beta-mercaptoethanol and a mixture of growth factors to generate IPCs from

MSCs.[54] IPCs derived using this method could normalise blood glucose in streptozocin (STZ) induced murine models of diabetes for a period of nine weeks.[54] However, this method still has similar limitations to that of IPCs derived from ESCs in that there is a low yield of IPCs and there is variability in the glucose responsiveness of these cells.

Another avenue being explored is the systemic administration of MSCs to treat diabetes. Intravenous administration of human bone marrow-derived MSCs has been shown to improve hyperglycaemia and increase beta cell mass in STZ-induced murine models of diabetes.[55] The mechanisms that mediate this seem to be a combination of the immunomodulatory, anti-apoptotic and regenerative properties of transplanted MSCs. Bone marrow-derived mesenchymal stem cells (BM-MSCs) have been shown to express chemokine receptors including CXCR4 and CX3CR1 that respond to chemokines such as CXCL23 and CXCCL1 secreted by the injured pancreas. This allows administered MSCs to migrate to the injured pancreas where they exert their effects on pancreatic beta cells.[54]

The mechanisms behind the regenerative effects demonstrated by transplanted MSCs that engraft in the pancreas is an area of debate. A study by Li *et al.* showed that the microenvironment of the injured pancreas can induce the expression of nestin, NGN3 and PDX1, which are genes specific for beta cell development and insulin production.[56] This suggests that MSCs could transdifferentiate into insulin-producing cells at the site of the pancreas. MSCs could also provide trophic support to viable beta cells within the pancreas. MSCs are known to secrete growth factors such as VEGF that promote angiogenesis and could improve transport of oxygen and nutrients to beta cells, thus improving beta cell viability and supporting growth in this manner.[57]

One issue with the systemic administration of MSCs is the 'pulmonary first pass effect'. MSCs tend to become trapped in the microvasculature of the lungs, resulting in few cells reaching the target therapeutic site.[58] Despite this, many studies have reported beneficial effects seen at the target site.[59,60] Furthermore, studies such as that by Nauta *et al.* have shown immunomodulation exerted by MSCs in a transwell system that separates the MSCs from immune cells by a semi-permeable membrane.[50] This indicates

that soluble factors play an important role in the therapeutic effects exerted by MSCs. The range of molecules and exomes secreted by MSCs have been termed the MSC secretome. Identifying the factors within the secretome that confer benefits in a wide range of diseases is an area of extensive research.

### 1.1.5 The Mesenchymal Stem Cell Secretome

The MSC secretome encompasses soluble factors as well as extracellular vesicles that are secreted by MSCs.[61] The study of this protein milieu has been gaining interest in recent years, as it provides several advantages over conventional stem cell therapy. The MSC secretome allows the therapeutic effects of MSCs to be utilised without the need for transplanting cells. This eliminates the risks of the surgery needed for engraftment and the risk of immune incompatibility, and reduces the risk of transmission of infections through grafted cells. Systemic administration of stem cells does however carry some risks, including the formation of pulmonary emboli and risks of tumorgenicity.[62] These risks can be ameliorated by a cell-free approach.

Proteomic assays of media conditioned by MSCs have been performed to determine the contents of the MSC secretome. Studies have found a wide

range of soluble factors that include angiogenic factors (e.g. VEGF, angiogenin), growth and trophic factors (e.g. BDNF, EGF, PIGF), chemokines (e.g. CCL1, CXCL2), anti-inflammatory cytokines (e.g. IL-10, IL-13) and haematopoietic cytokines, among others.[63] These factors provide the therapeutic properties associated with the MSC secretome. These include promoting angiogenesis via factors such as VEGF and angiogenin, which provides an exciting new therapy for vascular diseases including coronary artery disease and peripheral vascular disease.[64] The MSC secretome is also involved in the modulation of the immune system through factors such as PGE2, TGF6 and IL-10, which raises the potential for using the MSC secretome in the treatment of immune-mediated and autoimmune diseases such as type 1 diabetes and rheumatoid arthritis.[65] Studies have also shown the potential therapeutic benefits of using the stem cell secretome to treat neurological diseases such as Parkinson's disease and spinal cord injury. MSCs can secrete both neurotrophic and neuroprotective factors that can restore function to damaged areas of the nervous system.[66] These are but a few examples of the therapeutic potential of the MSC secretome.

Recently, the role of MSC-derived extracellular vesicles (EVs) in the MSC secretome has gained much interest. First described by Trams *et al.* in 1981, EVs were considered cellular waste.[67] It has since been found that they play important roles in intracellular communication and regulate a range of biological processes.[68] The International Society for Extracellular Vesicles has set out a list of minimum experimental standards for defining EVs and their functions.[69] Based on their structure and origin, EVs can be classified into exomes and microvesicles. Exomes are derived from the endosomal compartment and microvesicles are produced from direct budding from the plasma membrane. They contain proteins, polysaccharides, mRNA and microRNA.[67] EVs allow for the horizontal transfer of mRNA and miRNA between MSCs and target cells allowing for alterations in gene expression within these cells.[70] For example, MSC-derived EVs have been shown to induce proliferation and reduce apoptotic gene expression through the transfer of MSC-specific mRNAs in a murine model of acute kidney injury.[58] They have also been shown to induce genes for angiogenesis in models of renal ischaemia as well as improve post stroke neuroregeneration.[71,72] Studies also describe the potential therapeutic value of MSC-derived EVs in modulating the immune system in type 1 diabetes.[67]

### 1.1.6 Immunomodulatory and Anti-Apoptotic Properties of the MSC Secretome

Autoimmune diabetes is classically described as a TH1-mediated response against beta cells in the pancreas leading to progressive destruction of the beta cell mass, which results in clinically overt diabetes.[73] MSCs have been shown to exert immunomodulatory effects on a wide range of immune cells, and their ability to dampen the immune response and modulate it away from a TH1 phenotype is one of the major mechanisms behind the therapeutic effect of MSCs seen in murine models of diabetes.

MSCs are able to modulate the responses of T–cells, a key mediator in the pathology of type 1 diabetes. MSCs have been shown to inhibit the proliferation of T-cells and induce anergy.[65,74] Several mechanisms have been proposed for this. MSCs can induce IDO (indolamine 2-3 dioxygenase), which catalyses the conversion of tryptophan to kynurenine. This leads to the depletion of tryptophan and a build-up of its metabolites locally, which inhibits T-cell proliferation.[65,74,75] Direct cell-to-cell contact between MSCs and T-cells is another mechanism implicated. Engagement of the inhibitory PD-1 to its ligand PD-L1/PD-L2 also inhibits proliferation of T-cells. MSCs could

also induce T-cell anergy.[74] Activation of naïve T-cells requires the binding of MHC II to T-cell receptors as well as the binding of co-stimulatory molecules. MSCs could interact with T-cells through their receptors, but they lack the co-stimulatory molecules B7-1/B7-2, thus they could induce T-cell anergy in this manner.[50] MSCs could mediate a shift from a TH1 to a TH2 response by decreasing IFNγ production by differentiating T-cells and increasing IL-4 production.[75]

Soluble factors in the MSC secretome including PGE2, TSG6, TGF-β, HGF and IL-10 are known to have immunomodulatory properties. As examples, PGE2 increases the expression of IL-10 by macrophages and inhibits the proliferation of T-cells.[76,50] TSG6 can decrease the production of pro-inflammatory cytokines at the islets by inhibiting the translocation of the transcription factor NF-κB to the nucleus.[76] IL-10 is discussed in more detail in Chapter 3.

Apart from the effects seen on T-cells, MSCs also exert immunomodulatory effects on a wide range of other immune cells. They have been shown to modulate dendritic cell maturation and generation, block natural killer cell

proliferation and cytotoxicity as well as inhibit B cell proliferation and maturation.[65] The stem cell secretome has also been shown to have a number of cytoprotective and anti-apoptotic effects. Cytoprotective factors known to be secreted by MSCs include growth factors like VEGF, PIGF, FGF-2 and HGF, as well as cytokines such as IL-10 and IL-4.[67, 77] Extracellular vesicles secreted by MSCs have also been shown to downregulate the expression of pro-apoptotic genes (i.e. CASP1, CASP8, LTA) and upregulate anti-apoptotic genes (i.e. Bcl-xL, Bcl-2) in human tubular epithelial cells treated with cisplatin.[78]

# 1.2 Pathophysiology of Type 1 Diabetes

## 1.2.1 Maintenance of Self-Tolerance

Autoimmunity can be viewed as resulting from a breakdown in the mechanisms inherently present in preventing the expression of and reaction to self-antigens by the immune system. These can be subdivided into central and peripheral mechanisms of self-tolerance.[79] Central mechanisms for self-tolerance include the education of naïve lymphocytes within the thymus and bone marrow, as well as generation of natural T regulatory cells (nTregs) in the thymus.[79,80] Peripheral mechanisms involve the detection of self-reactive cells in the periphery and the subsequent induction of anergy or deletion of these self-reactive cells.[79,81] Defects in central and peripheral tolerance have been implicated in the pathogenesis of autoimmune diabetes and this section aims to provide an overview of the mechanisms involved.

## 1.2.2 The Thymus

### 1.2.2.1 Development of the Thymus

The thymus contains two distinct groups of cells: the epithelial cells and the lymphoid thymocytes.[82] The epithelium of the thymus develops embryologically from the third pharyngeal pouch endoderm and the ectoderm of the third branchial cleft.[82,83] Mature thymic epithelium contains cortical thymic epithelial cells (cTEC) and medullary thymic epithelial cells (mTEC).[82,83] The thymus attracts cells of haematopoietic origin from the bone marrow during its development, including thymocytes, dendritic cells and macrophages.[82,83] These cells colonise the thymus at around 8 weeks gestation in humans.[84] The fully-developed thymus consists of many lobules that are differentiated into an outer cortical region and an inner medulla. Less mature thymocytes can be found in the cortex and they progressively become more differentiated and mature as they enter the medulla.[85] From foetus up until adulthood the thymus is a major source of new lymphocytes.[85] Development of new T-cells slows down in adults and the thymus involutes with age.[86] T-cell numbers in the adult are largely maintained through division of mature T-cells in the periphery.[85]

### 1.2.2.2 Thymic Education of T-Lymphocytes

At roughly 8 weeks gestation in the human and day 11.5 of embryogenesis in mice, the thymus recruits haematopoietic cells.[84] Chemokines including CCL21 and CCL25 have been shown to play important roles in mediating this process, which involves attracting T-cell precursors from the bone marrow to the thymus.[84] Initially, the cells that enter the thymus lack most of the surface markers that characterise mature T-cells.[84,85,87] Interaction with the thymic stroma causes initial differentiation resulting in the expression of T-cell-specific markers. These cells lack the CD3/T-cell receptor complex and the co-receptors CD4/CD8, and are described as 'double negative' thymocytes.[84,85,87]

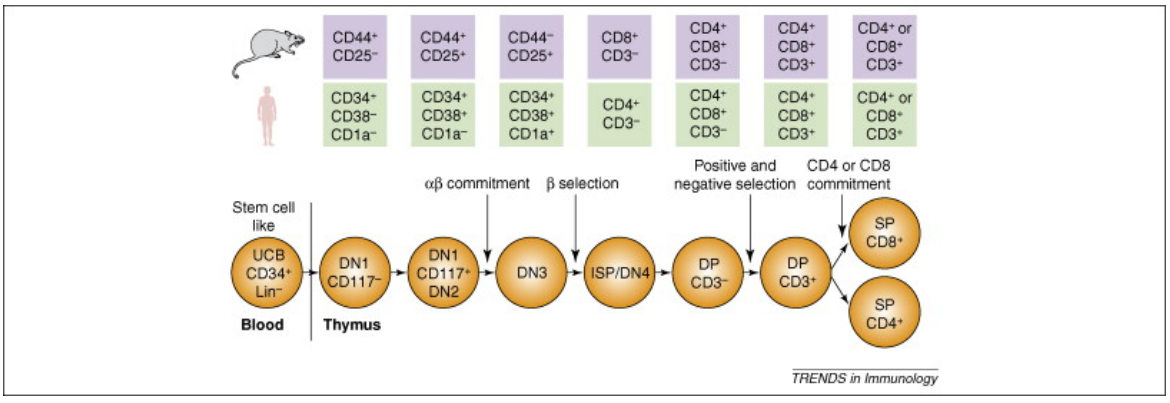


*Figure 1.4 : T-cell development and surface marker expression profile at different stages of development for human and murine T-cells (Image adapted from Weerkamp et al, 2006).*[88]

The expression of specific adhesion molecules can be used to stage the development of double-negative thymocytes in humans and mice (Figure 1.4).

Using mice as an example, the expression of CD44, CD25 and c-kit vary depending on the stage of development (Figure 1.4). Initially, double-negative thymocytes express c-kit and CD44 but not CD25. This is known as the double-negative 1 (DN1) stage.[84,85,87] As the thymocytes mature, they begin to express CD25 and the expression of CD44/c-kit is reduced.[84,85,87] This is the DN2 stage. In cells that reach the DN3 stage (CD4- CD8- CD25+ CD44-) beta selection occurs. Only cells that succeed in an in-frame rearrangement of the gene encoding the TCR-beta chain survive.[84,85,87] Eventually the cells lose CD25 expression again at the DN4 stage. During the maturation of double-negative thymocytes, they migrate from the corticomedullary junction to the subcapsular region of the thymic cortex.[89] This is mediated by CXCR4, CCR7 and CCR9.[84] The beta chains pair with surrogate pre-TCR alpha chains resulting in the formation of a pre-T-cell receptor. The assembly of the CD3/pre-T-cell receptor complex leads to arrest in beta chain rearrangement, replacement of the pre-TCR alpha chain with a rearranged TCR alpha chain, and allows further development into double-positive thymocytes.[84,85,87]

The double-positive (DP) thymocytes express both CD8 and CD4 on their cell surface. These cells undergo selection to ensure that functional T-cells that are not auto-reactive enter the periphery. The 'affinity model of selection' describes this process.[89,90] Double-positive thymocytes interact with peptide-MHC complexes that are expressed by stromal cells in the cortex such as cTECs and dendritic cells via their T-cell receptors. In a process known as positive selection, double-positive thymocytes with T-cell receptors capable of binding to MHC/peptide complexes are selected to receive "survival signals" that allow them to develop further into single positive thymocytes. [89,90] In this process, very low affinity interactions between the T-cell receptor and MHC/peptide complex leads to death by neglect. [89,90]

Positively selected thymocytes relocate from the cortex to the medulla via the chemokine CCR7 to undergo negative selection.[89] in this process, auto-reactive thymocytes undergo further deletion via interactions with mTECs.[89] mTECs express a wide range of self antigens including Tissue Restricted antigens (TRAs) whose expression is not normally found outside of specific tissues.[89]This is controlled in part by the autoimmune regular (AIRE) gene.[89] Auto-reactive T-cells that interact strongly with self-peptides undergo

deletion.[89] T regulatory cells (T-regs) only undergo positive selection in the cortex and do not progress to negative selection in the medulla as T-reg development is driven by a TCR avidity that is above that required for positive selction but below that required for negative selection.[91] T-regs are discussed in more detail in Section 1.2.2.4.Development is summarised in Figure 1.5.

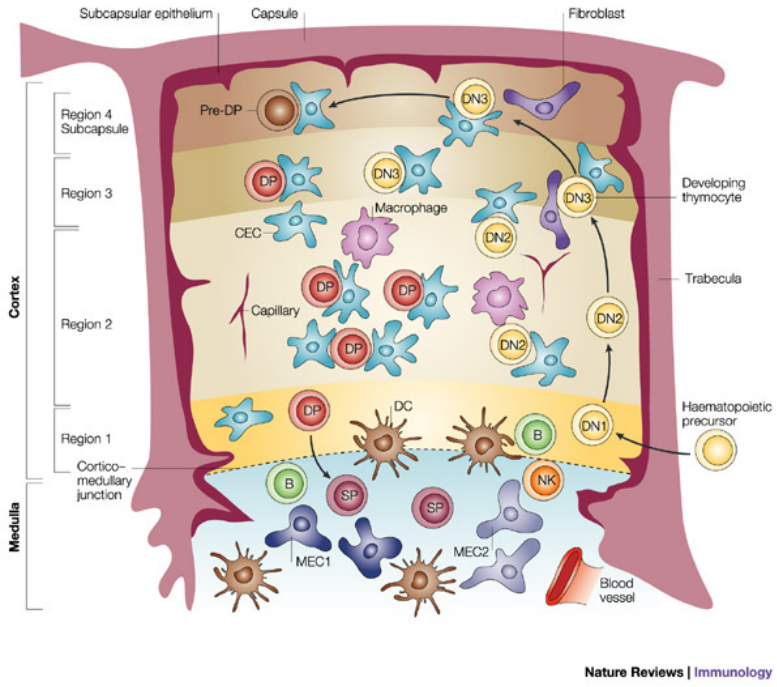


*Figure 1.5 : Development of the thymocyte within the thymus. DN1 cells migrate to the subcapsular region as they mature. Double positive cells undergo negative and positive selection in the cortex where affinity to MHC class I or MHC class II determines development into single positive CD4+ or CD8+ cells respectively. Further maturation occurs in the medulla (Image adapted from Blackburn et al, 2004).*[92]

#### 1.2.2.3 Breakdown of Central Tolerance in Autoimmune Diabetes

As alluded to earlier, defects in the central tolerance mechanisms described above can lead to autoimmunity. The susceptibility loci are gene regions associated with a specific disease. In type 1 diabetes, association studies and linkage analysis have uncovered a number of susceptibility loci containing candidate genes implicated in the pathogenesis of type 1 diabetes.[93] These regions are noted using the abbreviation IDDM followed by a number (eg. IDDM1).[93] Variations of genes associated with the susceptibility loci can result in defects in peptide presentation and subsequent failure of negative selection in the thymus.[94-100] An example of gene variations affecting the expression of peptides is variations in the AIRE gene. The AIRE gene contributes to the expression of tissue-specific antigens by mTECs in the medulla.[94] Defects in the gene lead to autoimmune polyendocrinopathy-candidiasis-ectodermal dystrophy (APECED), which results in the dysfunction of multiple endocrine glands due to autoimmunity.[94] It has been shown that disruption of a single tissue-specific gene molecule is sufficient to trigger autoimmunity against that tissue, albeit rarely.[95]

The HLA DR3/DR4 haplotypes confer susceptibility to developing autoimmune diabetes.[96] A number of mechanisms have been proposed to explain the link between HLA DR3/DR4 and autoimmune diseases. One theory suggests these alleles could result in MHC II complexes that are defective in their binding and presentation of self-peptides in the thymus and the periphery.[97] It is believed that this could lead to failure of negative selection and the subsequent survival of auto-reactive T-cells. Polymorphisms in the PTPN22 gene, which is located on region 1p13, is another susceptibility locus for autoimmune diabetes. It is implicated in defective thymic education of T-cells.[98] PTPN22 encodes a lymphoid-specific phosphatase, LYP, that negatively regulates TCR signalling. Mutations in PTPN22 lead to lower T-cell activation and IL-2 production.[98,82,99] This could potentially result in defects in the signal strength required for negative selection.

The insulin gene which is located on region 11p15.5 is another susceptibility locus implicated in thymic education.[99,100] Alleles for the gene are classified into three classes (classes I-III) which depend on the number of tandem repeats located 586 base pairs upstream of the INS locus. Class I alleles (26 to 63 repetitions) lower the expression of insulin in the thymus, thus increasing

the risk of T-cells auto-reactive against insulin evading negative selection.[99,100] Class III alleles (140-210 repetitions) conversely increase insulin expression and may offer protection against the development of diabetes.[99,100] A study by Cai *et al.* showed that the Class III VNTR haplotype is associated with an average threefold increase of insulin in the thymus compared to the Class I VNTR allele, thus increasing the effectiveness of central tolerance mechanisms.[101] Similar mechanisms of susceptibility have been reported for other immune diseases such as myasthenia gravis. [101]

#### 1.2.2.4 Regulatory T-Cells

Regulatory T-cells play an important role in modulating the immune response. They can largely be subdivided into natural T-regs (nTregs) generated in the thymus and induced T-regs (iTregs) that form in the periphery.[102] FOXP3 expressing CD4+ T-cells generated in the thymus (nTregs) are well characterised as regulatory T-cells. Mutations in FOXP3 result in immunodysregulation polyendocrinopathy enteropathy X-linked syndrome (IPEX) that leads to dysfunction of regulatory T-cells and autoimmunity.[103] This highlights the importance of these cells in regulating the immune response.

The production of nTregs that express FOXP3 appears to occur in the medulla of the thymus in a process known as clonal diversion.[79,104] The process that leads to the production of nTregs is largely unknown, although Hassall's corpustules appear to play a role through the production of thymic stromal lymphopoietin (TSLP).[105] Within the thymus, the mechanisms that control whether a thymocyte undergoes clonal deletion to form effector T-cells or clonal diversion to form nTregs is very much debated. TCR avidity or the 'Goldilocks theory' suggests that cells which bind strongly with the MHC II complex undergo clonal deletion, but a moderate strength of the signal might trigger clonal diversion. Differences in TCR/ligand properties may also play a role in this process (Figure 1.6).[106]

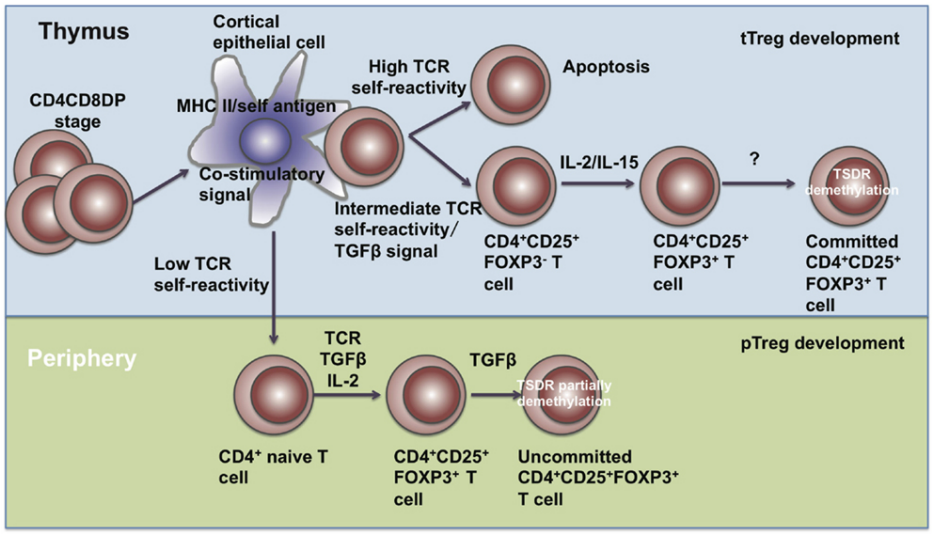


*Figure 1.6 : T-reg development in the thymus and periphery. An intermediate level of reactivity to self-peptides is believed to result in the development of T-regs via clonal diversion (Image adapted from Nie et al, 2015).* [104]

T-regs have been shown to exert their immunomodulatory effect through the production of anti-inflammatory cytokines like IL-10 and TGF-β, direct cell to cell contact, as well as modulating the activation state and functions of antigen-presenting cells.[107] In the context of autoimmune diabetes, studies have shown nTregs play an important role in the pathogenesis of the disease. FOXP3 T-cells are important in the pathogenesis of type 1 diabetes.[81,108] Indeed depletion of FOXP3-expressing T-cells in BD25TCR transgenic mice resulted in fulminant diabetes within 3 days.[81,108]

### 1.2.3 Mechanisms of Peripheral Tolerance

Clonal deletion within the thymus is not a perfect process and some auto-reactive cells survive the process and enter the periphery. Mechanisms exist in the periphery to prevent the activation and clonal expansion of these self-reactive T-cells. The activation of T-cells requires the TCR signal, which involves the binding of the TCR receptor to MHC class II/peptide complexes on antigen-presenting cells. A second signal involving co-stimulatory molecules is required to fully activate the cell. Cells that fail to receive this signal become anergic and are unable to elicit an immune response.[109] This positive co-stimulatory signal is mediated by the interaction of CD28 on T-cells with B7 molecules (CD80/CD86) on antigen-presenting immune cells (e.g. B-cells, macrophages, dendritic cells).[109] CTLA-4 is a homolog of CD28 and its upregulation controls T-cell activation by binding the B7 family of co-stimulatory molecules which conversely inhibits the activation initiated when the CD3 complex binds to the MHC II complex on antigen-presenting cells. [110] This transduces an inhibitory signal that prevents cell cycle progression and induces T-cell apoptosis.[110] Thus the balance between the positive signal from CD28 and the inhibitory signal form CTLA-4 controls T-cell activation.

Polymorphisms in the CTLA-4 gene have been shown to be linked with susceptibility to type 1 diabetes.[111]

Another negative regulator of T-cells is Programmed Death 1 (PD-1). PD-1 is a member of the CD28 superfamily of receptors and binds to ligands PD-L1 and PD-L2. PD-1/PD-L1 plays a crucial role in inhibiting T-cell activation during persistent antigen expression.[112] Blockage of the PD-1/PD-L1 pathway has been shown to result in diabetes in NOD Mice. [112]

### 1.2.4 Pro-Inflammatory Cytokines and their Role in Beta Cell Dysfunction

Autoimmune diabetes is characterised by an infiltration of the islets in the pancreas by immune cells leading to inflammation in a process termed insulitis.[113] Infiltrating cells secrete a range of pro-inflammatory cytokines into the microenvironment of the islets. These cytokines, IL-1β and TNFα, perpetuate this inflammatory response by activating immune cells, upregulating ICAM-1 on the vascular endothelium and stimulating the secretion of chemokines that attract autoreactive T-lymphocytes,

macrophages and antigen-presenting cells to the inflamed islets.[114,115] Pancreatic beta cells have also been shown to secrete pro-inflammatory cytokines in response to a pro-inflammatory environment.[116] This positive feedback mechanism leads to progressive destruction of beta cells and depletion of the beta cell mass, eventually resulting in clinical diabetes. A number of these cytokines have been implicated in the pathogenesis of autoimmune diabetes. These include IFNγ, TNFα, and IL-1β.[117] This section aims to explore the mechanisms whereby pro-inflammatory cytokines prime and induce beta cell apoptosis and the role they play in inducing diabetes.

#### 1.2.4.1 The NF-κB Pathway

NF-κB is a nuclear transcription factor found in all cells. It has been shown to be activated in response to stress, free radicals and bacterial/viral antigens.[118] Exposure of pancreatic beta cells to the pro-inflammatory IL-1β and TNFα has been shown to result in the activation of NF-κB and the expression of associated pro-apoptotic genes.[119] NF-κB is known to have both pro- and anti-apoptotic roles. However, the predominantly pro-apoptotic role of NF-κB on pancreatic beta cells is well established.[118-121] Indeed, blockage of the NF-κB pathway in experimental models has been shown to halt the

development of autoimmune diabetes.[122] NF-κB has been shown to regulate a diverse gene network in pancreatic beta cells. These include genes involved in beta cell function, defence and repair, as well as pro-apoptotic genes.[123]

#### 1.2.4.2 Signal Transduction in the NF-κB Pathway

The NF-κB transcription factor is a complex of related gene products from a family of five proteins: RelA/p65, c-Rel, RelB, p50 and p52.[124] These form homo- or heterodimers that vary depending on the stimulus and species.[120] These proteins have a Rel homology domain (RHD) that functions in DNA binding, dimerization and interaction with IκB forms.[124] NF-κB1 (p105) and NF-κB2 (p100) have ankyrin repeats on their C-termini (Figure 1.7). Processing of p105 and p100 leads to the production of p52 and p50 proteins.[120,124] P50 and p52 monomers on their own are repressors of NF-κB function, but can play a transactivation role through their interactions with RelA, RelB and c-Rel.[120]

The activity of NF-κB is controlled by proteins known as inhibitors of NF-κB. The IκB family of proteins consists of IκB-α, IκB-β, IκB-γ and BCL3.[124,125] These inhibitors contain ankyrin repeats that interact with the Rel homology domain

of the NF-κB family of proteins (Figure 1.7). This interaction results in the retention of NF-κB in the cytoplasm by masking its nuclear localisation sequence (NLS).[118,121,124]

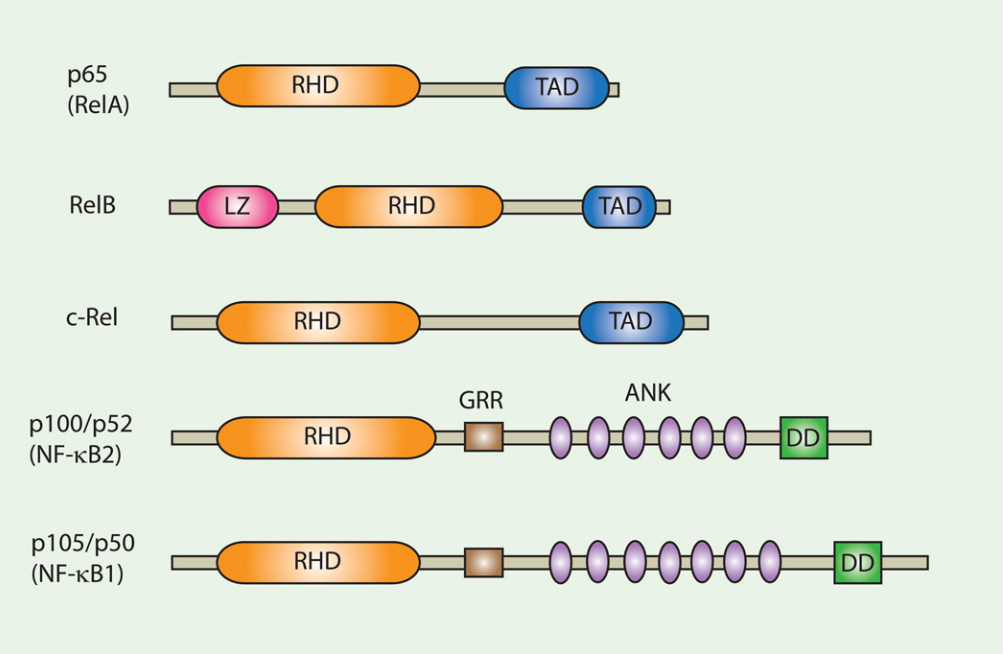


*Figure 1.7 : The NF-κB family of transcription factors. All members express the Rel homology domain (RHD). P52 and p53 have ankyrin repeats on their c-termini and as monomers they act as repressors of NF-κB function. (Image adapted from Oh et al, 2013).* [126]

Binding of IL-1β or TNFα to their respective receptors leads to the signal being transduced to an IκB kinase (IKK) complex consisting of IKKα and IKKβ as well as the regulatory IKKγ/NEMO.[118,121,124] This results in the phosphorylation of the IκB protein that targets the protein for ubiquitination and degradation via

the proteasome. NF-κB that has been liberated can translocate to the nucleus. RelA, RelB and c-Rel contain transcriptional activation domains and act as transcriptional factors for a wide network of genes.[118,121,124] This process is summarised in Figure 1.8.

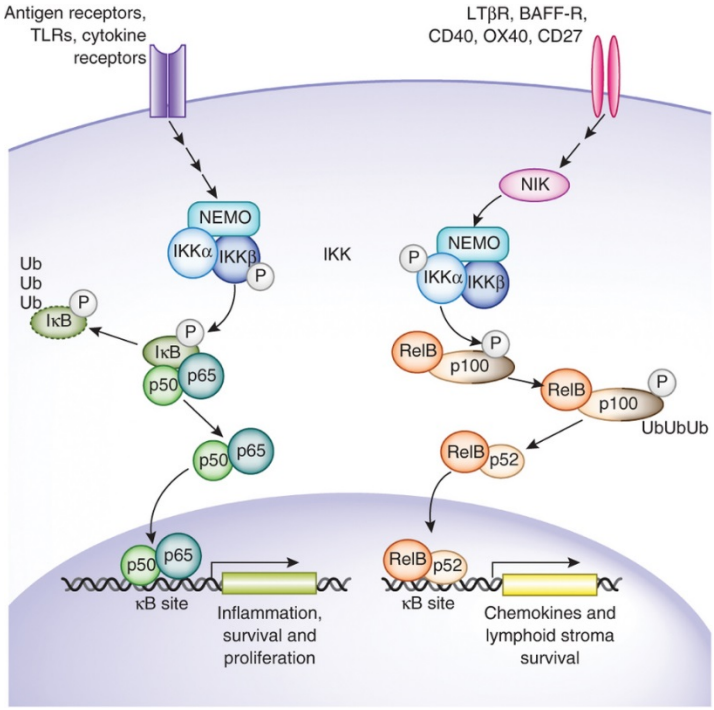


*Figure 1.8 : Depiction of the NF-κB pathway. Binding of pro-inflammatory cytokines (e.g. TNFα) to their receptors results in the activation of the IKK/NEMO complex and subsequent ubiquitination of IκB via the proteasome. NF-κB translocates to the nucleus to transcribe target genes (Image adapted from Gerondakis et al, 2014) .*[127]

### 1.2.4.3 Mechanisms of NF-κB-Induced Beta Cell Death

#### 1.2.4.3.1 Activation of Inducible Nitric Oxide Synthase (iNOS)

Nitric oxide (NO) is a compound involved in many biological processes. It is produced by macrophages in response to pathogens, where NO plays an important role in the destruction of pathogens.[128] It regulates blood vessel diameter,[129] as well as many cellular functions, including cell division and proliferation.[130] Production is controlled by the regulation of nitric oxide synthase (NOS).[131] Its role in cell survival is complex. It has been shown to have an anti- or pro-apoptotic signal depending on the concentration of NO and the cell type in question. NO can prevent apoptosis at many points in the apoptotic pathway. These include nitrosylation of caspases leading to their inactivation, activation of bcl-2 and bcl-xL and regulation of the expression of death receptors.[132,133,134] However in beta cells production of NO after exposure to pro-inflammatory cytokines appears primarily to induce apoptosis.[118,119,120,121,123] Activation of NF-κB by pro-inflammatory cytokines has been shown to increase the expression of inducible nitric oxide synthase (iNOS) and subsequent formation of NO.[135] The iNOS promoter contains two binding sites for NF-κB which are activated by IL-1β and TNFα as well as a

binding site for STAT1.[136] Activation of the pathway results in the liberation of reactive oxygen species (ROS) and oxidative stress. ROS damage critical cellular components.[137] High concentrations can damage DNA leading to activation of p53 at checkpoints in the cell cycle and subsequent apoptosis via the intrinsic mechanism (Figure 1.9).[137]

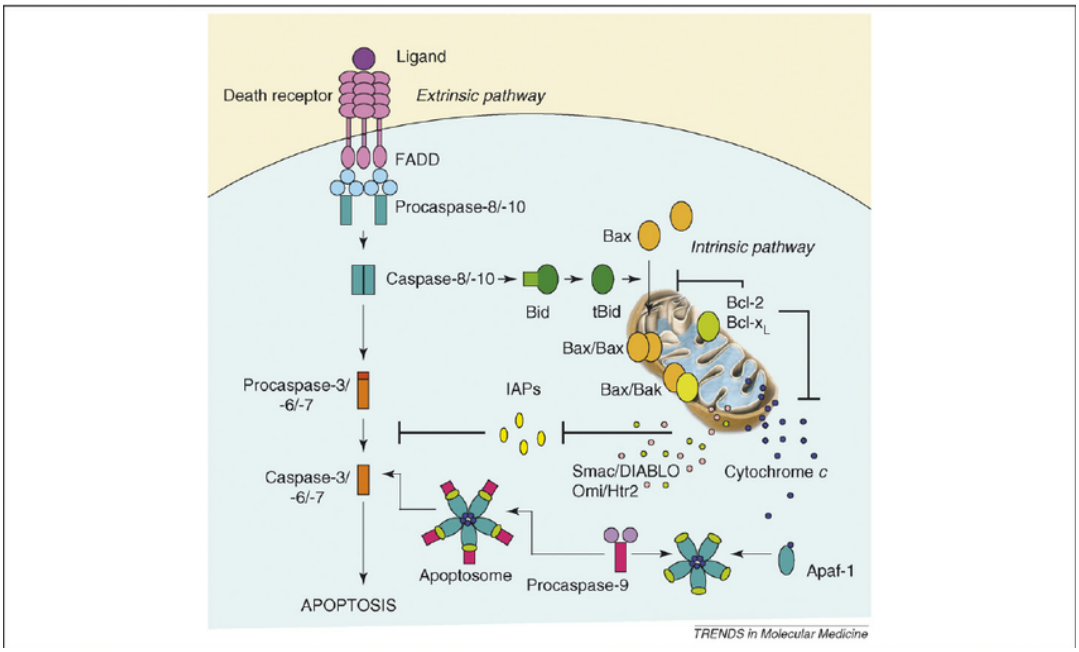


*Figure 1.9 : Simplified diagram of the pathways of apoptosis. In the intrinsic mechanism, stresses (e.g. DNA damage) lead to activators such as P53. BAX is phosphorylated and forms pores in the mitochondria releasing cytochrome c in to the cytosol. Cytochrome c binds to APAF-1 and caspase-9 forming the apoptosome which subsequently leads to apoptosis (Image adapted from Ramaldo et al, 2008).*[138]

NO has also been shown to inactivate the mitochondrial enzyme aconitase required for the generation of ATP via the Krebs cycle in aerobic respiration.[139] Increased DNA damage can lead to overactivation of poly ADP ribose polymerase (PARP), an enzyme that detects single strand DNA breaks. This results in the depletion of $NAD^+$ and subsequent depletion of ATP. Progressive ATP depletion via these mechanisms can induce necrotic cell death.[140] PARP can also independently trigger apoptosis via the production of PAR which stimulates mitochondrial release of AIF.[141] NO can nitrosylate specific cysteine residues of proteins resulting in the formation of nitrosothiols. This process affects the proteins' stability and activity within the cell.[134] Production of NO has also been shown to be a cause of ER stress and subsequent apoptosis in beta cells.

#### 1.2.4.3.2 Disruption of Endoplasmic Reticulum (ER) Homeostasis

The endoplasmic reticulum (ER) is an organelle that functions in the synthesis of new proteins in the cell. Pancreatic beta cells have the specialised function of rapidly producing insulin in response to fluctuations in blood sugar levels. This rapid and constantly changing protein synthesis leaves beta cells susceptible to dysregulation of ER homeostasis.[123] Accumulation of

misfolded proteins in the ER triggers a regulatory response known as the unfolded protein response. This response is protective and it prevents further accumulation of misfolded proteins within the ER.[142] It is mediated by three ER transmembrane receptors: protein kinase RNA-like ER kinase (PERK), activating transcriptional factor 6 (ATP6) and inositol-requiring enzyme 1 (IRE1).[142] When misfolded proteins accumulate the protein BiP dissociates from these receptors leading to the activation of the UPR.[142] The UPR protects the cell via translational attenuation, upregulation of ER chaperones and increased degradation of misfolded proteins.[140] Prolonged ER stress will however trigger apoptosis in spite of the protective mechanisms in place.[123,140]

Overexpression of NF-κB and subsequent generation of NO has been shown to inhibit SERCA2b, a calcium pump found on the endoplasmic reticulum that actively pumps calcium from the cytoplasm into the ER.[123] SERCA2b contains conserved binding sites for the zinc finger transcription factor Sp1. Downregulation of Sp1 via NO leads to downregulation of SERCA2b expression.[136] Inactivation and downregulation of the pump leads to subsequent depletion of ER calcium stores, eventually resulting in ER

stress.[123,140] ER stress leads to the expression of CHOP via the transmembrane proteins IRE1α, PERK and ATF6. The mechanisms through which CHOP induces apoptosis remain controversial.[140] Whether cytokine-induced ER stress is a direct cause of beta cell apoptosis or a parallel event is a question currently under debate.

#### 1.2.4.3.3 Disruption of Beta Cell-Specific Functions

Exposure to pro-inflammatory cytokines has been shown to negatively affect beta cell-specialised functions. A number of genes that regulate beta cell functionality have been shown to be downregulated on exposure to these cytokines. PDX1 is a gene that governs the embryonic development of the pancreas and is also involved in the differentiation of beta cells in later development.[143] Deficiencies in the gene have been shown to result in severe beta cell dysfunction with homozygous mutations resulting in pancreatic agenesis.[144] PDX1 downregulation occurs with NF-κB activation potentially indirectly via upregulation of NO via iNOS induction. Studies have implicated a potential therapeutic benefit of PDX1 gene therapy in the treatment of autoimmune diabetes.[145] The ISL1 gene is another important gene in the

embryogenesis of the pancreas that is downregulated by NF-κB induction in beta cells.[123]

Several genes involved in secretion and production of insulin are also implicated, including GLUT2, glucokinase and insulin. GLUT2 is a membrane-bound protein channel that facilitates the transport of glucose across the cell membrane.[146] As previously discussed the channel is important in the mechanisms regulating insulin release from the beta cells. NF-kB has been shown to be important in the expression of GLUT2, potentially inhibiting its expression and affecting glucose homeostasis.[118,123]

#### 1.2.4.3.4 Protective Role of NF-κB on Beta Cells

Activation of NF-κB by cytokines such as TNFα is known to have a protective role on many cell types.[121] The pro- or anti-apoptotic nature of NF-κB depends on the cell type and inciting stimulus.[121] Potential mechanisms for NF-κB anti–apoptotic effects include inhibition of caspase activation as well as the ability of NF-κB to negatively regulate JNK-mediated apoptosis.[132,147]

Cytokines in the inflammatory response induce the production of free radicals such as superoxides (O2-) and NO.[118,119,120,121,123] NF-κB has been shown to induce the expression of a wide array of 'defence genes' that protect the cell against free radical-induced cytotoxicity and apoptosis. Some of the genes implicated include manganese superoxide dismutase (MnSOD). This is an essential scavenger enzyme that detoxifies the free radical superoxide, preventing ROS-mediated cellular damage.[148] Expression of this protein in insulinoma cells has been shown to prevent IL-1β-induced cytotoxicity and reduce NO production in the cells.[148] Heat shock proteins (HSPs) have also been shown to be upregulated in response to NF-κB activation.[120] These proteins are expressed by cells in response to stressful conditions. They are evolutionarily conserved proteins that act as chaperones as well as stabilising biomolecules such an mRNA.[149] Studies have shown that HSPs protect beta cells from apoptosis on exposure to pro-apoptotic cytokines like LPS. Selective overexpression of a specific HSP70 has been shown to improve resistance of beta cells to NO-induced apoptosis in rat experimental models.[150] Human beta cells are known to naturally express higher levels of HSP70 compared to murine cells, which could account for the greater resistance of human beta cells to NO-induced apoptosis. [151]

In the case of beta cells, studies have shown that exposure to IL-1β initially causes an increase in the expression of MnSOD and other 'defence genes'. Prolonged exposure to the cytokine however resulted in the increased expression of iNOS and other mediators of beta cell apoptosis, leading to cell death.[152] Beta cells are known to be more susceptible to pro-inflammatory cytokine-mediated apoptosis compared to other cell types. A greater expression of pro-apoptotic genes on prolonged exposure to pro-apoptotic cytokines could overwhelm the protective mechanisms in beta cells and tip the balance in favour of apoptosis.

#### 1.2.4.4 The Mitogen-activated protein kinase Pathway (MAPK)

The mitogen-activated protein kinase signalling pathway (MAPK) is involved in cellular responses to a wide range of stimuli, including stress and growth stimuli. [153,154] The pathways classically consist of three family members, the c-Jun NH2-terminal kinase (JNK), extracellular signal-regulated kinase (ERK) and the p38-MAPKs.[153,154] MAPKKK (MAP kinase kinase kinase) activate MAPKK (MAP kinase kinase) which in turn activate MAPK that goes on to regulate gene expression by activating transcription factors.[153,154] These

factors are kinases that activate their targets via phosphorylation of tyrosine and serine residues. The pathways are illustrated in Figure 1.10.

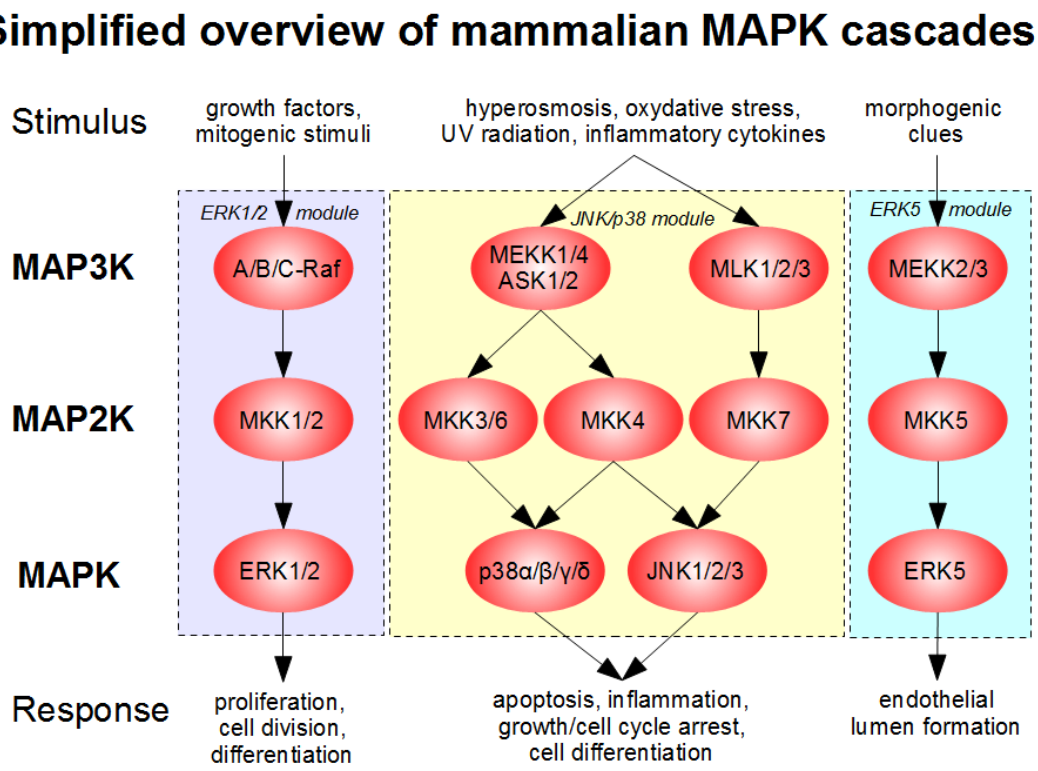


*Figure 1.10 : Simplified overview of the MAPK pathways. P38/JNK are known as the stress pathways and are activated in response to a wide range of stressors and are implicated in cellular apoptosis. In contrast, the ERK pathways are well characterised as pro-survival/growth. (Image adapted from Wikipedia, 2017).* [155]

The JNK and p38 pathways are known as the stress pathways and are activated by a wide range of stress stimuli including heat shock, DNA damage, pro-inflammatory cytokines and UV radiation.[153,156,157] ERK is well-characterised as having a pro-survival and proliferative role in cells. The JNK family of MAPKs

consist of three isotypes (JNK1, JNK2, JNK3). JNK1 and JNK2 are widely expressed in all cell types, but JNK3 is mainly expressed in neuronal and heart tissue.[157] Upstream activators of this pathway include ASK1, HPK1, MLK3 and TAK1. These factors activate MKK4/7 that in turn activate JNK via phosphorylation at TYR183/TYR185.[157] The p38 family of MAPK consists of four isoforms (p38α, p38β, p38γ and p38δ).[154] Upstream activators of this pathway largely overlap with those of the JNK pathway, and include factors such as ASK1, MEKK and TAK1. These activate MKK3/6 which in turn activate p38.[153] The ERK family of factors are involved in cell proliferation, differentiation and cell migration.[154] They classically consist of isotypes ERK1 and ERK2 although other isotypes have been described, the functions of which are largely unexplored.[154] The upstream activators RAS/RAF activate MEK1/2 that in turn activate ERK1/2.[154]

#### 1.2.4.4.1 The Mechanisms of MAPK-Induced Beta Cell Death

Binding of TNFα and IL-1β leads to the activation of the map kinase pathways in beta cells (Figure 1.11).

The importance of the MAPK pathway in the pathogenesis of autoimmune diabetes has been evaluated via the use of inhibitors of p38 and MEK1/2 signalling in several studies. These studies have shown that blocking p38 and ERK provided protection against beta cell apoptosis.[158,159,160,161] The mechanisms whereby p38 and ERK mediate an apoptotic response are however not well characterised. P38 is known to potentially inhibit Bcl-2, a protein that controls the release of cytochrome c by the mitochondria into the cytosol and initiation of the intrinsic pathway of apoptosis.[162] ERK is known as a pro-survival transcription factor. However, the pathway could play a role in beta cell apoptosis. ERK has been shown potentially to augment NF-κB activity downstream of nuclear translocation and DNA binding leading to mechanisms of beta cell apoptosis discussed previously.[161] It also promotes caspase 8 signalling, controls cytochrome c release by the Bcl-2 family of proteins and promotes p53 activity.[163]

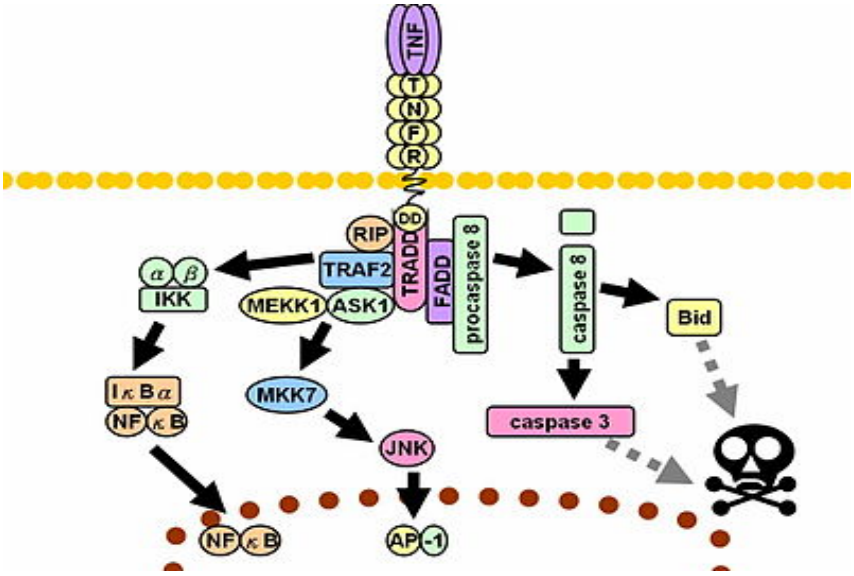


*Figure 1.11 : Signal transduction pathways of TNFα. Binding of TNFα is known to induce apoptosis via activating the JNK stress pathway and expression of AP-1 associated genes (Image adapted from Wikipedia, 2017).* [(164)]

JNK is another factor implicated in the pathogenesis of autoimmune diabetes. Multiple gene knockout models have shown that JNK exerts pro- and anti-apoptotic effects depending on the cell type and inciting stimuli.[(165)] JNK was initially identified as a UV-response protein kinase involved in the phosphorylation of c-Jun on its N-terminal transactivation domain ser60/ser73. Evidence of its pro-apoptotic role came from studies on embryonic fibroblasts from transgenic mice. These JNK1-/-, JNK2-/- mice showed resistance to apoptosis in response to UV radiation.[(166)]

Activation of JNK by exposure to pro-inflammatory cytokines is known to induce apoptosis in beta cells.[167,168,169] Previous studies have shown that blocking this factor can ameliorate the onset of diabetes in both murine and human models, indicating that it plays an important role in regulating beta cell apoptosis.[168] JNK is known to phosphorylate the AP-1 family of transcription factors including c-Fos, c-Jun, ATF and JDP.[168] AP-1 transcription factors are implicated in regulating a range of cellular processes including cell proliferation, differentiation and apoptosis.[170] The AP-1 transcription factor has been shown to upregulate the transcription of a number of genes that induce apoptosis including FAS-L, TNFα and BAK.[170,171] This pathway is implicated in the regulation of apoptosis in several cell types, including cells in the central nervous system in which blockage leads to reduced apoptosis.[170] The expression of AP-1 target genes on exposure to pro-inflammatory cytokines may play a crucial role in triggering beta cell apoptosis. Using the ATF3 transcription factor as an example, transgenic mice expressing ATF3 developed abnormal islets.[169] Knockout models of ATF3 have been shown to partially inhibit NO-mediated beta cell death.[169] Thus JNK may regulate apoptosis via the induction of these transcription factors.

Apart from modulating transcription factors and the expression of genes, JNK has also been shown to interact with proteins implicated in the apoptotic pathways. These proteins include the Bcl-2 protein family which consists of pro-apoptotic members (BAX/BAK) that form the mitochondrial apoptosis-induced channel (MAC) on the mitochondrial membrane, leading to the release of cytochrome c, formation of the apoptosome and subsequent apoptosis. The anti-apoptotic members include Bcl-2 and Bcl-xL that inhibit MAC formation. [172] JNK may modulate the activity of Bim and Bmf of the Bcl-2 family of proteins. Their activation could lead to the activation of BAX and initiation of the intrinsic pathway of apoptosis.[171] Phosphorylation of Bim could also bind and neutralise the antiapoptotic activity of Bcl-2 and Bcl-xL. JNK has also been shown to phosphorylate and activate the p53 tumour suppressor protein which could be another potential mechanism for JNK-mediated beta cell apoptosis.[171]

# 1.3 The Role of IL-10 in Immunomodulation in Type 1 Diabetes

## 1.3.1 The role of Interleukin 10 in Immunomodulation

Interleukin 10 (IL-10) is a cytokine that is well characterised for its anti-inflammatory properties.[173,174] It was the first cytokine to be discovered in the IL-10 family of cytokines whose members include IL-10, IL-20, IL-22 and IL-26.[175] The gene encoding interleukin 10 is located on chromosome 1 at 1q21-32 in the human genome.[176,177] It is expressed by both myeloid and lymphoid cells and it plays a central role in the modulation of the immune response.[178,177]

### 1.3.1.1 IL-10 Signal Transduction

IL-10 is secreted as a paracrine factor that binds to its cognate receptor IL-10R on its target cells. IL-10R is a tetramer consisting of two copies of IL-10R1 and IL-10R2 respectively (Figure 1.12).[179,180] IL-10R1 is specific to the binding of IL-10, and binding of the cytokine results in a conformational change in

structure that allows oligomerisation with IL-10R2.[181] IL-10R2 is less specific and is involved in the signal transduction of other cytokines including IL22, IL26, IL28 and IL29.[182]

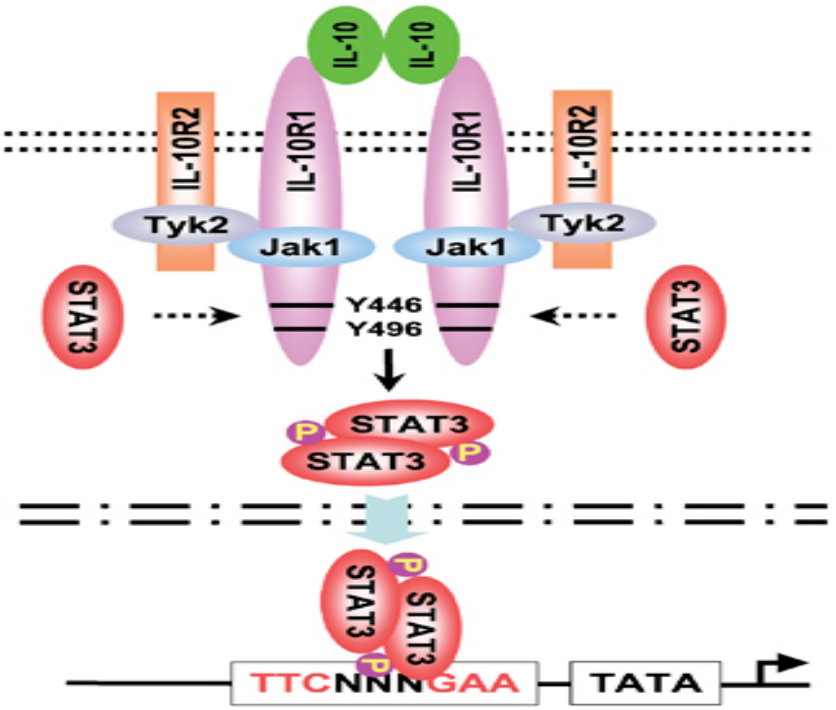


*Figure 1.12 : Depiction of IL-10 signal transduction. (Image adapted from Mosser et al, 2008).* [177]

Binding of IL-10 to its receptor leads to the formation of protein complexes in the cytoplasm. IL-10R1 recruits Janus Kinase 1 (JAK 1) and IL-10R2 recruits Tyrosine Kinase 2 to the protein complex.[183] The protein complex trans-phosphorylates JAK 1, activating it. Activated JAK 1 phosphorylates tyrosine

residues on the cytoplasmic tail of the IL-10 receptor.[184,185] STAT3 monomers are recruited to the phosphorylated residues and interact with the tyrosine residues via their C-terminal SH2 domain.[185] This interaction leads to the phosphorylation of STAT3 by JAK 1.[184,185] Phosphorylated STAT3 form dimers via interaction of their SH2 domains in the cytosol and translocate to the nucleus of the cell where they act as promoters for gene transcription.[186] The signal transduction pathway is summarised in Figure 1.12.

#### 1.3.1.2 Regulation of NF-κB via STAT3 Signalling

As previously discussed, NF-κB is an important factor involved in the pro-inflammatory response, insulitis and subsequent apoptosis of pancreatic beta cells in the pathology of autoimmune diabetes.[118,119,120,187] STAT3 is known to inhibit the expression of pro-inflammatory genes by NF-κB.[174,188] Proposed mechanisms underlying this include those at the nuclear and the cytoplasmic level.

STAT3 has been shown to induce the expression of anti-inflammatory response genes (AIR genes) that repress the expression of pro-inflammatory genes at the level of transcription (Figure 1.13). AIR factors identified include

BCL3 that impairs the ability of NF-κB to bind to DNA and express pro-inflammatory genes by acting as an IκB.[174,189,190] ETV3 is a co-repressor that inhibits NF-κB activity.[174] ZFP36 interferes with TNFα production by destabilising its mRNA.[191] SOCS3 inhibits pro-inflammatory effects of IL-6 via inhibition of the IL-6 receptor.[192] These are but a few of the AIR factors identified. STAT3 has been shown to have approximately 1,700 genomic targets associated with the anti-inflammatory response.[174]

In addition to its regulation of gene expression, IL-10 has been shown to inhibit NF-κB at the cytoplasmic level, probably via the phosphorylation and stabilisation of the IκB protein. This prevents the proteosomic degradation of IκB and the subsequent translocation of NF-κB to the nucleus.[188]

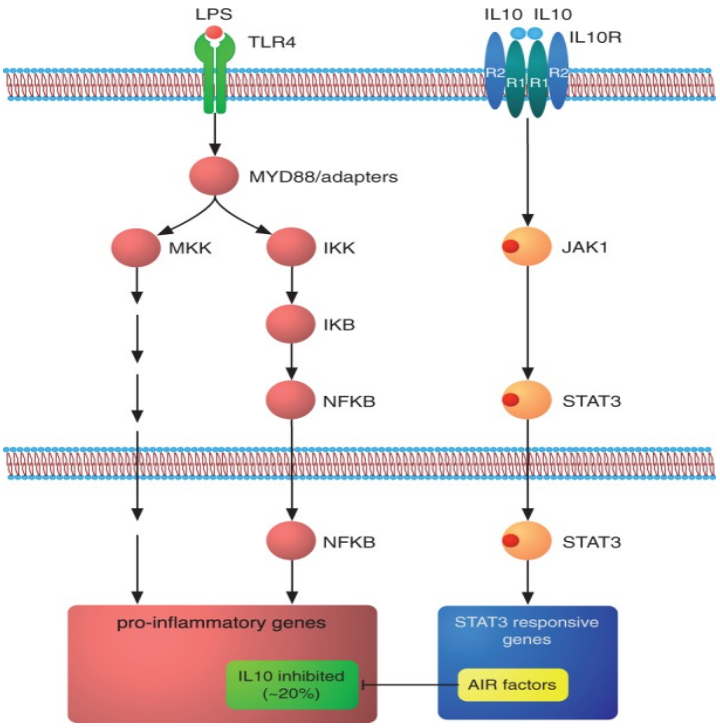


*Figure 1.13 : The IL-10-dependent AIR response in macrophages as described by Hutchkins et al. STAT3 activates target genes leading to the expression of AIR factors that act as repressors to NFκB transcription. (Image adapted from Hutchkins et al, 2013).* [174]

### 1.3.1.3 The Pleiotropic Nature of STAT3

Studies have shown that although the binding of IL-10 and IL-6 to their receptors both activate STAT3, IL-10 has a predominantly anti-inflammatory effect on dendritic cells and IL-6 elicits a predominately pro-inflammatory response.[193] Indeed, under the right conditions, both IL-6 and IL-10 are known to have pro-inflammatory effects on certain cells.[194,195,196,197] This highlights the fact that STAT3 is pleiotropic and many of its functions are cell-

specific. Studies by Hutchkins *et al.* have shown that transcription factors and co-factors associated with STAT3 signalling are pre-bound on sections of DNA that are 'primed' to express predetermined genes upon activation of STAT3.[174] The genomic targets vary between cell types resulting in the differing responses. However, there appears to be a small core of evolutionarily-conserved genomic targets in all cell types.

#### 1.3.1.4 IL-10 Ameliorates the TH1 Cell-Mediated Immune Response

As previously discussed, autoimmune diabetes is classically described as predominantly TH1 or cell-mediated autoimmune disease where the activation of cytotoxic T-cells and the expression of pro-inflammatory cytokines at the islets of Langerhans leads to insulitis and the progressive destruction of beta cells.[198] Although a TH2 response is implicated in the pathogenesis of Type 1 diabetes.[198] IL-10 was first described for its role in TH1/TH2 cross-regulation. IL-10 produced by TH2 cells directly suppresses the polarisation of TH0 CD4+ cells into TH1 cells and the generation of a cell-mediated immune response (Figure 1.14).

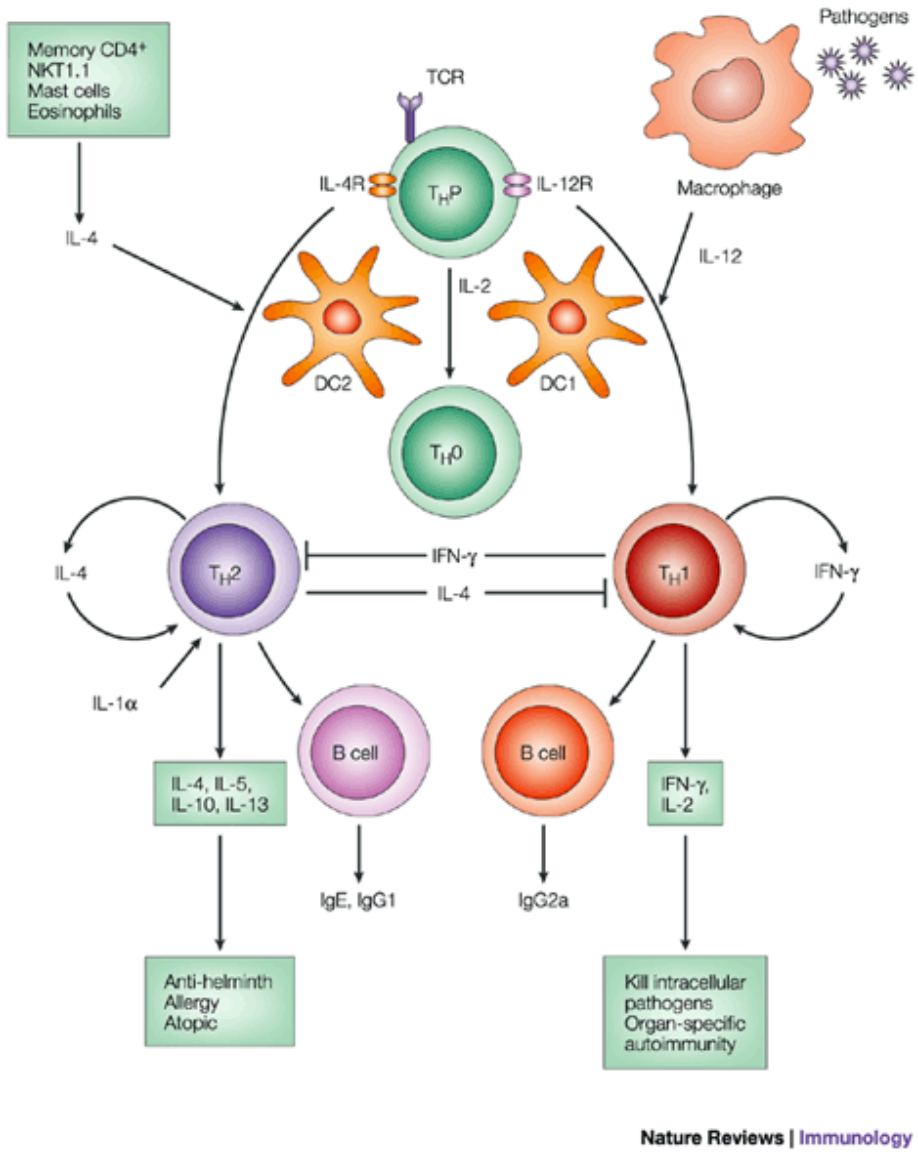


*Figure 1.14 : Figure depicting cross-regulation between the TH1 and TH2 responses. TH1 cytokines are known to inhibit TH2 polarisation of naïve T-cells cells and vice versa. (Image adapted from Liew et al, 2001).* [(199)]

IL-10 has also been shown to regulate the expression of MHC class I and MHC class II molecules in immune cells and could affect the expression of autoantigens in the context of autoimmune diabetes. IL-10 has been shown

to downregulate the expression of MHC class II molecules by antigen-presenting cells (APCs) as well as the co-stimulatory molecule CD86 required for T-cell activation and survival.[200,201] IL-10 is also known to downregulate MHC class I molecules in tumour cells, allowing cancers to evade immune detection.[202] MHC class I is required for the expression of auto-antigens and CD8 cytotoxic T-cell-mediated apoptosis. A similar mechanism in beta cells could protect them from cell-mediated apoptosis.

As discussed previously, T-regulatory cells play a pivotal role in modulating the immune system and preventing an auto-immune response through downregulating the induction and proliferation of T-cells.[203] Indeed, ablation of Tpl2, a MAP3K8 that regulates innate/adaptive immunity and inflamation has been shown to increase intestinal inflammation in mice by inhibiting T-reg cells and IL-10 production.[204] IL-10-secreting T-regs exert most of their immunomodulatory effects via the secretion of IL-10. IL-10 is a known promoter of the production of IL-10-secreting T-reg (IL-10Treg) cells and these cells are known to be a key producer of IL-10.[205,206] Thus a positive feedback loop involving IL-10 is present for the regulation of T-cell immune responses in this T-cell subset.

The pro-inflammatory cytokines TNFα, IL-1β, TGFβ and lPS have been implicated in the pathology of diabetes.[207] They activate NF-κB in immune cells leading to the expression of pro-inflammatory genes and recruitment via chemotaxis of TH1-induced cells to the pancreatic islets.[208] As alluded to earlier, IL-10 is able to block the expression of NF-κB, thus dampening the immune response in this manner. Thus a number of potential mechanisms exist whereby IL-10 can modulate the immune system and reduce the degree of TH1/cell-mediated autoimmunity in type 1 diabetes.

### 1.3.2 The Contrasting Effects of IL-10 on Pancreatic Beta Cells

The promising immunomodulatory properties of IL-10 have made it an attractive option for the treatment of TH1-mediated autoimmune diseases. IL-10 has previously been shown to be effective in modulating autoimmune conditions such as inflammatory bowel disease, where systemic administration of IL-10 reduced colonic inflammation in murine models.[209] However, studies on the efficacy of IL-10 in the treatment of autoimmune diabetes have shown contrasting results.[210,211,212,213,214] Systemic treatment

through intramuscular injection of IL-10 plasmid DNA has been shown to play a protective role in the development of autoimmune diabetes.[211] In contrast, local expression of IL-10 by pancreatic islet cells has been shown to accelerate the progression of autoimmune diabetes.[210] In addition, administration of anti-IL-10 antibodies negated this effect in transgenic NOD mice.[213]

This dichotomy could be explained by the immune-stimulatory properties of IL-10. In high concentrations IL-10 can conversely enhance the differentiation and cytotoxicity of T-cells.[216] Thus high concentrations of IL-10 expressed by islet cells in the islet microenvironment could enhance T-cell-mediated beta cell apoptosis. IL-10 can also induce the MHC II molecule on B cells and enhance B cell growth and differentiation.[213] A study by B Balasa et al. has shown that local expression of IL-10 increases the expression of ICAM1 at the site of the islets, potentially enhancing the extravasation and recruitment of TH1-induced autoimmune cells into the damaged islets.[212]

Interestingly, studies have shown that local expression of viral IL-10 (vIL-10) seems to protect pancreatic beta cells from apoptosis. vIL-10 is known to lack most of the immunostimulatory properties of IL-10 and may indeed supress

TH1/cell-mediated immune responses more specifically than IL-10.[213,214] This dichotomy highlights the complexities of IL-10's role in immune modulation. Although IL-10 is conceptually an attractive option for the treatment of autoimmune diabetes, it is clear that many challenges remain. More studies need to be done into the roles of IL-10 and other immunosuppressive cytokines in the MSC secretome in modulating the immune response before they can be used effectively in treating autoimmune diseases.

### 1.3.3 IL-10's Regulation of Apoptosis in the Pancreatic Beta Cell

In addition to its immunomodulatory properties, IL-10 has been shown *in vitro* to directly offer cytoprotection to pancreatic beta cells after co-administration with pro-inflammatory cytokines implicated in the pathology of autoimmune diabetes.[217]

A number of anti-inflammatory cytokines including IL-4 and IL-13 have been shown to offer cytoprotection directly to pancreatic beta cells. IL-4 and IL-13 have been shown to induce anti-apoptotic genes including Bcl-xL and sIL-1Ra

through the activation of STAT6 in the pancreatic beta cell.[218] Figure 1.15 summarises the signal transduction of IL-4 and IL-13.

In the pancreatic beta cell, the downstream signalling events following binding of IL-10 to its receptors remains largely unexplored. NF-κB plays a key role in the pathology of diabetes through the activation of stress-activated protein kinases (e.g. c-Jun, JNK and p38) as well as triggering ER stress and the release of death signals from the mitochondria.[219]

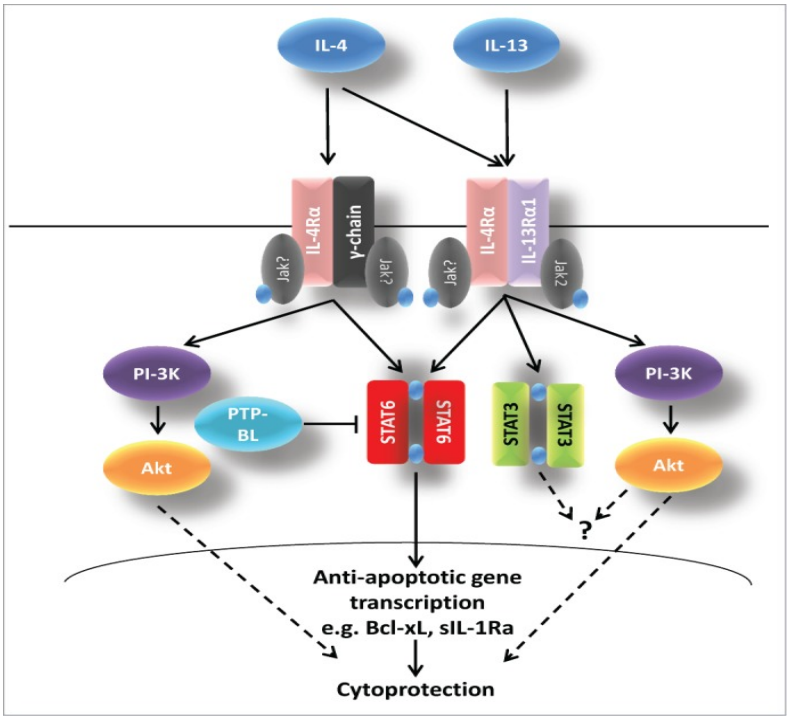


*Figure 1.15 : Proposed signaling pathway for IL-4 and IL-13-mediated cytoprotection of pancreatic beta cells. Binding of IL-4 and IL-13 leads to recruitment of JAK kinases that phosphorylate STAT6. Phosphorylated STAT6 subsequently forms dimers that translocate to the nucleus promoting the expression of anti-apoptotic genes (Image adapted from Russel et al, 2014).*[218]

In our study, we hypothesize that IL-10's ability to block the downstream gene expression of NF-κB may play a central role in the cytoprotective role of IL-10 on the pancreatic beta cell.

Reviewing the role of IL-10 in other cell types, a number of potential mechanisms can be suggested:

1) Binding of IL-10 to beta cells could result in the expression of repressors much like the AIR response seen in immune cells, preventing the expression of pro-apoptotic genes/cytokines via inhibition of NF-κB/AP-1.

2) IL-10 could stabilise IκB in the cytosol preventing its degradation via the proteasome and subsequent translocation of NF-κB to the nucleus.

3) STAT3 has been shown to have some capacity to promote gene expression. IL-10 signalling could result in the expression of anti-apoptotic genes as seen in IL-4 and IL-13.

Further research needs to be carried out to determine the mechanism of the cytoprotection shown to be offered by IL-10. This would shed some light on the value of IL-10 in the treatment of autoimmune diabetes.

### 1.3.4 Thesis Aims and Objectives

In the introduction, we determined that treating type 1 diabetes presents many challenges. The stem cell secretome may present a novel and viable method of treating type 1 diabetes in the future. Determining the therapeutic potential of the MSC secretome in ameliorating the pathogenesis of type 1 diabetes as well as characterising the components of the secretome that confers its therapeutic benefit would be paramount in determining it's efficacy as a treatment modality. With this in mind, the following objectives were laid out for the thesis:

Chapter 3

Chapter 3 will attempt to determine whether MSC conditioned media (MSC-CM) is able to prevent pro-inflammatory cytokine driven falls in cellular

viability by measuring the metabolic activity of beta cells *in vitro*. The specific objectives of this chapter are:

- Culture human bone marrow derived MSCs, characterise the cells through trilineage differentiation and collect conditioned media derived from these MSCs.
- Determine the effect of pro-inflammatory cytokines (TNF$\alpha$, IL-1$\beta$ and IFN$\gamma$) on the mitochondrial metabolism of beta cell lines *in vitro* using MTT assys
- Determine if MSC-CM is able to ameliorate pro-inflammatory cytokine driven falls in mitochondrial metabolism of beta cell lines *in vitro* using MTT assays.

Chapter 4

Chapter 4 will attempt to determine if MSC-CM is able to improve the functionality and morphology of islet in an *in vivo* model of type 1 diabetes. The specific objectives of this chapter are:

- Establish a murine model of type 1 diabetes via multiple low dose Intraperitoneal injections of streptozocin (STZ).
- Determine if MSC-CM improves islet functionality using terminal plasma insulin ELISAs.
- Determine if MSC-CM improves retention of body fat/weight via DEXA scans.
- Determine if MSC-CM improves islet morphology through pancreatic histology.

Chapter 5

Chapter 5 will explore whether IL-10 could play a role in the direct cytoprotection of beta cells. The specific objectives of this chapter are:

- Characterise the presence of IL-10 in MSC-CM using ELISA assays
- Characterise the presence of the IL-10 receptor on beta cell lines through Electrophoresis
- Characterise the presence of the IL-10 receptor on beta cell lines through immunofluorescence.

This study will shed some light on the immunomodulatory properties of the stem cell secretome in the context of autoimmune diabetes. The ultimate goal of research into the stem cell secretome is to be able to offer personalised medication consisting of patient-specific cocktails of cytokines and factors that can be administered to halt the progression and treat a wide range of autoimmune and degenerative conditions.


# Chapter 2: Materials and Methods

# 2.1 Materials

To avoid repetition in the methods, materials used in this thesis were obtained from the following suppliers as detailed in the following table for reference:

| Name | Catalogue No. | Supplier |
|---|---|---|
| (3-(4,5-dimethylthiazol-2yl)-2,5 diphenyltetrazolium bromide (MTT) | M2128 | Sigma-Aldrich, Gillingham, Dorset, UK |
| 3-isobutyl-1-methylxanthine (IBMX) | I7018 | Sigma-Aldrich, Gillingham, Dorset, UK |
| 4',6-Diamidino-2-phenylindole (DAPI) | D9542 | Sigma-Aldrich, Gillingham, Dorset, UK |
| ABTS | A3219 | Sigma-Aldrich, Gillingham, Dorset, UK |
| ALPCO RAT Ultrasensitive ELISA | 80-INSRTH-E01 | ALPCO, Salem , New Hampshire, USA |
| Agarose | BP1356-500 | Fisher Scientific, Loughborough, Leicestershire, UK |
| Alcain Blue | A3157 | Sigma-Aldrich, Gillingham, Dorset, UK |
| Alizarin Red S | A5533 | Sigma-Aldrich, Gillingham, Dorset, UK |

| Name | Catalogue No. | Supplier |
|---|---|---|
| Applied Biosystem ™Microamp™ Optical 8-Cap Strips | 10321515 | Fisher Scientific, Loughborough, Leicestershire, UK |
| Applied Biosystem ™Microamp™ Reaction tube with cap 0.2ml | 10630806 | Fisher Scientific, Loughborough, Leicestershire, UK |
| Ascorbic acid phosphate | A8960 | Sigma-Aldrich, Gillingham, Dorset, UK |
| Bovine serum albumin (BSA) | BP9703-100 | Fisher Scientific, Loughborough, Leicestershire, UK |
| Bone Marrow Mono cells cryoamp (25 million) (MSCs) | 2M-125C | Lonza, Walkersville, Maryland, USA |
| BlueJuice™ Gel Loading Buffer | 10816015 | Fisher Scientific, Loughborough, Leicestershire, UK |
| C57/BL6 inbred mice | Nil | ENVIGO, Huntingdon, Cambridgeshire, UK |
| Centifuge tube 15ml | 62.554.502 | SARSTEDT, Leicester, UK |
| CellStar® Cell Culture Flask (75cm$^2$) T75 | 658170 | Griener bio-one, Glouchestershire, Stonehouse, UK |
| CellStar® Cell Culture Flask (25cm$^2$) T25 | 690160 | Griener bio-one, Glouchestershire, Stonehouse, UK |
| CellStar® Cell Culture Multiwell Plate (24 Well) | 662160 | Griener bio-one,Glouchestershire, Stonehouse, UK |

| Name | Catalogue No. | Supplier |
|---|---|---|
| Desamethosone | D2915 | Sigma-Aldrich, Gillingham, Dorset, UK |
| Direct Load Wide Range DNA Marker | D7058 | Sigma-Aldrich, Gillingham, Dorset, UK |
| DMSO | D2650 | Sigma-Aldrich, Gillingham, Dorset, UK |
| Dulbecco's Eagle Modified Medium (DMEM) high glucose without L-glutamine | BE12-614F | Lonza, Slough, UK |
| Dulbecco's Eagle Modified Medium (DMEM) low glucose without L-glutamine | BE12-707F | Lonza, Slough, UK |
| Ethidium Bromide | E1510 | Sigma-Aldrich, Gillingham, Dorset, UK |
| Ethanol 100% | E0650/17 | Fisher Scientific, Loughborough, Leicestershire, UK |
| Foetal Bovine Serum (FBS) | DE14-801F | Lonza, Slough, Uk |
| Fibronectin | F0895 | Sigma-Aldrich, Gillingham, Dorset, UK |
| Human IL-10 mini ABTS ELISA Development Kit | 900-M21 | Peprotech, London, Uk |

| Name | Catalogue No. | Supplier |
|---|---|---|
| IL10RA Polyclonal Antibody | bs-2459R-A555 | Bioss Antibodies, Woburn, Massachusetts, USA |
| IL10RB Polyclonal Antibody | bs-2602R-FITC | Bioss Antibodies, Woburn, Massachusetts, USA |
| Indomethacin | I7378 | Sigma-Aldrich, Gillingham, Dorset, UK |
| Insulin | I9278 | Sigma-Aldrich, Gillingham, Dorset, UK |
| Insulin, Transferrin, Selenium (ITS) | I3146 | Sigma-Aldrich, Gillingham, Dorset, UK |
| Isopropanol | P/7500/17 | Fisher Scientific, Loughborough, Leicestershire, UK |
| L-Glutamine | BE17-605E | Lonza, Slough, Uk |
| L-Proline | P5607 | Sigma-Aldrich, Gillingham, Dorset, UK |
| Methanol | M/3900/17 | Fisher Scientific, Loughborough, Leicestershire, UK |
| Microplate (96 well) | 650101 | Griener bio-one, Glouchestershire, Stonehouse, UK |
| Non-essential amino acids | BE13-114E | Lonza, Slough, Uk |
| Nunc™ 1.8ml Crotube | 11311665 | Fisher Scientific, Loughborough, Leicestershire, UK |

| Name | Catalogue No. | Supplier |
|---|---|---|
| Oil Red O | O0625 | Sigma-Aldrich, Gillingham, Dorset, UK |
| Paraformaldehyde | P/0840/53 | Fisher Scientific, Loughborough, Leicestershire, UK |
| Penicillin, streptomycin, amphotericin B | BE17-745E | Lonza, Slough, UK |
| Penicillin-Streptomycin (P.S) | 17-602F | Lonza, Slough, UK |
| Phosphate buffered saline | BE17-516F | Lonza, Slough, UK |
| Polysine™ Poly-l-lysine coated Microscope slides. | P4981 | Fisher Scientific, Loughborough, Leicestershire, UK |
| Rabbit IgG Isotype control, FITC conjugated | bs-0295P-FITC | Bioss Antibodies, Woburn, Massachusetts, USA |
| Rabbit IgG Isotype control, A555 conjugated | bs-0209P-A555 | Bioss Antibodies, Woburn, Massachusetts, USA |
| Recombinant human IFNγ | 300-02 | Peprotech, London, UK |
| Recombinant human IFNγ | 300-02 | Peprotech, London, UK |
| Recombinant human IL-1β | 200-01 | Peprotech, London, UK |

| Name | Catalogue No. | Supplier |
|---|---|---|
| Recombinant human TNFα | 300-01 | Peprotech, London, UK |
| RNase Zap | R2020 | Sigma-Aldrich, Gillingham, Dorset, UK |
| RNeasy Mini Kit | 74104 | Qiagen, Manchester, UK |
| Roswell Park Memorial Institute (RPMI) High glucose without-L-glutamine or phenol red | 12-918F | Lonza, Slough, UK |
| Syringe filtration Unit Filtrospur 2.0 | 83.1826.001 | SARSTEDT, Leicester, UK |
| Streptozocin | Ab142155 | Abcam, Milton, Cambridge, UK |
| SuperScript™ III One-Step RT-PCR System with Platinum™ *Taq* DNA Polymerase | 12574018 | Fisher Scientific, Loughborough, Leicestershire, UK |
| Tris-Acetate EDTA (TAE) buffer 50x | EC-872 | Fisher Scientific, Loughborough, Leicestershire, UK |
| Tween-20 | 85113 | Fisher Scientific, Loughborough, Leicestershire, UK |
| Xylene | X3S-4 | Fisher Scientific, Loughborough, Leicestershire, UK |

# 2.2 Cell Culture Methods

All Cell Culture procedures were conducted at the Guy Hilton Research Center, Stoke on Trent, UK.

**Ethical statement:** Bone Marrow Mononuclear cells were purchased from Lonza (Slough, Uk), (Lot Number: 0000562133). Cells were isolated from donor tissue obtained with informed consent and legal authorisation.

## 2.2.1 Preparation of Growth Media

BRIN-bd11 cells were cultured in Roswell Park Memorial Institute (RPMI) medium with 4.5g/l glucose. This was supplemented with 10% foetal bovine serum (FBS) and 1% Penicillin-Streptomycin (5,000 U/L)

The TC6 cell line was initially cultured in low glucose Dulbecco's Modified Eagles Medium (DMEM) with 1g/L glucose due to the potential sensitivity of TC6 cells to higher concentrations of glucose.[220] This was supplemented with 10% heat inactivated foetal bovine serum (FBS) and 1% Penicillin-Streptomycin. To prepare heat inactivated FBS, FBS was heated to 50$^{o}$C in a

water bath for 30 minutes before it was added to the medium. After several unsuccessful attempts at culturing the cells a preparation of 4.5g/L glucose DMEM supplemented with 15% heat-inactivated foetal bovine serum was found to provide good growing conditions for these cells. This optimised preparation was used throughout the experiments. MSCs were cultured in complete MSC medium consisting of DMEM with 1g/L glucose supplemented with 5% FBS, 1% L-glutamine, 1% non-essential amino acids and 1% Penicillin-Streptomycin with Amphotericin B.

### 2.2.2 Cell Lines Utilised

The cell lines utilised in the experiments are depicted in Figure 2.1 below.

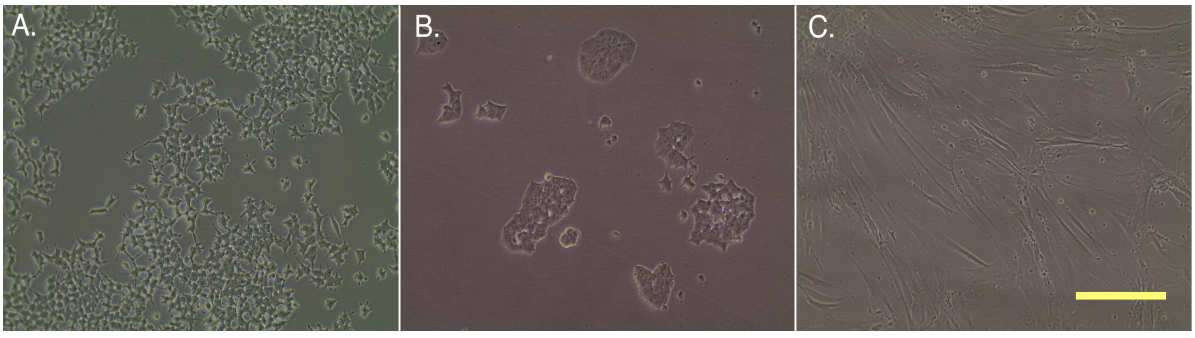


*Figure 2.1 : Microscopy images of cells utilised. Images taken at x20 magnification. A - BRIN-bd11 cells, B - TC6 Cells, C - Mesenchymal Stem Cells (MSCs) Scale bar =200μm.*

Brin-bd11 cells used in this thesis were a kind gift from Ulster university. The BRIN-bd11 cell line is a hybrid cell line produced via the electrofusion of a primary culture of NEDH rat pancreatic cells with RINm5F, which is a cell line derived from NEDH rat insulinoma cells.[221] They are stable, glucose-responsive insulin secreting cells expressing the GLUT2 transporter, and have applications in the study of pancreatic beta cell function.[221] These cells were utilised between passages (P) 38 to 67.

TC6 cells were ordered from ATCC as detailed in Section 2.1. The TC6 cell line is derived from insulinoma cells obtained from transgenic mice.[222] These mice carry the pseudogene construct composed of the SV40 early region controlled by the rat insulin II promoter gene.[222] They secrete insulin in response to glucose. These cells were utilised between passages (P) 7 to 20.

MSCs were obtained from bone marrow aspirate. 25 million bone marrow mononuclear cells were purchased from Lonza and cultured as detailed in Section 2.2.8. Cells were utilised between passages (P) 2 to 3 before cells were discarded.

## 2.2.3 Culturing of Cells

Cells were cultured in the cell culture lab at the Guy Hilton Research Centre, Stoke-on-Trent, UK. Cell culture methods were performed in laminar flow cabinets using aseptic techniques. Cells were incubated in a MCU-18AC-PE Incusafe $CO_2$ Incubator (Panasonic, Leicester, UK) at 37$^{o}$C with 5% $CO_2$ and 21% $O_2$.

## 2.2.4 Thawing Cells from Liquid Nitrogen

BRIN-bd11 and TC6 cells were thawed from liquid nitrogen before being used in cell culture. Cryovials containing the cells were removed from liquid nitrogen. The cryovials were heated in a 37$^{o}$C Grant JB Nova (Grant, Royston, UK) water bath to facilitate rapid defrosting of the cells. The defrosted cell suspension in each cryovial was added to a 15ml centrifuge tube containing 4ml of medium and mixed well. The cell suspension was centrifuged in a Heraeus$^{TM}$ Megafuge$^{TM}$ 8 Small Benchtop Centrifuge (Thermo Scientific , Osterode am Harz, Germany) at 900rpm for 5 minutes. The supernatant was decanted and the cell pellet re-suspended in 2ml of medium. 1ml of re-

suspended cell solution was added to labelled flasks containing growth medium.

T75 flasks were used to culture BRIN-bd11 cells. 15ml of RPMI growth medium as prepared in Section 2.2.1 was added to each T75 flask. T25 flasks were used to culture TC6 cells. 5ml of DMEM medium as prepared in Section 2.2.1 was added to each T25 flask.

### 2.2.5 Passaging of cells

BRIN-bd11 cells were passaged at 80-90% confluence. TC6 cells tend to form clusters much like islets and cells in the centre of these clusters will undergo necrosis if left too long due to the limited diffusion of nutrients to these cells. Therefore, TC6 cells were passaged at around 50-60% confluence. To passage cells 0.25% trypsin, PBS and growth medium were pre-heated in a 37$^{o}$C Grant JB Nova (Grant, Royston, UK) water bath. When the optimal confluence was reached, the growth medium was removed from the flasks and the flasks were washed with 4ml of PBS to remove excess medium. 2ml of 0.25% trypsin was added to each T75 flask and 0.7ml to each T25 flask. The trypsin-treated flasks were kept in a MCU-18AC-PE Incusafe $CO_2$ Incubator (Panasonic, Leicester,

UK) at 37$^{o}$C for 4-5 minutes to allow cells to detach from the flasks. After incubation, the cells were viewed under a Olympus CKX41 (Olympus, Tokyo, Japan) light microscope to visualise the detachment of the cells from the culture flasks. Care was taken not to agitate the flasks to avoid clumping of the cells. Cells were returned to the incubator if inadequate detachment was observed, and subsequently viewed again under the microscope. The process was repeated until all the cells had detached. When all the cells had detached, 4ml of medium was added to each flask to inactivate the trypsin. The medium was used to wash the flask several times, to maximise the number of cells retrieved. The suspension of cells was aspirated from the flasks and added to a 50ml centrifuge tube and centrifuged in a Heraeus$^{TM}$ Megafuge$^{TM}$ 8 Small Benchtop Centrifuge (Thermo Scientific , Osterode am Harz, Germany) at 900rpm for 5 minutes. On removal from the centrifuge the tube was inspected to ensure that a cell pellet was visible at the base of the centrifuge tube. The supernatant was decanted and the cell pellet resuspended in 5ml of growth medium. At this point the cells could be counted to be used in other experiments as detailed in Section 2.2.6. Growth medium was added to culture flasks and the desired number of cells added to each flask. The flasks were labelled with the passage number as well as the date the passage took

place and the cell type contained in the flask. Cells were incubated in a MCU-18AC-PE Incusafe $CO_2$ Incubator (Panasonic, Leicester, UK) at 37$^{o}$C with 5% $CO_2$ and 21% $O_2$. 100% media changes were carried out twice a week.

## 2.2.6 Performing Cell Counts

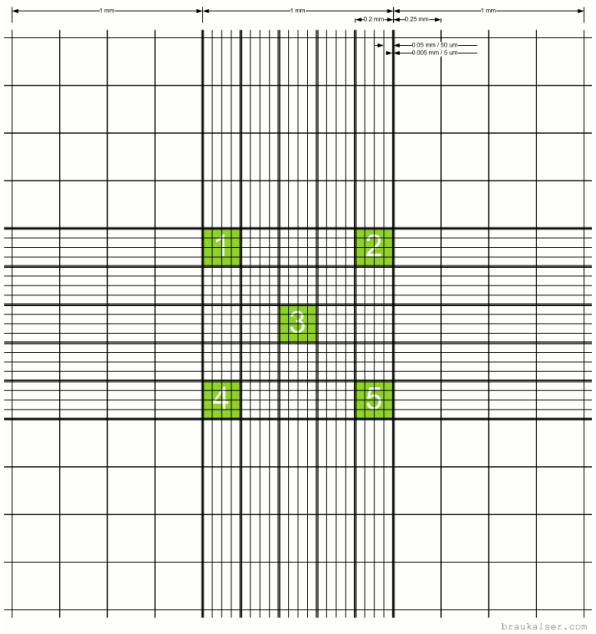


*Figure 2.2 : Depiction of haemocytometer grid. In each corner of the grid 16 small squares can be seen. Cells within these squares were counted. Four separate counts were obtained, one for each corner of the grid. The values were added together and divided by four to obtain the average cell count. (Image adapted from Braukaiser.com,2017)* [(223)]

Cell counts were performed manually using a Neubauer-improved with dark lines haemocytometer (Marienfield, Lauda-Konigshoen, Germany). After cells

were trypsinised and re-suspended in media as detailed in Section 2.2.5, 15 µL of cell suspension was added to the haemocytometer and the cells were visualised under an Olympus CKX41 (Olympus, Tokyo, Japan) light microscope and counted using a handheld counter (Figure 2.2).

The total number of cells was calculated using the following formula:

***Total cell count = average cell count x dilution factor x 10,000***

The method for obtaining the average cell count is described in Figure 2.2. The dilution factor is the number of millilitres of medium in which the cells were re-suspended.

## 2.2.7 Recovery and Expansion of MSCs

Bone marrow mononuclear cells were purchased from Lonza as a cryoamp of 25 million cells. T75 flasks were pre-treated with a sterile 10ng/ml solution of fibronectin in PBS and incubated in a MCU-18AC-PE Incusafe $CO_2$ Incubator (Panasonic, Leicester, UK) at 37$^{o}$C for an hour. After this period, the fibronectin solution was removed and 20ml of complete MSC medium added to each flask. The cells were thawed in accordance with the procedure

detailed in Section 2.2.4. The thawed mononuclear cells were seeded at a density of $10^5$ cells/$cm^2$ in the fibronectin pre-treated flasks. The cells were incubated in a MCU-18AC-PE Incusafe $CO_2$ Incubator (Panasonic, Leicester, UK) at 37°C with 5% $CO_2$ and 21% $O_2$. After one week, a 50% medium change was performed. After a further week, a 100% medium change was carried out. Subsequently 100% medium changes were carried out twice a week.

### 2.2.8 Isolation and Culture of MSCs

After three weeks in culture, MSCs were isolated from mononuclear cells. The medium was removed from the T75 flasks. The flasks were washed with 4ml of PBS. 2ml of 0.25% trypsin was added to each flask and the flasks were incubated in a MCU-18AC-PE Incusafe $CO_2$ Incubator (Panasonic, Leicester, UK) at 37°C. MSCs generally detach after 3-4 minutes of exposure to 10% trypsin, while other mononuclear cells take much longer (~10-15 minutes). This allows for the isolation of MSCs from other cells in culture. After 3-4 minutes of exposure to trypsin, 4ml of complete MSC medium was added to each flask to inactivate the trypsin. The resulting cell suspension was added to

a 15ml centrifuge tube and centrifuged in a Heraeus™ Megafuge™ 8 Small Benchtop Centrifuge (Thermo Scientific , Osterode am Harz, Germany) at 900rpm for 5 minutes. The supernatant was carefully pipetted away leaving around 2ml at the base of the tube. The remaining 2ml was then mixed well and added to a T75 flask containing 20ml of complete MSC medium. The cells were incubated MCU-18AC-PE Incusafe $CO_2$ Incubator (Panasonic, Leicester, UK) at 37$^{o}$C with 5% $CO_2$ and 21% $O_2$, and medium changes were carried out twice a week. The MSCs can be visualised as adherent fibroblastic (spindle shaped) cells as depicted in Figure 2.1.

### 2.2.9 Freezing Cells in Liquid Nitrogen

Superfluous cells were frozen in liquid nitrogen for future use. Cryopreservative was prepared consisting of 10% dimethyl sulfoxide (DMSO). 20% FBS and 70% culture medium. Cells in suspension to be cryopreserved were counted as described in Section 2.2.6. The cells were centrifuged at 900rpm in a Heraeus™ Megafuge™ 8 Small Benchtop Centrifuge (Thermo Scientific , Osterode am Harz, Germany)for 5 minutes and the supernatant decanted. Cryopreserving fluid was added and mixed well to obtain a

suspension of 1 million cells per ml. 1ml of cryopreservant cell suspension was added to each 2.5ml cryotube. The cryovials were stored in a Mr Frosty cryopreserving container (Thermo Scientific, Windsford , UK) in a MDF-U5386S-PE PRO ULT Upright Freezer (Panasonic, Leicester, UK) set at -80$^{o}$C overnight. The tubes were subsequently transferred into liquid nitrogen. This helps to slow the freezing process and inhibits ice from forming within cells, which could break the cell membranes and reduce cell viability.

## 2.2.10 Producing MSC-CM

MSCs were cultured and expanded as detailed in Section 2.2.7. MSCs were subsequently isolated from mononuclear/haematopoietic cells and cultured as detailed in Section 2.2.8. MSC-CM was produced using cells in early passages (P2-P3) before signs of cellular senescence were seen. (e.g. cellular enlargement, increase in cellular vacuoles/debris). [224] Senescent cells have been shown to mount a pro-inflammatory response by activation of a process known as the senescence-associated secretory phenotype (SASP). This involves a factor of 10-800 increase in the production of pro-inflammatory cytokines including IL-8, IL-6 and GM-CSF.[224,225] Senescent cells do not exert

immunomodulatory properties and could conversely exacerbate the immune response in immune mediated disease.[226] Senescence associated changes including changes in cellular morphology and differentation potential become increasingly more apparent after around passages 4-5. As a result, MSC-CM was collected from cells between passage 2 and 3.

When MSCs were between 70-80% confluence, the growth medium was removed and cells were washed with PBS. 15ml of RPMI medium was added to each T75 flask containing MSCs and cells were incubated MCU-18AC-PE Incusafe $CO_2$ Incubator (Panasonic, Leicester, UK) for 24 hours at 37$^{o}$C, 21% $O_2$, 5% $CO_2$. 70%-80% confluence corresponds to the density where the time taken for the MSC population to double is the shortest (i.e. the rate of proliferation is greatest at 70-80% confluence).[227] Theoretically this would correspond to the time when the cells are metabolically the most active and are secreting the greatest quantities of soluble factors into the medium being conditioned.

After 24 hours in culture, the conditioned medium was removed from the T75 flasks and growth medium replaced. The conditioned medium was

centrifuged in a Heraeus™ Megafuge™ 8 Small Benchtop Centrifuge (Thermo Scientific , Osterode am Harz, Germany) and sterile filtered to remove debris. The conditioned medium was subsequently aliquotted into 5ml bijou tubes and stored in a MDF-U5386S-PE PRO ULT Upright Freezer (Panasonic, Leicester, UK) set at -80°C until needed for experimentation.

Multiple freeze/thaw cycles of conditioned medium were avoided as this could potentially damage proteins/exomes in the samples. Conditioned medium was collected from passages 2 and 3 and cells were subsequently discarded.

# 2.3 In Vitro Methodologies

All *in vitro* experiments were conducted at the Guy Hilton Research Center, Stoke on Trent, UK.

## 2.3.1 Trilineage Differentiation of MSCs

Preparation of Differentiation Medium

To induce adipogenic differentiation, cells were cultured in adipogenic medium. Complete MSC growth medium was used consisting of DMEM with 1g/L glucose, supplemented with 1% NEAA, 1% L-glut and 10% FBS. This was supplemented with 0.5µM dexamethasone, 0.5mM IBMX , 10ug/ml insulin and 100µM indomethacin.

To induce osteogenic differentiation, cells were cultured in osteogenic medium. Complete MSC growth medium was used consisting of DMEM with 1g/L glucose, supplemented with 1% NEAA, 1% L-glut and 10% FBS. This was supplemented with 50µM ascorbic acid , 10mM β-glycerophosphate and 0.1µM dexamethosone.

To induce chondrogenic differentiation, cells were cultured in chondrogenic medium. MSC growth medium was used consisting of DMEM with 1g/l glucose supplemented with 1% NEAA, 1% L-glut and 1% FBS. This was supplemented with 1% v/v ITS , 0.1µM dexamethosone, 50µM ascorbic acid, 40µg/ml L-proline, 1% v/v sodium pyruvate and 10ng/ml TGF-B3.

Preparation of Stains

Stock solution of Oil Red O was prepared by mixing 300mg of Oil Red O powder with 100ml of 99% isopropanol.

Working solution Oil Red O only remains stable for approximately 2 hours, so should be prepared immediately before staining. In a fume hood, 3 parts stock solution of Oil Red O were mixed with 2 parts water. The addition of water results in precipitates forming in solution. The solution was passed through a 20µl syringe filter to remove precipitates that would affect image quality.

A solution of Alizarin Red was prepared by dissolving 2g Alizarin Red powder in 100ml distilled water. The solution was sterile filtered before use.

A solution of Alcain Blue was prepared by mixing 1g Alcain Blue powder with a 3% solution of acetic acid. PH should be adjusted to 2.5 with acetic acid. The solution was sterile filtered before use.

Seeding of MSCs

To prepare a monoloyer for staining, cells were trypsonised and re-suspended in medium and counted. 30,000 cells were seeded per well in a 24 well plate. Two wells were seeded for each of adipogenic, chondrogenic and osteogenic differentiation, with two additional wells seeded for each type of differentiation as negative controls.

To prepare a micromass for staining, cells were trypsonised and re-suspended in medium and counted. Cells were centrifuged in a Heraeus™ Megafuge™ 8 Small Benchtop Centrifuge (Thermo Scientific , Osterode am Harz, Germany) and supernatant decanted. 32μL of medium was added and mixed well. 8μL of cells was applied as a drop to the center of each of four wells in a 24 well plate. Medium was added after the cells attached.

Culturing of MSCs for Differentiation

MSCs were incubated in a MCU-18AC-PE Incusafe $CO_2$ Incubator (Panasonic, Leicester, UK) at 37$^{o}$C with 21% $O_2$ and 5% $CO_2$. After three days, Complete MSC growth medium was replaced with differentiation medium for the wells undergoing differentiation. Complete MSC growth medium was added to the negative controls. The medium was subsequently changed every two days.

Fixing of MSCs

Following 3 weeks in culture the medium was removed and cells were washed with 2ml PBS, taking care not to disturb the monolayer. Cells were subsequently fixed by the addition of 4% paraformaldehyde for 15 minutes. Cells were washed again in PBS.

Staining of Cells

To stain adipogenic MSCs, 1ml of isopropanol was added to each well and left for 2 minutes. Isopropanol was aspirated and 1ml of working solution of Oil Red O added and allowed to stand for 5 minutes. Wells were subsequently washed with PBS until the PBS remained clear.

To stain chondrogenic MSCs, 1ml of Alcain Blue was added to each well. The stain was left overnight at room temperature. Before viewing, cells were washed with PBS until the PBS remained clear.

To stain osteogenic MSCs, 1ml of Alizarin Red was added to each well and left for 15 minutes. Before viewing, cells were washed with PBS until the PBS remained clear.

Staining was viewed with a EVOS$^{TM}$ XL Core Imaging System (Thermo Scientific, Windsford, UK).

### 2.3.2 MTT Assay Optimisation Experiment

Preparation of Media/Reagents.

Cells were treated with four different types of media in this experiment: MSC-CM, RPMI, MSC-CMS (MSC-CM with serum) and RPMIS (RPMI with serum).

MSC-CM was produced as detailed in Section 2.2.10. 5% FBS was added to RPMI and MSC-CM media to produce PRMIS and MSC-CMS respectively.

To prepare a stock solution of MTT reagent, MTT reagent (Sigma-Aldrich) was dissolved in PBS to a concentration of 5mg/ml. MTT stock solution should be stored in the dark as the reagent is photosensitive.

To prepare a working solution of MTT, Stock MTT solution was dissolved in plain RPMI (1:10).

To prepare solvent for formazan crystals, equal parts of DMSO and isopropanol were mixed.

Seeding Cells

Cells were trypsonised and re-suspended in medium as detailed in Section 2.2.5. The cells were counted as detailed in Section 2.2.6. 40,000 BRIN-bd11 cells were seeded per well in 96 well plates. Over-confluent cells can affect metabolism and disrupt the linear relationship between absorbance and cell number, thus cells should be seeded at an optimum density.[228] 40,000 cells per well was the seeding density deemed to reach ~80% confluence after 24 hours' incubation which was standardised across experiments to avoid overconfluence. In each of three 96 well plates, 9 wells were seeded for

treatment with each type of medium respectively. Cells were incubated for 24 hours in a MCU-18AC-PE Incusafe $CO_2$ Incubator (Panasonic, Leicester, UK)at 37$^{o}$C, 21% $O_2$, 5% $CO_2$.

Treating Cells with Prepared Media

Growth medium was removed from the cells and cells were washed twice with PBS. To each of three 96 well plates, 200μl of each of the four types of media was added to 9 wells seeded with cells respectively. Medium that had been conditioned by MSCs (MSC-CM/MSC-CM+serum) were used as positive controls. Cells were incubated for 24 hours in a MCU-18AC-PE Incusafe $CO_2$ Incubator (Panasonic, Leicester, UK) at 37$^{o}$C, 21% $O_2$, 5% $CO_2$.

Treating Cells with MTT Reagent

Medium was removed from the cells and cells were washed twice with PBS. 220μl of working MTT solution was added to each well containing cells. Culture conditions can affect the ability of cells to reduce MTT reagents to formazan. Presence of compounds such as ascorbic acid and coenzyme A can interfere with the MTT assay, mandating the need for media and cell-free controls for each experiment.[228,229] Thus, 220μl of working MTT solution was added to 9 cell-free wells in each 96 well plate to act as cell-free negative

controls. Addition of MTT reagent to each 96 well plate was staggered at 1 hour intervals to allow for the first plate of cells treated to be exposed to MTT for 3 hours, the second plate to be exposed for 2 hours and the final plate to be exposed to MTT reagent for 1 hour.

Dissolving Formazan Crystals

Plates were centrifuged for 1 minute at 1,000 rpm. 195μl of MTT reagent was removed from each well and 100μl of formazan solvent was added to each well. The plates were incubated for 45 minutes in a MCU-18AC-PE Incusafe $CO_2$ Incubator (Panasonic, Leicester, UK) at 37$^{o}$C, 21% $O_2$, 5% $CO_2$.

Reading Absorbance

Wells were pipetted to ensure formazan crystals were uniformly dissolved. Bubbles in wells can affect absorbance and were removed before plates were read. Plates were read at 570nm absorbance using a Synergy 2 Multi-Mode Reader (Bio-Tek, Swindon, UK).

Data Analysis

To determine the relationship between MTT incubation time and absorbance readings, we fitted exponential curves to the data in Figure 3.10 and determined that the relationship between absorbance and length of time in MTT is exponential in nature. Nine replicate samples from one experiment were used for each data point. Data is expressed as mean +/- standard deviation. Differences between experimental groups were evaluated using unpaired T-tests assuming unequal variance. A p value of $<0.05$ was deemed to be significant. All data points were compared to the negative (0 hour in MTT) control.

To determine the effect of conditioned media on BRIN-bd11 cells, viability readings for MSC-conditioned medium treated cells were normalised to their respective non-conditioned media controls for comparison. Nine replicate samples from one experiment were used for each data point. Data is expressed as mean +/- standard deviation. Differences between experimental groups were evaluated using unpaired T-tests assuming unequal variance. A p value of $<0.05$ was deemed to be significant.

## 2.3.3 Cytokine-Induced Apoptosis MTT Assays

Preparation of Reagents

*1) Stock Solution of Cytokines*

Vials of cytokines (TNFα, IFNγ and IL-1β ) were centrifuged in a MicroCL 17 Microcentrifuge (Thermo Scientific, Windsford, UK) and reconstituted in sterile distilled water to 0.1mg/ml. Resulting stock solutions of cytokines were aliquotted and stored in a Bosch Clasixx (Boshh, Liverpool, UK) -30$^{o}$C freezer until needed for experimentation.

*2) Working Solution of Cytokines*

Serial dilutions of each cytokine were made in RPMI media from 1,000ng/ml to 0.1ng/ml. A cytomix of all three cytokines in equal parts in RPMI was also prepared to a total concentration of 1,000ng/ml and serial dilutions subsequently made from 1,000ng/ml to 0.1ng/ml. For cells treated with MSC-CM, a working solution of 1,000ng/ml was prepared for each cytokine as well as a cytomix of all three cytokines in equal parts for a final total concentration of 1,000ng/ml.

*3) MTT Reagent and Formazan Diluent.*

MTT reagents and formazan diluent were prepared as detailed in Section 2.3.2.

Seeding Cells

Cells were seeded in a 96 well plate. 40,000 cells were seeded per well for BRIN-bd11 cells and 60,000 per well for TC6 cells. These seeding densities resulted in 80% confluence after 24 hours' incubation for each cell line respectively. This is to prevent over-confluence as described in Section 2.3.2. Nine wells were seeded for treatment with each concentration of cytokine respectively. Nine further wells were seeded as untreated control cells. Cells were incubated in a MCU-18AC-PE Incusafe $CO_2$ Incubator (Panasonic, Leicester, UK) for 24 hours at 37$^{o}$C, 21% $O_2$, 5% $CO_2$.

Treatment with Pro-inflammatory Cytokines

Medium was removed from the cells and cells were washed twice with PBS. 200μl of media+cytokines was added in to each of 9 wells containing cells for

each concentration of cytokines respectively. This is to account for variability between medias used as described in Section 2.3.2. Cells were incubated in a MCU-18AC-PE Incusafe $CO_2$ Incubator (Panasonic, Leicester, UK) for 24 hours at 37$^{o}$C, 21% $O_2$, 5% $CO_2$.

Treating Cells with MTT Reagent

Medium was removed from the cells and cells were washed twice with PBS. 220μl of working MTT solution was added to each well containing cells. In addition, 220μl of working MTT solution was added to 9 cell-free wells to act as cell-free negative controls. MTT treated cells were incubated in a MCU-18AC-PE Incusafe $CO_2$ Incubator (Panasonic, Leicester, UK) for 3 hours at 37$^{o}$C, 21% $O_2$, 5% $CO_2$.

Dissolving Formazan Crystals

Plates were centrifuged for 1 minute at 1,000 rpm. 195μl of MTT reagent was removed from each well and 100μl of formazan solvent was added to each well. The plates were incubated for 45 minutes in a MCU-18AC-PE Incusafe $CO_2$ Incubator (Panasonic, Leicester, UK at 37$^{o}$C, 21% $O_2$, 5% $CO_2$.

Reading Absorbance

Wells were pipetted to ensure formazan crystals were uniformly dissolved. Bubbles in wells can affect absorbance and were removed before plates were read. Plates were read at 570nm absorbance using a Synergy 2 Multi-Mode Reader (Bio-Tek, Swindon, UK)

Data Analysis

Nine replicate samples from one experiment were used for each data point. Data is expressed as mean +/- standard deviation. Differences between experimental groups were evaluated using unpaired T-tests assuming unequal variance. A p value of $<0.05$ was deemed to be significant. Viability readings are normalised to their respective untreated cell controls.

### 2.3.4 IL-10 Serial ELISAs

Preparation of Materials

The Human IL-10 Mini ELISA Development Kit was utilised for this experiment. Reagents were centrifuged before being reconstituted in distilled water.

Capture antibody was reconstituted to a concentration of 100μg/ml, detection antibody to a concentration of 100μg/ml and human IL-10 standard to a concentration of 1μg/ml. Reagents were aliquotted and stored at -30$^{o}$C until required for experimentation. Avidin-HRP conjugate was aliquotted into two 9μL vials prior to storage in a Bosch Clasixx (Bosch, Liverpool, UK) -30$^{o}$C freezer.

Wash buffer consisted of 0.05% tween in PBS. Block buffer consisted of 1% BSA in PBS. Diluent consisted of 0.05% tween and 0.1% BSA in PBS. Block buffer and diluent were sterile filtered and stored at 4$^{o}$C prior to use.

Plate Preparation

Capture antibody was diluted to a concentration of 1μg/ml in PBS. 100μL of diluted capture antibody was added to each ELISA plate well. Three ELISA plates were prepared (Plate1-Plate3). The plates were sealed and incubated for 24 hours at room temperature.

Serial ELISA Protocol

A stepwise protocol was designed to allow all three ELISA plates to run in tandem. This is detailed below:

**Step 1**: After 24 hours' incubation with capture antibody, the wells of Plate 1 were aspirated and washed four times using 300μL of wash buffer per well. After the final wash, the plate was blotted dry using a paper towel. 300μL of block buffer was added to each well and the plates were sealed and left to incubate for 1 hour.

**Step 2**: Serial dilutions of standard were made from 5ng/ml to 0ng/ml. 100μL of each concentration of standard was added to each well in the first ELISA plate in duplicate. 100μL of MSC-CM was added to eight of the wells. The plates were sealed and left to incubate at room temperature for two hours.

**Step 3**: An hour after completion of Step 2, Plate 2 was washed four times with wash buffer. After the final wash, the plate was blotted dry using a paper towel. 300μL of block buffer was added to each well and the plate was left to incubate for 1 hour.

**Step 4**: An hour after completion of Step 3, The wells of Plate 2 were aspirated and washed four times with wash buffer. A new batch of serial dilutions of standard was made from 5ng/ml to 0ng/ml. 100μL of each concentration of standard was added to each well in the second ELISA plate in duplicate. At this stage, the wells of Plate 1 were aspirated and MSC-CM was transferred from Plate 1 to Plate 2. Plate 2 was sealed and left to incubate for 2 hours. Plate 1 was washed four times with wash buffer. Detection antibody was diluted to a concentration of 0.5μg/ml and 100μL was added to each well. Plate 1 was sealed and incubated at room temperature for 2 hours.

**Step 5**: An hour after completion of Step 4, Plate 3 was aspirated and washed four times with wash buffer. After the final wash, the plate was blotted dry using a paper towel. 300μL of block buffer was added to each well and the plate was left to incubate for 1 hour.

**Step 6**: An hour after completion of Step 5, The wells of Plate 3 were aspirated and washed four times with wash buffer. A new batch of serial dilutions of standard was made from 5ng/ml to 0ng/ml. 100μL of each concentration of

standard was added to each well in the second ELISA plate in duplicate. At this stage the wells of Plate 2 were aspirated and MSC-CM was transferred from Plate 2 to Plate 3. Plate 3 was sealed and left to incubate for 2 hours. Plate 2 was washed four times with wash buffer. Detection antibody was diluted to a concentration of 0.5μg/ml and 100μL was added to each well. Plate 2 was sealed and incubated at room temperature for 2 hours. Plate 1 was washed four times. Avidin was diluted in diluent (1:2,000). 100μL of diluted Avidin was added to each well. Plate 1 was sealed and left to incubate at room temperature for 30 minutes.

**Step 7**: 30 minutes after completion of Step 6, Plate 1 was aspirated and washed four times with wash buffer. 100μL of ABTS substrate was added to each well. Plate 1 was read in a Synergy 2 Multi-Mode Reader (Bio-Tek, Swindon, UK) (absorbance 405nm) at 15 minute intervals for 1 hour.

**Step 8**: 90 minutes after completion of Step 6, Plate 3 was washed four times with wash buffer. Detection antibody was diluted to a concentration of 0.5μg/ml and 100μL was added to each well. Plate 3 was sealed and incubated at room temperature for 2 hours. Plate 2 was washed four times Avidin was

diluted in diluent (1:2,000). 100μL of diluted Avidin was added to each well. Plate 1 was sealed and left to incubate at room temperature for 30 minutes.

**Step 9**: 30 minutes after completion of Step 8, Plate 2 was aspirated and washed four times with wash buffer. 100μL of ABTS substrate was added to each well. Plate 2 was read in a Synergy 2 Multi-Mode Reader (Bio-Tek, Swindon, UK) (absorbance 405nm) at 15 minute intervals for 1 hour.

**Step 10:** 90 minutes after completion of Step 8, Plate 3 was washed four times. Avidin was diluted in diluent (1:2,000). 100μL of diluted Avidin was added to each well. Plate 1 was sealed and left to incubate at room temperature for 30 minutes.

**Step 11**: 30 minutes after completion of Step 10, Plate 3 was aspirated and washed four times with wash buffer. 100μL of ABTS substrate was added to each well. Plate 3 was read in a Synergy 2 Multi-Mode Reader (Bio-Tek, Swindon, UK) (absorbance 405nm) at 15 minute intervals for 1 hour.

Data Analysis

Concentrations of cytokines in each well were determined by comparing raw absorbance data to standard curves of IL-10 of known concentration. The standard curves used are depicted in Figure 2.3.

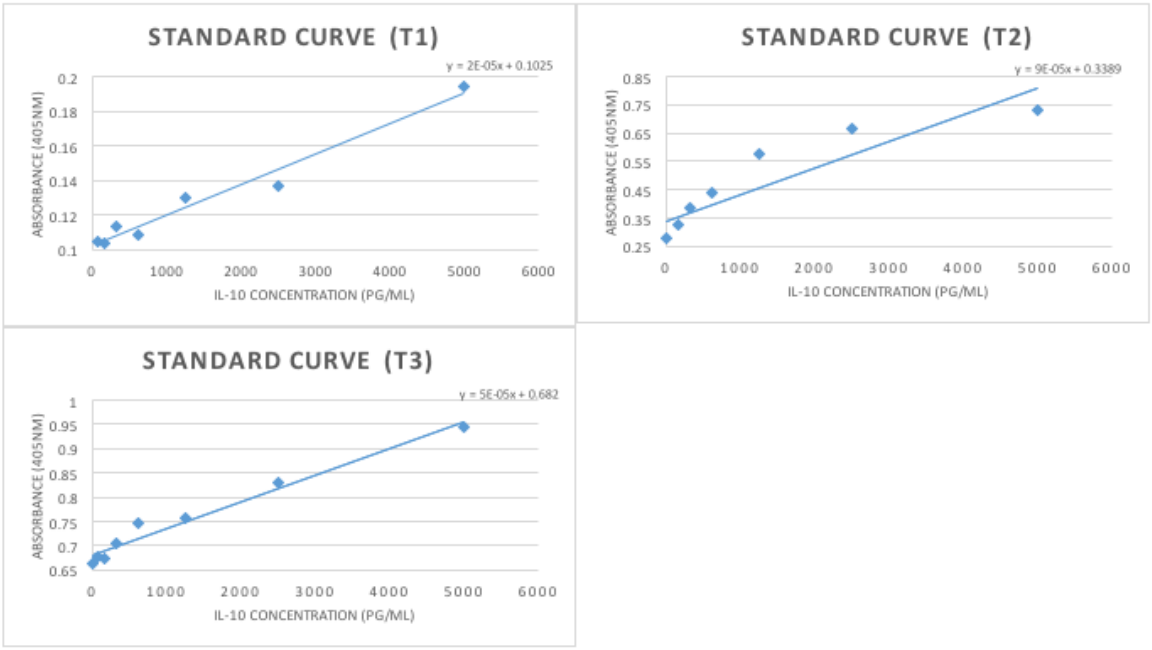


*Figure 2.3 : Standard curves for Plate 1 (T1), Plate 2 (T2) and Plate 3 (T3). Graphs show absorbance over IL-10 concentration.*

Eight replicate samples from one experiment were used for each data point. Data is expressed as mean +/- standard deviation. Differences in concentrations of IL-10 between transfers were evaluated using two-tailed unpaired T-tests assuming unequal variance. A p value of <0.05 was deemed

to be significant. A linear trend line was fitted to the graph to determine the gradient of depletion of IL-10.

### 2.3.5 RNA Extraction

Cells were trypsinised and resuspended in medium as detailed in Section 2.2.5 and the cells were counted as detailed in Section 2.2.6. 100,000 cells were seeded into three wells in a 24 well plate and the cells were incubated in a MCU-18AC-PE Incusafe $CO_2$ Incubator (Panasonic, Leicester, UK)for 24 hours at 37$^{o}$C with 5% $CO_2$ and 21% $O_2$.

The RNeasy Mini Kit was utilised for RNA extraction. Medium from the wells was aspirated and the cells were washed with PBS. PBS was removed and 700µL of lysis buffer added to the wells. The cells were left to lyse for 10 minutes. Complete lysis of the cells was visualised using a Olympus CKX41 (Olympus, Tokyo, Japan) light microscope. 300µL of ethanol was added to each well and mixed well. 700µL of lysate was added to extraction tubes with a filter membrane and centrifuged at 11.0g for 15 seconds. The Eppendorf® Minispin® microcentrifuge (Eppendorf, Stevenage, UK) was used throughout RNA extraction. The filtrate was discarded. This was repeated until all the

lysate had been processed. 700µL of RW1 buffer was added to the extraction tube and centrifuged at 11.0g for 15 seconds. The filtrate was discarded. 500µL of RPE buffer was added to the extraction tube and it was centrifuged at 11.0g for 15 seconds. The filtrate was discarded. 500µL of RPE buffer was added to the tube again and centrifuged at 11.0g for 2 minutes. The filtrate was discarded. The membrane in the extraction tube was transferred to a new sterile extraction tube for membrane drying and centrifuged at 11.0g for 1 minute. The filtrate was discarded. The membrane was transferred to a new sterile cap vial. 30µL RNase-free water was added and the cap vial was centrifuged at 11.0g for 1 minute. The sample within the cap vial was kept for analysis of RNA content and stored in a MDF-U5386S-PE PRO ULT Upright Freezer (Panasonic, Leicester, UK) set at -80$^{o}$C.

### 2.3.6 RNA Analysis

The concentration of RNA within the sample was analysed using a Nanodrop 2000 Spectrophometer (Thermo Scientific, Windsford, UK). The machine was calibrated using 1µL of RNase-free water. 1µL of sample was subsequently added and read to obtain the RNA concentration in the sample.

For electrophoresis, an RNA concentration of 25ng/µL was used. The following formula was used to calculate the dilution factor:

$$N1V1 = N2V2$$

$$V1 = (25 \times 25)/N1$$

(where N1 is the sample concentration, V1 is the required volume of the sample, N2 is the desired concentration (i.e. 25ng/µL) and V2 the desired volume (i.e. 25 µL))

The volume obtained (V1) was made up to 25µL using Rnase-free water to obtain the desired RNA concentration of 25ng/µL.

### 2.3.7 Reverse Transcriptase Polymerase Chain Reaction (RT-PCR)

Reverse transcriptase polymerase chain reaction was carried out using the SuperScript™ III One-Step RT-PCR System with Platinum® Taq High Fidelity Kit (Invitrogen).

Sterile techniques were used throughout the experiment. RNaseZAP (Thermo Fisher Scientific) was used to clean the workbench to avoid RNA contamination. Pipettes and cap vials were sterilised under ultraviolet light for two minutes before use in the experiment.

The kit was thawed and reagents kept cold on ice during the experiment. A master mix was prepared consisting of 6.25µL of 2x reaction mix, 4.5µL of RNase-free water, 0.25µL of Taq (enzyme) and 0.25µL of desired forward and reverse primer for each sample. 1µL of RNA from the desired cell type (25ng/µL) was added to samples as detailed in Figure 2.4.

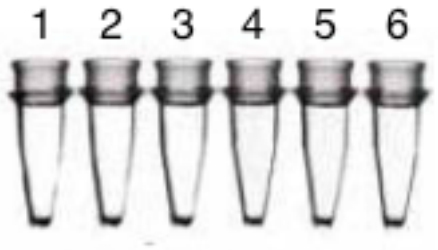


*Figure 2.4 : RT-PCR micro-ampule setup: 1 - 13 IL10RA primer mix + 1 RNA; 2 - 13 IL10RA primer mix (negative control); 3 - 13 IL10RB primer mix + 1 RNA; 4 - 13 IL10RB primer mix (negative control); 5 - GAPDH primer mix + 1 BRIN-bd11 RN; 6 - GAPDH primer mix (negative control). (Image adapted from Thermo Fisher Scientific, 2017)* [(230)]

Primer mixes without the addition of RNA were used as negative controls to determine whether any RNA contamination had affected the results. Bands appearing after electrophoresis of these negative controls would indicate RNA contamination.

GAPDH is an enzyme expressed in all cell types, and was used as a positive control in the experiments. It acts as a standard that should work regardless of the IL-10 receptor expression profile of the cells. A negative IL-10 receptor result with a positive GAPDH result indicates lack of expression of IL-10 receptors. However, if the GAPDH result is also faulty, issues with the experiment or RNA samples are likely.

After addition of RNA the microamp tubes were sealed and placed in a Stratagene MX3005P thermocycler set to the specifications detailed in Table 2.1.

| Step | Temperature ($^{o}$C) | Time | Number of cycles |
|---|---|---|---|
| Conversion to cDNA | 50 | 30 mins | 1 |
| Initial denaturation | 94 | 2 mins | 1 |
| Denaturation | 94 | 15 sec | 40 |
| Primer annealing | 55 | 30 sec | |
| Primer extension | 68 | 1 min | |
| Final extension | 15 | □ | - |

*Table 2.1 : Settings used for RT-PCR thermocycler.*

### 2.3.8 Primer Design

New IL10RA and IL10RB primers were designed using the NCBI gene database. The target gene and desired gene template were located in the database. The NCBI reference sequence for the target gene's mRNA was found and the NCBI primer design tool was used to design primers specific to the target mRNA sequence. The forward and reverse primer sequences were obtained for the desired base pair length of the RT-PCR product.

Custom DNA oligos were ordered from Thermo Fisher Scientific. Primers used for RT-PCR in individual experiments are detailed in Chapter 5.

## 2.3.9 Electrophoresis

Preparing the Gel Mould

A gel mould was prepared by taping the edges well to ensure a good seal to avoid leakage of the agarose solution before it had set. A 20 well comb was used to form wells in the agarose gel.

Preparation of Agarose Gel

A solution of 2% TAE and 2% agarose gel powder in 200ml of distilled water was prepared. The solution was heated in the microwave until all the agarose powder had dissolved and a clear agarose solution had been obtained. 5µL of ethidium bromide was added to the agarose solution in a fume cupboard, as ethidium bromide is a carcinogen. The solution was mixed well and poured gently into the prepared gel mould to avoid generating bubbles in the gel. The gel was left to set for 40 minutes before it was ready for use.

Loading the Gel

Once the gel had set, the tape and comb were removed and the gel was placed in the electrophoresis buffer. On completion of RT-PCR, 4µL of Blue Juice gel loading buffer (10x) (Invitrogen) was added to each microamp tube and mixed well. 10µL of the mixture from each microamp tube was subsequently added to its respective well in the agarose gel. For determination of base pair length of the PCR product, 10µL of direct load wide range DNA marker (Sigma, UK) was added to two wells in each experiment for comparison.

The gel electrophoresis machine was manually set to run at 100 volts for one hour. Upon completion, the gel was removed from the mould and imaged in an ultraviolet transilluminator using Syngene gel documenting system (Cambridge, UK).

## 2.3.10 IL-10 Receptor Immunofluorescence

Conjugated primary antibodies were ordered from Bioss Antibodies for use in the electrophoresis experiments. The antibodies used are detailed in Table 2.2.

| Product | Catalogue number | conjugate | Host | Target Protein | Isotype | Excitation/Emission |
|---|---|---|---|---|---|---|
| IL10RB Polyclonal Antibody | bs-2602R-FITC | FITC | Rabbit | IL10RB | IgG | 494nm/518nm |
| IL10RA Polyclonal antibody | bs-2459R-A555 | Alexa Flour 555 | Rabbit | IL10RA | IgG | 553nm/568nm |
| Rabbit IgG isotype control | bs-0295P-FITC | FITC | Rabbit | - | IgG | 494nm/518nm |
| Rabbit IgG isotype control | bs-0209P-A555 | Alexa Flour 555 | Rabbit | - | IgG | 553nm/568nm |

*Table 2.2 : Antibodies used in the immunofluorescence experiments*

Immunofluorescence Controls

In this experiment isotype controls were used to confirm whether fluorescence is due to specific binding of antibodies. Isotype controls are antibodies that are not specific to any proteins in the tissue sample, thus any staining seen with these antibodies would be the result of non-specific binding

of the antibodies to the sample (background staining).[231] Apart from differences in specificity to the antigen of interest, the isotype controls are otherwise identical to their respective antigen-specific antibodies[231] as detailed in Table 2.2. This allows comparison between the stains to be made.

In addition to this, autofluorescence of cells could result in false positives. Autofluorescence is the natural emission of light from biological structures such as mitochondria and lysosomes when they absorb light from the fluorescence microscope.[232] To determine if autofluorescence is affecting the results, negative controls using only DAPI nuclear staining without fluorescent tagged antibodies were used for comparison.

Preparing Cells

Cells were trypsonised and re-suspended in medium as detailed in Section 2.2.5. The cells were counted as detailed in Section 2.2.6. 50,000 cells were seeded per well in a 96 well plate. Two wells were seeded for staining with the IL10RB polyclonal antibodies, IL10RA polyclonal antibodies, FITC isotype control, Alexa Fluor® isotype control and DAPI control respectively. The cells

were incubated overnight in a MCU-18AC-PE Incusafe $CO_2$ Incubator (Panasonic, Leicester, UK) at 37$^{o}$C with 5% $CO_2$ and 21% $O_2$.

Fixation

Medium was removed from cells and cells were washed twice with PBS. 200μL of 4% paraformaldehyde was added to each well and allowed to incubate for 15 minutes at room temperature. The wells were subsequently washed twice with PBS.

Blocking

200μL of 2% BSA was added to each well and the plate was sealed and allowed to incubate for 1 hour. BSA binds to non-specific epitopes and reduces non-specific staining of the sample. In theory, BSA should compete equally with antibodies for binding to epitopes to which the antibodies are not specific. However, antibodies should preferentially bind to epitopes to which the antigen binding site is specific, thus non-specific antibody binding is reduced.

Staining

Antibodies were diluted in PBS to a ratio of 1:67 antibodies to PBS. 100μL of diluted antibody was added to each well and cells were incubated in the dark at 4°C overnight. Exposure to light was minimised during staining due to the potential for photobleaching of the stain.

Counterstaining

Antibody solution was removed and cells were washed twice with 0.05% tween in PBS (5 minute washes) to remove any residual stain. 100μL of 1:1,000 DAPI solution was added to each well for counterstaining of the nuclei and left for 10 minutes. DAPI solution was removed and cells were washed three times with 0.05% tween in PBS (5 minutes washes) to remove any residual stain. PBS was added to each well and cells were viewed under a Eclipse Ti-S (Nikon®, Miyagi, Japan) fluorescence microscope.

Image Capture and Data Analysis

Image capture was performed using an eclipse Ti-S (Nikon®, Miyagi, Japan) immunofluorescence microscope and NIS Elements 3.2 image capture

software (Nikon®, Miyagi, Japan). Images were captured at 20X and 40X magnification. The TRITC filter on the microscope was used for detection of staining with IL10RA polyclonal antibody (A555 conjugate) and rabbit IgG isotype control (A555 conjugate). The FITC filter was used for detection of staining with IL10RB polyclonal antibody (FITC conjugate) and rabbit IgG isotype control (FITC conjugate). The DAPI filter was used for detection of DAPI nuclear stain.

Acquisition parameters between isotype controls and their corresponding antigen-specific antibodies were kept consistent to allow for effective comparison between fluorescence of the isotype controls and the positive stains. IL10RA polyclonal antibody (A555 conjugate) and rabbit IgG isotype control (A555 conjugate) were captured with 1 second exposure and 4.00X gain. Images for IL10RB polyclonal antibody (FITC conjugate) and rabbit IgG isotype control (FITC conjugate) were captured with 3 second exposure and 2X gain. DAPI stain was consistently captured with exposure set at 0.1 seconds with 2X gain. These were determined to be the optimum parameters to obtain acceptable images in the positive samples without saturation of pixels in the image (Figure 2.5).

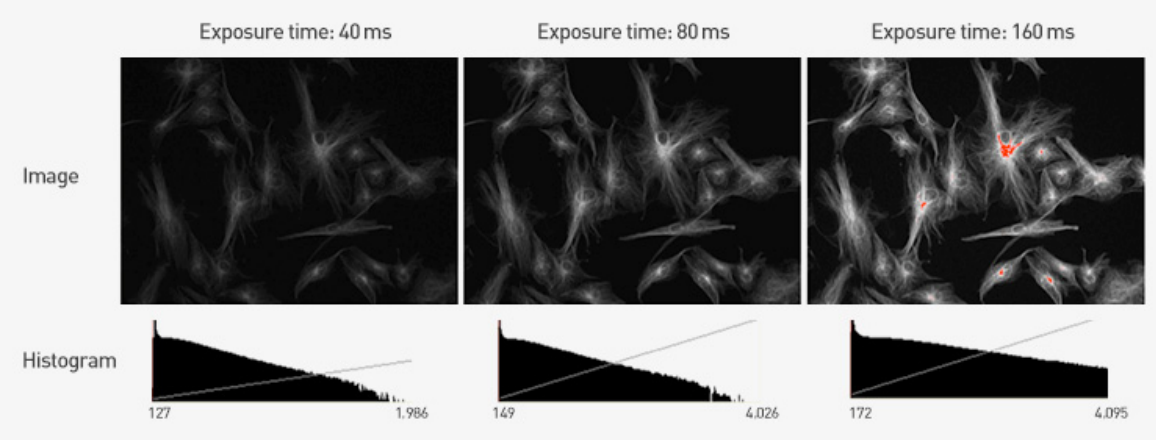


*Figure 2.5 : Depiction demonstrating optimal exposure for immunofluorescence imaging. Acquisition parameters should be optimised for each stain to ensure images are not underexposed as seen with an exposure time of 60ms or overexposed as depicted with an exposure time of 160ms where saturation of pixels can be seen. (Image adapted from Thermo Fisher Scientific, 2017)* [(233)]

For a qualitative comparison of the images of the positive stain to the isotype control, The LUTS settings of the isotype were adjusted to the threshold where staining is no longer visible. These settings were subsequently applied to the corresponding images of the antigen-specific antibodies to allow for a comparison between the two stains. This process subtracts the stain seen in the isotype control from that of the antigen-specific antibody. Thus any visible stain in the positive results after adjustments are made should in theory be that of staining specific to the antigen of interest.

To quantitatively measure[(c)] the difference between the positive stain and the isotype control, ImageJ image analysis software was used to quantify the intensity of staining in the images. Quantitative measurements are only necessary if a comparison between levels of protein expression between cells is needed. This could be to test changes in protein expression after cells are exposed to different experimental conditions or treatments. Characterising the presence of a protein like the IL-10 receptor in the case of this experiment only requires a qualitative analysis. However, providing additional quantitative data demonstrating the difference in isotype control and positive staining does improve the robustness of the results.

Images of fields taken at both x20 and x40 magnifications were used for comparison. Multiple intensity readings from at least 4 areas of measurement taken at random from each field were used for each data point. To obtain intensity data specific to antibody staining, background intensity readings were subtracted from intensity readings of stained cells in the image. Values are expressed as mean +/- standard deviation. Two-tailed unpaired T-tests assuming unequal variance were used to determine the significance of the difference between the positive images and their corresponding isotype controls. Significance was determined as $p<0.05$.

## 2.4 In Vivo Methodologies

Animal experiments described in this section were conducted as a collaboration with Dr Catriona Kelly in Ulster University. All *in vivo* experiments were conducted at the Biomedical Sciences Research Institute at Ulster University. Islet histology was sent to the Guy Hilton Research Center, Stoke on Trent, UK for analysis.

**Ethical statement**: All *in vivo* experiments were performed according to *The Principles of Laboratory Animal Care* (NIH publication no. 86-23, revised 1985) and UK Home Office Regulations (UK Animals Scientific Procedures Act 1986). The experiments were approved by Ulster University Animal Ethics Review Committee. All necessary steps were taken to avoid animal suffering during the experiment. The *in vivo* experiments were conducted under project licence PPL 2804- Hormonal and metabolic studies.

## 2.4.1 Animal Husbandry

Induction of Mouse T1D Model

Male C57BL/6 mice were used for all experiments, which commenced when the animals were 12 weeks old. C57BL/6 mice were used for the purposes of the experiment as they have been described as relatively sensitive to the induction of diabetes via STZ.[234] The gender of mice was also considered in the method. Female mice are known to be more resistant to the effects of STZ, potentially due to the protective effect of oestrogen on the pancreatic beta cells.[234] Administration of STZ to male mice tends to result in a more consistent and rapid onset of a diabetic state.[234] Therefore, for consistency, only male mice were used in this experiment. Mice were housed individually in an IVC-ventilated housing system in an aseptic animal room at a temperature of ~20$^{o}$C-25$^{o}$C with humidity at ~40-70% with a 12:12 hour light dark cycle and unrestricted access to water and standard laboratory feed

Mice were randomised into three groups: Group 1: 8 untreated controls; Group 2: 8 STZ-induced diabetic mice; Group 3: 8 STZ-induced diabetic mice treated with MSC-CM. To induce diabetes, a low dose STZ regimen was used.

50mg/kg/day of STZ in 0.1M sodium citrate buffer (pH 4.5) was administered via intraperitoneal (i.p.) injections over a period of five days. STZ is taken up by GLUT2 membrane transporters in beta cells and alkylates DNA within cells, resulting in the activation of intrinsic mechanisms of apoptosis and depletion of beta cell mass.[235] A multiple low dose method of administration (e.g. 50mg/kg/day over five days) has been described to result in a TH1-mediated autoimmune response and subsequent depletion of the beta cell mass.[236,237] This is thought to be the result of the induction of glutamic acid decarboxylase (GAD) antigens. GAD is subsequently presented to immune cells, precipitating autoimmunity.[236,237] As this mimics the autoimmune destruction implicated in the pathogenesis of type 1 diabetes, it makes the low dose method ideal for the purposes of this experiment.

Monitoring of Mice

Blood glucose concentrations were checked via tail prick after 10 days and diabetes was accepted as a random blood glucose of >15mmol/L. Mice in Group 3 received 300μL MSC-CM i.p. once weekly commencing 5 days after streptozocin treatment. MSC-CM was produced as detailed in Section 2.2.10. 300μL MSC-CM was subsequently administered weekly until the animals were

culled. Animals were maintained for 3 months and monitored for weight loss twice weekly. GLUT2 is also expressed in high levels by the liver and kidneys; indeed, the side effects of STZ include hepatotoxicity and nephrotoxicity.[236] In addition to acute organ toxicity, STZ treatment in mice results in complications including weight loss, life threatening hypoglycaemia and respiratory distress.[237] Any animal that was poorly or lost >10% of its body weight was euthanized using Schedule 1 methods.

Processing of Mice

After 3 months mice were euthanized via cervical dislocation. Mice were terminally bled via cardiac puncture and serum used for insulin ELISAs as detailed in Section 2.4.2. DEXA scans were performed on mice using the Lunar PIXImus Densitometer (GE Medical Systems, Slough, UK) as described in Section 2.4.3. The pancreata of the mice were removed and the tail of the pancreas was fixed in 4% paraformaldehyde in phosphate buffered saline (PBS) for subsequent histological analysis (Section 2.4.4). The head of the pancreas was wrapped in tin foil and flash frozen in liquid nitrogen for subsequent protein extraction.

## 2.4.2 Insulin ELISA

To determine insulin concentrations in terminal plasma samples from mice, the ALPCO ultrasensitive ELISA was used.

Preparation of Reagents

To prepare a working conjugate solution, conjugate stock solution was dissolved in conjugate buffer in a 1:10 ratio. To prepare wash buffer (21x) stock buffer solution was dissolved in distilled water in a 1:20 ratio.

ELISA Protocol

5μL of samples and 5μL of standards were added to the provided insulin-coated 96 well plate. 75μL of working conjugate solution was added to each well. The plate was sealed and incubated at room temperature for 2 hours on a plate shaker (600 rpm). The plate was subsequently washed 6 times with 350μL of wash buffer per well. The plate was blotted on a paper towel to remove excess wash buffer between washing steps. 100μL of TMB (tetramethyl benzidine) substrate was added to each well and the plate was sealed and incubated for 30 minutes at room temperature on a plate shaker

(600 rpm). 100μL of stop solution was added to each well and the plate returned briefly to the plate shaker to ensure thorough mixing of the contents. Absorbance was read with a Synergy 2 Multi-Mode Reader (Bio-Tek, Swindon, UK) at a wavelength of 450nm.

Data Analysis

Concentrations of insulin were determined by comparing raw absorbance data to standard curves of known insulin concentration. The standard curve used is shown in Figure 2.6.

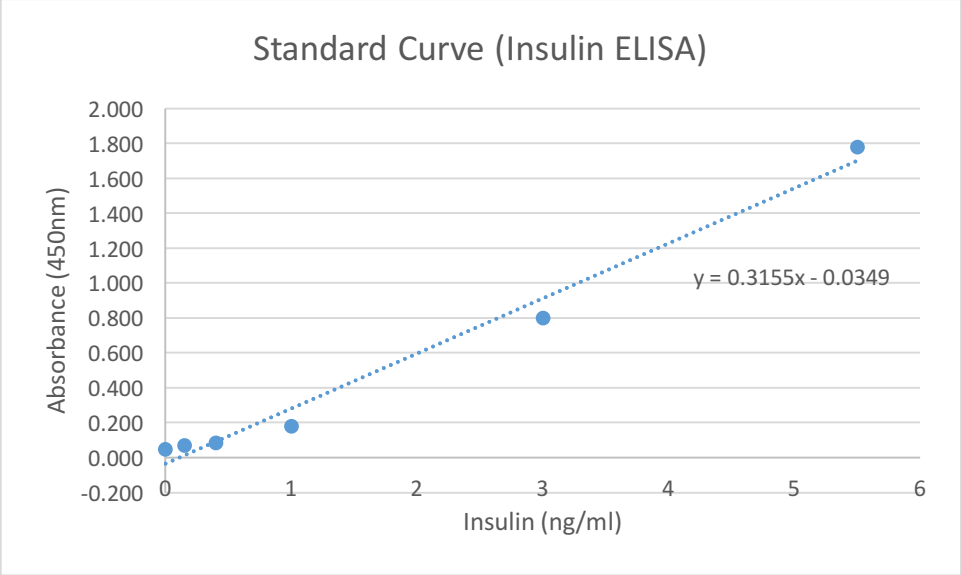


*Figure 2.6 : Standard curve for insulin ELISA assay. Figure shows absorbance over insulin. Standards were prepared for 0, 0.15, 0.4, 1, 3 and 5.5ng/ml.*

Data from each group consists of 8 plasma samples, one from each animal respectively. Data is expressed as mean +/- standard deviation. Differences in concentrations of insulin between groups of mice were evaluated using two-tailed unpaired T-tests assuming unequal variance. A p value of $<0.05$ was deemed to be significant.

### 2.4.3 DEXA Scans

DEXA scans were performed on culled mice using a LUNAR PIXImus densitometer (GE Medical Systems, Slough, UK). This allowed determination of body composition (lean and fat mass) as well as bone mineral content. Body fat content, lean mass and body weight were compared between non-diabetic mice, diabetic mice treated with MSC-CM and non-treated diabetic mice. Figure 2.7 depicts a sample of results obtained.

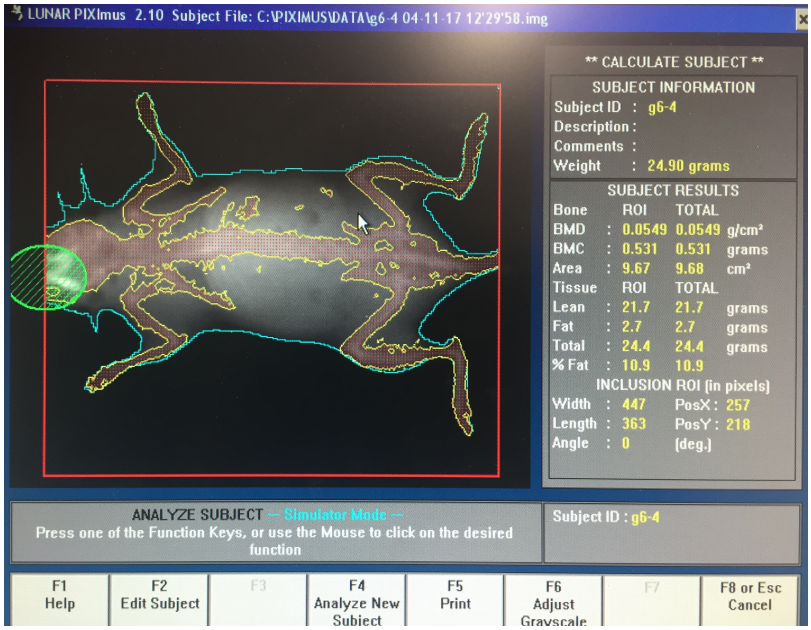


*Figure 2.7 : Sample of DEXA scan results obtained using the LUNAR PIXImus densitometer.*

## Data analysis

Data for each group consists of 8 measurements, one from each animal respectively. Data is expressed as mean +/- standard deviation. Differences between experimental groups were evaluated using unpaired T-tests assuming unequal variance. A p value of $<0.05$ was deemed to be significant.

## 2.4.4 Pancreata Histology

Tissue Preparation

Pancreatic tissue was excised immediately after mice were culled. The tail of the pancreas was collected from each animal for further analysis. Tissue was fixed immediately in 4% PFA in phosphate-buffered saline (PBS) for 48 hours at 4$^{o}$C. As water present in tissue is hydrophobic tissue needs to be dehydrated before wax embedding. Pancreata were processed using a a Leica TP1020 (Leica Microsystems, Nussloch, Germany) automated tissue processor Dehydration of samples was performed with increasing concentrations of ethanol solution (50%, 70%, 80%, 95%, 100%). Tissue was incubated at each concentration for 10 minutes (with a final 30-minute incubation in 100% ethanol). Clearing was performed with incubation in xylene (two 20-minute and one 45-minute wash).

Embedding and Preparation of Slides

Pancreata were infiltrated with wax using a Leica TP1020 (Leica Microsystems, Nussloch, Germany)automated tissue processor (Leica TP120) and subsequently embedded in paraffin wax. Tissue blocks were sectioned to 8μm

thickness using a Shandon™ Finesse™ 325 microtome (Thermo Scientific, Hemel Hempsted, UK) and mounted directly on to poly-L-lysine coated microscope slides for imaging.

Imaging

Histology Images were taken using an EVOS™ Core imaging system (Thermo Scientific, Windsford, UK). Scale bars were manually calibrated using stage rulers.

Data analysis

Islet areas were measured on ImageJ image processing software. Areas obtained were converted from pixels to $\mu m^2$. At least 15 islets taken from multiple pancreatic sections were used for each data point. Data for islet size is expressed as mean +/- standard deviation. Differences between experimental groups were evaluated using unpaired T-tests assuming unequal variance. A p value of $<0.05$ was deemed to be significant.


# Chapter 3: Exploration of the Effect of MSC-CM on an *in Vitro* Model for Cytokine-Induced Reduction of Mitochondrial Metabolism in Beta Cells

# 3.1 Introduction

As described in Chapter 1, MSCs present an attractive option in regenerative medicine. Previous studies have shown that MSCs are capable of modulating and shifting the immune response away from a TH1 to a TH2 response through production of soluble factors. [65,74] MSCs are also capable of inducing T-cell anergy through direct cell-to-cell contact, as they lack the co-stimulatory molecules required for the activation of autoreactive T-cells.[50,74]

In addition to the immunoregulatory effects, it could be proposed that the MSC-CM may directly confer cytoprotection to beta cells from inflammatory factors implicated in the pathogenesis of type 1 diabetes. In the diseased state, immune cells are known to secrete factors, namely TNFα, IFNγ and IL1β, in the pro-inflammatory environment.[117, 207] These factors are capable of inducing apoptosis of beta cells through mechanisms such as INO induction and ER stress as described in Chapter 1.[118-123,140] The MSC-CM has been shown through proteomic studies to contain a number of cytoprotective factors including VEGF, IL-10, IL-4, PIGF and HGF to name a few.[63] This

indicates that it is plausible that the MSC-CM could help maintain beta cell mass through the inhibition of these apoptotic mechanisms.

Previous studies by Yeung *et al.* investigated the effect of co-culturing MSCs with islet cells from pancreatic islets. They treated islet cells with an inflammatory cytokine cocktail of TNF$\alpha$, IFN$\gamma$ and IL-1$\beta$ and demonstrated apoptosis through TUNEL assays.[238] TUNEL assays are a method of detecting DNA fragmentation by immunolabelling the 3'-hydroxyl termini in double-strand DNA breaks that occur during apoptosis.[239] They demonstrated that the number of apoptotic cells were reduced in the presence of MSCs.[238] This experiment cultured MSCs together in the same compartment, allowing MSCs to interact by direct cellular contact as well as paracrine factors. Other studies demonstrated improved islet function and survival when MSCs were co-cultured in separate compartments, indicating soluble factors contributed to the benefits conferred.[240]

To test the hypothesis that MSCs could directly prevent pro-inflammatory cytokine driven falls in cellular viability of beta cells through paracrine actions, MTT assays were used in the experiments presented in this chapter. The MTT viability assay measures mitochondrial metabolism of cells and can reflect the number of viable cells present. The objectives of this chapter are:

- Culture human bone marrow derived MSCs, characterise the cells through trilineage differentiation and collect conditioned media derived from these MSCs.
- Determine the effect of pro-inflammatory cytokines (TNF$\alpha$, IL-1$\beta$ and IFN$\gamma$) on the mitochondrial metabolism of beta cell lines *in vitro* using MTT assays.
- Determine if MSC-CM is able to ameliorate pro-inflammatory cytokine driven falls in mitochondrial metabolism of beta cell lines *in vitro* using MTT assays.

The following experiment should shed some light on whether the MSC-CM as a whole confers direct cytoprotection to cells in the presence of pro-inflammatory cytokines implicated in the pathogenesis of type 1 diabetes.

# 3.2 Trilineage Differentiation of MSCs

## 3.2.1 Methods

Materials

Materials used in this procedure are detailed in Section 2.1.

MSC Culture Methods

MSCs were recovered and expanded as detailed in Section 2.2.7. Isolation and culture of MSCs is detailed in Section 2.2.8. Passaging of cells is detailed in Section 2.2.5. Cells were trypsonised and suspended in medium as detailed in Section 2.2.5. Cell counts were performed as detailed in Section 2.2.6.

Trilineage differentiation

Details of preparation of differentiation media, preparation of stains, seeding cells, fixing cells and staining cells can be found in Section 2.3.1

## 3.2.2 Results

### 3.2.2.1 Adipogenic Differentiation of MSCs

Adipogenic differentiation can be seen by accumulation of lipid vacuoles within cells. Lipid vacuoles accumulated over the three weeks of exposure to adipogenic differentiation medium and eventually filled the cells. Lipid vacuoles can be visualized via Oil Red O staining as depicted in Figure 3.1.

### 3.2.2.2 Osteogenic Differentiation of MSCs

Osteogenic differentiation medium induced changes in morphology including the development of cellular projections after a few days of exposure to osteogenic medium. After three weeks, the extracellular matrix stained an intense red with Alizarin Red staining as depicted in Figure 3.2, indicating mineralisation of the extracellular matrix associated with osteogenesis of MSCs.

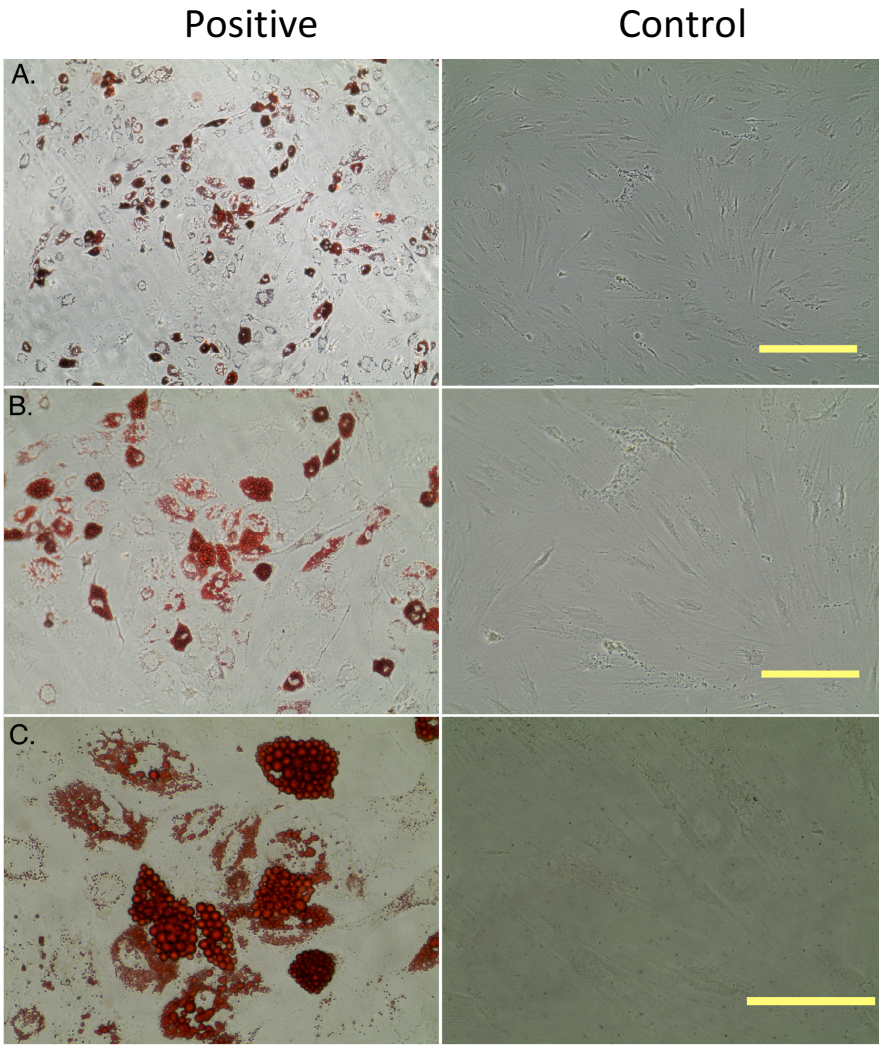


*Figure 3.1 : Oil Red O staining of adipogenic differentiation of MSCs. A - 10x magnification of positive results and control (scale bar = 400μm); B - 20x magnification of positive results and control (scale bar = 200μm); C - 40x magnification of positive results and control (scale bar = 100μm). Lipid vacuoles can be seen filling the cells and stained an intense red. Negative control shows absence of lipid vacuoles and staining.*

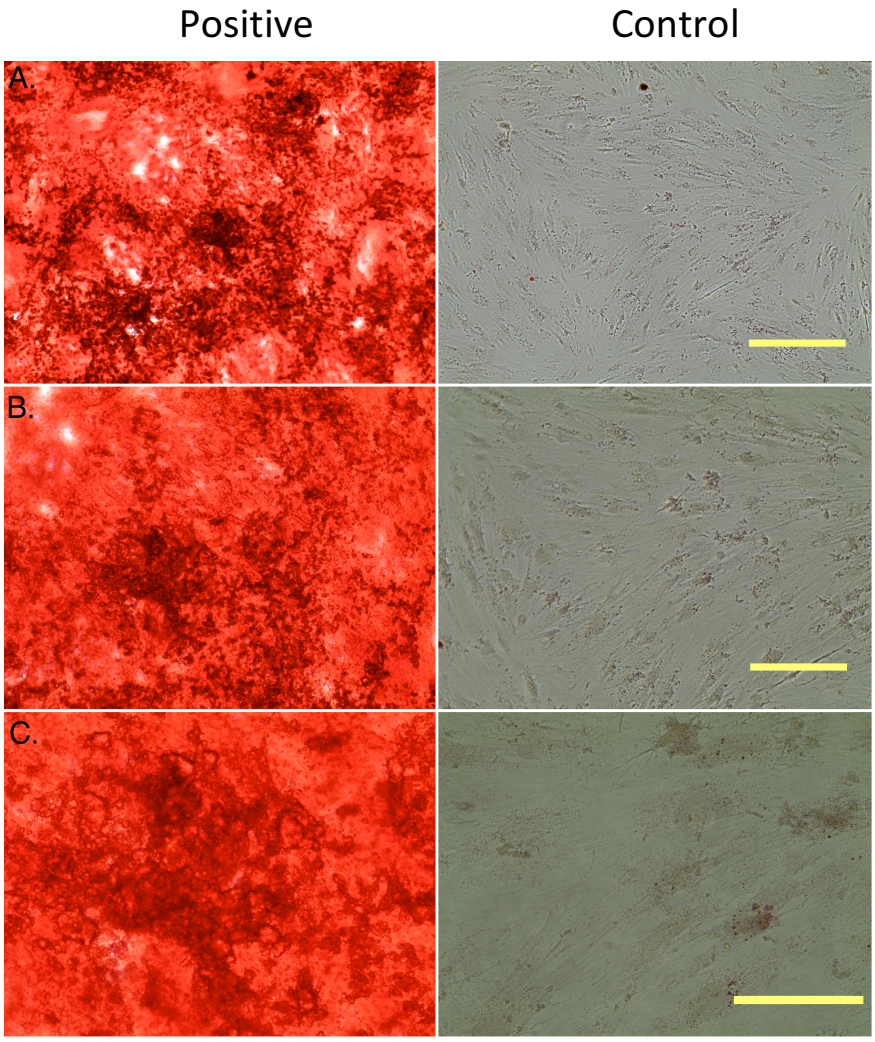


*Figure 3.2 : Alizarin Red staining of osteogenic differentiation of MSCs. A - 10x magnification of positive results and control (scale bar = 400μm); B - 20x magnification of positive results and control (scale bar = 200μm); C - 40x magnification of positive results and control (scale bar = 100μm). Extracellular matrix stains red indicating mineralisation of the extracellular matrix associated with osteogenesis. Negative controls do not exhibit ECM mineralisation.*

#### 3.2.2.3 Chondrogenic Differentiation of MSCs

Chondrogenic differentiation medium resulted in the deposition of proteoglycans that exhibited mild staining with Alcain Blue with some changes in morphology/lacunae development (Figure 3.3). However, cellular aggregates with intense blue staining expected with chondrogenic differentiation of MSCs were not observed. A longer incubation time in chondrogenic medium might have been required. Micromass clearly showed greater staining for proteoglycans compered to control (Figure 3.4).

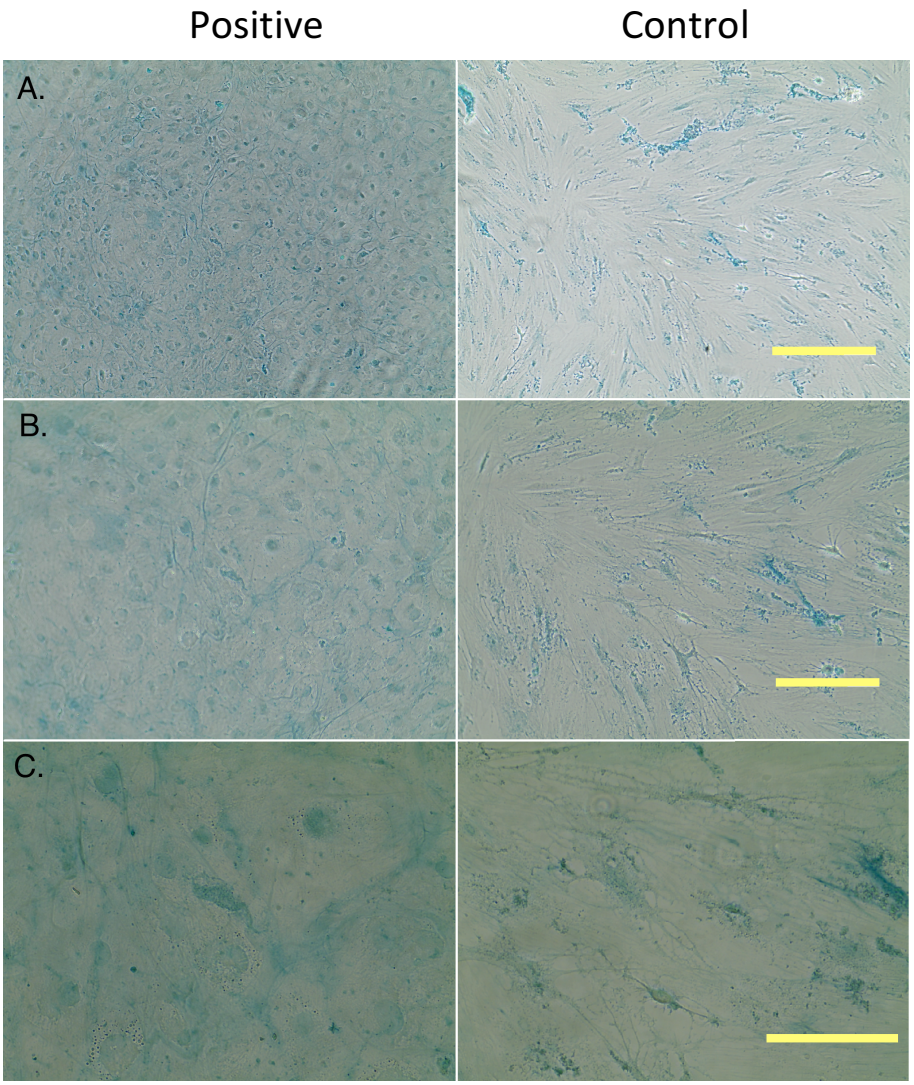


*Figure 3.3 : Alcain Blue staining of chondrogenic differentiation for monolayer of cells. A - 10x magnification of positive results and control (scalebar = 400μm); B - 20x magnification of positive results and control (scale bar = 200μm); C - 40x magnification of positive results and control (scale bar = 100μm). Some morphological changes can be seen compared to the control with mild blue staining of proteoglycans.*

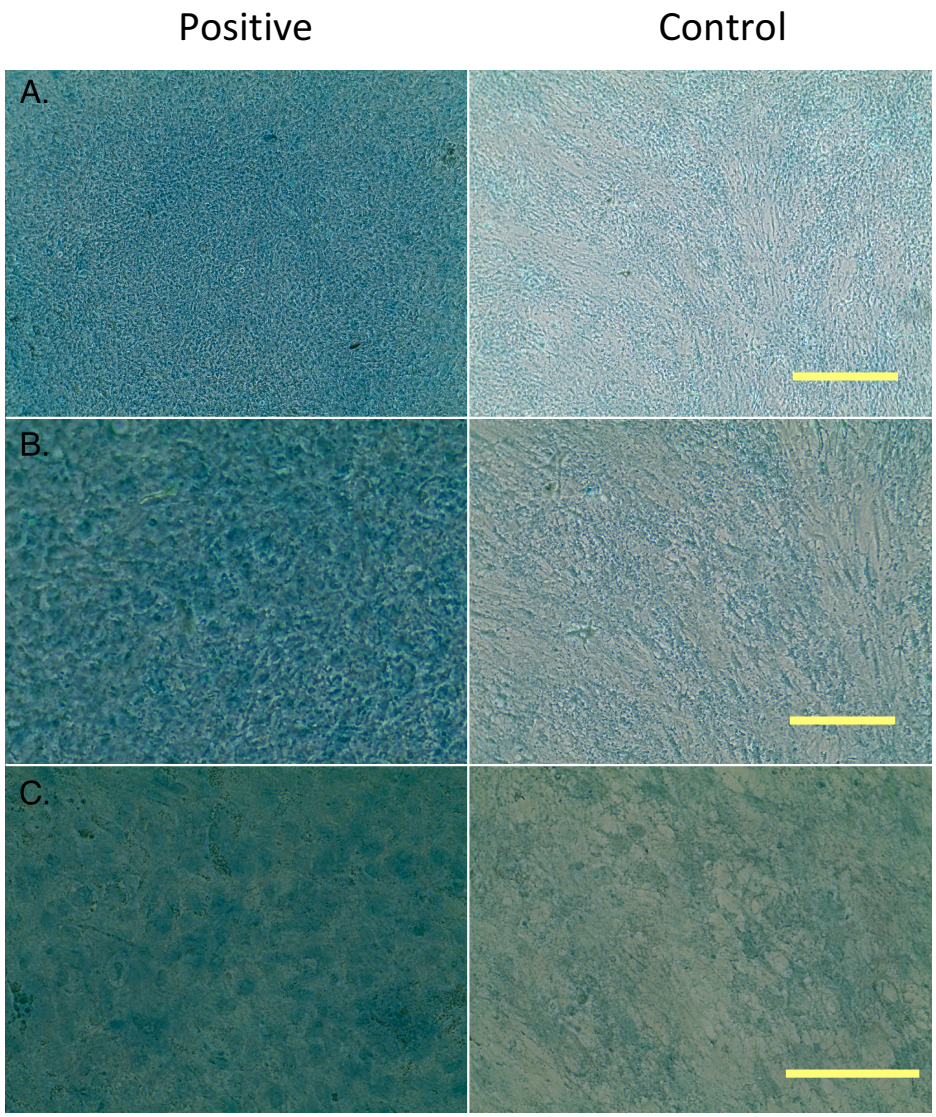


*Figure 3.4 : Alcain Blue staining of chondrogenic differentiation for micromass. A - 10x magnification of positive results and control (scale bar = 400μm); B - 20x magnification of positive results and control (scale bar = 200μm); C - 40x magnification of positive results and control (scale bar = 100μm).*

# 3.3 MTT Assay

## 3.3.1 MTT Assay Optimisation Experiment

The quantity of signal generated depends on several factors including the length of incubation in MTT, the concentration of MTT and the metabolic activity of the cells. These parameters should be considered to ensure sufficient product is generated to be detected above background.

MTT assays on BRIN-bd11 cells were conducted to determine the relationship between MTT incubation time and absorbance readings. This allows for the optimal period of incubation in MTT solution at a set concentration of MTT working solution (0.05mg/ml) and cell density (80% confluence) to be determined. These experiments were also used to determine whether there is any significant difference in viability readings between BRIN-bd11 cells treated with MSC-CM and BRIN-bd11 cells treated with non-conditioned RPMI medium.

#### 3.3.1.1 Methods

Materials

Materials used for this experiment are detailed in Section 2.1.

Cell Lines Utilised

BRIN-bd11 cells were utilised in this experiment. Details of the cell line used can be found in Section 2.2.2.

Cell Culture Methods

Cells were obtained from liquid nitrogen dewars located at the Guy Hilton Research Center, Stoke-on-Trent, UK, and thawed as detailed in Section 2.2.4. Cells were trypsonised and suspended in medium as detailed in Section 2.2.5. Cell counts were performed as detailed in Section 2.2.6.

MTT Assay Optimisation

Details of the preparation of reagents, MTT procedure and data analysis used in the experiment can be found in Section 2.3.3.

#### 3.3.1.2 Results

##### 3.3.1.2.1 Relationship Between Absorbance and MTT Incubation Time

The relationship between absorbance and incubation time in MTT reagent was determined to be exponential in nature (Figure 3.5). Data analysis is described in Section 2.3.2. All incubation times in MTT resulted in absorbance readings significantly above the negative control for a cell density of ~80% confluence and 0.05mg/ml concentration of MTT working solution (Figure 3.5).

As the absorbance reading appears to saturate just after 3 hours of incubation in MTT. Thus, 3 hours was standardised as the incubation time that would be used for further experimentation.

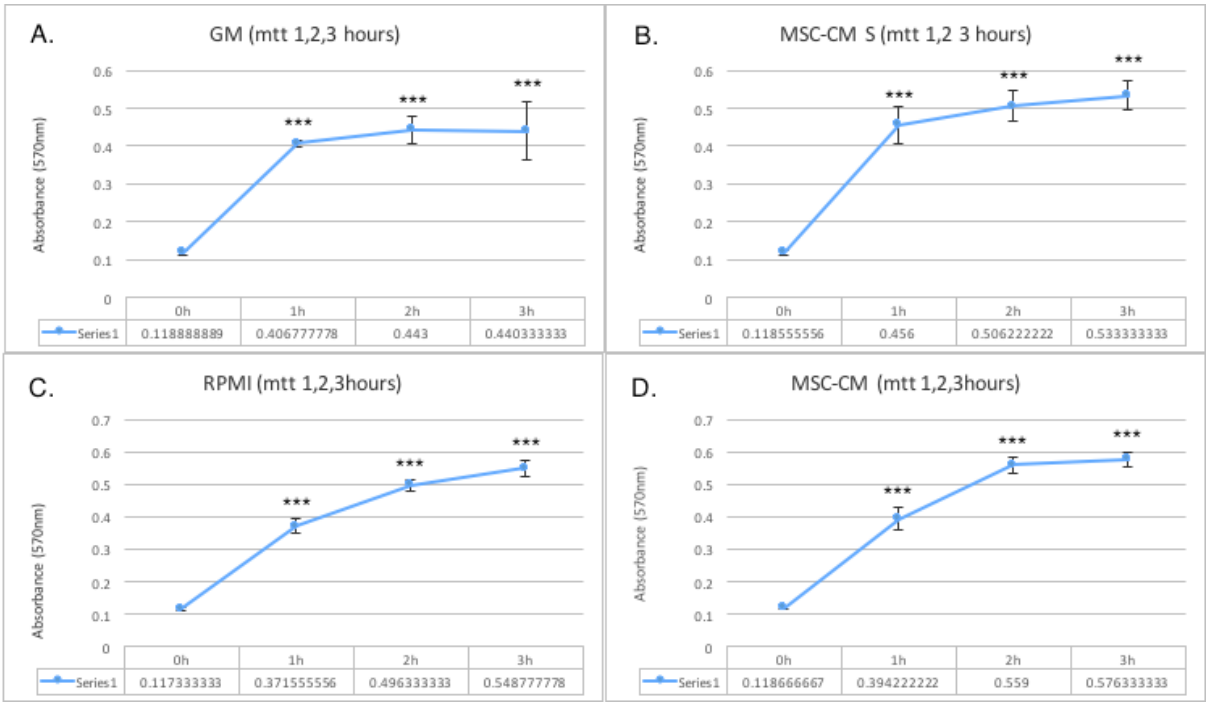


*Figure 3.5 : Graphs depicting the relationship between absorbance and incubation time in MTT reagent for cells incubated in different media for 24 hours. Data presented as mean +/- standard deviation for absorbance read at 570nm. All data comparted to their respective negative (0 hour) control. A - BRIN-bd11 cells exposed to RPMI (with serum); B - BRIN-bd11 cells exposed to MSC-CM (with serum); C - BRIN-bd11 cells exposed to RPMI; D - BRIN-bd11 cells exposed to MSC-CM. ***p<0.001*

#### 3.3.1.2.2 Effect of MSC-CM on BRIN-bd11 Cell Viability (1h MTT incubation)

To determine the effect of MSC-CM on the viability of BRIN-bd11 cells, viabilities of cells cultured in MSC-CM and RPMI for 24 hours were compared. For cells exposed to MTT reagent for 1 hour, cells cultured in MSC-CM+serum

showed +12.1% ($p<0.05$) greater viability reading compared to cells cultured in RPMI+serum (MSC-CM+serum 1.0± 0.0352 $nA_{570}$, RPMI+serum 1.12+0.138 $nA_{570}$) (Figure 3.6). Viability readings were +6.1% ($p<0.1$) greater for BRIN-bd11 cells treated with MSC-CM compared to cells treated with RPMI, however the difference was not significant at the 5% threshold ($p<0.1$) (MSC-CM 1.0 ± 0.0809 OD $nA_{570}$, RPMI 1.061 ± 0.111 $nA_{570}$) (Figure 3.6).

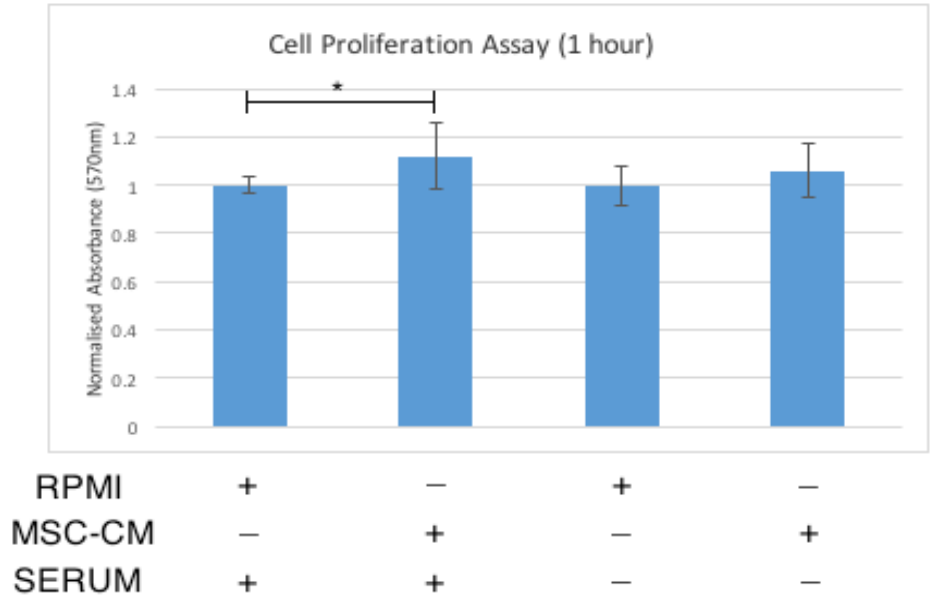


*Figure 3.6 : Effect of MSC-CM on the viability of BRIN-bd11 cells. Following 24 hours' incubation of BRIN-bd11 cells in MSC-CM and RPMI media, viability was compared using MTT assays with 1 hour incubation in MTT reagent. Viabilities were tested both with and without addition of serum to the media. Values for cells treated with conditioned media have been normalised to their respective non-conditioned media controls for comparison. Data presented as mean +/- standard deviation for normalised absorbance read at 570nm. *p<0.05*

#### 3.3.1.2.3 Effect of MSC-CM on BRIN-bd11 Cell Viability (2h MTT incubation)

To determine the effect of MSC-CM on the viability of BRIN-bd11 cells, viability of cells cultured in MSC-CM and RPMI for 24 hours were compared. For cells exposed to MTT reagent for 2 hours, a similar picture was observed. BRIN-bd11 cells cultured in MSC-CM+serum displayed +14.3% ($p<0.01$) greater viability compared to RPMI+serum (MSC-CM+serum 1.0 $\pm$ 0.0920 $nA_{570}$, RPMI+serum 1.143 $\pm$ 0.109 $nA_{570}$) (Figure 3.7). Viability readings were also greater (+12.6%; $p<0.01$) for cells exposed to MSC-CM compared to RPMI medium without the addition of FBS (MSC-CM 1.0 $\pm$ 0.0435 $nA_{570}$, RPMI 1.126 $\pm$ 0.0587 $nA_{570}$) (Figure 3.7).

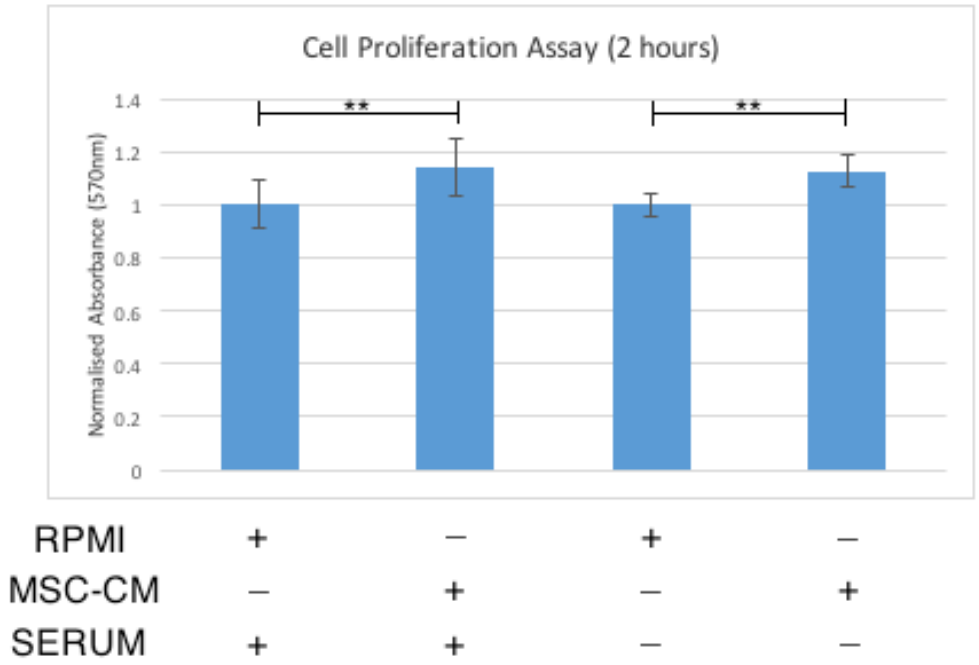


*Figure 3.7 : Effect of MSC-CM on the viability of BRIN-bd11 cells. Following 24 hours' incubation of BRIN-bd11 cells in MSC-CM and RPMI media, viability was compared using MTT assays with 2 hours' incubation in MTT reagent. Viabilities were tested both with and without addition of serum to the media. Values for cells treated with conditioned media have been normalised to their respective non-conditioned media controls for comparison. Data presented mean +/- standard deviation for normalised absorbance measured at 570nm. **p<0.01*

#### 3.3.1.2.4 Effect of MSC-CM on BRIN-bd11 Cell Viability (3h MTT incubation)

To determine the effect of MSC-CM on the viability of BRIN-bd11 cells, viability of cells cultured in MSC-CM and RPMI for 24 hours were compared. Cells exposed to MTT reagent for 3 hours showed +21.1% ($p<0.01$) greater viability readings for cells cultured in MSC-CM+serum compared to RPMI+serum (MSC-CM+serum 1.0 $\pm$ 0.191 $nA_{570}$, RPMI+serum 1.211+0.0975 $nA_{570}$) (Figure 3.8). Viability readings were also greater (+5.0%; $p<0.05$) for cells treated with MSC-CM compared with RPMI (MSC-CM 1.0 $\pm$ 0.0526 $nA_{570}$, RPMI 1.05 $\pm$ 0.0612 $nA_{570}$) (Figure 3.8).

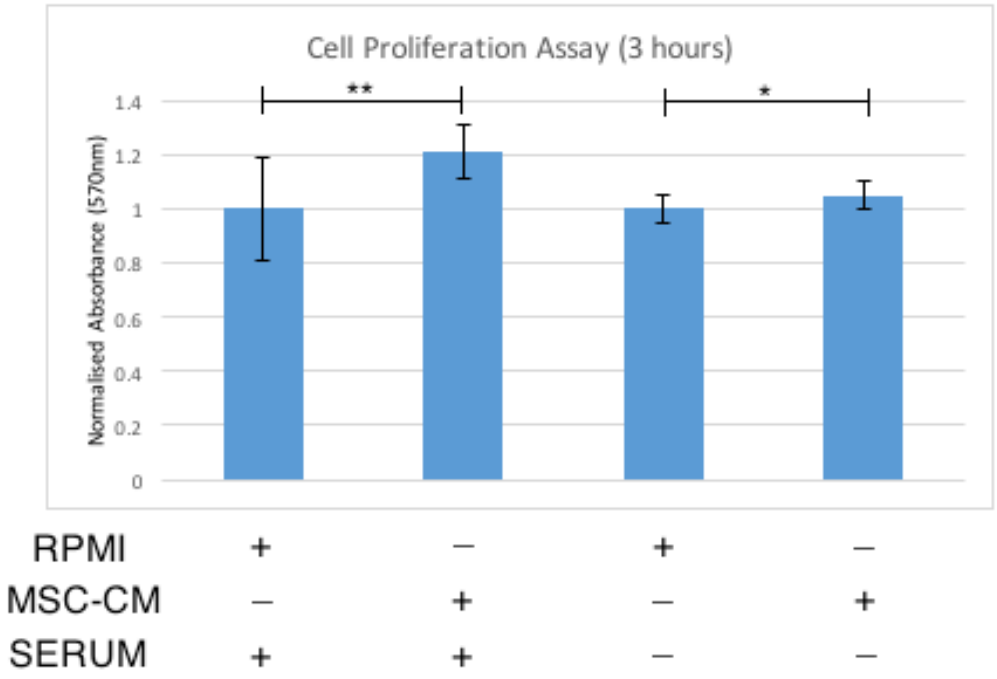


*Figure 3.8 : Effect of MSC-CM on the viability of BRIN-bd11 cells. Following 24 hours' incubation of BRIN-bd11 cells in MSC-CM and RPMI media, viability was compared using MTT assays with 3 hours' incubation in MTT reagent. Viabilities were tested both with and without addition of serum to the media. Values for cells treated with conditioned media have been normalised to their respective non-conditioned media controls for comparison. Data presented mean +/- standard deviation for normalised absorbance measured at 570nm **p<0.01, *p<0.05*

### 3.3.2 Determining Effects of Pro-Inflammatory Cytokines on Beta Cells in Vitro

Several pro-inflammatory cytokines have previously been shown to be implicated in the pathogenesis of type 1 diabetes including TNFα, IFNγ and IL-1β. Exposure of beta cells to these cytokines has been shown to result in beta cell dysfunction and cellular apoptosis as described in Chapter 1. To test this hypothesis in vitro, we planned to expose BRIN-bd11 cells to increasing concentrations of these cytokines individually as well as a cytomix of all three to determine the effects on cellular viability. Concentrations of cytokines that resulted in the greatest fall in viability determined from these experiments were determined to be optimal for use in further experiments

We theorise that the MSC-CM has cytoprotective properties that could counteract the cytotoxic effects of these pro-inflammatory cytokines. BRIN-bd11 cells were also cultured with MSC-CM in the presence of these cytokines individually as well as a cytomix of all three cytokines at the predetermined optimal concentrations. This allowed us to determine whether treating cells with MSC-CM can ameliorate the falls in viabilities associated with exposure to these pro-inflammatory cytokines.

### 3.3.2.1 Methods

Materials

Materials used for the experiment are detailed in Section 2.1.

Cell Lines Utilised

BRIN-bd11 and TC6 cells were utilised in this experiment. Details of the cell line used can be found in Section 2.2.2.

Cell Culture Methods

Cells were obtained from liquid nitrogen dewers located at the Guy Hilton Research Center, Stoke-on-Trent, UK, and thawed as detailed in Section 2.2.4. Cells were trypsonised and suspended in medium as detailed in Section 2.2.5. Cell counts were performed as detailed in Section 2.2.6.

MSC Culture Methods

MSCs were recovered and expanded as detailed in Section 2.2.7. Isolation and culture of MSCs is detailed in Section 2.2.8. Passaging of cells is detailed in Section 2.2.5.

Procurement and Collection of MSC-CM

Production of MSC-CM is detailed in Section 2.2.10.

Cytokine-Induced Apoptosis MTT Assays

Details of preparation of reagents, reconstitution of cytokines, treatment of cells with pro-inflammatory cytokines, measurement of viabilities via MTT calorimetric assays and data analysis are detailed in Section 2.3.3.

### 3.3.2.2 Results

#### 3.3.2.2.1 Effect of Increasing Concentrations of TNFα on BRIN-bd11 Cells

To determine the effect of TNFα on the viability of BRIN-bd11 cells, cells were treated with increasing concentrations (0-1,000 ng/ml) of TNFα for 24 hours. Significant falls in viability were seen for concentrations of TNFα of 100ng/ml (-12.2%; $p<0.05$) compared to the control (cell control 1.0 $\pm$ 0.102 $nA_{570}$, 100ng/ml TNFα 0.878 $\pm$ 0.091 $nA_{570}$) (Figure 3.9) as well as 1,000ng/ml (-21.1%; $p<0.01$) compared to the control (cell control 1.0 $\pm$ 0.102 $nA_{570}$, 1,000ng/ml TNFα 0.789 $\pm$ 0.133 $nA_{570}$) (Figure 3.9). 1,000ng/ml TNFα

achieved greatest falls in viability and was therefore used for subsequent experiments.

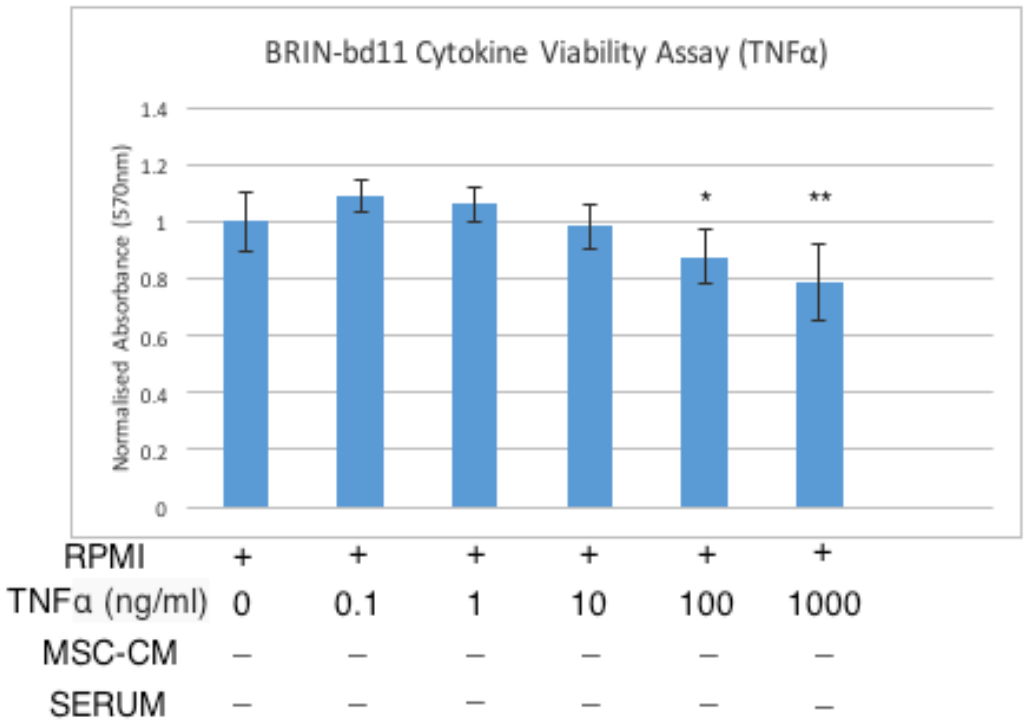


*Figure 3.9 : Effect of 24 hours' exposure to rising concentrations (0.1ng/ml-1,000ng/ml) of TNF$\alpha$ on the viability of BRIN-bd11 cells cultured in RPMI medium without serum. Viability of BRIN-bd11 cells was determined by calorimetric MTT assays after 24 hours' exposure to rising concentrations of TNF$\alpha$. Data normalised to untreated control and presented as mean +/- standard deviation. **p<0.01, ***p<0.001*

#### 3.3.2.2.2 Effect of Increasing Concentrations of IFNγ on BRIN-bd11 Cells

To determine the effect of IFNγ on the viability of BRIN-bd11 cells, cells were treated with increasing concentrations (0-1,000ng/ml) of IFNγ for 24 hours. Significant falls in viability were seen for 10ng/ml IFNγ (-10.6%; $p<0.05$) compared to the control (cell control 1.0 $\pm$ 0.113 $nA_{570}$, 10ng/ml IFNγ 0.894 $\pm$0.045) (Figure 3.10). Significant falls were also seen for 100ng/ml IFNγ (-10.1%; $p<0.05$) compared to the control (cell control 1.0 $\pm$ 0.113 $nA_{570}$, 100ng/ml IFNγ 0.899 $\pm$ 0.064) (Figure 3.10). The greatest fall in viability was achieved with 1,000ng/ml IFNγ (-18.3%; $p<0.01$) compared to the control (cell control 1.0+ 0.113$nA_{570}$, 1,000ng/ml IFNγ (0.817 $\pm$ 0.099 $nA_{570}$) (Figure 3.10). As a result, 1,000ng/ml IFNγ was selected for subsequent experiments.

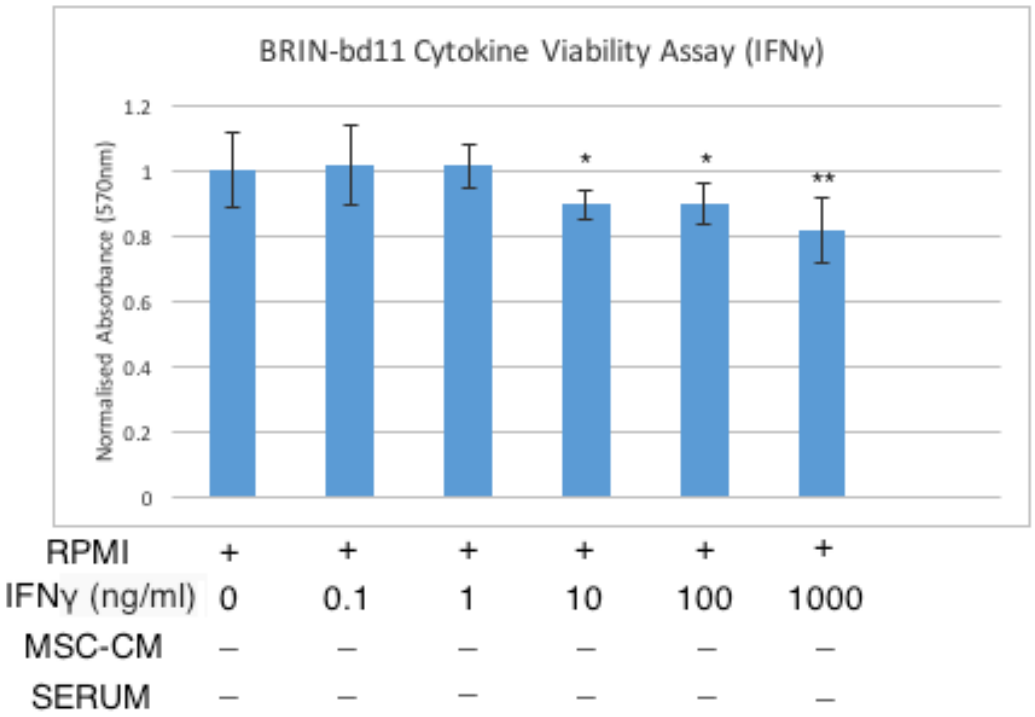


*Figure 3.10 : Effect of 24 hours' exposure to rising concentrations (0.1ng/ml-1,000ng/ml) of INFγ on the viability of BRIN-bd11 cells cultured in RPMI medium without serum. Viability of BRIN-bd11 cells was determined by calorimetric MTT assays after 24 hours' exposure to rising concentrations of INFγ. Data normalised to untreated control and presented as mean +/- standard deviation. **p<0.01, ***p<0.001.*

#### 3.3.2.2.3 Effect of Increasing Concentrations of IL-1β on BRIN-bd11 Cells

BRIN-bd11 cells were cultured for 24 hours in increasing concentrations (0-1,000ng/ml) of IL-1β to determine the effect of IL-1β on the viability of BRIN-bd11 cells. Treatment of BRIN-bd11 cells with 1,000ng/ml resulted in a 11.3% drop in viability. However, this was not significant at the 5% significance cut-off. (p = 0.075) (Figure 3.11). As 1,000ng/ml resulted in the largest fall in viability, it was used for subsequent experiments.

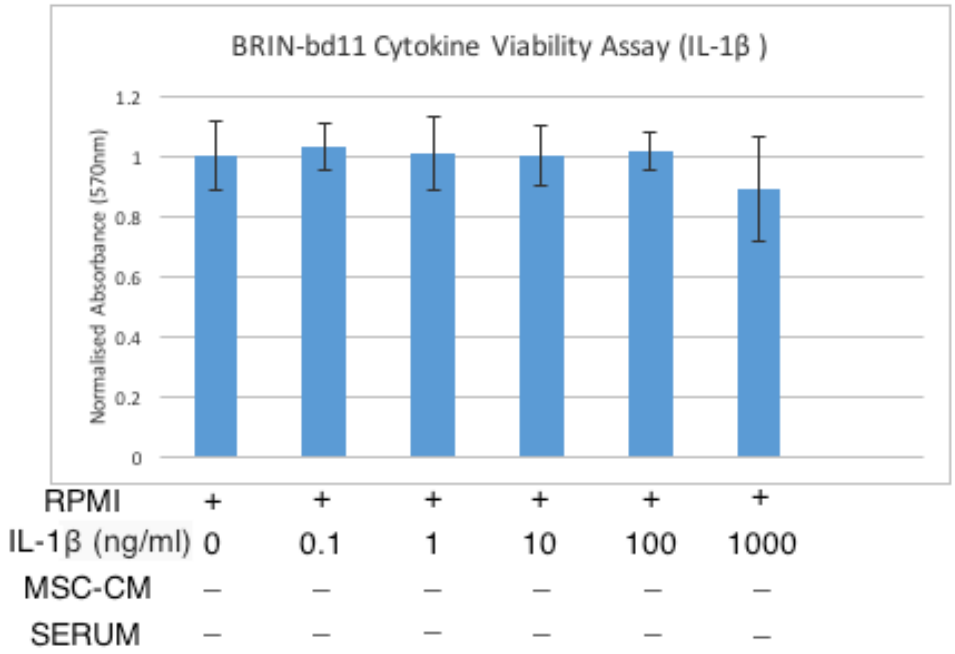


*Figure 3.11 : Effect of 24 hours' exposure to rising concentrations (0.1ng/ml-1,000ng/ml) of IL-1β on the viability of BRIN-bd11 cells cultured in RPMI medium without serum. Viability of BRIN-bd11 cells was determined by calorimetric MTT assays after 24 hours' exposure to rising concentrations of IL-1β. Data normalised to untreated control and presented as mean +/- standard deviation.*

#### 3.3.2.2.4 Effect of Increasing Concentrations of Cytomix on BRIN-bd11 Cells

To determine the effect of a cytomix of all three cytokines, TNF$\alpha$, IFN$\gamma$ and IL-1$\beta$ were mixed in equal quantities and applied as a cytomix in increasing concentrations (0-1,000ng/ml) to BRIN-bd11 for 24 hours. 100ng/ml of cytomix resulted in a significant fall in viability (-9.7%; $p<0.01$) compared to the control (cell control 1.0 $\pm$ 0.054, 100ng/ml cytomix 0.903 $\pm$ 0.075). (Figure 3.12). 1,000ng/ml cytomix resulted in a greater fall in viability (-15.3%; $p<0.001$) than the control (cell control 1.0 $\pm$ 0.054, 1,000ng/ml cytomix 0.847 $\pm$ 0.038) (Figure 3.12). As a result, 1,000ng/ml of cytomix was used for subsequent experiments.

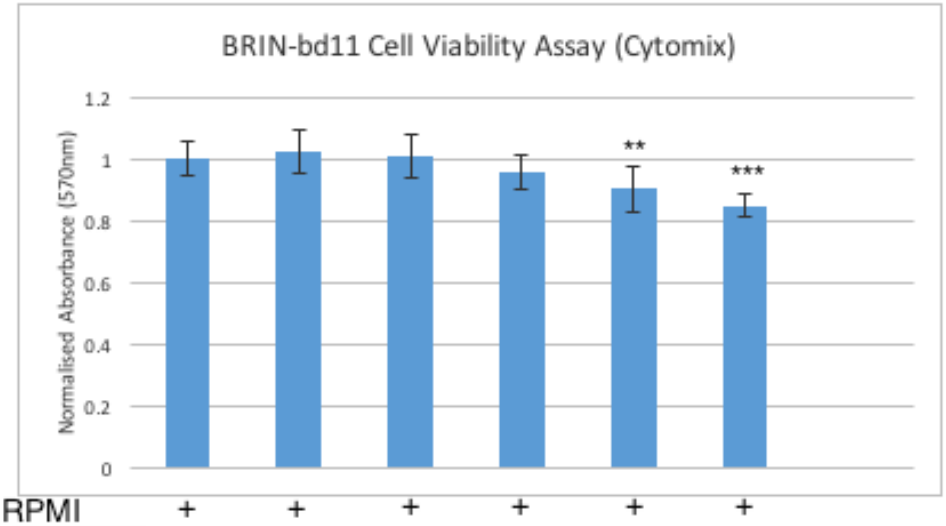


| | | | | | | |
|---|---|---|---|---|---|---|
| RPMI | + | + | + | + | + | + |
| TNFα (ng/ml) | – | 0.0333 | 0.333 | 3.33 | 33.3 | 333 |
| IFNγ (ng/ml) | – | 0.0333 | 0.333 | 3.33 | 33.3 | 333 |
| IL-1β (ng/ml) | – | 0.0333 | 0.333 | 3.33 | 33.3 | 333 |
| MSC-CM | – | – | – | – | – | – |
| SERUM | – | – | – | – | – | – |

*Figure 3.12 : Effect of 24 hours' exposure to rising concentrations (0.1ng/ml-1000ng/ml) of cytomix on the viability of BRIN-bd11 cells cultured in RPMI medium without serum. Viability of BRIN-bd11 cells was determined by MTT assay after 24 hours' exposure to rising concentrations of cytomix. Data normalised to untreated control and presented as mean +/- standard deviation. **p<0.01, ***p<0.001*

#### 3.3.2.2.5 MSC-CM Attenuates Cytokine-Driven Falls in Viability in BRIN-bd11 Cells

To determine the effect of MSC-CM on the viability of BRIN-bd11 cells when exposed to pro-inflammatory cytokines, BRIN-bd11 cells were exposed to pro-inflammatory cytokines for 24 hours in the presence and absence of MSC-CM. MTT viability assays were used to determine differences in viability. Optimised concentrations of cytokines determined in previous experiments were used.

Figure 3.13 demonstrates that for all types of pro-inflammatory cytokines, treatment with MSC-CM resulted in significantly greater viabilities for BRIN-bd11 cells compared to cells that were not treated with MSC-CM.

For BRIN-bd11 cells exposed to 1,000ng/ml TNF$\alpha$, BRIN-bd11 cells showed significantly greater viability (+77.3%; $p<0.001$) for cells treated with MSC-CM compared to untreated cells (Figure 3.13). For BRIN-bd11 cells exposed to 1,000ng/ml of cytomix, viabilities were also significantly greater for cells treated with MSC-CM (+27.4%; $p<0.01$) compared to cells that were not treated with MSC-CM. For cells treated with 1,000ng/ml IFN$\gamma$, viability was (+72.8%; $p<0.001$) greater for MSC-CM treated cells compared to untreated

cells (Figure 3.13). Finally, for cells exposed to 1,000ng/ml IL-1β, viabilities were (+38.2%; p<0.01) compared to cells that were not treated with MSC-CM (Figure 3.13).

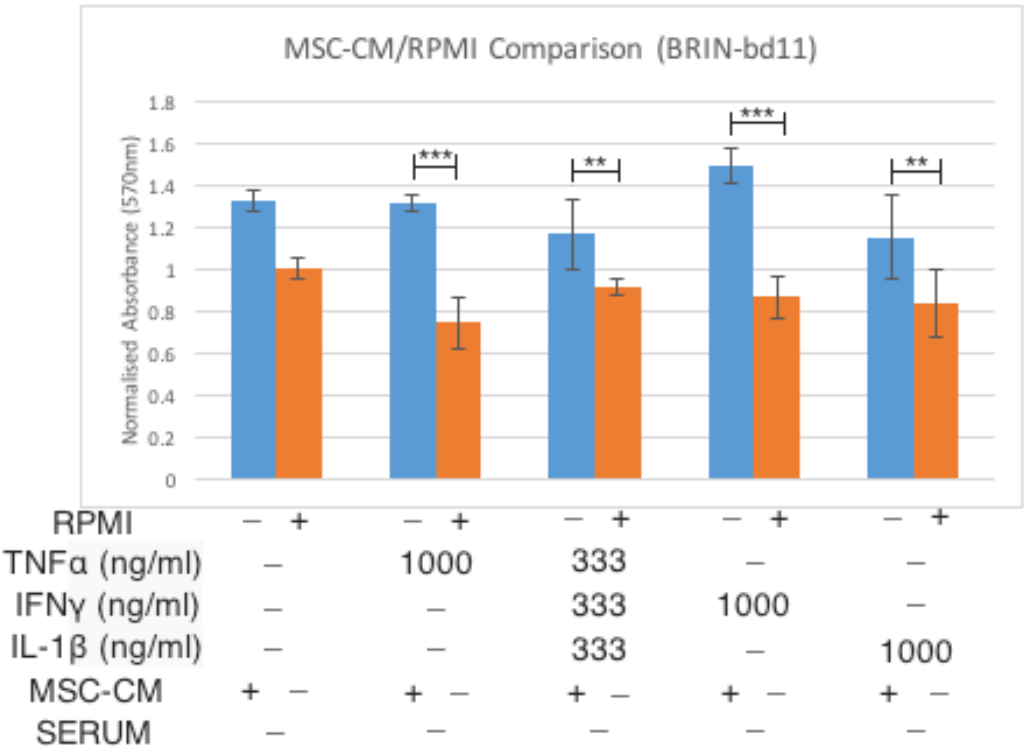


*Figure 3.13 : Determining the effect of MSC-CM on the viability of BRIN-bd11 cells exposed to pro-inflammatory cytokines. Viability of BRIN-bd11 cells was determined by MTT assay after 24 hours' exposure to pro-inflammatory cytokines (TNFα, IFNγ, IL-1β and cytomix). Data normalised to untreated RPMI control and presented as mean +/- standard deviation. **p<0.01, ***p<0.001*

#### 3.3.2.2.6 Effect of Increasing Concentrations of TNFα on TC6 Cells

To determine the effect of TNFα on the viability of TC6 cells, cells were treated with increasing concentrations (0-1,000ng/ml) of TNFα for 24 hours. In Figure 3.14 we can see progressive falls in viability with increasing concentrations of the cytokine. TC6 cells appear more susceptible to TNFα-induced falls in viability compared to BRIN-bd11 cells. Significant falls in viability were observed for concentrations of TNFα of 1ng/ml (-16.8%; $p<0.001$) compared to the control (cell control $1.0 \pm 0.079$ $nA_{570}$, 1ng/ml TNFα $0.832 \pm 0.077$ $nA_{570}$) (Figure 3.14). Treatment with 10ng/ml TNFα also resulted in a significant fall in viability (-12.8%; $p<0.01$) compared to the cell control (cell control $1.0 \pm 0.079$ $nA_{570,}$ 10ng/ml TNFα $0.872 \pm 0.090$ $nA_{570}$) (Figure 3.14). 100ng/ml TNFα resulted in a significant fall in viability (-18.4%; $p<0.001$) compared to the cell control (cell control $1.0 \pm 0.079$ $nA_{570}$, 100ng/ml TNFα $0.816 \pm 0.103$ $nA_{570}$) (Figure 3.14). 1,000ng/ml TNFα resulted in the greatest fall in viability (-29.8%; $p< 0.001$) compared to the control (cell control $1.0 \pm 0.079$ $nA_{570,}$ 1,000ng/ml TNFα $0.702 \pm 0.093$ $nA_{570}$) (Figure 3.14). As a result, 1,000ng/ml of TNFα was used for subsequent experiments.

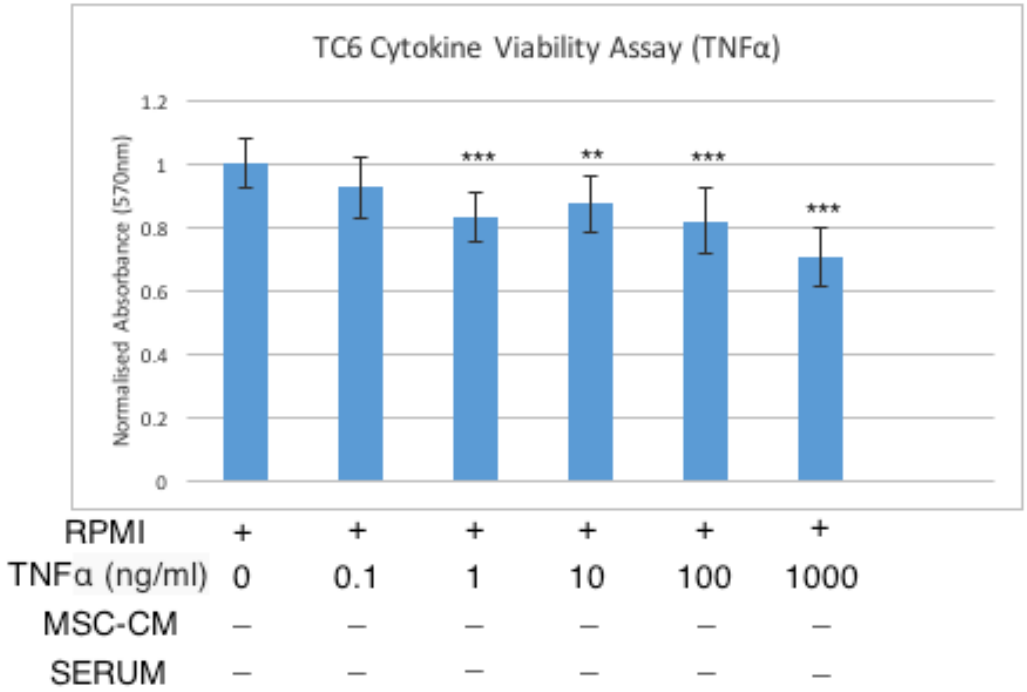


*Figure 3.14 : Effect of 24 hours' exposure to rising concentrations (0.1ng/ml-1,000ng/ml) of TNF$\alpha$ on the viability of TC6 cells cultured in RPMI medium without serum. Viability of TC6 cells was determined by calorimetric MTT assays after 24 hours' exposure to rising concentrations of TNF$\alpha$. Data normalised to untreated control and presented as mean +/- standard deviation. **p<0.01, ***p<0.001*

#### 3.3.2.2.7 Effect of Increasing Concentrations of IFNγ on TC6 Cells

TC6 cells were cultured with increasing concentrations (0-1,000ng/ml) of IFNγ for 24 hours to determine the effects of IFNγ on this cell line. In Figure 3.15 we can observe that increasing concentration of IFNγ results in progressive falls in the viability of TC6 cells. Significant falls in viability were seen for TC6

cells treated with 1ng/ml IFNγ (-12.0%; $p<0.05$) compared to the cell control (cell control 1.0 ± 0.112 $nA_{570}$, 1ng/ml IFNγ 0.880 ± 0.079 $nA_{570}$) (Figure 3.15). 10ng/ml of IFNγ resulted in a significant fall of -13.4% ($p<0.05$) compared to the cell control (cell control 1.0 ± 0.112 $nA_{570}$, 10ng/ml IFNγ 0.866 ± 0.086 $nA_{570}$) (Figure 3.15). 100ng/ml resulted in a fall in viability of (-19.9%; $p<0.001$) compared to the control (cell control 1.0 ± 0.112 $nA_{570}$, 100ng/ml IFNγ 0.801 ± 0.078 $nA_{570}$) (Figure 3.15). 1,000ng/ml of IFNγ resulted in the greatest fall in viability (-30.0%; $p<0.001$) compared to the cell control (cell control 1.0 ± 0.112 $nA_{570}$, 1,000ng/ml IFNγ 0.700 ± 0.117 $nA_{570}$) (Figure 3.15). TC6 cells appear to be more susceptible to IFNγ-mediated falls in viability compared to BRIN-bd11 cells.

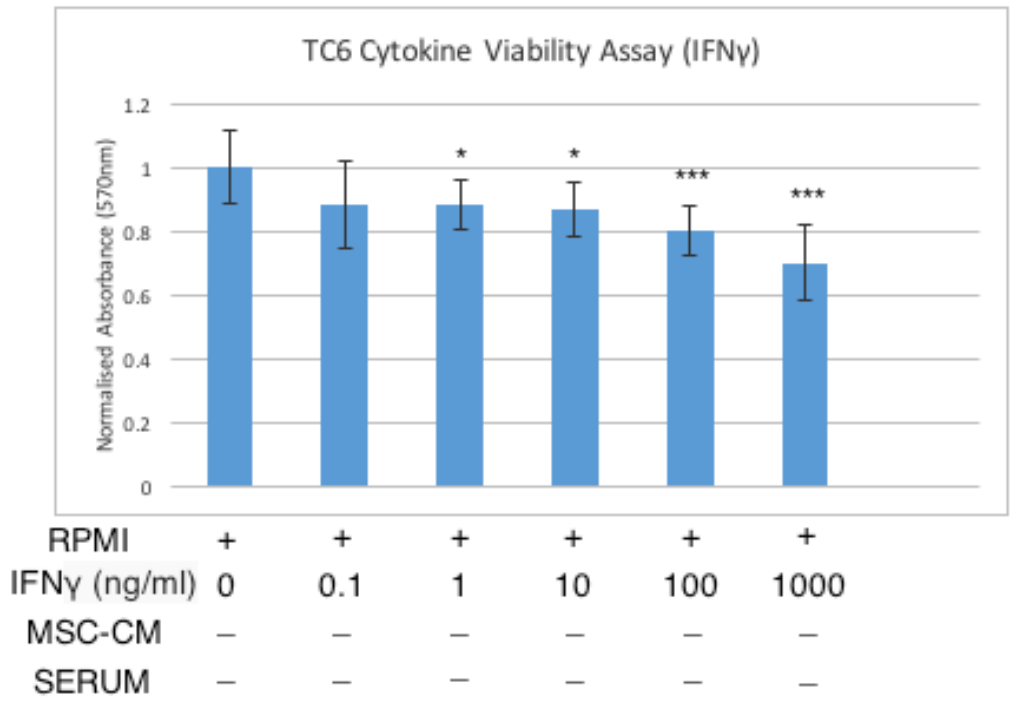


*Figure 3.15 : Effect of 24 hours' exposure to rising concentrations (0.1ng/ml-1,000ng/ml) of INFγ on the viability of TC6 cells cultured in RPMI medium without serum. Viability of TC6 cells was determined by calorimetric MTT assays after 24 hours' exposure to rising concentrations of INFγ. Data normalised to untreated control and presented as mean +/- standard deviation. *p<0.05, ***p<0.001.*

#### 3.3.2.2.8 Effect of Increasing Concentrations of IL-1β on TC6 Cells

To determine the effect of IL-1β on the viability of TC6 cells, TC6 cells were treated with increasing concentrations of IL-1β (0-1,000ng/ml) for 24 hours. From Figure 3.16, we can observe that increasing concentrations of IL-1β results in progressive falls in the viability of TC6 cells. TC6 cells also appear to have a much greater impact on the viability of TC6 cells compared to BRIN-bd11 cells. Treatment of TC6 cells with 1ng/ml of IL-1β resulted in a significant (-18.9%; $p<0.001$) fall in viability compared to the cell control (cell control 1.0 $\pm$ 0.102 $nA_{570}$, 1ng/ml IL-1β 0.811 $\pm$ 0.082 $nA_{570}$) (Figure 3.16). 10ng/ml resulted in a significant decrease (-24.2%; $p<0.001$) compared to the cell control (cell control 1.0 $\pm$ 0.102 $nA_{570}$, 10ng/ml IL-1β 0.758 $\pm$ 0.107 $nA_{570}$) (Figure 3.16). 100ng/ml resulted in the greatest fall in viability (-25.7%; $p<0.001$) compared to the cell control (cell control 1.0 $\pm$ 0.102 $nA_{570}$, 100ng/ml IL-1β 0.743 $\pm$ 0.076 $nA_{570}$) (Figure 3.16). As a result, 100ng/ml of IL-1β was used for subsequent experimentation on TC6 cells.

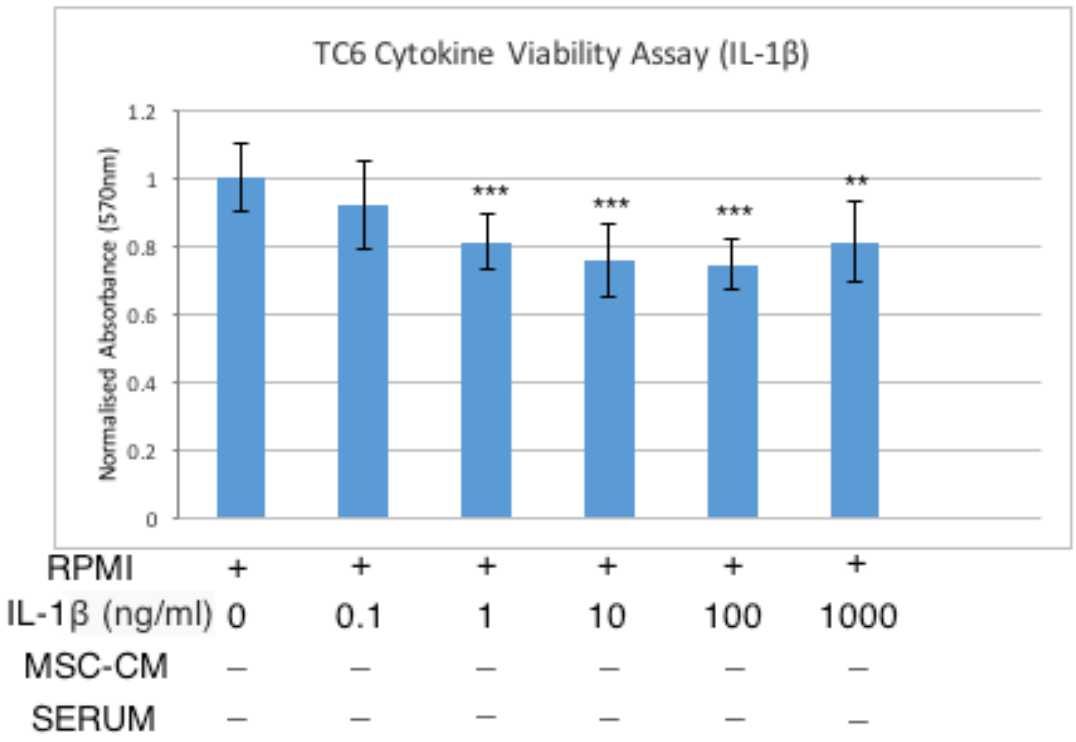


*Figure 3.16 : Effect of 24 hours' exposure to rising concentrations (0.1ng/ml-1,000ng/ml) of IL-1β on the viability of TC6 cells cultured in RPMI medium without serum. Viability of TC6 cells was determined by calorimetric MTT assays after 24 hours' exposure to rising concentrations of IL-1β. Data normalised to untreated control and presented as mean +/- standard deviation. **p<0.01, ***p<0.001.*

#### 3.3.2.2.9 Effect of Increasing Concentrations of Cytomix on TC6 Cells

To determine the effect of a cytomix of TNF$\alpha$, IFN$\gamma$ and IL-1$\beta$ on the viability of TC6 cells, TC6 cells were incubated with increasing concentrations (0-1,000ng/ml) mixture of all three cytokines for 24 hours. Figure 3.17 demonstrates that the cytomix was very effective at reducing TC6 cell viability with progressively greater falls in viability with increasing concentrations of the cytomix. Incubation with 1ng/ml of cytomix was sufficient to result in a significant fall in viability (-28.0%; $p<0.001$) compared to the cell control (cell control 1.0 $\pm$ 0.117 $nA_{570}$, 1ng/ml cytomix 0.720 $\pm$ 0.091 $nA_{570}$) (Figure 3.17). 10ng of cytomix resulted in a significant fall (-24.6%; $p<0.001$) compared to the cell control (cell control 1.0 $\pm$ 0.117 $nA_{570}$, 10ng/ml cytomix 0.754 $\pm$ 0.092 $nA_{570}$) (Figure 3.17). 100ng/ml again resulted in a significant fall in viability (-26.5%; $p<0.001$) compared to the cell control (cell control 1.0 $\pm$ 0.117 $nA_{570}$, 100ng/ml cytomix 0.735 $\pm$ 0.054 $nA_{570}$) (Figure 3.17). Finally, 1,000ng/ml of cytomix resulted in the greatest fall in viability (-39.7%; $p<0.001$) compared to the cell control (cell control 1.0 $\pm$ 0.117 $nA_{570}$, 1,000ng/ml cytomix 0.603 $\pm$ 0.121 $nA_{570}$) (Figure 3.17). As a result, 1,000ng/ml of cytomix was used for subsequent experimentation.

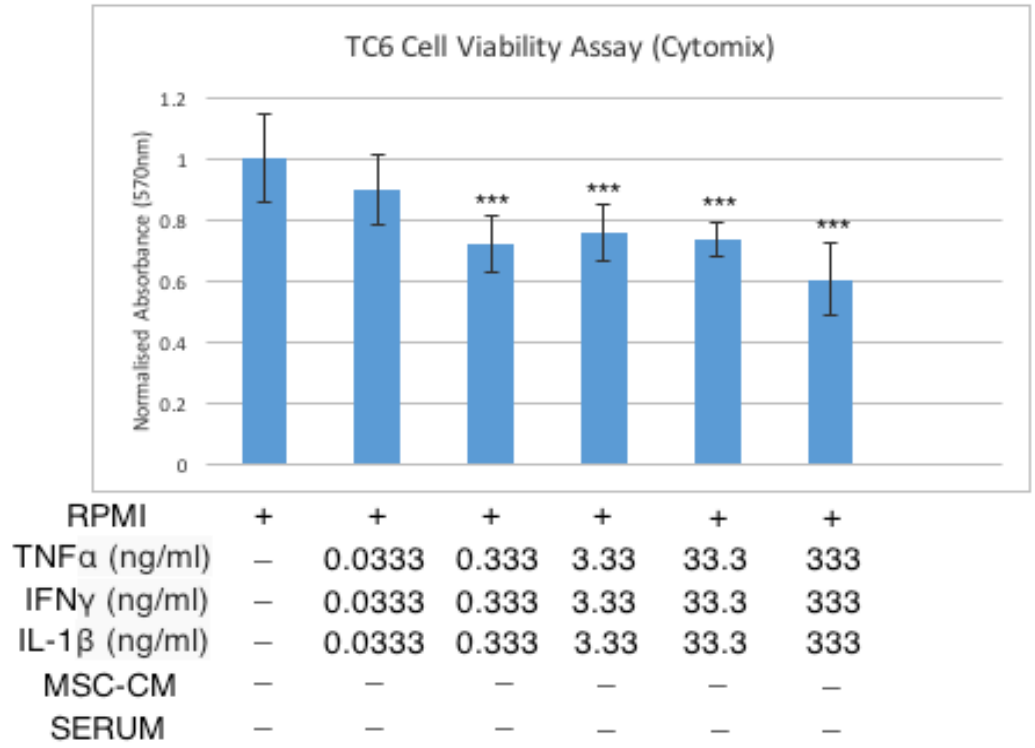


| | | | | | | |
|---|---|---|---|---|---|---|
| RPMI | + | + | + | + | + | + |
| TNFα (ng/ml) | – | 0.0333 | 0.333 | 3.33 | 33.3 | 333 |
| IFNγ (ng/ml) | – | 0.0333 | 0.333 | 3.33 | 33.3 | 333 |
| IL-1β (ng/ml) | – | 0.0333 | 0.333 | 3.33 | 33.3 | 333 |
| MSC-CM | – | – | – | – | – | – |
| SERUM | – | – | – | – | – | – |

*Figure 3.17 : Effect of 24 hours' exposure to rising concentrations (0.1ng/ml-1,000ng/ml) of cytomix on the viability of TC6 cells cultured in RPMI medium without serum. Viability of TC6 cells was determined by calorimetric MTT assays after 24 hours' exposure to rising concentrations of cytomix. Data normalised to untreated control and presented as mean +/- standard deviation. ***p<0.001.*

#### 3.3.2.2.10 MSC-CM Attenuates Cytokine-Driven Falls in Viability in TC6 Cells

To determine the effect of MSC-CM on the viability of TC6 cells when exposed to pro-inflammatory cytokines, TC6 cells were exposed to pro-inflammatory cytokines for 24 hours in the presence and absence of MSC-CM. MTT viability assays were used to determine differences in viability. Optimised concentrations of cytokines determined in previous experiments were used.

Figure 3.18 demonstrates that for all types of pro-inflammatory cytokines, treatment with MSC-CM resulted in significantly greater viabilities for BRIN-bd11 cells compared to cells that were not treated with MSC-CM.

For TC6 cells exposed to 1,000ng/ml TNF$\alpha$, TC6 cells showed significantly greater viability (+12.3%; $p<0.05$) for cells treated with MSC-CM compared to untreated cells (Figure 3.18). For TC6 cells exposed to 1,000ng/ml of cytomix, viabilities were also significantly greater for cells treated with MSC-CM (+29.8%; $p<0.05$) compared to cells that were not treated with MSC-CM. For cells treated with 1,000ng/ml IFN$\gamma$, viability was (+42.6%; $p<0.001$) greater for MSC-CM treated cells compared to untreated cells (Figure 3.18). Finally, for

cells exposed to 100ng/ml IL-1β, viabilities were (+25.7%; p<0.001) compared to cells that were not treated with MSC-CM (Figure 3.18).

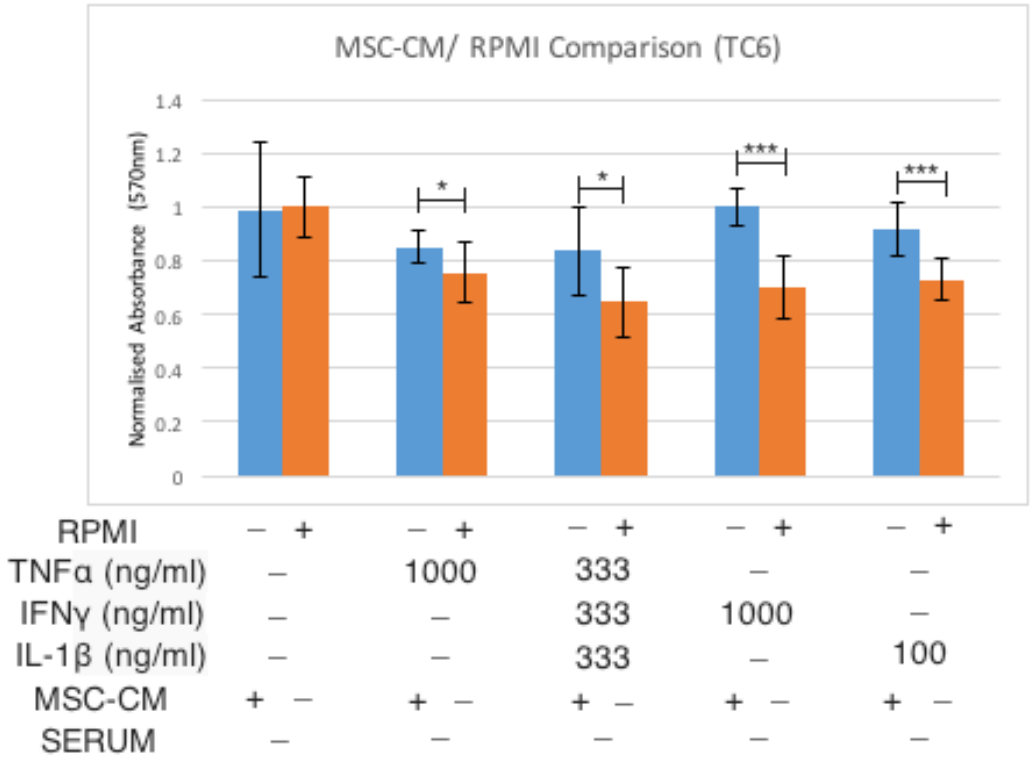


*Figure 3.18: Determining the effect of MSC-CM on the viability of TC6 cells exposed to pro-inflammatory cytokines. Viability of TC6 cells was determined by MTT assay after 24 hours' exposure to pro-inflammatory cytokines (TNFα, IFNγ, IL-1β and cytomix). Data normalised to untreated RPMI control and presented as mean +/- standard deviation. *p<0.05, *p<0.01, ***p<0.001.*

## 3.4 Discussion

Previous studies have shown that beta cell death in the context of type 1 diabetes may be mediated by both direct cell-to-cell contact between immune cells and pancreatic beta cells, as well as the generation of pro-inflammatory cytokines in the microenvironment of the pancreas. These cytokines, TNFα, IL-1β and IFNγ, induce beta cell dysfunction and cell death, eventually resulting in clinically overt diabetes.[118,207]

Mesenchymal stem cells have been shown to protect several cell types from diabetes-induced apoptosis through paracrine actions. In an in vivo model of diabetic cardiomyopathy, MSCs have been shown to protect cardiac myocytes from apoptosis via an Akt-dependent anti-apoptotic signalling cascade.[241] In another study, MSCs protected podocytes from apoptosis in an in vitro model of diabetic nephropathy.[242] Our study aimed to determine whether the MSC-CM is capable of preserving cellular viability when cells are treated with pro-inflammatory cytokines. This was determined by measurements of mitochondrial metabolisms of cells by MTT assays.

The findings presented in this chapter confirmed that cellular viability progressively decreases with increasing concentrations of pro-inflammatory cytokines in the BRIN-bd11 and TC6 beta cell lines. It has also demonstrated that MSC-CM appears to attenuate this fall in viability in both BRIN-bd11 and TC6 cells, indicating that the MSC secretome could contain factors that inhibit cytokine-induced falls in viability. However, it is important to note that due to limitations in the experimental method, the data presented in this chapter needs to be interpreted with caution. The MTT assay does not determine the mechanisms of cell death, and only looks at mitochondrial metabolism which can be used to quantify metabolically active cells remaining in the wells. Ideally further experiments should be performed to confirm that apoptosis via pro-inflammatory cytokines is indeed attenuated by the MSC-conditioned medium.

In addition to these findings, we have also observed consistently increased viability readings of BRIN-bd11 cells treated for 24 hours in MSC-CM compared to cells that are not treated with MSC-CM in the absence of pro-inflammatory cytokines were observed. The MSC-CM has previously been

shown to contain trophic factors, including VEGF, HGF and IGF.[63] Thus we could hypothesise that in addition to inhibiting apoptotic mechanisms, the MSC-CM may indeed promote cellular growth and division of beta cells. This could be another mechanism to account for the increased islet size of MSC-CM-treated mice in previous murine models of diabetes. Previous studies have shown the capabilities of the MSC secretome in promoting the proliferation of a number of cell types. A study by Gao *et al.* demonstrated proliferation of beta cells in MSC-CM-treated mice in a STZ model of diabetes.[243] They confirmed that MSC-CM could upregulate the expression of pERK and pAKT in this model. Subsequent blockage of the pAKT pathway ameliorated the proliferative effect observed, indicating that the pathway plays a crucial role in beta cell proliferation.[243]

An *in vitro* study conducted by Y Zhou *et al.* demonstrated that umbilical-derived MSCs (uMSCs) secreted factors that improved the viability of isolated rat islets separated from the uMSCs via a trans-well plate.[240] MTS viability assays were used to measure changes in viability in this experiment. Furthermore, in a subsequent, streptozocin-induced murine model of diabetes, uMSCs were shown to migrate to the pancreas and express IGF-1,

HGF and PDGFA. These factors were shown to activate the Pi3K and pERK pathways in the pancreatic beta cells. Further analysis of cell-cycle genes, including cyclin D1, cyclin D2, p21 and p27, showed doubling of cyclin D2 but no significant changes in other cell cycle genes.[240] Thus the conclusion was drawn that the anti-apoptotic activities of uMSCs played the predominant role in the improved islet size seen in this experiment.

The MSC-CM has been shown to increase the rate of proliferation of other cell types. A study by Li *et al*. demonstrated that MSC-CM reversed the downregulation of MEK 1/2 and ERK 1/2 phosphorylation via LPS in keratinocytes in a model of diabetic wound healing.[244] Senescent MSCs release factors that promote proliferation and migration of cancer cells.[245,246] Indeed, cancer is widely recognised to be a disease caused by gain of function mutations of proto-oncogenes that drive the cell cycle forward, and loss of functions of tumour suppressor genes that prevent apoptosis of dysfunctional cells.[247] The tumorigenicity of stem cell products is one of the limitations and a potential drawback that needs to be overcome before these therapies could be considered safe for clinical use.

In the context of the results presented in this chapter, the potential proliferative effect of MSC-CM on beta cells presents an unexpected and exciting additional factor. These results could point toward the MSC-CM having a direct trophic effect on beta cells in addition to attenuating cytokine-induced apoptosis. However, the MTT assay does not strictly measure proliferation or viability, but rather is a measure of the metabolic activity of the cells, which may not directly mirror the number of cells in culture. Should the MSC-CM increase the metabolic rate of cells, this could have resulted in misleading results. Thus, although these results are interesting, they need to be substantiated with further experimentation.

In this chapter, we aimed to test the theory that MSC-CM improves the viability as measured by mitochondrial metabolism of beta cells in vitro when exposed to pro-inflammatory cytokines implicated in the pathogenesis of type 1 diabetes. The results appear to suggest that this is the case; however, the components of the secretome that confer these benefits and the mechanisms by which they do so remain to be elucidated, and further research is required to answer the many questions raised.


# Chapter 4: Exploration of the Effect of MSC-CM on an in Vivo Model of Autoimmune-Mediated Diabetes

# 4.1 Introduction

Chapter 3 explored the effect of the MSC-CM on an in vitro model of cytokine-mediated beta cell apoptosis, a key element of the pathophysiology of type 1 diabetes. We demonstrated that that the MSC-CM could improve viabilities of beta cell lines via calorimetric MTT assays. In this chapter, we aim to determine whether the beneficial effects of the MSC-CM can be extended to and demonstrated in an in vivo model of diabetes.

The MSC-conditioned medium has been shown in previous in vivo studies to promote the repair of islets from diabetic mice in vivo through paracrine actions. These studies showed homing of the MSCs to the damaged pancreas and subsequent improvements in beta cell mass and insulin secretion in mice treated with systemic MSCs.[238,240] As alluded to in Chapter 3, the observed effects could be due to a number of factors. These could include attenuation of immune response through actions of the MSC-CM on immune cells, provision of trophic support to beta cells through factors like VEGF that promotes angiogenesis to damaged islets, as well as the potential transdifferentiation of MSCs to insulin-secreting cells as proposed by Li *et al*.[50.56,57,,65,74]

The experiments in his Chapter were conducted to determine whether the MSC secretome contained in the MSC-CM is able to ameliorate the Type-1 diabetic state *in vivo.* The objectives of this study are:

- Establish a murine model of type 1 diabetes via multiple low dose Intraperitoneal injections of streptozocin (STZ).
- Determine if MSC-CM improves islet functionality using terminal plasma insulin ELISAs.
- Determine if MSC-CM improves retention of body fat/weight via DEXA scans.
- Determine if MSC-CM improves islet morphology through pancreatic histology.

The success of this study would lend further support to the therapeutic potential of the MSC secretome on a live model of diabetes, and determine its potential for use as a therapeutic option in diabetes.

## 4.2 Methods

Materials

Materials used in the in vivo experiments are listed in Section 2.1.

Animal Husbandry

Animals were reared in accordance to procedures detailed in Section 2.4.1. Induction of diabetes, monitoring of mice and processing of mice are described in Section 2.4.1.

Insulin ELISA

Blood plasma was obtained from mice as detailed in Section 2.4.1. Insulin ELISAs were performed on obtained serum samples as described in Section 2.4.2.

DEXA Scans

DEXA scans were performed on mice to determine body fat percentage and lean mass as described in Section 2.4.3.

Pancreatic Histology

Pancreata were obtained from mice and preserved in formaldehyde as described in Section 2.4.1. Tissue was processed and imaged as described in Section 2.4.4.

# 4.3 Results

## 4.3.1 Terminal Insulin ELISAs

To determine the secretory profile of the pancreatic beta cells, Insulin ELISAs were performed on terminal plasma obtained from the mice. Figure 4.1 demonstrates that treatment with STZ significantly reduced (-23.7%; $p<0.05$) terminal plasma insulin compared to the non-diabetic control (non-diabetic control 0.477 $\pm$ 0.090ng/ml, STZ 0.364 $\pm$ 0.040ng/ml). MSC-CM appears to partially restore insulin secretion in STZ-treated mice. Mice treated with STZ and MSC-CM had greater (+24.4%; $p = 0.08$) terminal plasma insulin compared to mice treated with STZ alone (STZ + MSC-CM 0.453 $\pm$ 0.098ng/ml, STZ 0.364 $\pm$ 0.040ng/ml) although this was not significant at the 5% confidence interval (Figure 4.1).

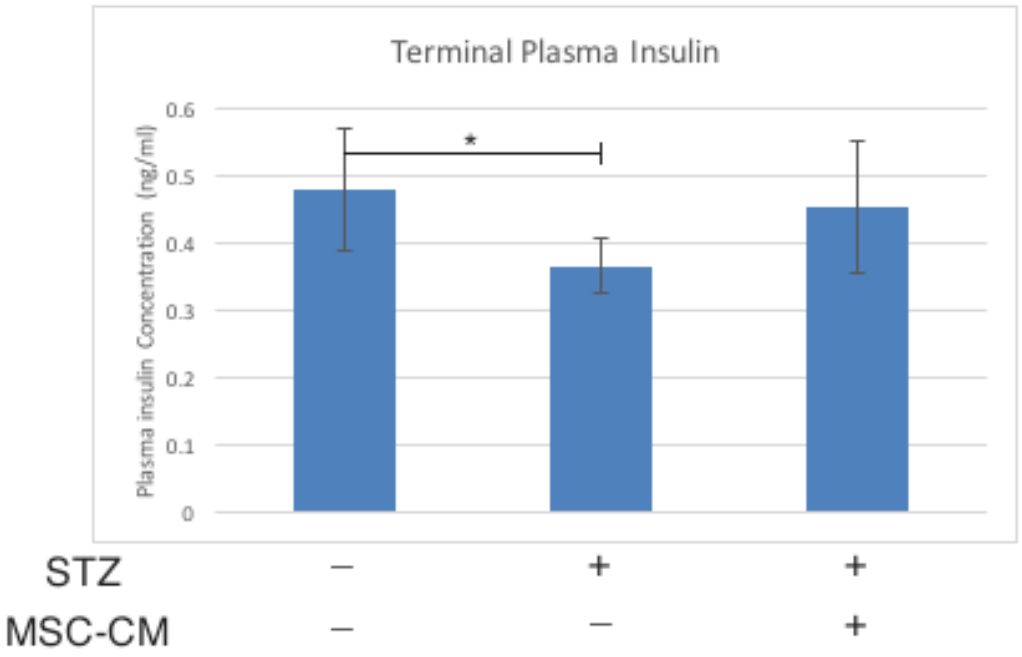


*Figure 4.1: Graph of terminal plasma insulin concentrations for untreated controls, STZ diabetic mice and STZ diabetic mice treated with MSC-CM. Insulin concentration was determined by ELISA. Data presented as mean +/- standard deviation. *p<0.05*

### 4.3.2 DEXA Scans

DEXA scans were performed to compare body composition of mice. Mice treated with STZ had a significantly reduced (-25.6%; $p<0.01$) total body fat compared to non-diabetic control mice (non-diabetic control $3.68 \pm 0.705$g, STZ $2.74 \pm 0.504$g) (Figure 4.2). Treatment with MSC-CM did not result in a significant improvement in fat content in STZ treated mice (STZ $2.74 \pm 0.504$g,

STZ + MSC-CM 2.61 ± 0.695g) (Figure 4.2). These results are reflected in the body fat percentages with significant falls in percentage body fat seen in both STZ-treated mice (-19.2%; $p<0.05$) and STZ + MSC-CM-treated mice (-24.8%; $p<0.01$). Significant falls in body weight were seen for both untreated diabetic mice (-5.4%; $p<0.001$) and MSC-CM-treated diabetic mice (-6.4%; $p<0.001$) compared to the non-diabetic controls (non-diabetic control 27.05 ± 0.926g, STZ 25.58 ± 1.463g, STZ + MSC-CM 25.325 ± 0.721g). No significant differences were seen between groups for lean masses (Figure 4.2).

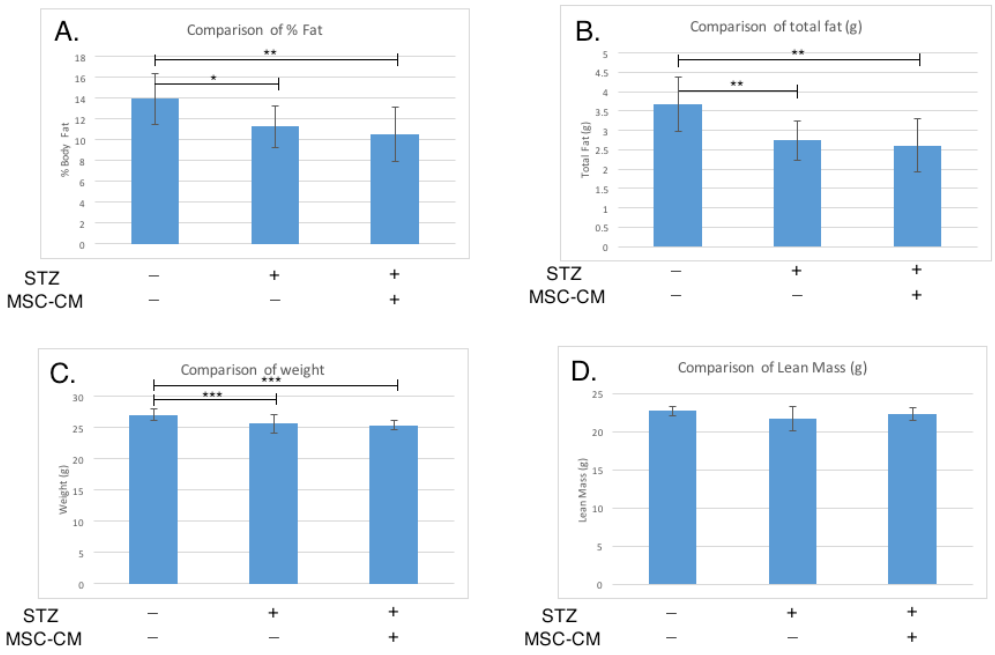


*Figure 4.2 : Comparison of percentage fat, total fat, weight and lean mass measured using DEXA scans. A - comparison of percentage fat; B - Comparison of total fat; C - Comparison of weight; D - Comparison of lean mass. Data presented as mean +/- standard deviation. *p<0.05, **p<0.01, ***p<0.001*

### 4.3.3 Pancreatic Histology

Pancreatic histology shows Islets of Langerhans which can be seen as clusters of cells marked by asterisks for illustration in Figure 4.3. These are surrounded by the secretory acinar cells which function as the exocrine part of the pancreas.

Histological analysis revealed a significant reduction in islet size and number in the STZ diabetic mice compared to both the non-diabetic control and STZ diabetic mice treated with MSC-CM. Representative examples of histological images obtained are shown in Figure 4.3. Measurement of islet area revealed a significant reduction (-27.3%; $p<0.01$) in islet size in mice treated with STZ compared to the non-diabetic control (non-diabetic control 56,419 $\pm$ 14,246$\mu m^2$, STZ 40,995 $\pm$ 10,899$\mu m^2$) (Figure 4.4). Treatment with MSC-CM appeared to restore islet morphology and size as seen with the significantly greater (+32.7%; $p<0.05$) islet size in MSC-CM + STZ-treated mice compared to mice treated with STZ alone (STZ 40,995 $\pm$ 10,899$\mu m^2$, STZ + MSC-CM 54,391 $\pm$ 13,472$\mu m^2$) (Figure 4.4).

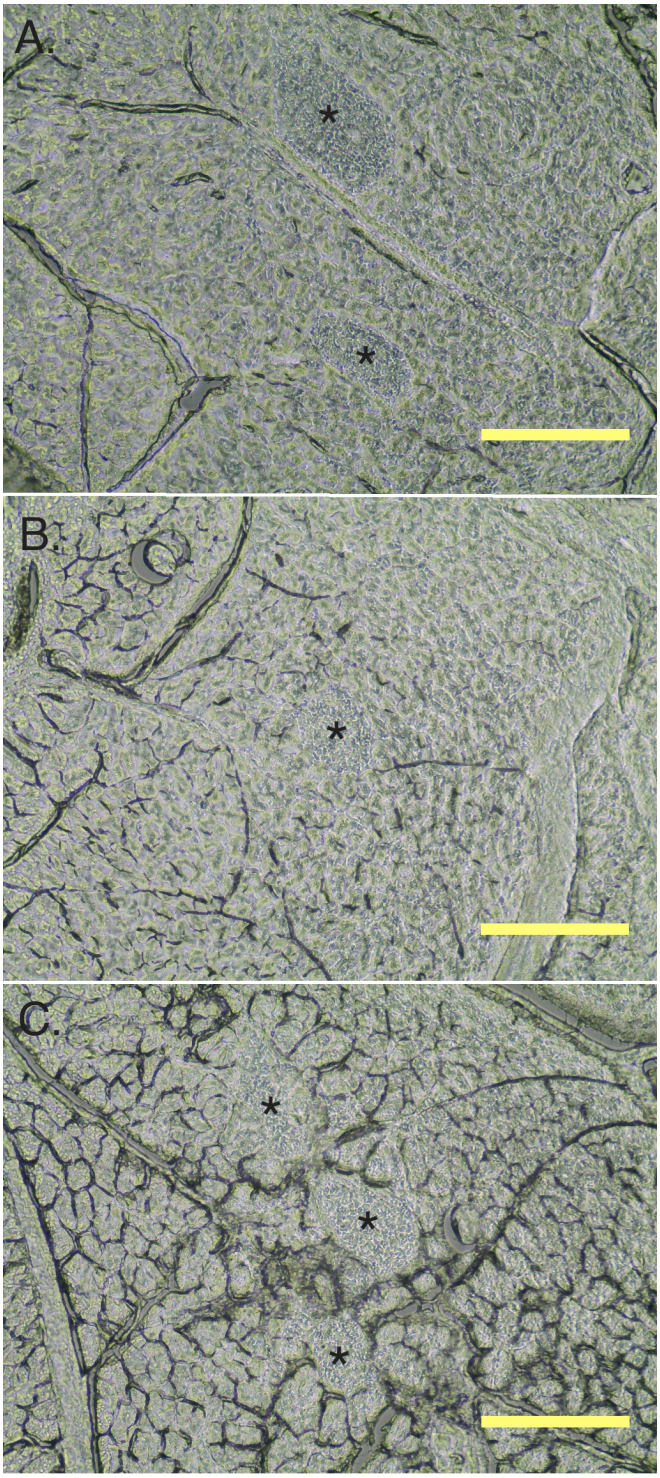


*Figure 4.3: Images depicting pancreatic islet histology of mice. A - histology from non-diabetic control mice; B - histology from STZ diabetic mice; C - histology from STZ diabetic mice treated with MSC-CM. Asterisk denotes location of islets (scale bar = 200μm).*

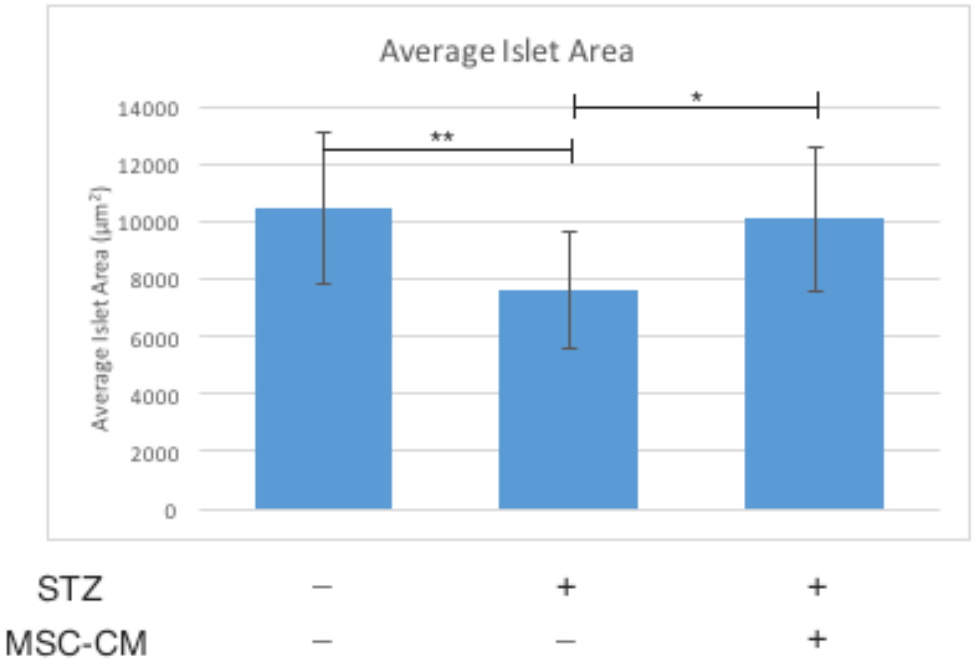


*Figure 4.4 : Graph of average islet area for untreated controls, STZ diabetic mice and STZ diabetic mice treated with MSC-CM. Data presented as mean +/- standard deviation. *p<0.05, **p<0.01*

## 4.4 Discussion

This chapter aimed to explore the effect of MSC-CM on a streptozocin-induced model of diabetes in mice. Our study shows that as expected, treatment of mice with streptozocin resulted in decreased body weight and loss of body fat. This is thought to result from an inability of diabetic mice to metabolise carbohydrate food stores, leading to a shift to fatty acid metabolism and subsequent loss of body fat as depicted in the DEXA scans we conducted.[248] Treatment with MSC-CM appears to have improved islet function and islet morphology as determined by serum ELISAs and histological analysis at the time of death. However, no significant difference between the weight and body fat of MSC-CM treated diabetic mice and non-treated diabetic mice was observed.

The diabetic microenvironment in type-1 diabetes is known to cause beta cell dysfunction.[117, 123,143,144,146] Although the beta cell mass in the STZ treated mice may be maintained by the trophic and cytoprotective effects of the MSC-CM, the beta cells may be dysfunctional and unable to appropriately secrete insulin in response to changes in blood glucose. Thus a shift to fatty acid metabolism may still occur in the MSC-CM treated diabetic mice. Further

study involving functional tests such as intraperitoneal glucose tolerance tests (IPGTT) could provide insight in to the functionality of beta cells in mice treated with streptozocin and whether MSC-CM could prevent beta cell dysfunction and improve insulin responsiveness. STZ is also known to cause hepatotoxicity and nephrotoxicity which could result in stress and subsequent weight loss.[237] This may account for some of the weight loss seen in both groups of STZ treated mice.

There are significant limitations to the experimental method used in this chapter. The study looked at a snapshot of the insulin profile, islet histology and body fat content at the time of culling. This does not allow for a trend to be determined for glycaemic control and body habitus. Ideally, the experiment should be conducted to allow for periodic monitoring of the blood glucose and body weight as well as serum insulin over the course of the experiment. The experiment was also performed with 8 animals in each group, which presents a relatively small sample size. Ideally, a larger sample size could be used to reduce the propensity for error. Furthermore, the experiment does not allow us to determine the components of the MSC-CM that confers its therapeutic benefit.

In conclusion, periodic IP injections of MSC-CM appeared to improve insulin secretion and islet histology of diabetic mice in this experiment, although further research is needed to determine the components of the MSC secretome that exert these therapeutic effects and whether MSC-CM is able to ameliorate beta cell dysfunction in type 1 diabetes.


# Chapter 5: Characterising the IL-10 Receptor on Beta Cells

# 5.1 Introduction

Type 1 diabetes, as described in Chapter 1, is a TH1-mediated immune response resulting in the death of pancreatic beta cells.[189] Pro-inflammatory cytokines, namely TNF$\alpha$, IFN$\gamma$ and IL-1$\beta$, have been shown to be implicated in its pathogenesis.[207] These factors activate the NF-κB and AP-1 pathways in pancreatic beta cells leading to apoptosis, depletion of the beta cell mass and eventually clinically overt diabetes.[118-120,158-161,187]

Clinical trials utilising stem cell therapy for the treatment of type 1 diabetes have shown promising results. A number of studies including a study by Voltarelli et al. have shown improved biochemical markers for patients receiving treatment, indicating improved insulin production and beta cell function.[249] However, the factors that mediate this therapeutic effect largely remain unknown.

We theorise that the MSC secretome may contain factors that directly protect beta cells from apoptosis induced by pro-inflammatory cytokines. In Chapter 3, we demonstrated that conditioned medium containing the MSC secretome significantly improves the viability of BRIN-bd11 cells in vitro measured using

MTT assays. We have also demonstrated improved islet function in rats treated with MSC-CM in an in vivo streptozocin model of diabetes. The components of the secretome that confer these therapeutic properties remain to be fully characterised, and this is an area that is being studied extensively. Proteomic assays have uncovered many factors in the MSC secretome that could potentially confer this benefit.[63]

Previous studies have shown IL-10 to be a soluble factor secreted by MSCs.[63] IL-10 is known to broadly act as an immune-regulatory cytokine, despite also having immune-stimulatory effects on certain cell types.[200-206,212,213,216] The immune-regulatory properties of this cytokine could potentially explain some of the therapeutic effects observed.

It could be hypothesised that in addition to these immune-regulatory effects, IL-10 may directly interact with beta cells and prevent cellular dysfunction and subsequent apoptosis. As alluded to in Chapter 1, IL-10 has been shown to potentially inhibit the NF-κB pathway through the expression of AIR factors, as well as stabilising IκB in the cytosol and preventing the translocation of NF-κB to the nucleus.[174,188,189-192].

The IL-10 receptor is known to be expressed on haematopoietic cells and is involved with immunoregulation.[180] Expression has also been characterised in tissues such as epithelial cells of the lung and small intestine.[250,251] The expression of the IL-10 receptor on pancreatic beta cells however remains poorly characterised.

This chapter aims to determine whether IL-10 could directly interact with beta cells and contribute to the cytoprotection of beta cells conferred by the MSC-CM. The Objectives of this Chapter are:

- Characterise the presence of IL-10 in MSC-CM using ELISA assays
- Characterise the presence of the IL-10 receptor on beta cell lines through Electrophoresis
- Characterise the presence of the IL-10 receptor on beta cell lines through immunofluorescence.

Confirming the presence of IL-10 receptors on pancreatic islet cells and IL-10 in MSC-CM are the first steps in determining whether this factor plays an important role in the direct cytoprotection of pancreatic islet cells conferred by the mesenchymal stem cell secretome.

# 5.2 Serial ELISAs for IL-10

## 5.2.1 Methods

Materials

Materials used in this experiment are detailed in Section 2.1.

MSC Culture Methods

MSCs were recovered and expanded as detailed in Section 2.2.7. Isolation and culture of MSCs is detailed in Section 2.2.8. Passaging of cells is detailed in Section 2.2.5.

Procurement and Collection of MSC-CM

Production of MSC-CM for subsequent use in ELISAs is detailed in Section 2.2.10.

IL-10 Serial ELISAs

ELISAs were conducted to determine concentrations of IL-10 in MSC-CM and determine falls in concentrations of IL-10 after transfers between ELISA plates. Details of the methodology including preparation of materials, plate preparation and serial ELISA protocol can be found in Section 2.3.4.

## 5.2.2 Results of Serial ELISAs for IL-10 on MSC-CM

The concentration of IL-10 in MSC-CM was determined to be 3,529 $\pm$ 195 pg/ml. The concentration of IL-10 fell significantly (-54.4%; $p<0.001$) after one transfer (T0 3,529 $\pm$ 195pg/ml, T1 1,610 $\pm$ 506pg/ml). After the second transfer, the concentration was determined to have fallen significantly again (-88.1%; $p<0.001$) as compared to T1 (T1 1,610 $\pm$ 195pg/ml, T2 192 $\pm$ 655) (Figure 5.1). This confirms that sequential ELISAs are a viable method of depleting IL-10 from conditioned medium.

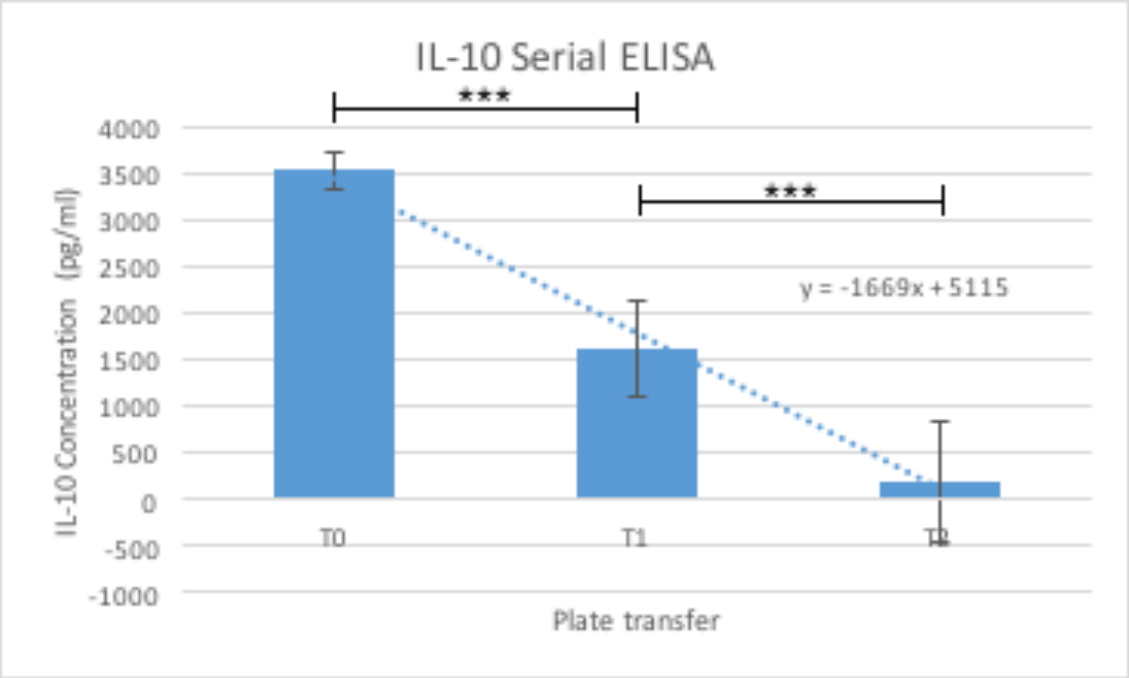


*Figure 5.1 : Serial ELISAs for detection of IL-10 concentrations in MSC-conditioned RPMI medium (MSC-CM). T0 represents concentrations of IL-10 in MSC-CM (Plate 1). T1 shows concentration of IL-10 remaining in MSC-CM transferred from Plate 1 to Plate 2. T2 shows concentration of IL-10 remaining in MSC-CM after transfer from Plate 2 to Plate 3. Data presented as mean +/- standard deviation. ***P<0.001.*

# 5.3 Characterising the IL-10 Receptor on Beta Cells by RT-PCR and Electrophoresis

## 5.3.1 Methods

Materials

Materials used in this experiment can be found in Section 2.1.

Cell Lines Utilised

BRIN-bd11, TC6 cells and MSCs cells were utilised in this experiment. Details of the cell lines used can be found in Section 2.2.2.

Cell Culture Methods

Cells were obtained from liquid nitrogen dewars located at the Guy Hilton Research Center, Stoke-on-Trent, UK, and thawed as detailed in Section 2.2.4. Cells were trypsonised and suspended in medium as detailed in Section 2.2.5. Cell counts were performed as detailed in Section 2.2.6.

MSC Culture Methods

MSCs were recovered and expanded as detailed in Section 2.2.7. Isolation and culture of MSCs is detailed in Section 2.2.8. Cells were trypsonised and suspended in medium as detailed in Section 2.2.5. Cell counts were performed as detailed in Section 2.2.6.

RT-PCR Method

RNA was extracted from BRIN-bd11 cells, TC6 cells and MSCs as detailed in Section 2.3.5. RNA analysis was performed on extracted RNA as described in Section 2.3.6. RT-PCR was performed on extracted RNA as described in Section 2.3.7. Primer design for use in RT-PCR is described in Section 2.3.8.

Electrophoresis Method

Electrophoresis was performed on RT-PCR products to determine their base pair length. Protocol for electrophoresis and imaging of gels can be found in Section 2.3.9.

## 5.3.2 Results

### 5.3.2.1 Gel Electrophoresis of PCR Products for the IL-10 Receptor from BRIN-bd11 Cells (Experiment 1)

To determine the presence of IL10 receptors on BRIN-bd11 cells, RNA was extracted from BRIN-bd11 cells and RT-PCR performed on the RNA extract. Base pair length of RT-PCR products was determined by electrophoresis. Primers used are detailed in Table 5.1.

In addition to the GAPDH positive control, excess primer mixes were used to run the experiment with RNA extracted from Jurkat cells. Jurkat cells are cells known to express the IL-10 receptor and this allows a comparison between the BRIN-bd11 cells and Jurkat IL10RA and IL10RB results.

In Figure 5.2, laddering of the bands can be seen for the BRIN bd-11 IL10RA and IL10RB samples as well as splitting of the IL10RA Jurkat band. This could be a result of several causes, including RNA contamination of the original BRIN-bd11 RNA sample and non-specific binding of the primers. The negative controls showed no bands, indicating that RNA contamination did not occur over the course of the RT-PCR and electrophoresis experiments. The end

product of the IL10RA for the Jurkat cells was in the correct position with an expected base pair value of 175 (Figure 5.2) The IL10RB result for the Jurkat cells was also as expected with an expected base pair value of 259 (Figure 5.2). In contrast to this, the BRIN-bd11 IL10RA and IL10RB bands were not of the expected base pair value. The experiment was repeated with alterations detailed in Section 5.3.2.2.

| Gene ID | Accession number | Primer Pair | Sequence (5'-3') | Product length | Melting Temp (°C) |
|---|---|---|---|---|---|
| IL10RA | NM_001558.3 Homo sapiens interleukin 10 receptor, alpha (IL10RA), transcript variant 1, mRNA | 3 | Forward AGTCACTTCCGAG AGTATGA<br><br>Reverse TAGACCACATCCC CTTGTTA | 175 | Forward 55.03<br><br>Reverse 55.13 |
| IL10RB | NM_000628.4 Homo sapiens interleukin 10 receptor, beta (IL10RB), mRNA | 7 | Forward CTCCCCAGTATGA CTTTGAG<br><br>Reverse AAGGCGTACTTTG TCTTCTT | 259 | Forward 59.75<br><br>Reverse 59.60 |
| GAPDH | NM_001256799.2 Homo sapiens glyceraldehyde-3-phosphate dehydrogenase (GAPDH), transcript variant 2, mRNA | 2 | Forward GAAAGCCTGCCG GTGACTAA<br><br>Reverse TTCCCGTTCTCAG CCTTGAC- | 301 | Forward 60.32<br><br>Reverse 59.97 |

*Table 5.1 : Primers used in BRIN-bd11 electrophoresis (Experiment 1)*

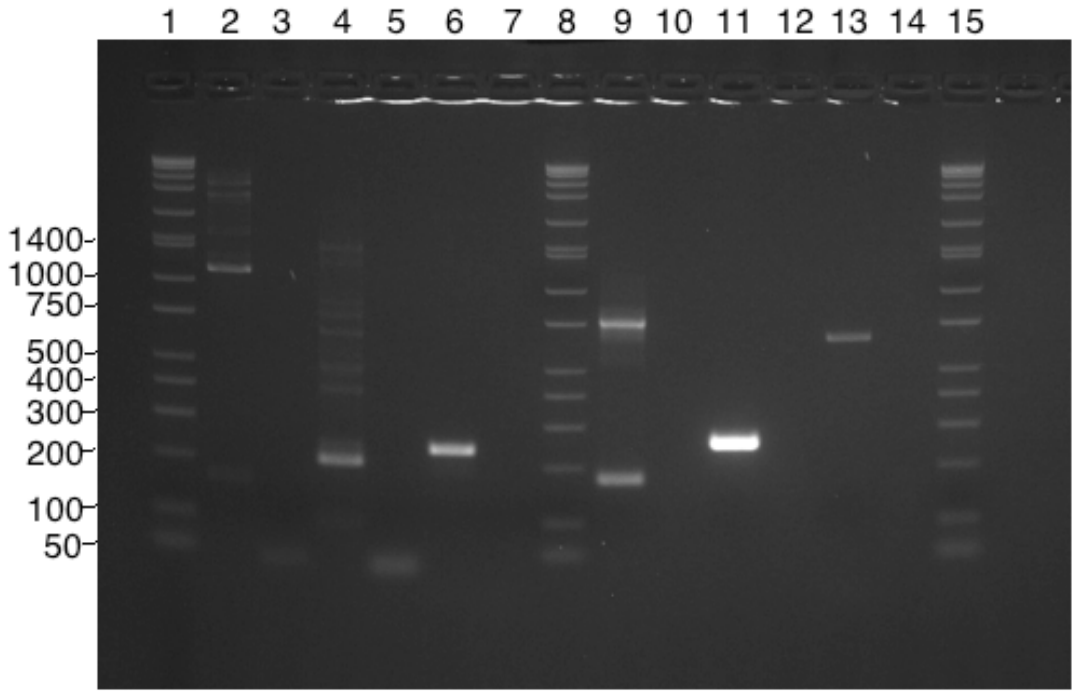


*Figure 5.2 : Electrophoresis of BRIN-bd11 cells (Experiment 1). 1 - DNA ladder; 2 - IL10RA (BRIN-bd11); 3 - IL10RA (negative control); 4 - IL10RB (BRIN-bd11); 5 - IL10RB (negative control); 6 - GAPDH (BRIN-bd11); 7 - GAPDH (negative control); 8 - DNA ladder; 9 - IL10RA (Jurkat); 10 - IL10RA (negative control); 11 - IL10RB (Jurkat); 12 - IL10RB (negative control); 13 – GAPDH (Jurkat); 14 - GAPDH (negative control); 15 - DNA ladder.*

#### 5.3.2.2 Gel Electrophoresis of PCR Products for the IL-10 Receptor from BRIN-bd11 Cells (Experiment 2)

Due to the potential RNA contamination of the original sample during RNA extraction, a new batch of RNA was extracted from BRIN-bd11 cells. RT-PCR and electrophoresis were subsequently performed. New primers were designed for this experiment. Primers used are detailed in Table 5.2.

In the second experiment, no bands were seen for IL10RA for either the BRIN-BD11 or Jurkat cells. A clear band for IL10RB was seen for the Jurkat cells with the correct base pair length of 618; however, no clear bands for IL10RB were seen for the BRIN-bd11 cells (Figure 5.3).

Both experiments 1 and 2 showed that in most cases the primers worked for the Jurkat cells but not the BRIN-bd11 cells. Jurkat cells are a human line of cells whereas BRIN-bd11 are derived from rat pancreatic cells. The primers used in the first two experiments were based on the human gene template. Thus this confirms that species-specific primers should be designed for use in the experiment. Primers based on *rattus norvegicus* (the brown Norway rat) gene template were designed and used for the third experiment.

| Gene ID | Accession number | Primer Pair | Sequence (5'-3') | Product length | Melting Temp (°C) |
|---|---|---|---|---|---|
| IL10RA | NM_001558.3 Homo sapiens interleukin 10 receptor subunit alpha (IL10RA), transcript variant 1, mRNA | 2 | Forward AGAGGGCCTCAATCTCCCAT<br>Reverse CAAGCCAGCTTGGTAGTCCA | 129 | Forward 60.03<br>Reverse 59.96 |
| IL10RB | NM_000628.4 Homo sapiens interleukin 10 receptor subunit beta (IL10RB), mRNA | 1 | Forward CAGACCCTGGACTTAGCCAC<br>Reverse GAGCTGACCACCCTTGAGTT | 618 | Forward 59.75<br>Reverse 59.60 |
| GAPDH | NM_001256799.2 Homo sapiens glyceraldehyde-3-phosphate dehydrogenase (GAPDH), transcript variant 2, mRNA | 2 | Forward GAAAGCCTGCCGGTGACTAA<br>Reverse TTCCCGTTCTCAGCCTTGAC | 301 | Forward 60.32<br>Reverse 59.97 |

*Table 5.2 : Primers used in BRIN-bd11 electrophoresis (Experiment 2)*

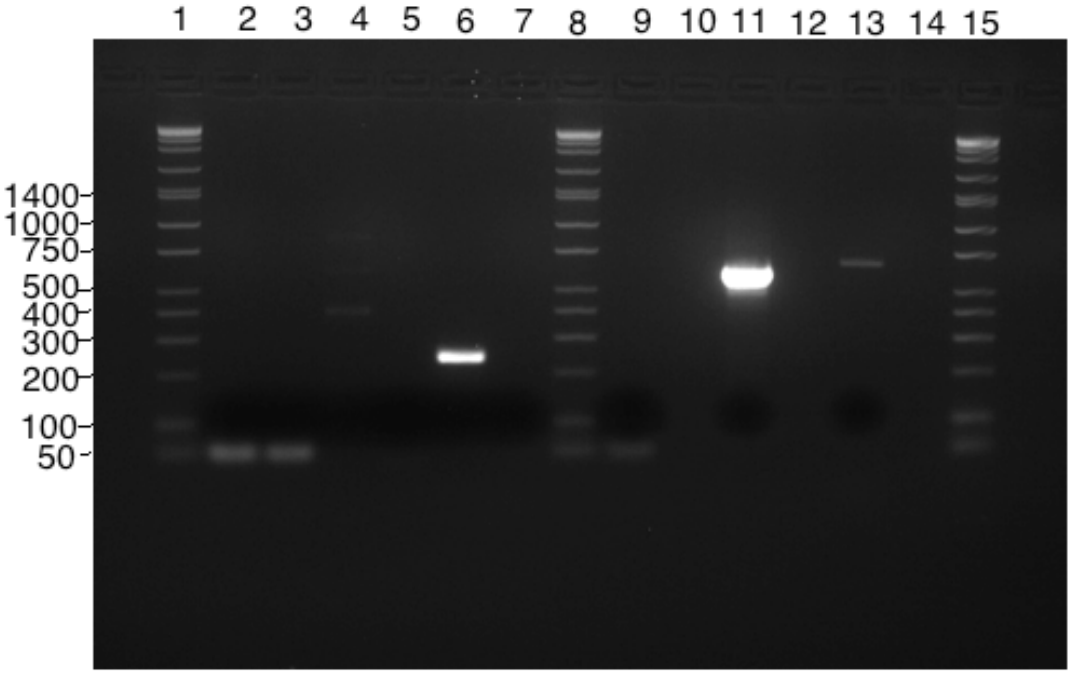


*Figure 5.3 : Electrophoresis of BRIN-bd11 cells (Experiment 2). 1 - DNA ladder; 2 - IL10RA (BRIN-bd11); 3 - IL10RA (negative control); 4 - IL10RB (BRIN-bd11); 5 - IL10RB (negative control); 6 - GAPDH (BRIN-bd11); 7 - GAPDH (negative control); 8 - DNA ladder; 9 - IL10RA (Jurkat); 10 - IL10RA (negative control); 11 - IL10RB (Jurkat); 12 - IL10RB (negative control); 13 – GAPDH (Jurkat); 14 - GAPDH (negative control); 15 - DNA ladder.*

#### 5.3.2.3 Gel Electrophoresis of PCR Products for the IL-10 Receptor from BRIN-bd11 Cells (Experiment 3)

A new batch of RNA was extracted from BRIN-bd11 cells. RT-PCR and electrophoresis were subsequently performed. However, in this experiment the Jurkat positive control was omitted as primers designed to be specific to the gene template of rattus norvegecus will not work for a human derived Jurkat T-cell line. New primers were designed using the gene template for *rattus norvegicus* and custom oligos were ordered from Thermo Fisher Scientific. These primers are detailed in Table 5.3.

The final product size for IL10RA, IL10RB and GAPDH was as expected as illustrated in Figure 5.4b. This demonstrates that species-specific primers should be designed for RT-PCR. There was however laddering of the bands as shown in Figure 5.4a. This could again be due to non-specific binding of the primers or RNA contamination of the RNA sample. The experiment was repeated with a new batch of RNA and the annealing temperature was increased from 55$^{o}$C to 56$^{o}$C to increase the specificity of primer binding. The results are shown in Figure 5.5.

Further raising the annealing temperature to 59$^{o}$C to increase the specificity of primer binding was shown to remove laddering as depicted in Figure 5.6a. The product size was as expected for IL10RA, IL10RB and GAPDH as depicted in Figure 5.6b. This experiment demonstrates that closely matching the annealing temperature of the thermal cycler to the melting temperature of the primers utilised can improve results by increasing specificity of primer binding.

In summary, gel electrophoresis of PCR products from BRIN-bd11 cells using primers specific to the IL10RA, IL10RB and GAPDH genes of *rattus norvegicus* showed positive results for IL10RA as depicted in Lane 2 of Figure 5.6a (expected bp 313). Positive results were shown for IL10RB as depicted in Lane 4 of Figure 5.6a (expected bp 483). Positive results were shown for GAPDH as depicted in Lane 6 of Figure 5.6a (expected bp 262). Individual base pair comparisons are shown in Figure 5.6b.

| Gene ID | Accession number | Primer Pair | Sequence (5'-3') | Product length | Melting Temp ($^{o}$C) |
|---|---|---|---|---|---|
| IL10RA | NM_057193.2 Rattus norvegicus interleukin 10 receptor subunit alpha (IL10RA), mRNA | 2 | Forward GATTCCCTTGGCAGAAGCCT<br><br>Reverse CAATGGCAGGGTGACCAGAT | 313 | Forward 60.03<br><br>Reverse 60.03 |
| IL10RB | NM_001107111.1 Rattus norvegicus interleukin 10 receptor subunit beta (IL10RB), mRNA | 1 | Forward TGGTACTTCCAAGACCGCTG<br><br>Reverse GGGAGGGGTTGTTTCATCAC | 483 | Forward 59.68<br><br>Reverse 58.45 |
| GAPDH | NM_017008.4 Rattus norvegicus glyceraldehyde-3-phosphate dehydrogenase (GAPDH), mRNA | 1 | Forward GCATCTTCTTGTGCAGTGCC<br><br>Reverse GATGGTGATGGGTTTCCCGT | 262 | Forward 60.11<br><br>Reverse 60.03 |

*Table 5.3: Primers used in BRIN-bd11 electrophoresis (Experiment 3)*

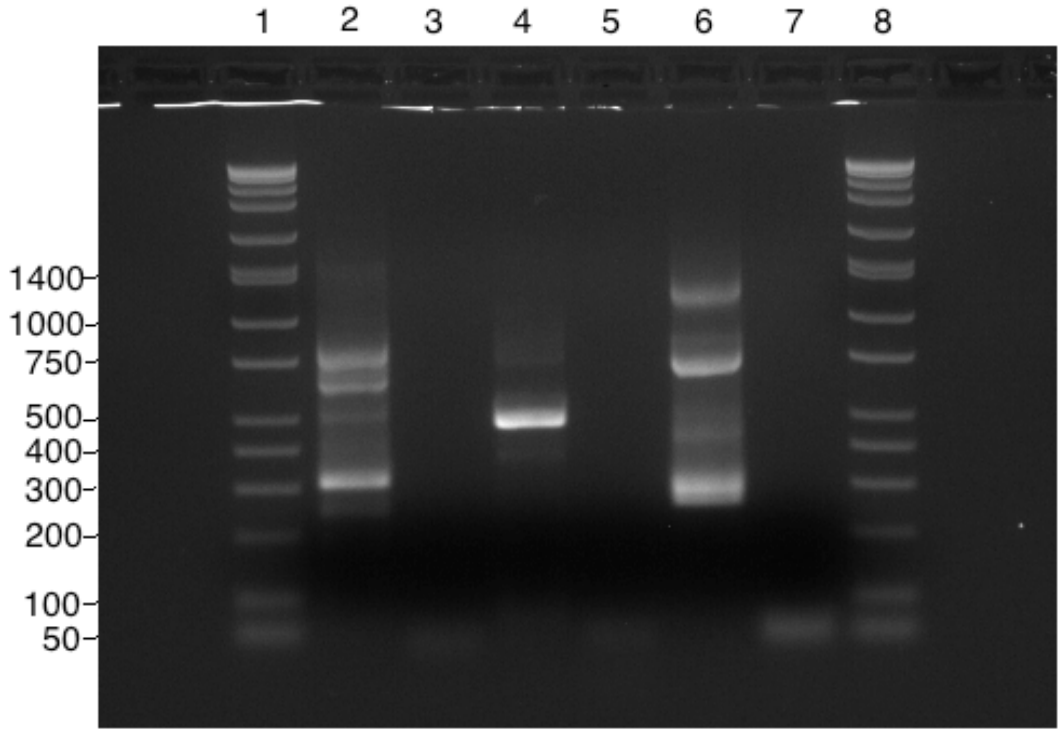


*Figure 5.4a : Electrophoresis of BRIN-bd11 cells (Experiment 3) (I). 1 - DNA ladder; 2 - IL10RA; 3 - IL10RA (negative control); 4 - IL10RB; 5 - IL10RB (negative control); 6 – GAPDH; 7 -GAPDH (negative control); 8 - DNA ladder.*

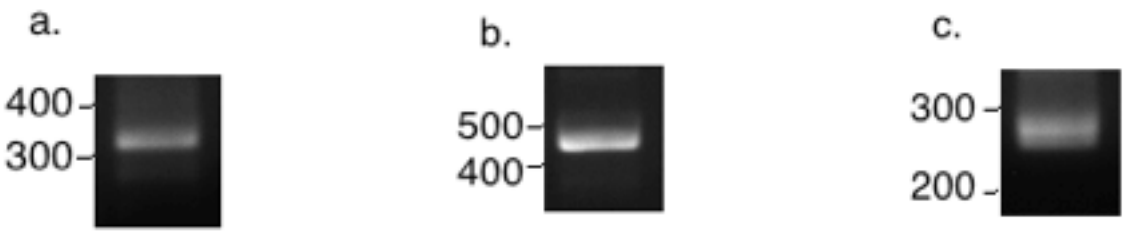


*Figure 5.4b : Electrophoresis of BRIN-bd11 cells (Experiment 3) (I) a - IL10RA (expected bp 313); b - IL10RB (expected bp 483); c -GAPDH (expected bp 262).*

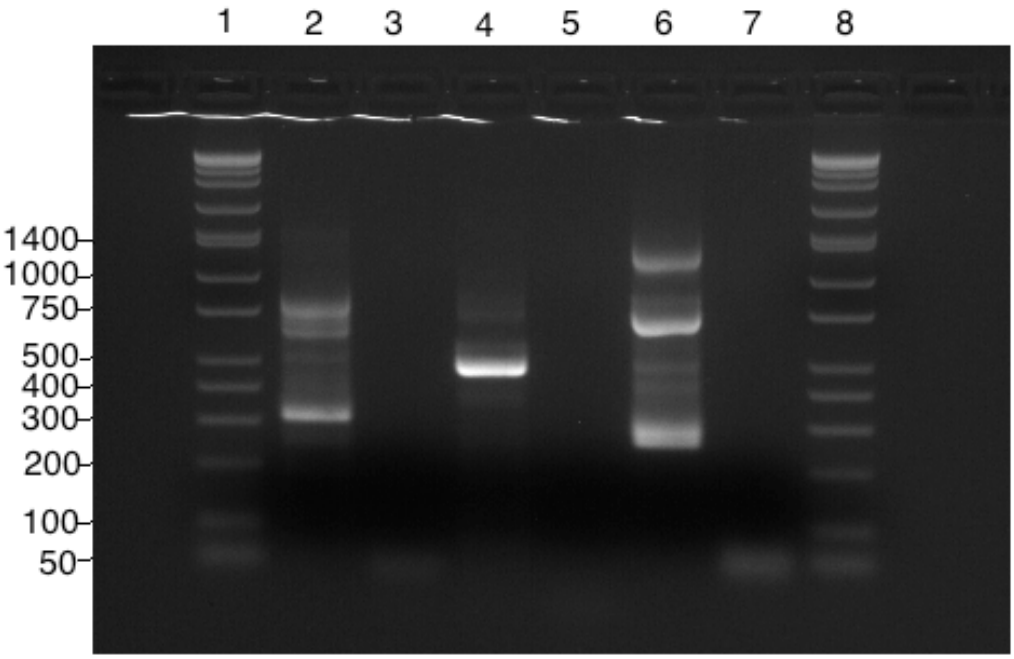


*Figure 5.5: Electrophoresis of BRIN-bd11 cells (Experiment 3) (II). 1 - DNA ladder; 2 - IL10RA; 3 - IL10RA (negative control); 4 - IL10RB; 5 - IL10RB (negative control); 6 – GAPDH; 7 -GAPDH (negative control); 8 - DNA ladder.*

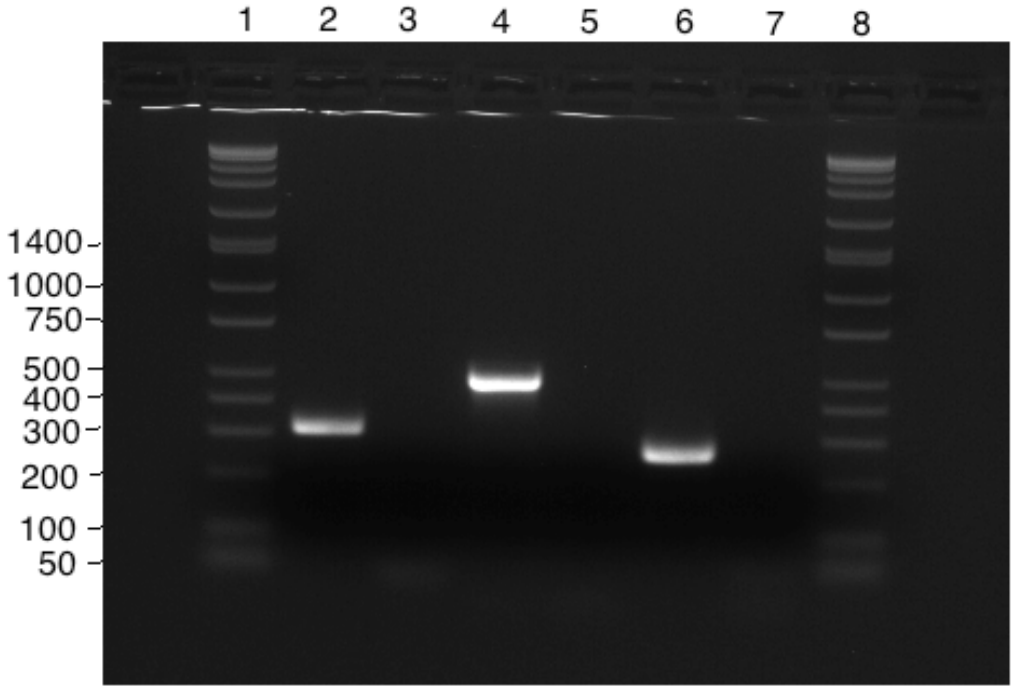


*Figure 5.6a : Electrophoresis of BRIN-bd11 cells (Experiment 3) (III). 1 - DNA ladder; 2 - IL10RA; 3 - IL10RA (negative control); 4 - IL10RB; 5 - IL10RB (negative control); 6 – GAPDH; 7 -GAPDH (negative control); 8 - DNA ladder.*

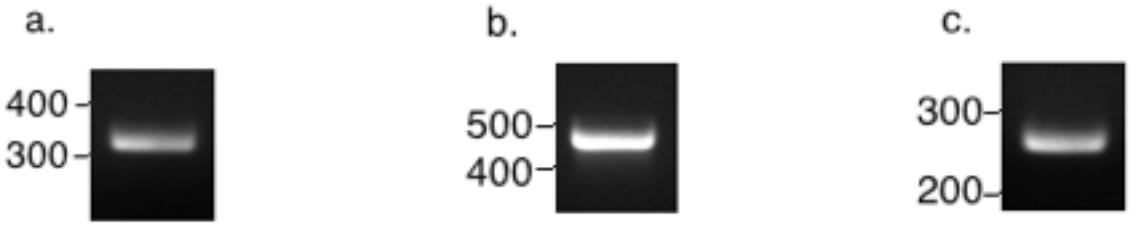


*Figure 5.6b : Electrophoresis of BRIN-bd11 cells (Experiment 3) (III). a - IL10RA (expected bp 313); b - IL10RB (expected bp 483); c -GAPDH (expected bp 262).*

#### 5.3.2.4 Gel Electrophoresis of PCR Products for the IL-10 Receptor from Mesenchymal Stem Cells

To determine the presence of IL10 receptors on MSC cells, RNA was extracted from MSC cells and RT-PCR performed on the RNA extract. Base pair length of RT-PCR products was determined by electrophoresis. Primers were designed using the gene template for *homo sapiens* and custom oligos were ordered from Thermo Fisher Scientific. These primers are detailed in Table 5.4.

Gel electrophoresis of PCR products from MSC cells using primers specific to the IL10RA, IL10RB and GAPDH genes of *homo sapiens* showed positive results for IL10RA as depicted in Lane 2 of Figure 5.7a (expected bp 360). Positive results were shown for IL10RB as depicted in Lane 4 of Figure 5.7a (expected bp 618). Positive results were seen for GAPDH as depicted in Lane 6 of Figure 5.7a (expected bp 311). Individual base pair comparisons are depicted in Figure 5.7b.

| Gene ID | Accession number | Primer Pair | Sequence (5'-3') | Product length | Melting Temp (°C) |
|---|---|---|---|---|---|
| IL10RA | NM_001558.3 Homo sapiens interleukin 10 receptor subunit alpha (IL10RA), transcript variant 1, mRNA | 8 | Forward CAATAGCACAGACAGCGGGA<br>Reverse GCCTCATCAACCAGGCATCT | 360 | Forward 60.11<br>Reverse 60.11 |
| IL10RB | NM_000628.4 Homo sapiens interleukin 10 receptor subunit beta (IL10RB), mRNA | 1 | Forward CAGACCCTGGACTTAGCCAC<br>Reverse GAGCTGACCACCCTTGAGTT | 618 | Forward 59.75<br>Reverse 59.60 |
| GAPDH | NM_001289745.1 Homo sapiens glyceraldehyde-3-phosphate dehydrogenase (GAPDH), transcript variant 3, mRNA | 1 | Forward TGAAGACGGGCGGAGAGAAA<br>Reverse TTCCCGTTCTCAGCCTTGAC | 311 | Forward 61.18<br>Reverse 59.97 |

*Table 5.4: Primers used in MSC electrophoresis experiment*

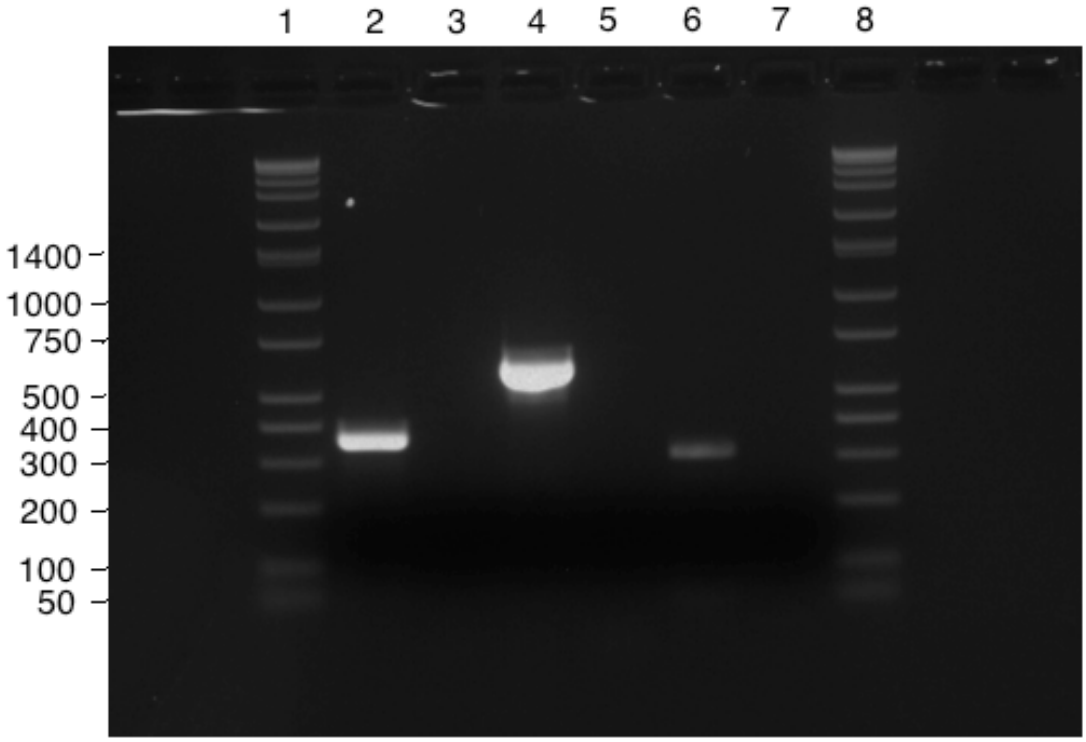


*Figure 5.7a : Electrophoresis of MSCs. 1 - DNA ladder; 2 - IL10RA; 3 - IL10RA (negative control); 4 - IL10RB; 5 - IL10RB (negative control); 6 – GAPDH; 7 - GAPDH (negative control); 8 - DNA ladder.*

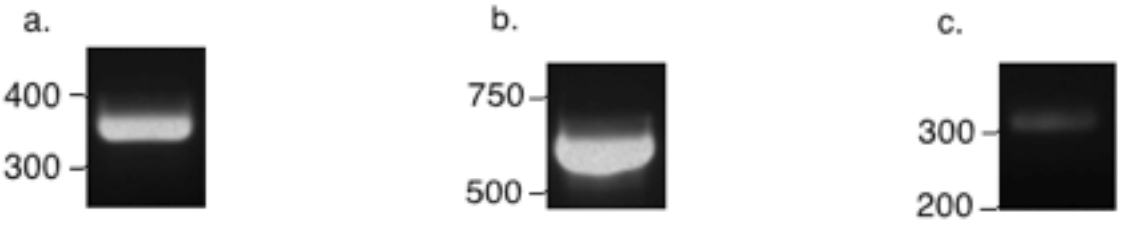


*Figure 5.7b : Electrophoresis of MSCs. a - IL10RA (expected bp 360); b - IL10RB (expected bp 618); c - GAPDH (expected bp 311).*

#### 5.3.2.5 Gel Electrophoresis of PCR Products for the IL-10 Receptor from TC6 Cells

To determine the presence of IL10 receptors on TC6 cells, RNA was extracted from TC6 cells and RT-PCR performed on the RNA extract. Base pair length of RT-PCR products was determined by electrophoresis.

Primers were designed using the gene template for *mus musculus* and custom oligos were ordered from Thermo Fisher Scientific. These primers are detailed in Table 5.5.

Gel electrophoresis of PCR products from TC6 cells using primers specific to the IL10RA, IL10RB and GAPDH genes of *mus musculus* showed positive results for the IL10RB as depicted in Lane 4 of Figure 5.8a (expected bp 998). Positive results were seen for GAPDH as depicted in Lane 6 of Figure 5.8a (expected bp 302). A band with a higher than expected base pair size was seen for IL10RA as depicted in Lane 2 of Figure 5.8a (expected bp 370). Individual base pair comparisons are depicted in Figure 5.8b.

| Gene ID | Accession number | Primer Pair | Sequence (5'-3') | Product length | Melting Temp (°C) |
|---|---|---|---|---|---|
| IL10RA | NM_008348.3 Mus musculus interleukin 10 receptor, alpha (IL10RA), transcript variant 1, mRNA | 9 | Forward ATTGCATACGGGACAGAACTGC<br>Reverse AGATGATGCCGTCCATTGCT | 370 | Forward 61.26<br>Reverse 59.82 |
| IL10RB | NM_008349.5 Mus musculus interleukin 10 receptor, beta (IL10RB), mRNA | 1 | Forward CTTCCTTCTGGTGCCAGCTCTA<br>Reverse TGAGCAGTTTGGGGTCATCG | 998 | Forward 61.74<br>Reverse 60.32 |
| GAPDH | NM_001289726.1 Mus musculus glyceraldehyde-3-phosphate dehydrogenase (GAPDH), transcript variant 1, mRNA | 5 | Forward TAAGAGGGATGCTGCCCTTAC<br>Reverse GATGGGCTTCCCGTTGATGA | 302 | Forward 59.23<br>Reverse 60.11 |

*Table 5.5 : Primers used in TC6 electrophoresis experiment.*

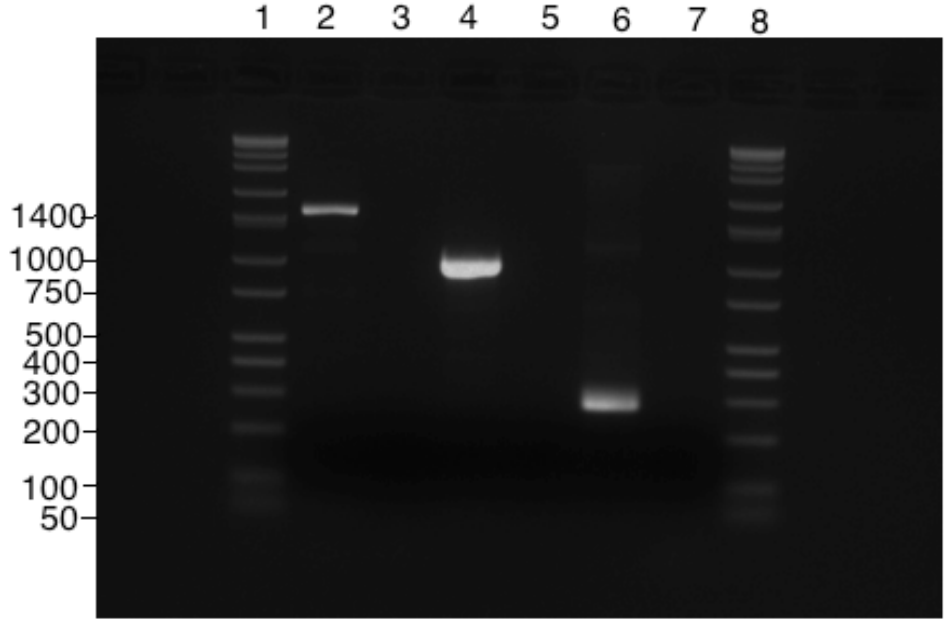


*Figure 5.8a : Electrophoresis of TC6 cells. 1 - DNA ladder; 2 - IL10RA; 3 - IL10RA (negative control); 4 - IL10RB; 5 - IL10RB (negative control); 6 – GAPDH; 7 - GAPDH (negative control); 8 - DNA ladder.*

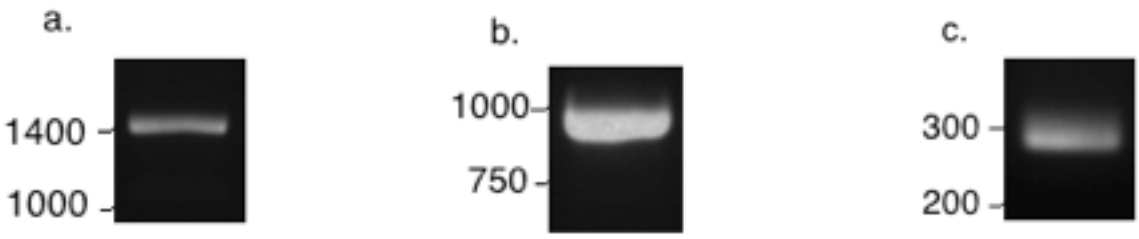


*Figure 5.8b : Electrophoresis of TC6 cells. a - IL10RA (expected bp 370); b - IL10RB (expected bp 998); c -GAPDH (expected bp 302).*

# 5.4 Characterising the IL-10 Receptor on Beta Cells by Immunofluorescence

## 5.4.1 Methods

Materials

Materials used in this experiment can be found in Section 2.1.

Cell lines Utilised

BRIN-bd11, TC6 cells and MSCs cells were utilised in this experiment. Details of the cell lines used can be found in Section 2.2.2.

Cell Culture Methods

Cells were obtained from liquid nitrogen dewars located at the Guy Hilton Research Center, Stoke-on-Trent, UK, and thawed as detailed in Section 2.2.4. Cells were trypsonised and suspended in medium as detailed in Section 2.2.5. Cell counts were performed as detailed in Section 2.2.6.

MSC Culture Methods

MSCs were recovered and expanded as detailed in Section 2.2.7. Isolation and culture of MSCs is detailed in Section 2.2.8. Cells were trypsonised and suspended in medium as detailed in Section 2.2.5. Cell counts were performed as detailed in Section 2.2.6.

Immunofluorescence Protocol

Details of seeding cells, fixing of cells, blocking, staining of cells as well as image capture and data analysis can be found in Section 2.3.10.

## 5.4.2 Results

### 5.4.2.1 IF Characterisation of IL-10 Receptor in BRIN-bd11 Cells

To determine whether BRIN-bd11 cells express the IL-10 receptor in culture conditions detailed in Section 2.2.3, fluorescent conjugated antibodies specific to the IL10RA and IL10RB components of the receptor were utilised to allow visualisation of receptor expression. Staining with antibodies specific to IL10RA resulted in a fluorescent intensity visibly greater than that of the isotype control (Figure 5.9). No autofluorescence was seen for BRIN-bd11 cells stained with DAPI (Figure 5.9). Quantification of fluorescence intensity demonstrated a significantly greater (+69.2%; $p<0.001$) intensity of the positive stain compared to the control (Figure 5.11). Staining with antibodies specific to the IL10RB resulted in fluorescence that was greater in the positive stain compared to the isotype control (Figure 5.10). The stain was determined to be significantly greater (+61.4%; $p<0.001$) on quantitative analysis (Figure 5.11).

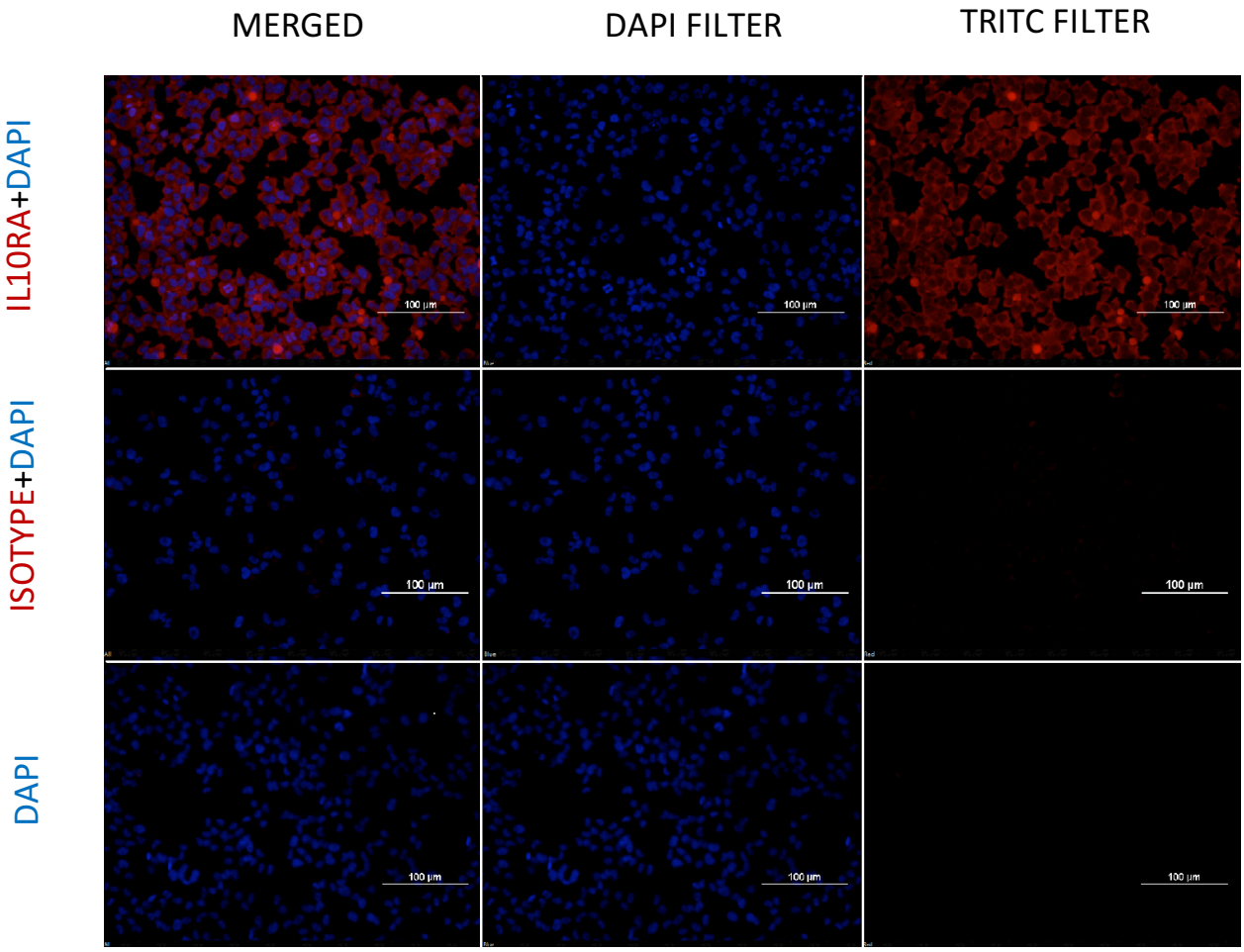


*Figure 5.9 : Immunofluorescence images demonstrating expression of IL10RA receptors by BRIN-bd11 cells. IL10RA-specific antibodies resulted in a significantly greater fluorescence intensity than the isotype control. DAPI controls displayed no autofluorescence. Images were taken at x20 magnification. Scale bar = 100µm*

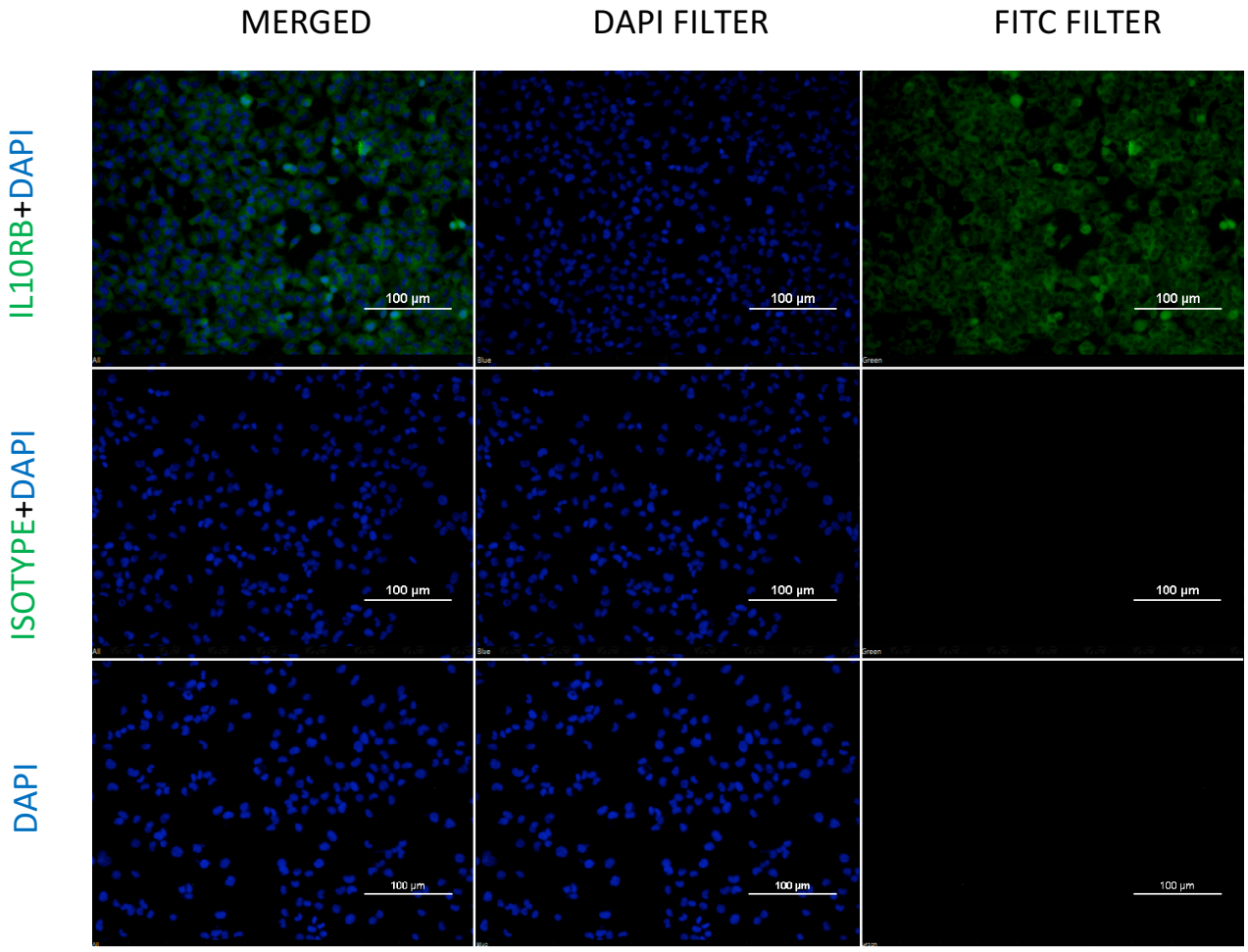


*Figure 5.10 : Immunofluorescence images demonstrating expression of IL10RB receptors by BRIN-bd11 cells. IL10RB-specific antibodies resulted in a significantly greater intensity than the isotype control. DAPI controls displayed no autofluorescence. Images were taken at x20 magnification. Scale bar = 100$\mu$m*

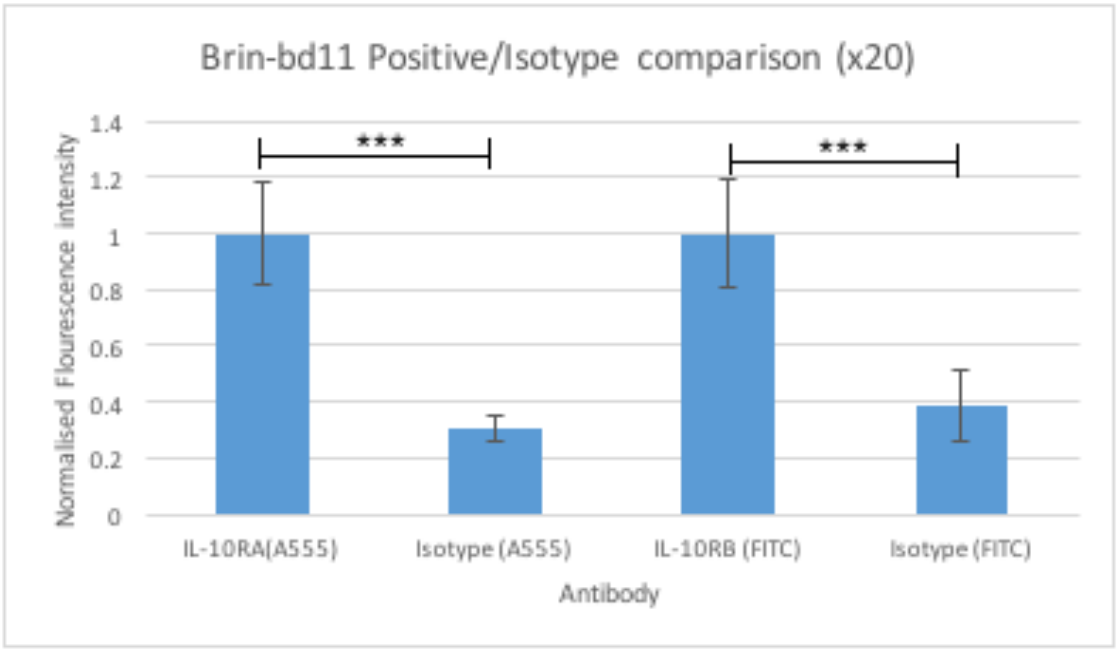


*Figure 5.11 : Quantification of immunofluorescence for characterisation of IL-10 receptors expressed by BRIN-bd11 cells. Fluorescence intensities of antigen-specific antibodies are compared to their respective isotype controls for fields taken at x20 magnification. Isotype intensities are normalised to their respective antigen-specific antibody. Data presented as mean +/- standard deviation. ***P<0.001*

#### 5.4.2.2 IF Characterisation of IL-10 Receptor in MSCs.

To determine whether MSCs express the IL-10 receptor in culture conditions detailed in Section 2.2.3, fluorescent conjugated antibodies specific to the IL10RA and IL10RB components of the receptor were utilised to allow visualisation of receptor expression. Staining with antibodies specific to IL10RA resulted in a fluorescent intensity visibly greater than that of the isotype control (Figure 5.12). No autofluorescence was seen for MSCS stained with DAPI (Figure 5.12). Quantification of fluorescence intensity demonstrated a significantly greater (+60.0%; $p<0.001$) intensity of the positive stain compared to the control (Figure 5.14). Staining with antibodies specific to the IL10RB resulted in fluorescence that was greater in the positive stain compared to the isotype control (Figure 5.13). The stain was determined to be significantly greater (+70.1%; $p<0.001$) on quantitative analysis (Figure 5.14).

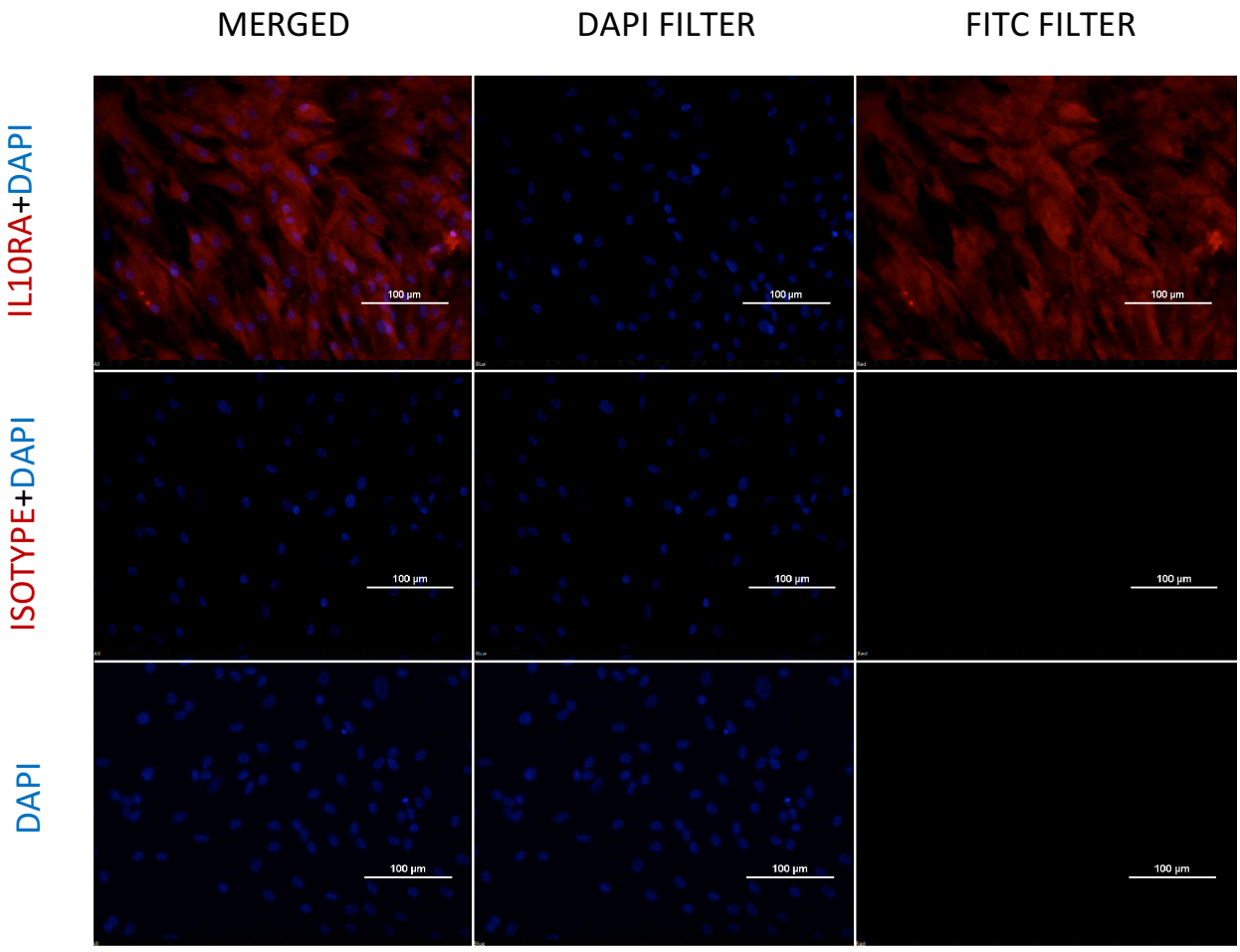


*Figure 5.12 : Immunofluorescence images demonstrating expression of IL10RA receptors by MSCs. IL10RA-specific antibodies resulted in a significantly greater fluorescence intensity than the isotype control. DAPI controls displayed no autofluorescence. Images were taken at x20 magnification. Scale bar = 100µm.*

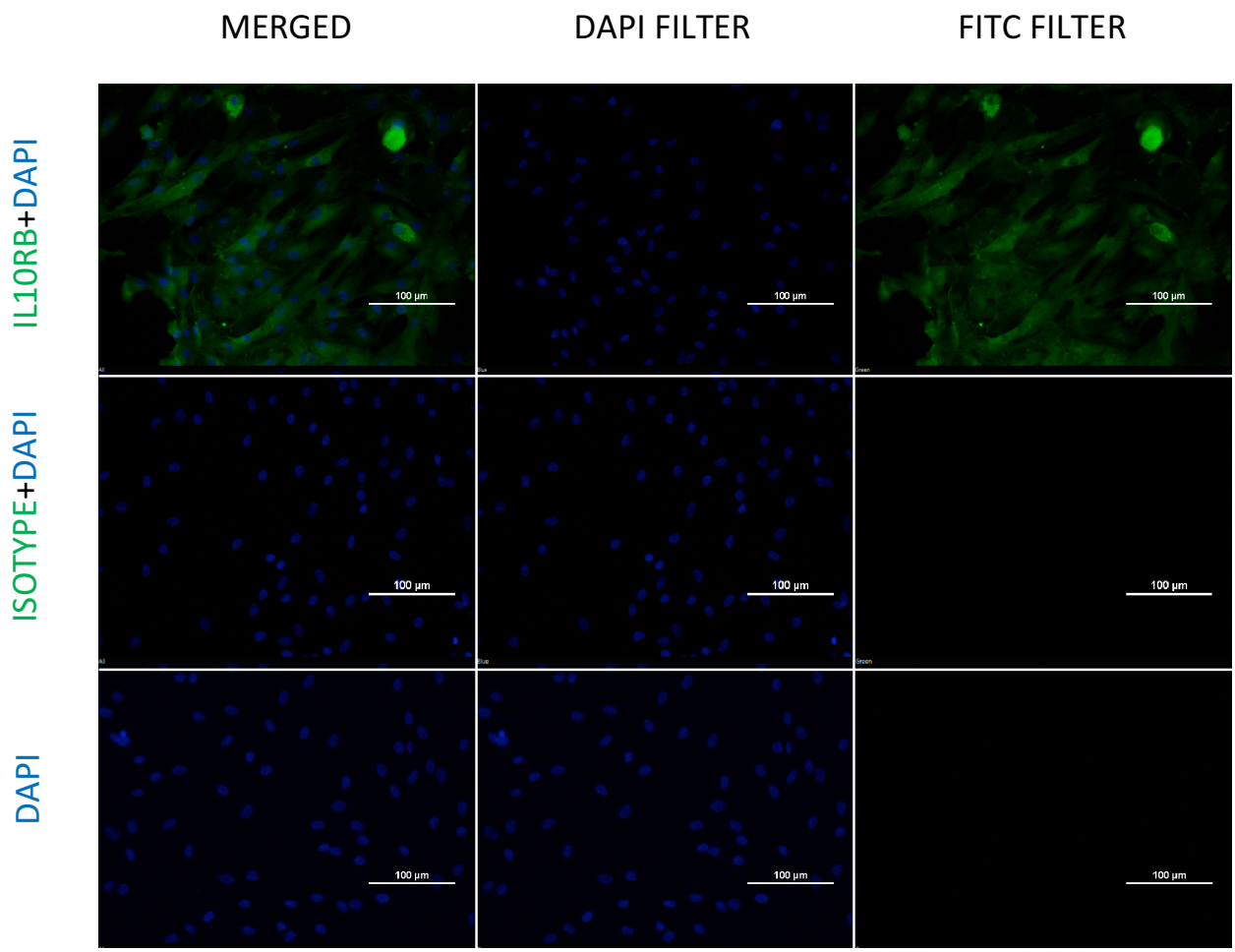


*Figure 5.13 : Immunofluorescence images demonstrating expression of IL10RB receptors by MSCs. IL10RB-specific antibodies resulted in a significantly greater intensity than the isotype control. DAPI controls displayed no autofluorescence. Images were taken at x20 magnification. Scale bar = 100µm.*

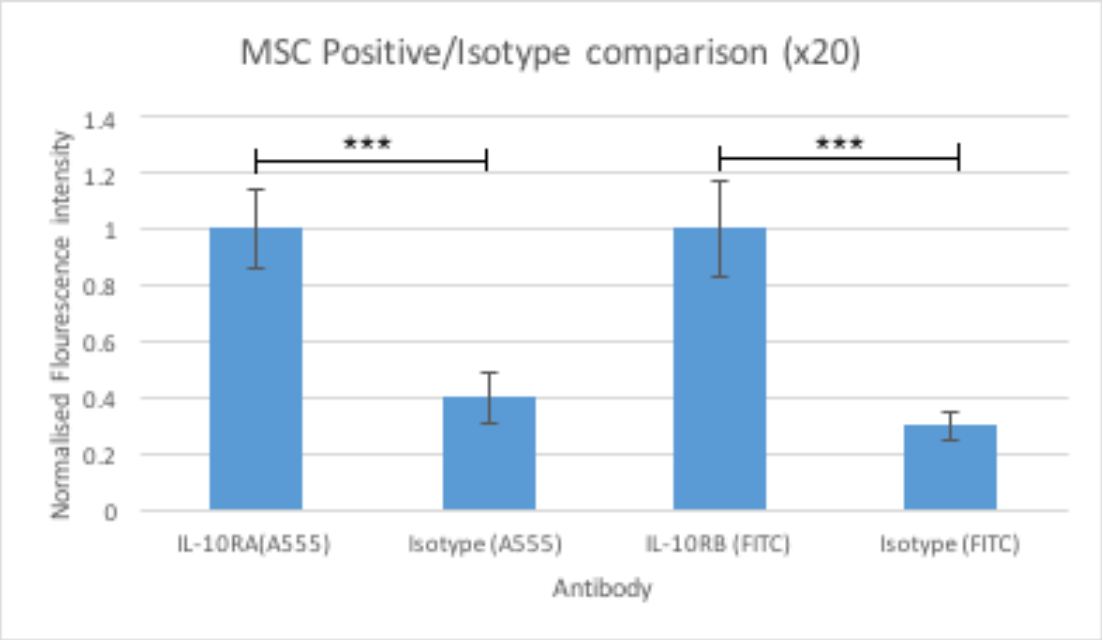


*Figure 5.14 : Quantification of immunofluorescence for characterisation of IL-10 receptors expressed by MSCs. Fluorescence intensities of antigen-specific antibodies are compared to their respective isotype controls for fields taken at x20 magnification. Isotype intensities are normalised to their respective antigen-specific antibody. Data presented as mean +/- standard deviation. ***P<0.001*

#### 5.4.2.3 IF Characterisation of IL-10 Receptor in TC6 Cells

To determine whether TC6 cells express the IL-10 receptor in culture conditions detailed in Section 2.2.3, fluorescent conjugated antibodies specific to the IL10RA and IL10RB components of the receptor were utilised to allow visualisation of receptor expression. Staining with antibodies specific to IL10RA resulted in a fluorescent intensity visibly greater than that of the isotype control (Figure 5.15). No autofluorescence was seen for TC6 cells stained with DAPI (Figure 5.15). Quantification of fluorescence intensity demonstrated a significantly greater (+56.3%; $p<0.001$) intensity of the positive stain compared to the control (Figure 5.17). Staining with antibodies specific to IL10RB resulted in fluorescence that was greater in the positive stain compared to the isotype control (Figure 5.16). The stain was determined to be significantly greater (+55.5%; $p<0.001$) on quantitative analysis (Figure 5.17).

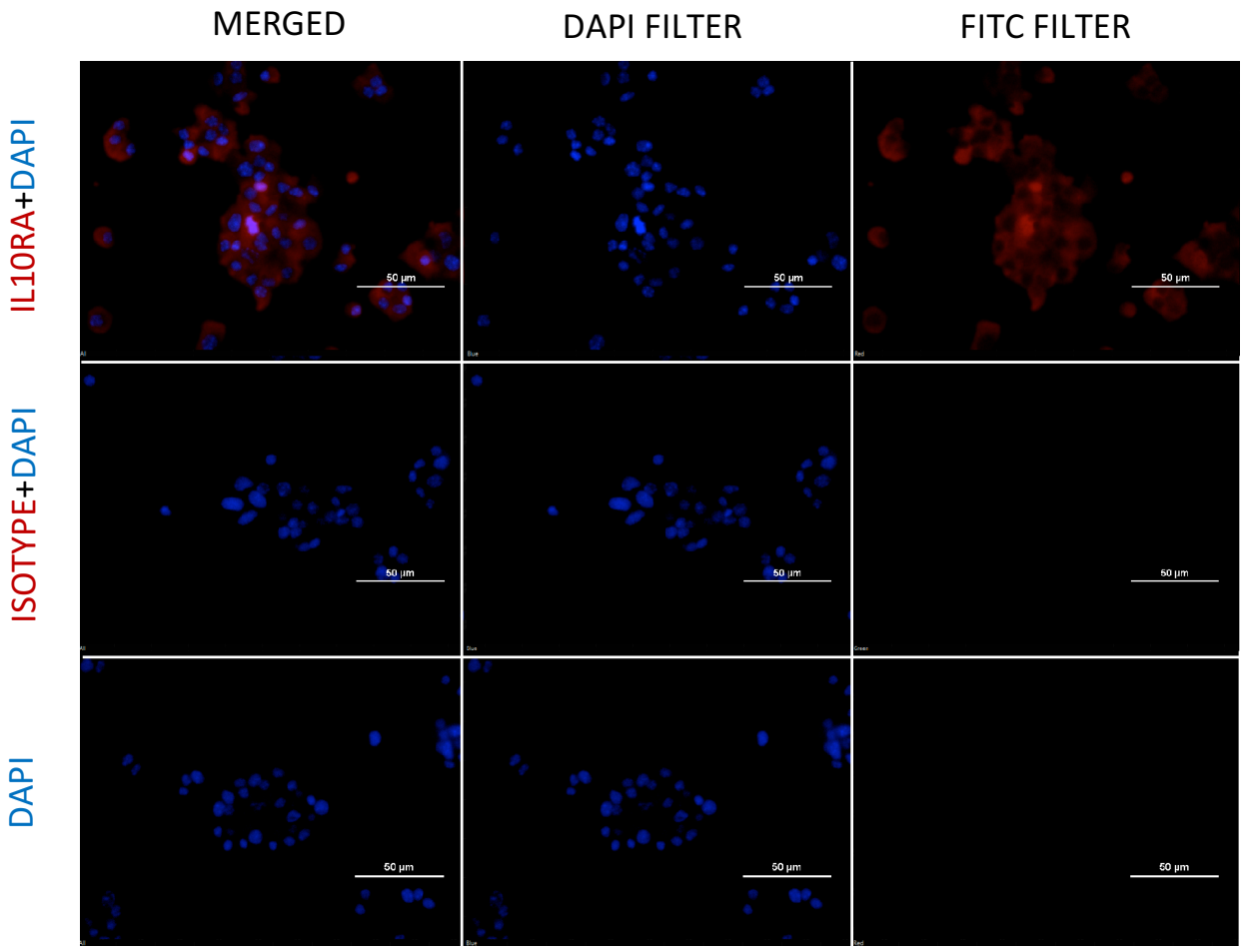


*Figure 5.15 : Immunofluorescence images demonstrating expression of IL10RA receptors by TC6 cells. IL10RA-specific antibodies resulted in a significantly greater fluorescence intensity than the isotype control. DAPI controls displayed no autofluorescence. Images were taken at x40 magnification. Scale bar = 100µm*

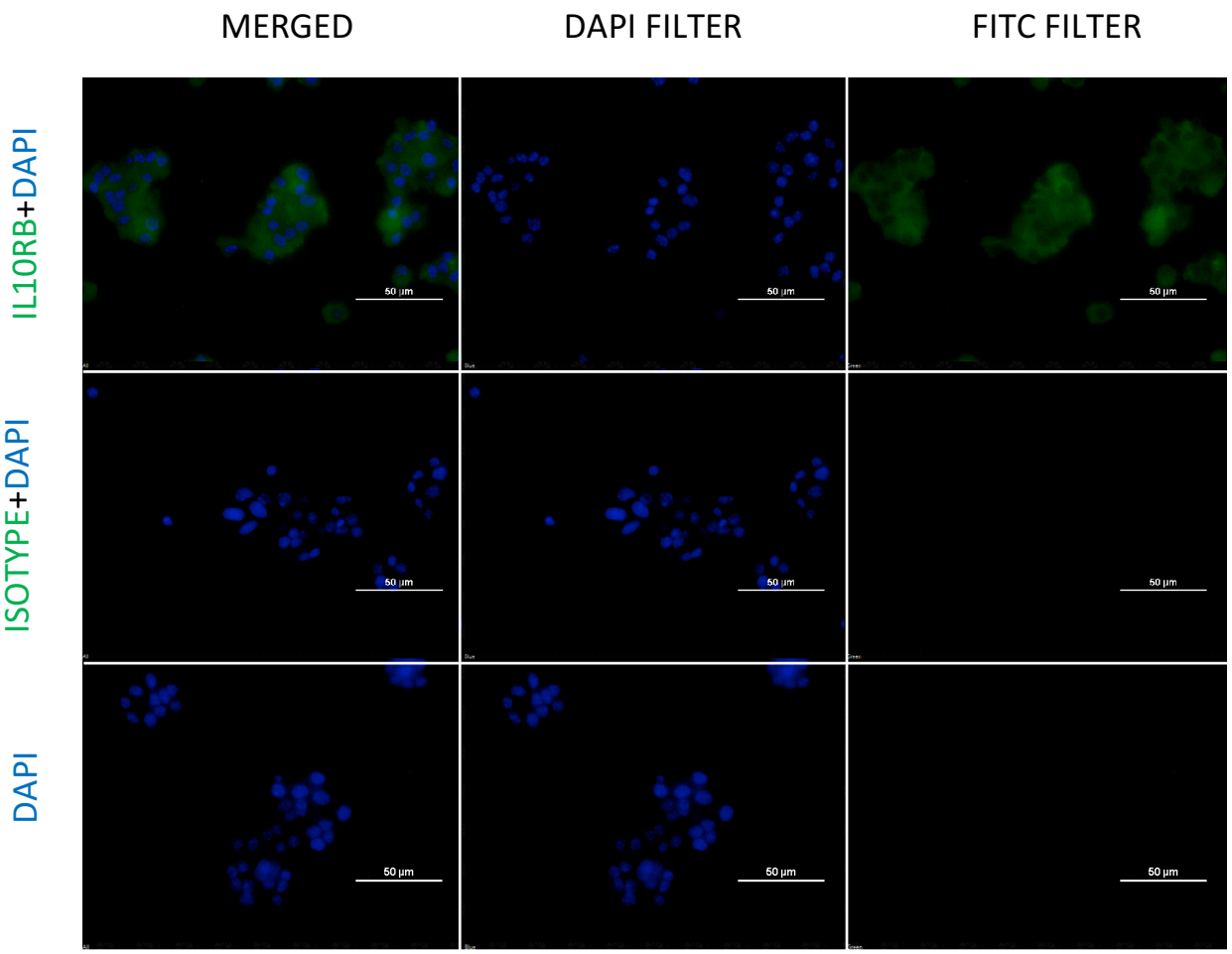


*Figure 5.16 : Immunofluorescence images demonstrating expression of IL10RB receptors by TC6 cells. IL10RB-specific antibodies resulted in a significantly greater intensity than the isotype control. DAPI controls displayed no autofluorescence. Images were taken at x40 magnification. Scale bar = 100µm.*

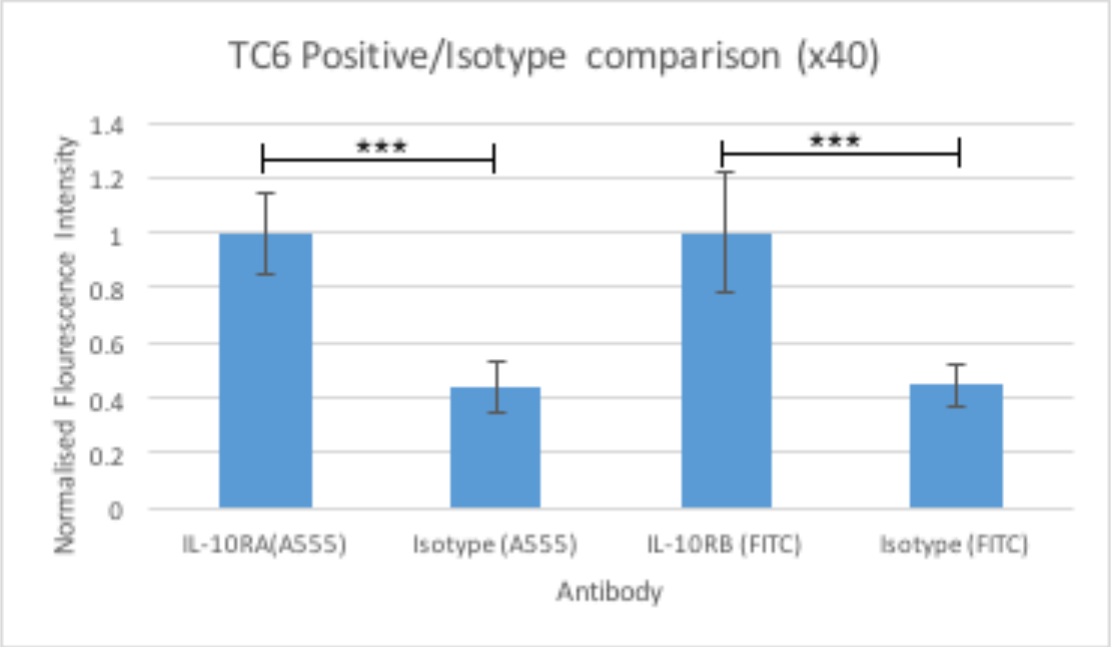


*Figure 5.17 : Quantification of immunofluorescence for characterisation of IL-10 receptors expressed by TC6 cells. Fluorescence intensity of antigen-specific antibodies are compared to their respective isotype controls for fields taken at x40 magnification. Isotype intensities are normalised to their respective antigen-specific antibody. Data presented as mean +/- standard deviation. ***P<0.001*

## 5.5 Discussion

The mesenchymal stem cell secretome presents an exciting and novel area of research in the field of stem cell therapy. Proteomic studies have uncovered a complex cocktail of soluble factors that are secreted by the MSCs. These include angiogenic factors (e.g. VEGF, angiogenin), Growth and trophic factors (e.g. BDNF, EGF, PIGF), chemokines (e.g. CCL1, CXCL2), anti-inflammatory cytokines (e.g. IL-10, IL-13) and haematopoietic cytokines, among others.[63]

As discussed in Chapter 1, these factors have been shown to mediate therapeutic benefits in a number of disease models, including autoimmune conditions, cardiac disease and neurological disease. [64-66]

To uncover the factors present in the MSC-CM, we conducted ELISA assays. We have demonstrated a high concentration of IL-10 in MSC-CM using ELISA assays, and as described in Chapter 1, IL-10 is a cytokine that acts through STAT3 signalling and is well-characterised for its immunomodulatory functions. IL-10 has been studied in the context of autoimmune diseases such as inflammatory bowel disease (IBD) where administration of IL-10 has been shown to prevent the development of the disease in murine models by acting

as an immunosuppressant and attenuating the autoimmune response.[200] Administration of IL-10 to diabetic mice has shown mixed results. Systemic administration appears to be beneficial and improve insulin metabolism. However, local expression at high levels appears to exacerbate the immune response.[210-214]

Previous studies of IL-10 in autoimmune diseases have largely focussed on its immunosuppressive properties via its actions on immune cells involved in the pathogenesis of autoimmune diseases. The ability of IL-10 to directly confer cytoprotection to beta cells in the context of type 1 diabetes has to my knowledge not previously been explored. As previously discussed we theorised that IL-10 may directly confer cytoprotective effects to beta cells by blocking NF-κB through a number of mechanisms.[174,188, 189-191] As a result, we started the process of characterising the presence of receptors on beta cell lines.

In this chapter, we have demonstrated the presence of the IL-10 receptor in BRIN-bd11 beta cell lines via electrophoresis and immunofluorescence, and TC6 cells via immunofluorescence. This indicates that IL-10 could directly bind

to receptors on the surface of these cells and initiate in STAT3 transduction to the nucleus. As alluded to earlier, IL-10 may be able to attenuate pro-inflammatory cytokine-driven apoptosis in beta cells through the blockage of NF-κB signal transduction. Further study is however required to determine the extent of the cytoprotective effect conferred by IL-10 and the mechanisms whereby IL-10 exerts these effects.


# Chapter 6: Summary and Future Directions

## 6.1 Summary

The objective of this thesis was to determine the effects of the MSC secretome on *in vitro* and *in vivo* models of diabetes. An Exploration of the current understandings of the pathophysiology of diabetes has uncovered that destruction of beta cells is mediated both by direct cellular toxicity as well as by pro-inflammatory cytokines. These cytokines mediate beta cell dysfunction and apoptosis and perpetuate the immune response within the islet leading to progressive depletion of the beta cell mass and eventual clinical manifestation of the disease.[113-117] Finding a way to inhibit biochemical pathways activated by these cytokines may present the possibility of slowing or even halting the progression of the disease. Studying the stem cell secretomes ability to ameliorate beta cell destruction could provide an avenue to unravel the biochemical pathways involved in conferring its therapeutic benefits, and could ultimately pave the way for targeted drug therapies in the future. The results of this thesis as summarised below shows that the MSC-CM has therapeutic potential in the context of Type 1 diabetes and further study in this field could realise these goals.

Chapter 3 of this thesis demonstrated that the MSC-CM appears to improve the viability of beta cells exposed to cytokines implicated in the pathogenesis of type 1 diabetes (TNF$\alpha$, IFN$\gamma$ and IL-1$\beta$). In addition to this, we looked at the effects of the MSC-CM on a cytomix of all three cytokines as previous studies have indicated a possible synergistic effect of these cytokines in mediating beta cell apoptosis. The in vitro study by Yeung *et al.* demonstrated decreased apoptosis and improved survival of islet cells exposed to a cytomix of these three pro-inflammatory cytokines when co-cultured in the same compartment with MSCs.[238] We demonstrated via colorimetric MTT assays that secreted factors in the form of the MSC-CM appear to improve the viability as measured by mitochondrial metabolism of beta cell lines in vitro thus supporting the findings of these previous studies.

In addition, in chapter 4 we tested the effects of MSC-CM on a multiple low dose streptozocin *in vivo* model of diabetes. Our results demonstrated improved islet function and restoration of insulin secretion in MSC-CM-treated mice. Previous studies have demonstrated the ability of the MSC-CM to repair islets from diabetic mice through trophic actions of MSCs, which could account for the improved metabolic profiles seen in our MSC-CM-

treated mice.[240,242] However, we did not determine the mechanisms which conferred the improved insulin metabolism seen in our experiment. Immunoregulation and increased proliferation of beta cells are potential mechanisms cited in previous studies. [74,238,240]

The mechanisms whereby the MSC-CM protects cytokine-mediated reductions in beta cell viability seen in our *in vitro* experiments remain to be elucidated. The NF-κB and AP-1 pathways have been implicated in the pathogenesis of the disease.[118-120,158-161,187] Indeed, the use of NF-κB inhibitors has been shown to significantly reduce IL-1β+IFNγ-induced apoptosis of beta cells.[120] Furthermore, Blockage of NF-κB in the multiple-low dose streptozocin-induced model of diabetes protected against beta cell death and lymphocytic infiltration into the diseased islets.[120] Thus, the NF-κB pathway appears to be a key mediator of beta cell death in type 1 diabetes.

It could be theorised that factors in the MSC-CM may exert their therapeutic effect through the blockage of the NF-κB pathway in beta cells. Using ELISAs, we demonstrated that MSC-CM contains a significant concentration of IL-10. Previous studies have indicated that IL-10 could block the signal transduction

of NF-κB by the induction of AIR factors as well as stabilising IκB in the cytosol, thereby preventing translocation of NF-κB to the nucleus and the subsequent expression of pro-inflammatory mediators.[174,188,189-192] The effect of IL-10 in inhibiting the immune response through the blockage of NF-κB in immune cells is well documented.[174,188] Chapter 5 of the thesis demonstrated the presence of IL-10 receptors on beta cell lines, which indicates that IL-10 could directly interact with beta cells and may as a result confer cytoprotective effects to beta cells in addition to modulating the immune response. Further study is needed to determine the role IL-10 plays in the cytoprotective effect of MSCs on the beta cell.

Type 1 diabetes is a chronic condition that requires lifelong treatment to prevent complications. Complications associated with diabetes are still a major cause of morbidity and mortality for diabetics worldwide. Finding treatments that could stop the progression of the disease in susceptible individuals before it presents clinically would eliminate complication-associated morbidity and mortality in patients who would otherwise go on to develop the disease.

In the future, it may be possible screen for susceptibility to the development of Type 1 diabetes using autoanibody titres and genetic profile as proposed by Bonifacio *et al* [252] With a viable treatment to halt the progression of the disease and a screening method acceptable to the patient, intervening before depletion of islet mass and onset of clinical diabetes occurs may be a possibility.

In this thesis, we have demonstrated that the mesenchymal stem cell secretome appears to have therapeutic properties on beta cells in both in vitro and in vivo models. Our study has however only scratched the surface in developing an understanding of the therapeutic potential of the MSC secretome in the treatment of diabetes. The MSC secretome represents a novel method to further our understanding of a wide range of diseases beyond diabetes, and further research in this area of regenerative medicine could revolutionise the practice of medicine in the future.

## 6.2 Future Directions

Over the course of this nine month project, I have explored the viability of MSC-CM as a potential option for the treatment of type 1 diabetes and have started some of the characterisation experiments for IL-10 signalling to begin looking at the biochemical pathways that may confer the beneficial effects seen. The findings represent the groundwork for a potentially much larger project, and given more time, there were many areas that could have been explored in greater depth. This section aims to lay out a plan of work for future investigation to further the goals of this project.

This results of this thesis demonstrated improved viabilities as measured by mitochondrial metabolism using MTT assays for cell lines treated with MSC-CM after exposure to pro-inflammatory cytokines. We also showed that IL-10 is a factor secreted in significant quantities in the MSC secretome. MTT assays looking for the effect of recombinant IL-10 alone in the concentrations found in MSC-CM could be used to isolate this soluble factor and determine the extent to which it contributes to the cytoprotective effect seen for MSC-CM as a whole.

The next logical step would be to confirm the mechanisms that confer the cytoprotective effects observed. A limitation in the experiments presented in chapter 3 are that MTT assays only measure mitochondrial metabolism, which can reflect cell viability. It is not a test for apoptosis and does determine if the improved metabolic results on treatment with MSC-CM is caused by reduced apoptosis or increased proliferation of beta cells. To address this a number of further studies can be proposed. TUNEL assays have been used in the past to confirm and quantify the extent of apoptosis. Furthermore, exploring the expression of pro-apoptotic genes such as p53 using western blot could be carried out. This could be done to determine the extent to which MSC-CM as a whole and recombinant IL-10 suppress apoptosis in beta cells when exposed to pro-inflammatory cytokines.

A potential proliferative effect of the MSC-CM on beta cell lines in vitro has also been hypothesised. To confirm this, growth curves could be plotted to demonstrate differences in population-doubling times for beta cells in the presence and absence of MSC-CM. This could be performed using a viability assay such as Alamar Blue or through periodic cell counts. Previous studies have also measured the expression of cell cycle proteins such as cyclins, as

well as proteins that inhibit cell cycle progression such as p21, to determine if there is a difference in the rate of proliferation.

Future studies could involve unravelling the signal transduction pathways which the soluble factors in the MSC-CM act upon in beta cells. We were particularly interested in the potential of IL-10 to confer cytoprotective effects directly to beta cells and its potential ability to block NF-κB signal transduction. Thus, further study into the activity of NF-κB in cells challenged with pro-inflammatory cytokines could be undertaken comparing cells treated with MSC-CM and untreated controls. This would allow us to determine whether MSC-CM blocks NF-κB activation.

The *in vivo* experiment in this thesis presented a number of limitations as discussed in Chapter 4. Further study could involve conducting the experiment with periodic measurement of blood glucose and serum insulin, as well as body weights to determine if trends in glycaemic control can be established. Subsequent experiments could involve determining whether IP injections of individual components or combinations of factors present in the MSC-CM are capable of achieving improvements in islet function and morphology in

diabetic mice. This would complement the in vitro studies to determine the components of the MSC secretome that confer its therapeutic benefit. Another limitation highlighted in chapter 4 is that the functionality of beta cells were not tested in this thesis. Measuring insulin secretion through glucose challenges could be used to determine whether the MSC secretome can ameliorate beta cell dysfunction in addition to preserving beta cell mass.

Recent discoveries have shown that in addition to soluble factors, exomes play an important role in modifying the disease state. Being capable of mediating horizontal transfer of genetic material between MSCs and target cells, they could play a key role in mediating the protective effects seen in our model of type 1 diabetes. Characterising the exomes released by MSCs and the genes they transfer to beta cells and immune cells implicated in the pathogenesis of diabetes is another avenue that could be explored in the future.

The use of stem cell products for the treatment of diseases is an exciting field that shows promise as a potential therapeutic option in the future. Further research in this field may result in treatments that could halt and reverse the pathogenesis of diseases like type 1 diabetes.

Keele University

# References

(1) Ward CW, Lawrence MC, **"Landmarks in Insulin Research"**, Front Endocrinol (Lausanne). 2011;2:76.

(2) Mazur A, **"Why Were "Starvation Diets" Promoted for Diabetes in the Pre-Insulin Period?"**, Nutr J. 2011;10:23.

(3) Pambianco G, Costacau T, Ellis D, Becker DJ, Klein R, Orchard TJ (2006) **"The 30-Year Natural History of Type 1 Diabetes Complications: the Pittsburgh Epidemiology of Diabetes Complications Study Experience"**, Diabetes. 2006 May;55(5):1463-1469.

(4) The Diabetes Control and Complications Trial Research Group, **"The Effect of Intensive Treatment of Diabetes on the Development and Progression of Long-Term Complications in Insulin-Dependent Diabetes Mellitus"**, N Engl J Med. 1993 Sep 30;329(14):977-986.

(5) Williams PW, **"Notes on Diabetes Treated with Extract and by Graft of Sheep's Pancreas"**, Br Med J. 1894;2:1303-1304.

(6) Kemp CB, Knight MJ, Scharp DW, Lacy PE, Ballinger WF, Lacy PE, **"Transplantation of Isolated Pancreatic Islets into the Portal Vein of Diabetic Rats"**, Nature. 1973 Aug 17;244(5416):447.

(7) Ricordi C, Lacy PE, Scharp DW, **"Automated Islet Isolation from Human Pancreas"**, Diabetes. 1989 Jan;38 Suppl 1:140-142.

(8) James Shapio AM, Lakey JRT, Ryan EA, Korbutt GS, Toth E, Warnock GL, Kneteman NM, Rajotte RV, **"Islet Transplantation in Seven Patients with Type 1 Diabetes Mellitus Using a Glucocorticoid-Free Immunosuppressive Regimen"**, N Engl J Med. 2000 Jul 27;343(4):230-238.

(9) **"Video and Image Library."** Diabetes Research Institute, Diabetes Research Institute Foundation, 2016, www.diabetesresearch.org/video-and-image-library. Accessed at: 15th September 2016.

(10) James Shapio AM *et al*, **"International Trial of the Edmonton Protocol for Islet Transplantation"**, N Engl J Med. 2006 Sep 28;355(13):1318-1330.

(11) Brennan DC, Kopetskie HA, Sayre PH, Alejandro R, Cagliero E, Sharpio AM, Goldstein JS, DesMarais MR, Booher S, Bianchine PJ, **"Long –Term Follow-Up of the Edmonton Protocol of Islet Transplantation in the United States"**, Am J Transplant. 2016 Feb;16(2):509-517.

(12) Close N, Alejandro R, Hering B, Appel M, **"Second Annual Analysis of the Colaborative Islet Transplant Registry"**, Transplant Proc. 2007;39(1):179-182.

(13) Barton FB, Rickels MR, Alejandro R *et al*, **"Improvement in Outcome of Clinical Islet Transplantation: 1999-2010"**, Diabetes Care. 2012;35(7):1436-1445.

(14) Srinivasan P, Huang GC, Amiel SA, Heaton ND, **"Islet Cell Transplantation"**, Postgrad Med J. 2007;83(978):224-229.

(15) Robertson RP, **"Islet Transplantation for Type 1 Diabetes, 2015: What Have We Learned from Alloislet and Autoislet Successes"**, Diabetes Care. 2015;38(6):1030-1035.

(16) Matsumoto S, Kuroda Y, **"Perfluorocarbon for Organ Preservation before Transplantation"**, Transplantation. 2002 Dec 27;74(12):1804-1809.

(17) Health Quality Ontario, **"Pancreas Islet Transplantation for Patients With Type 1 Diabtes Mellitus: A Clinical Evidence Review",** Ont Health Technol Assess Ser. 2015; 15(16):1-84

(18) Rother KI, Harlan DM, **"Challenges Facing Islet Transplantation for the Treatment of Type 1 Diabetes Mellitus"**, J Clin Invest. 2004;114(7):877-883.

(19) Naziruddin B, Iwahashi S, Kanak MA, Takita M, Itoh T, Levy MF, **"Evidence for Instant Blood-Mediated Inflammatory Reaction in Clinical Autologous Islet Transplantation"**, Am J Transplant. 2014 Feb; 14(2):428-437.

(20) De Groot LJ, Chrousos G, Dungan K, Fiengold KR, Grossman A, Hershman JM, Koch C, Korbonitis M, McLachlan R, New M, Purnell J, Rebar R, Singer F, Vinik A , editors. **"Endotext [Internet].**" South Dartmouth (MA): MDText.com, Inc.; 2000-. Available from: https://www.ncbi.nlm.nih.gov/books/NBK278966/

(21) Posselt AM, Bellin MD, Tavakol M, Szot GL, Frassetto LA, Masharani U, Kerlan RK, Fong L, Vincenti FG, Hering BJ, Bluestone JA, Stock PG, **"Islet Transplantation in Type 1 Diabetics Using an Immunosuppressive Protocol Based on the Anti-Lfa-1 Antibody Efalizumab"**, Am J Transplant. 2010 Aug;10(8):1870-1880.

(22) Gaston RS.**"Chronic Calcineurin Inhibitor Nephrotoxicity: Reflections on an Evolving Paradigm"**, Clin J Am Soc Nephrol. 2009 Dec;4(12):2029-2034.

(23) Heerspink HJL, Holtkamp FA, Zeeuw DD, Ravid M, **"Monitoring Kidney Function and Albuminuria in Patients with Diabetes"**, Diabetes Care. 2011 May;34(suppl2):S325-S329.

(24) Lovell-Badge R, **"Many Ways to Pluripotency"**, Nat Biotechnol. 2007 Oct;25(10):1114-6.

(25) Hentze H, Soong PL, Wang ST, Phillips BW, Putti TC, Dunn NR **"Teratoma Formation by Human Embryonic Stem Cells: Evaluation of Essential Parameters for Future Safety Studies"**, Stem Cell Res. 2009 May;2(3):198-210.

(26) Polejaeva I, Mitalipov S **"Stem Cell Potency and the Ability to Contribute to Chimeric Organisms"**, Reproduction. 2013 Mar;145(3): R81-R88.

(27) Nelson TJ, Behfar A, Yamada S, Martinez-Fernandez A, Terzic A, **"Stem Cell Platforms for Regenerative Medicine"**, Clin Transl Sci. 2009 June; 2(3):222-227.

(28) Martin GR, **"Isolation of a Pluripotent Cell Line from Early Mouse Embryos Cultured in Medium Conditioned by Teratocarcinoma Stem Cells"**, Proc Natl Acad Sci USA. 1981 Dec;78(12):7634-8.

(29) Thomson JA, Itskovitz-Eldor J, Shapiro SS, Waknitz MA, Swiergiel JJ, Marshall VS, Jones JM, **"Embryonic Stem Cell Lines Derived from Human Blastocysts"**, Science. 1998 Nov 6;282(5391):1145-1147.

(30) Hayek A, King CC, **"Brief Review: Cell Replacement Therapies to Treat Type 1 Diabetes Mellitus"**, Clin Diabetes Endocrinol. 2016 Feb 25;2:4.

(31) Llames S, Garcia-Perez E, Meana A, Larcher F, del Rio M, **"Feeder Layer Cell Action and Applicaions"**, Tissue Eng Part B Rev. 2015 Aug 1;21(4):345-353.

(32) Eiselleova L, Peterkova I, Neradil J, Slaninova I, Hampl A, Dvorak P, **"Comparative Study of Mouse and Human Feeder Cells for Human Embryonic Stem Cells"**, Int J Dev Biol. 2008; 52(4):353-363.

(33) Assady S, Maor Gila, Amit M, Istkovitz-Eldor J, Skorechi KL, Tzukerman M, **"Insulin Production by Human Embryonic Stem Cells"**, Diabetes. 2001 Aug;50(8):1691-1697.

(34) Nakagawa M, Taniguchi Y, Senda Sm Takizawa N, Ichisaka T, Asano K, Morizane A, Doi D, Takahashi J, Nishizawa M, Yoshida Y, Toyoda T, Osafune K, Sekiguchi K, Yamanaka S, **"A Novel Efficient Feeder-Free Culture System for the Derivation of Human Induced Pluripotent Stem Cells"**, Sci Rep. 2014 Jan 8;4:3594.

(35) Maria R, Nicholas B, Austin S, **"Towards Consistent Generation of Pancreatic Lineage Progenitors from Human Pluripotent Stem Cells"**, Philos Trans RR Soc B. 2015 Oct 19;370(1680):1-11.

(36) Murry CE, Keller G, **"Differentiation of Embryonic Stem Cells to Clinically Relevant Populations: Lessons from Embryologic Development"**, Cell. 2008 Feb 22;132(4):661-680.

(37) Pugliese A, Reijonen HK, Nepom J, Burke GW, **"Recurrence of Autoimmunity in Pancreas Transplant Patients: Research Updates"**, Diabetes Manag (Lond). 2011 Mar;1(2):229-238.

(38) Lo B, Parham L, **"Ethical Issues in Stem Cell Research**", Endocr Rev. 2009 May;30(3):204-213.

(39) Yamanaka S, **"Induced Pluripotent Stem Cells: Past, Present and Future"**, Cell Stem Cell. 2012 Jun 14;10(6):678-684.

(40) Dieke S, Jung SM, Lee J, Ju JH, **"Recent Technological Updates and Clinical Applications of Induced Pluripotent Stem Cells"**, Korean J Intern Med. 2014 Sep;29(5):547-557.

(41) Takahashi K, Yamanaka S **"Induction of Pluripotent Stem Cells from Mouse Embryonic and Adult Fibroblast Cultures by Defined Factors"**, Cell. 2006 Aug 25; 126(4):663-676.

(42) Soejitno A, Prayudi PKA, **"The Prospect of Induced Pluripotent Stem Cells for Diabetes Mellitus Treatment"**, Ther Adv Endocrinol Metab. 2011 Oct;2(5):197-210.

(43) Alipo Z, Liao W, Roemer EJ, Waner M, Fink LM, Ward DC, Ma Y **"Reversal of Hyperglycemia in Diabetic Mouse Models Using Induced Pluripotent Stem (iPS)-Derived Pancreatic β-Like Cells"**, Proc Natl Acad Sci USA. 2010 Jul 27;107(30):13426-13431.

(44) Wernig M, Meissner A, Cassady JP, Jaenisch R, **"c-Myc Is Dispensable for Direct Reprogramming of Mouse Fibroblasts"**, Cell Stem Cell. 2008 Jan 10;2(1):10-12.

(45) Weltner J, Anisimov A, Alitalo K, Otonkoski T, Trokovic R, **"Induced Pluripotent Stem Cell Clones Reprogrammed via Recombinant Adeno-Associated Virus-Mediated Transduction Contain Integrated Vector Sequences"**, J Virol. 2012 Apr;86(8):4463-4467.

(46) Yu J, Vodyanik MA, Smugga-Otto K, Antosiewicz-Bourget J, Frane JL, Tian S, Nie J, Jonsdottir GA, Routti V, Stewart R, Slukvin II, Thomson JA, **"Induced Pluripotent Stem Cell Lines Derived from Human Somatic Cells"**, Science. 2007 Dec 21;318(5858):1917-1920.

(47) Fusaki N, Ban H, Nishyama A, Saeki K, Hasegawa M, **"Efficient Induction of Transgene-Free Human Pluripotent Stem Cells Using a Vector Based on Sendai Virus, an RNA Virus that Does Not Integrate into the Host Genome"**, Proc Jpn Acad Ser B Phys Biol Sci. 2009 Oct; 85(8):348-362.

(48) Bianco P, Robey PG, Simmons PJ, **"Mesenchymal Stem Cells: Revisiting History, Concepts, and Assays"**, Cell Stem Cell. 2008 Apr 10;2(4):313-319.

(49) Zhao Q, Ren H, Han Z, **"Mesenchymal Stem Cells: Immunomodulatory Capability and Clinical Potential in Immune Diseases"**, Journal of Cellular Immunotherapy. 2016 Mar;2(1):3-20.

(50) Nauta AJ, Fibbe WE, **"Immunomodulatory Properties of Mesenchymal Stromal Cells"**, Blood. 2007 Nov 15;110(10):3499-3506.

(51) Ryan JM, Barry FP, Murphy JM, Mahon BP, **"Mesenchymal Stem Cells Avoid Allogenic Rejection"**, J Inflamm (Lond). 2005;2:8.

(52) Nagwa E, Mohamed AG, "**Mesenchymal Stem Cell Therapy in Diabetes Mellitus Progress and Challenges",** J Nucleic Acids. 2013;2013:194858.

(53) Dominici M, Le Blanc K, Mueller I, Slaper-Cortenbach I, Marini F, Krause D, Deans R, Keating A, Prockop Dj, Horwitz E, **"Minimal Criteria for Defining Multipotent Mesenchymal Stromal Cells. The International Society for Cellular Therapy Position Statement"**, Cytotherapy. 2006;8(4):315-7.

(54) Wu XX, Shao JZ, Xiang C, **"Generation of Pancreatic B Cells From Mesenchymal Stem Cells to Treat Type 1 Diabetes"**, OA Stem Cells. 2014 Mar 22;2(1):5.

(55) Si Y, Zhao Y, Hao H, Liu J, Guo Y, Mu Y, Shen J, Cheng Y, Fu X, Han W, **"Infusion of Mesenchymal Stem Cells Ameliorates Hyperglycaemia in Type 2 Diabetic Rats: Identification of a Novel Role in Improving Insulin Sensitivity"**, Diabetes. 2012 Jun;61(6):1616-1625.

(56) Li L, Li F, Gao F, Yang Y, Liu Y, Guo P, Li Y, **"Transplantation of Mesenchymal Stem Cells Improves Type 1 Diabetes Mellitus"**, Cell Tissue Res. 2016 May;364(2):345-355.

(57) Figliuzzi M, Bonanadrini B, Silvani S, Remuzzi A, **"Mesenchymal Stem Cells Help Pancreatic Islet Transplantation to Control Type 1 Diabetes"**, World J Stem Cells. 2014 Apr 26;6(2):163-172.

(58) Fischer UM, Harting MT, Jimenez F, Monson-Posadas WO, Xue H, Savitz SI, Laine GA, Cox CS, **"Pulmonary Passage is a Major Obstacle for Intravenous Stem Cell Delivery: The Pulmonary First-Pass Effect"**, Stem Cell Dev. 2009 Jun;18(5):683-691.

(59) Darwin JP, Joo YO, **"Mesenchymal Stem/Stromal Cells (MSCs): Role as Guardians of Inflammation."**, Mol Ther. 2012 Jan;20(1):14-20.

(60) Katsha AM, Ohkouch S, Xin H, Kanehira M, Sun R, Nukiwa T, Saijo Y, "**Paracrine Factors of Multipotent Stromal Cells Ameliorate Lung Injury in an Elastase-Induced Emphysema Model**", Mol Ther. 2011 Jan;19(1):196-203.

(61) Tran C, Damaser MS, **"Stem Cells as Drug Delivery Methods: Application of Stem Cell Secretome for Regeneration"**, Adv Drug Deliv Rev. 2015 Mar;82-83:1-11.

(62) Lee RH, Seo MJ, Reger RL, Spees JL, Pulin AA, Olson SD, Prockop DJ, **"Multipotent Stromal Cells from Human Marrow Home to and Promote Repair of Pancreatic Islets and Renal Glomeruli in Diabetic NOD/Scid Mice"**, Proc Natl Acad Sci USA. 2006 Nov 14;103(46):17438-17443.

(63) Skalnikova HK, **"Proteomic Techniques for Characterization of Mesenchymal Stem Cell Secretome"**, Biochimie. 2013 Dec;95(12):2196-2211.

(64) Ranganath SH, Levy O, Inamdar MS, Karp JM, **"Harnessing the Mesenchymal Stem Cell Secretome for the Treatment of Cardiovascular Disease"**, Cell Stem Cell. 2012 March 2;10(3):244-258.

(65) Zhao Q, Ren H, Han Z, **"Mesenchymal Stem Cells: Immunomodulatory Capability and Clinical Potential in Immune Diseases"**, Journal of Cellular Immunotherapy. 2016 Mar;2(1):3-20.

(66) Teixeira FG, Carvalho MM, Sousa N, Salgado AJ, **"Mesenchymal Stem Cell Secretome: A New Paradigm for Central Nervous System Regeneration?"**, Cell Mol Life Sci. 2013 Oct;70(20):3871-3882.

(67) Carpanetto A, Gai C, Favaro E, Zanone MM, Camussi G, **"Potential Immune Modulatory Action of Mesenchymal Stem Cell-Derived Extracellular Vesicles in Type 1 Diabetes"**, Int J Stem Cell Res Ther. 2015;2(2):011.

(68) Shifrin DA, Beckler MD, Coffey RJ, Tyska MJ, **"Extracellular Vesicles: Communication, Coercion, and Conditioning"**, Mol Biol Cell. 2013 May;24(9):1253-1259.

(69) Yanez-Mo, Siljander PR, Andreu Z, Zavec AB, Borras FE, Buzas K, Casal E, Capello F, Carvalho J, Colas E, Cordeiro-da Silva A, Fais S, Falcon-Perez JM, Ghobrial IM, Giebel B Gimona M, Graner M, Gursel I, Gursel M, Heegard NH, Hendrix A, Kierulf P, Kokubun K, Kosanovic M, Kralj-Iglic V, Krammer-Albers EM, Laitinen S, Lasser C, Lener T, Ligeti E, Line A, Lipps G, Llorente A, Lotvall J, Mancek-Kerber M, Marcilla A, Mittelbrunn , Nazarenko I, Nolte-t Hoen EN, Nyman TA, O'Driscoll L, Olivan M, Oliveira C, Pallinger E, Del Portillo HA, Reventros J, Rigau M, Rohde E, Sammar M, Sanchez-Madrid F, Santarem N, Schallmoser K, Osteneld MS, Stoorvogel W, Stukelj R, Van der Grein SG,

Vasconcelos MH, Wauben MH, De Wever O, **"Biological Properties of Extracellular Vesicles and Their Physiological Functions"**, J Extracell Vesicles. 2015 May 14;4:27066.

(70) Bo Y, Xiaomin Z, Xiaorong L, "**Exosomes Derived from Mesenchymal Stem Cells"**, Int J Mol Sci. 2014 Mar 7;15(3):4142-4157.

(71) Camussi,G, Deregibus M, Tetta C, "**Paracrine/Endocrine Mechanism of Stem Cells on Kidney Repair: Role of Microvesicle-Mediated Transfer of Genetic Information"**, Curr Opin Nephrol Hypertens. 2010 Jan;19(1):7-12.

(72) Doeppner TR, Herz J, Gorgens A, Schletcher J, Ludwig A, Radtke S, Miroschedji KD, Horn PA, Giebel B, Hermann DM, **"Extracellular Vesicles Improve Post-Stroke Neuroregeneration and Prevent Postischaemic Immunosuppression"**, Stem Cells Transl Med. 2015 Oct;4(10):1131-1143.

(73) Azar ST, Tamim H, Beyhum HN, Habbal MZ, Almawi WY, **"Type 1 (Insulin-Dependent) Diabetes is a Th1- and Th2-Mediated Autoimmune Disease"**, Clin Diagn Lab Immunol. 1999 May;6(3):306-310.

(74) Abdi R, Fiorina P, Adra CN, Atkinson M, Sayegh MH, **"Immunomodulation by Mesenchymal Stem Cells - a Potential Therapeutic Strategy for Type 1 Diabetes"**, Diabetes. 2008 Jul;57(7):1759-1767.

(75) Aggarwal S, Pittenger MF, "**Human Mesenchymal Stem Cells Modulate Allogenic Immune Cell Responses**", Blood. 2005 Feb 15;105(4):1815-1822.

(76) Prockop DJ, Youn OJ, "**MSCs: Role as Guardians of Inflammation**", Mol Ther. 2012 Jan;20(1):14-20.

(77) Park KS, Kim YS, Kim JH, Choi BK, Kim SH, *Tan AH, Lee MS, Lee MK, Kwoh CH, Joh JW, Kim SJ, Kim KW*, "**Trophic Molecules Derived from Human Mesenchymal Stem Cells Enhance Survival, Function And Angiogenesis Of Isolated Islets after Transplantation"**, Transplantation. 2010 Mar 15;89(5):509-517.

(78) Bruno S, Grange C, Collino F, Deregibus MC, Cantaluppi V, Biancone L, Tetta C, Camussi G, **"Microvesicles derived from mesenchyml stem cells enhance survival in a lethal model of acte kidney injury"**, PLOS One 2012 Mar 14;7(3):e33115

(79) Xing X, Hogquist KA, **"T-cell Tolerance: Central and Peripheral"**, Cold Spring Harb Perspect Biol. 2012 Jun 1;4(6):a006957.

(80) Lio CW, Hseieh CS, **"Becoming Self-Aware: The Thymic Education of Regulatory T-Cells"**, Curr Opin Immunol. 2011 April;23(2):213-219.

(81) Jeker LT, Bour-Jordan H, Bluestone JA, **"Breakdown in Peripheral Tolerance in Type 1 Diabetes in Mice and Humans"**, Cold Spring Harb Perspect Med. 2012 Mar;2(3):a007807.

(82) van Ewijk W, **"T-Cell Differentiation is Influenced by Thymic Microenvironments"**, Annu. Rev. Immunol. 1991;9:591-615.

(83) Hollander G, Gill J, Iwanami N, Liu C, Takahama Y, **"Cellular and Molecular Events During Early Thymus Development"**, Immunol Rev. 2006 Feb;209:28-46.

(84) Yousuke T, **"Journey Through the Thymus: Stromal Guides for T-Cell Development and Selection"**, Nat Rev Immunol. 2006 Feb;6(2):127-35.

(85) Janeway CA Jr*, Travers P, Walport M*, **"Generation of Lymphocytes in the Bone Marrow and Thymus",** Immunobiology: The Immune System in Health and Disease. 5th Edition. New York: Garland Science; 2001.

(86) Lynch HE, GolbergGL, Chidgey A, Van der Bink MR, Boyd R, Sempowski GD, **"Thymic Involution and Immune Reconstruction"**, Trends Immunol. 2009 Jul;30(7):366-373.

(87) Germain RN, **"T-cell Development and the CD4-CD8 Lineage Decision"**, Nat Rev Immunol. 2002 May;2(5):309-22.

(88) Weerkamp F, Pike-Overzet K, Staal FJ, **"T-Sing Progenitors to Commit"**, Trends Immunol. 2006 Mar;27(3):125-131.

(89) Klein L, Hiterberger M, Wirnsberger G, Kyewski B, **"Antigen presentation in the thymus for positive selection and central tolerance induction**", Nat Rev Immunol. 2009 Dec;9(12):833-844.

(90) Sebzda E, Mariathasan S, Ohteki T, Jones R, Bachmann MF, Ohashi PS, **"Selection of the T Cell Repertoire"**, Annu Rev Immunol. 1999;17:829-874.

(91) Hsieh C, Lee H, Lio C, **"Selection of regulatory T cells in the Thymus"**, Nat Rev Immunol. 2012 Mar;12(3):157-167.

(92) Blackburn CC, Manly NR, **"Developing a new paradigm for thymus organogenesis"**, Nature Reviews Immunology. 2004 April; 4:278-289

(93) Froguel P, **"Genetics of type 1 insulin-dependent diabetes mellitus"**, Horm Res. 1997;48(Suppl 4):55-57.

(94) Zumer K, Saksela K, Peterlin BM, **"The Mechanism of Tissue-Restricted Antigen Gene Expression by AIRE"**, J Immunol. 2013;190(6):2479-2482.

(95) Su MA, Anderson MS, **"Monogenic Autoimmune Disease: Insights into Self-Tolerance"**, Pediatr Res. 2009 May;65(5 pt 2):20R-25R.

(96) Wong FS, Wen L, **"The Study of HLA Class II and Autoimmune Diabetes"**, Curr Mol Med. 2003 Feb;3(1):1-15.

(97) Gough SC, Simmonds MJ, **"The HLA Region and Autoimmune Disease: Associations and Mechanisms of Action"**, Curr Genomics. 2007 Nov;8(7):453-465.

(98) Sharp CS, Abdulrahim M, Naser ES, Naser SA, **"Genetic Variations of PTPN2 and PTPN22: Role in the Pathogenesis of Type 1 Diabetes and Crohn's Disease"**, Front Cell Infect Microbiol. 2015 Dec 24;5:95.

(99) Espino-Paisan L, Urcelay E, Santiago JL, **"An insight into the Genetics of Type 1 Diabetes"**, Immunologia. 2009;28(4):173-181.

(100) Pugliese A, **"The Insulin Gene In Type 1 Diabetes**", IUBMB Life. 2005 Jul;57(7):463-468.

(101) Cai CQ, Zhang T, Breslin MB, Giraud M, Lan MS, **"Both Polymorphic Variable Number of Tandem Repeats and Autoimmune Regulator Module Differential Expression of Insulin in Human Thymic Epithelial cells"**, Diabetes. 2011 Jan;60(1):336-344.

(102) Lin X, Chem M, Liu Y, Guo Z, He X, Brand D, Zheng SG, **"Advances In Distinguishing Natural From Induced Foxp3+ Regulatory T-Cells"**, Int J Clin Exp Pathol. 2013;6(2):116-123.

(103) van der Vilet HJJ, Nieuwenhuis EE, **"IPEX as a Result of Mutations in FOXP3"**, Clin Dev Immunol. 2007;2007:89017.

(104) Nie J, Li YY, Zheng SG, Tsun A, Li Ben, **"FOXP3$^+$ Treg Cells and Gender Bias in Autoimmune Disease"**, Front Immunol. 2015;6:493.

(105) Hanabuchi S, Watanabe N, Liu Y, **"TSLP and Immune Homeostasis"**, Allergol Int. 2012 Mar;61(1):19-25.

(106) Li MO, Rudensky AY, **"T-Cell Receptor Signalling in the Control of Regulatory T-Cell Differentiation and Function"**, Nat Rev Immunol. 2016 Apr;16(4):220-233.

(107) Vignali DA, Collison LW, Workman CJ, **"How Regulatory T-Cells Work"**, Nat Rev Immunol. 2008 Jul;8(7):523-532.

(108) Petzold C, Riewaldt J, Watts D, Sparwasser T, Schallenberg S, Kretschmer K, **"FOXP3$^+$ Regulatory T-Cells in Mouse Models of Type 1 Diabetes"**, J Diabetes Res. 2013;2013:941710.

(109) Lasalle JM, Hafler DA, **"T-Cell Anergy"**, FASEB J. 1994 Jun;8(9):601-608.

(110) Simmonds MJ, Gough SCL, **"Unvavelling the genetic complexity of autoimmune thyroid disease: HLA, CTLA-4 and beyond"**, Clinical and Experimental Immunology 2004 Jan;136(1):1-10

(111) Kavvoura FK, Loannidis JP, **"CTLA-4 Gene Polymorphism and Susceptibility to Type 1 Diabetes Mellitus: A HuGE Review and Meta-Analysis"**, Am J Epidemiol. 2005 Jul 1;162(1):3-16.

(112) Francisco LM, Sage PT, Sharpe AH, **"The PD-1 Pathway in Tolerance and Autoimmunity"**, Immunol Rev. 2010 Jul;236:219-242.

(113) Vield PI, **"Insulitis in Human Type 1 Diabetes: The Quest for an Elusive Lesion"**, Islets. 2011 Jul-Aug;3(4):131-138.

(114) Balasa B, La Cava A, Van Gunsk K, Mocnik L, Balakrshna D, Nguyen N, Tucker L, Sarvetnick N, **"A Mechanism for IL-10 Mediated Diabetes in the Nonobese Diabetic (NOD) Mouse: ICAM-1 Deficiency Blocks Accelerated Diabetes"**, J Immunol. 2000 Dec 15;165(12):7330-7337.

(115) Atkinson MA, Wilson SB, **"Fatal Attraction: Chemokines and Type 1 Diabetes"**, J Clin Invest. 2002 Dec;110(11):1611-1613.

(116) Kaminitz A, Stein J, Yaniv I, Askenasy N, "**The Vicious Cycle of Apoptotic β-Cell Death in Type 1 Diabetes"**, Immunol Cell Biol. 2007 Nov-Dec;85(8):582-589.

(117) Wang C, Guan Y, Yang J, **"Cytokines in the Progression of Pancreatic β-Cell Dysfunction"**, Int J Endocrinol. 2010;2010:515136.

(118) Patel S, Santani D, **"Role of NF-κB in the Pathogenesis of Diabetes and its Associated Complications"**, Pharmacol Rep. 2009 Jul-Aug;61(4):595-603.

(119) Ortis F, Pirot P, Naamane N, Kriens AY, Rasschaert J, Moore F, Theatre E, Verhaeghe C, Magnusson NE, Chariot A, Orntoft TF, Eizirik DL, **"Induction of Nuclear Factor-kappaB And its Downstream Genes by TNF-alpha and IL-1 beta has a Pro-Apoptotic Role in Pancreatic Beta Cells"**, Diabetologia. 2008 Jul;51(7):1213-1225.

(120) Melloul D, **"Role of NF-κB in Beta Cell death"**, Biochem Soc Trans. 2008 Jun;36(Pt 3):334-339.

(121) Barkett M, **"Control of Apoptosis by Rel/NF-κB Transcription Factors**", Oncogene. 1999 Nov 22;18(49):6910-6924.

(122) Eldor R, Yeffet A, Baum K, Doviner V, Amar D, Ben-Neriah Y, Christofori G, Peled A, Carel JC, Boitard C, Klein T, Serup P, Eizirik DL, Melloul D, **"Conditional and Specific NF-kappaB Blockade Protects Pancreatic Beta Cells From Diabetogenic Agents"**, Proc Natl Acad Sci USA. 2006 Mar 28;103(13):5072-5077.

(123) Cnop M, Welsh N, Jonas J, Jorns A, Lenzen S, Eizirik DL, **"Mechanisms of Pancreatic Beta-Cell Death in Type-1 and Type-2 Diabetes – Many Differences, Few Similarities"**, Diabetes. 2005 Dec;54 Suppl 2:S97-S107.

(124) Baldwin AS, **"The NF-κB and IκB Proteins: New Discoveries and Insights**", Annu Rev Immunol. 1996;14:649-683.

(125) Hayden MS, Gosh S, **"Signalling to NF-κB"**, Genes Dev. 2004 Sep 15;18(18):2195-2224.

(126) Oh H, Ghosh S, **"NF-κB: Roles and Rgulation in different CD4 (+) T-cell Subsets",** Immunol Rev. 2013 Mar;252(1):41-51.

(127) Gerondakis S, Fulford TS, Messina NL, Grumont RJ, **"NF-κB Control of T-Cell Development"**, Nat Immunol. 2014 Jan;15(1):15-25.

(128) MacMicking J, Xie QW, Nathan C, **"Nitric Oxide and Macrophage Function**", Annu Rev Immunol. 1997;15:323-350.

(129) Knowles RG, Moncada S, **"Nitric Oxide as a Signal in Blood Vessels"**, Trends Biochem Sci. 1992 Oct;17(10):399-402.

(130) Villalobo A, **"Nitric Oxide and Cell Proliferation"**, FEBS J. 2006 Jun; 273(11);2329-2344.

(131) Forstermann U, Sessa WC, **"Nitric Oxide Synthases: Regulation and Function"**, Eur Heart J. 2012 Apr;33(7):829-837.

(132) Kim YM, Talanian RV, Billiar TR, **"Nitric Oxide Inhibits Apoptosis by Preventing Increases in Caspase-3-Like Activity Via Two Distinct Mechanisms"**, J Biol Chem. 1997 Dec 5;272(49):31138-31148.

(133) Delikouras A, Hayes M, Malde P, Dorling A, **"Nitric Oxide-Mediated Expression of Bcl-2 and Bcl-Xl and Protection from Tumour Necrosis Factor-Alpha-Mediated Apoptosis in Porcine Endothelial Cells after Exposure to Low Concentrations of Xenoreactive Natural Antibody"**, Transplantation. 2001 Mar 15;71(5):599-605.

(134) Bernhard B, **"Nitric Oxide: NO Apoptosis or Turning it ON?"**, Cell Death Differ. 2003 Aug;10(8):864-869.

(135) Keklikoglu N, Akinci S, **"The Role of iNOS in Beta Cell Destruction in Diabetes"**, Oxid Antioxid Med Sci. 2013;2(4):251-254.

(136) Darville MI, Eizirik DL, "**Regulation by Cytokines of the Inducible Nitric Oxide Promoter in Insulin-Producing Cells"**, Diabetologia. 1998;41(9):1101-1108.

(137) Messmer UK, Brune B, **"Nitric Oxide-Induced Apoptosis: p53-Dependent and p53-Independent Signalling Pathways"**, Biochem J. 1996 Oct 1;319(Pt 1):299-305.

(138) Ramaldo R, Viana RJS, Low WC, Rodrigues C, **"Bile Acids and Apoptosis Modulation: An Emerging Role in Experimental Alzheimer's Disease"**, Trends Mol Med. 2008 Feb;14(2):54-62.

(139) Tortora V, Quijano C, Freedman B, Radi R, Castro L, **"Mitochondrial Aconitase Reaction with Nitric Oxide, S-Nitroglutathione and Peroxynitrite; Mechanisms and Relative Contributions of Aconitase Inactivation"**, Free Radic Biol Med. 2007 Apr;42(7):1075-1088.

(140) Pierre P, Alessandra KC, Decio LE, **"Mediators and Mechanisms of Pancreatic Beta-Cell Death in Type 1 Diabetes"**, Arq Bras Endocrinol Metabol. 2008 Mar;52(2):156-165.

(141) Wang Y, Kim NS, Haince JF, Kang HC, David KK, Andrabi SA, Poirier GG, Dawson VL, Dawson TM, **"Poly(ADP-Ribose) (PAR) Binding to Apoptosis-Inducing Factor is Critical for PAR Polymerase-1-Dependent Cell Death (Parthanatos)"**, Sci Signal. 2011 Apr 5;4(167):ra20.

(142) Oslowski CM, Urano F, **"Measuring ER Stress and the Unfolded Protein Response Using Mammalian Tissue Culture System**", Methods Enzymol. 2011;490:71-92.

(143) Kaneto H, Miyatsuka T, ShiraiwaT, Yamamoto K, Kato K, Fujitani Y, Matsuoka TA, **"Crucial Role of Pdx-1 in Pancreatic Development, Beta Cell Differentiation, and Induction of Surrogate Beta"**, Curr Med Chem. 2007;14(16):1745-1752.

(144) Gauthier BR, Wiederkehr A, Baquie M, Dai C, Powers AC, Kerr-Conte J, Pattou F, Macdonald RJ,Ferrer J, Wollheim CB, **"Pdx1 Deficiency Causes Mitochondrial Dysfunction and Defective Insulin Secretion through TFAM Suppression"**, Cell Metab. 2009 Aug;10(2):110-118.

(145) Shternhall-Ron K, Quintana FJ, Perl S, Meivar-Levy I, Barchack I, Cohen IR, Feber S, **"Ectopic PDX-1 Expression in Liver Ameliorates Type-1 Diabetes"**, J Autoimmun. 2007 Mar-May;28(2-3):134-142.

(146) Bernard T, **"GLUT2, Glucose Sensing and Glucose Homeostasis"**, Diabetologia. 2015 Feb;58(2):221-232.

(147) Delphine J, Francoise B, **"NF-kB Activation Results in Rapid Inactivation of JNK in TNF-Alpha Treated Ewing Sarcoma Cells: A Mechanism for the Anti-Apoptotic Effect of NF-kB"**, Oncogene. 2001 Jul 19;20(32):4365-4372.

(148) Hohmeier H, Thigpen A, Tran VV, Davis R, Newgard CB, **"Stable Expression of Manganese Superoxide Dismutase (MnSOD) in Insulinoma Cells Prevents IL-1β-induced Cytotoxicity and Reduces Nitric Oxide Production"**, J Clin Invest. 1998 May 1;101(9):1811-1820.

(149) Li Z, Srivastava P, **"Heat-Shock Proteins",** Curr Protoc Immunol. 2004 Feb;58:A.1T.1-A.1T.6.

(150) Hagiwara S, Iwasaka H, Shingu C, Matsumoto S, Hasegawa A, Asai N, Noguchi T, **"Heat Shock Protein 72 Protects Insulin-Secreting Beta Cells from Lipopolysaccharide-Induced Endoplasmic Reticulum Stress"**, Int J Hyperthermia. 2009 Dec;25(8):626-633.

(151) Burkart V, Liu H, Bellmann K, Wissing D, Jaattela M, Cavallo MG, Pozzilli P, Briviba K, Kolb H, **"Natural Resistance of Human Beta Cells toward Nitric Oxide is Mediated by Heat Shock Protein 70"**, J Biol Chem. 2000 Jun 30;275(26):19521-19528.

(152) Papaccio G, Graziano A, D'aquino R, Valiante S, Naro F, **"A Biophasic Role of Nuclear Transcription Factor (NF)-Kb in the Islet β-Cell Apoptosis Induced by Interleukin (IL)-1β"**, J Cell Physiol. 2005 Jul;204(1):124-130.

(153) Wada T, Penninger JM, **"Mitogen-Activated Protein Kinases in Apoptosis Regulation"**, Oncogene. 2004 Apr 12;23(16):2838-2849.

(154) Zhang W, Liu HT, **"MAPK Signal Pathways in The Regulation of Cell Proliferation in Mammalian Cells"**, Cell Res. 2002 Mar;12(1):9-18.

(155) **"Simplified Overview of Mammalian MAPK Cascades."** Wikipedia, Wikimedia Foundation, 29 Dec. 2012, en.wikipedia.org/wiki/File:MAPK-pathway-mammalian.png. Retrieved on: 12th October 2016.

(156) Dhanasekara DN, Reddy EP, **"JNK Signalling in Apoptosis"**, Oncogene. 2008 Oct 20;27(48):6245-6251.

(157) Liu J, Lin A, **"Role of JNK Activation in Apoptosis: A Double-Edged Sword"**, Cell Res. 2005 Jan;15(1):36-42.

(158) Saldden J, Lee JC, Welsh N, **"Role of P38 Mitogen-Activated Protein Kinases (P38mapk) in Cytokine-Induced Rat Islet Cell Apoptosis"**, Biochem Pharmacol. 2001 Jun 15;61(12):1561-1569.

(159) Widenmaiser SB, Ao Z, Kim SJ, Warnock G, Mclntosh CH, **"Suppression of P38 MAPK and JNK via Akt-Mediated Inhibition of Apoptosis Signal-Regulating Kinase 1 Constitutes a Core Component of the Beta-Cell Pro-Survival Effects of Glucose-Dependent Insulinotrophic Polypeptide"**, J Biol Chem. 2009 Oct 30;284(44):30372-30382.

(160) Pavlovic D, Andersen NA, Mandrup-Poulsen T, Eizirik DL, **"Activation of Extracellular Signal-Regulated Kinase (ERK) 1/ 2 Contributes to Cytokine-Induced Apoptosis in Purified Rat Pancreatic Beta-Cells"**, Eur Cytokine Netw. 2000 Jun;11(2):267-274.

(161) Larsen L, Storling J, Darville M, Eizirik DL, Bonny C, Billestrup N, Mandrup-Poulsen T, **"Extracellular Signal-Regulated Kinase is Essential for Interleukin-1-Induced and Nuclear Factor KB Mediated Gene Expression in Insulin-Producing INS-1E Cells"**, Diabetologia. 2005 Dec;48(12):2582-2590.

(162) Cal B, Chang SH, Becker EBE, Bonni A, Xia Z, **"p38 MAP Kinase Mediates Apoptosis through Phosphorylation of $Bim_{EL}$ at Ser-65"**, J Biol Chem. 2006 Sep 1;281(35):25215-25222.

(163) Cagnol S, Chambard J, **"ERK and Cell Death; Mechanisms of ERK-Induced Cell Death: Apoptosis, Autophagy and Senescence"**, FEBS J. 2010 Jan;277(1):2-21.

(164) **"Tumor necrosis factor alpha."** Wikipedia, Wikimedia Foundation, 18 Oct. 2016, en.wikipedia.org/wiki/Tumor_necrosis_factor_alpha. Retrieved on: 18th October 2016.

(165) Wada T, Penninger JM, **"Mitogen-Activated Protein Kinases in Apoptosis Regulation"**, Oncogene. 2004 Apr 12;23(16):2838-2849.

(166) Liu J, Lin A, **"Role of JNK Activation in Apoptosis: A Double-Edged Sword"**, Cell Res. 2005 Jan;15(1):36-42.

(167) Kaneto H, Matsuoka T, Katakami N, Kawamort D, Miyatsuka T, Yoshiuchi K, Yasuda T, Sakamoto K, Yamasaki Y, Matsuhisa M, **"Oxidative stress and the JNK pathway are Involved in the Development of Type 1 and Type 2 Diabetes"**, Curr Mol Med. 2007 Nov;7(7):674-686.

(168) Karin M, **"The Regulation of AP-1 Activity by Mitogen-Activated Protein Kinases"**, J Biol Chem. 1995 Jul 14;270(28):16483-16486.

(169) Hartman MG, Lu D, Kim M, Kociba GJ, Shukri T, Buteau J, Wang X, Frankel WL, Guttridge D, Prentki M, Grey ST, Ron D, Hai T, **"Role of Activating Transcription Factor 3 in Stress-Induced β-Cell Apoptosis"**, Mol Cell Biol. 2004 Jul;24(13):5721-5732.

(170) Shaulian E, Karin M, **"AP-1 in Cell Proliferation and Survival"**, Oncogene. 2001 Apr 30;20(19):2390-2400.

(171) Dhanasekaran DN, Reddy EP, **"JNK Signalling in Apoptosis"**, Oncogene. 2008 Oct 20;27(48):6245-6251.

(172) Tsujimoto Y, **"Role of Bcl2 family proteins in apoptosis: apoptosomes or mitochondria?"**, 1998 Nov;3(11):697-707.

(173) Couper KN, Blount DG, Riley EM, **"IL-10: The Master Regulator of Immunity to Infection"**, J Immunol. 2008 May 1;180(9):5771-5777.

(174) Hutchkins AP, Diez D, Miranda-Saavedra D, **"The IL-10/STAT3-Mediated Anti-Inflammatory Response: Recent Developments and Future Challenges"**, Brief Funct Genomics. 2013 Nov;12(6):489-498.

(175) Sabat R, **"IL-10 Family of Cytokines"**, Cytokine Growth Factor Rev. 2010 Oct;21(5):315-324.

(176) Kim JM, Brannan CI, Coopeland NG, Jenkins NA, Khan TA, Moore KW, **"Structure of the Mouse Interleukin-10 Gene and Chromosomal Localization of the Mouse and Human Genes"**, J Immunol. 1992 Jun 1;148(11):3618-3623.

(177) Mosser DM, Zhang X, **"Interleukin-10: New Perspective on an Old Cytokine"**, Immunol Rev. 2008 Dec;226:205-218.

(178) Hedrich CM, Bream JH, **"Cell Type-Specific Regulation of IL-10 Expression in Inflammation and Disease"**, Immunol Res. 2010 Jul;47(1-3):185-206.

(179) Walter MR, **"The Molecular Basis of IL-10 Function: From Receptor Structure to the Onset of Signalling"**, Curr Top Immunol. 2014;380:191-192.

(180) Moore KW, de Waal Malefyt R, Coffman RL, O'Gaara A, **"Interleukin-10 and the Interleukin-10 Receptor"**, Annu Rev Immunol. 2001;19:683-765.

(181) Yoon SI, Logsdon NJ, Sheikh F, Donnelly RP, Walter MR, **"Conformational Changes Mediate Interleukin-10 Receptor 2 (IL-10R2) Binding to IL-10 and Assembly of the Signalling Complex"**, J Biol Chem. 2006 Nov 17;281(46):35088-35096.

(182) Walter MR, "**The Molecular Basis of IL-10 Function: From Receptor structure to the Onset of Signalling**", Curr Top Microbiol Immunol. 2014;380:191-212.

(183) Kotenko SV, Krause CD, Izotova LS, Pollack BP, Wu W, Pestka S, "**Identification and Functional Characterisation of a Second Chain in the Interleukin-10 Receptor Complex"**, EMBO J. 1997 Oct 1;16(19):5894–5903.

(184) Rawlings JS, Rosler KM, Harrison DA (2004) "**The JAK/STAT Signalling Pathway"**, J Cell Sci. 2004 Mar 15;117(Pt 8):1281-1283.

(185) MA Russel, Morgan NG, "**The Impact of Anti-Inflammatory Cytokines on the Pancreatic Beta Cell"**, Islets. 2014;6(3):e950547.

(186) Kato K, Nomoto M, Izumi H, Ise T, Nakano S, Niho Y, Kohno K, **"Structure and Functional Analysis of the Human STAT3 Gene Promoter: Alteration of Chromatin Structure as a Possible Mechanism for the Upregulation in Cisplatin-Resistant Cells"**, Biochim Biophys Acta. 2000 Sep 7;1493(1-2):91-100.

(187) Saleem HH, Trojanowski B, Fiedler K, Maier HJ, Schirmbeck R, Wagner M, Boehm BO, Wirth T, Baumann B, **"Long-Term IKK2/NFκB Signalling in Pancreatic Beta Cells Induces Immune-Mediated Diabetes"**, Diabetes. 2014 Mar;63(3):960-975.

(188) Shames BD, Selzman CH, Meldrum DR, Pulido EJ, Barton HA, Meng X, Harken AH, McIntyre RC Jr, **"Interleukin-10 Stabilises Inhibitory KappaB-alpha in Human Monocytes"**, Shock. 1998 Dec;10(6):389-394.

(189) Kuwata H, Watanabe Y, Miyoshi H, Yamamoto M, Kaisho T, Takeda K, Akita S, **"IL-10-Inducible Bcl-3 Negatively Regulates LPS-Induced TNF-A Production in Macrophages"**, Blood. 2003 Dec 1;102(12):4123-4129.

(190) Zhang Q, Didonato JA, Karin M, McKeithan TW, **"BCL3 Encodes a Nuclear Protein Which Can Alter the Subcellular Location of NFκB Protein"**, Mol Cell Biol. 1994 Jun;14(6):3915-3926.

(191) Carbello E, Lai WS, Blackshear PJ, **"Feedback Inhibition of Macrophage Tumour Necrosis Factor - a Production by Tristetrapolin"**, Science. 1998 Aug 14;281(5379):1001-1005.

(192) Babon JJ, Varghese LN, Nicola NA, **"Inhibition of IL-6 Family Cytokines by SOCS3"**, Semin Immunol. 2014 Feb;26(1):13-19.

(193) Braun DA, Fribourg M, Sealfon SC, **"Cytokine Response is Determined by Duration of Receptor and Signal Transducers and Activators of Transcription 3 (STAT3) Activation"**, J Biol Chem. 2013 Feb 1;288(5):2986-2993.

(194) Scheller J, Chalaris A, Schmidt-Arras D, Rose-John S, **"The Pro- and Anti-Inflammatory Properties of the Cytokine Interleukin 6"**, Biochim Biophys Acta. 2011 May;1813(5):878-888.

(195) Herfath H, Scholmerich J, **"IL-10 Therapy in Crohn's Disease: at The Crossroads"**, Gut. 2002 Feb;50(2):146-147.

(196) Groux H, Bigler M, de Vries JE, Roncarolo MG, **"Inhibitory and Stimulatory Effects of IL-10 on Human CD8+ T Cells"**, J Immunol. 1998 Apr 1;160(7):3188-3193.

(197) Rousett F, Garcia E, Defrance T, Peronne C, Vezzio N, Hsu DH, Kastelein R, Moore KW, Banchereau J, **"Interleukin 10 is a Potent Growth and Differentiation Factor for Activated Human B Lymphocytes"**, Proc Natl Acad Sci USA. 1992 Mar 1;89(5):1890-1893.

(198) Azar ST, Tamim H, Beyhum HN, Habbal MZ, Almawi WY, **"Type 1 (Insulin-Dependent) Diabetes is a TH1- and TH2-Mediated Autoimmune Disease"**, Clin Diagn Lab Immunol. 1999 May;6(3):306-310.

(199) Liew FY, **"$T_H$1 and $T_H$2 cells : a historical perspective"**, Nat Rev Immunol. 2002 Jan;2(1):55-60.

(200) Chadban SJ, Tesh GH, Foti R, Lan HY, Atkins RC, Nikolic-Paterson DJ, **"Interleukin-10 Differentially Modulates MHC Class II Expression by Mesangial Cells and Macrophages in Vitro and in Vivo"**, Immunology. 1998 May;94(1):72-78.

(201) Buelens C, Willems F, Delvaux A, Pierard G, Delville JP, Velu T, Goldman M, **"Interleukin-10 Differentially Regulates B7-1(CD80) and B7-2(CD86) Expression on Human Peripheral Blood Dendritic Cells"**, Eur J Immunol. 1995 Sep;25(9):2668-2672.

(202) Ren YX, Yang J, Sun R, Zhang L, Zhao L, Li B, Li L, Long H, Sun Q, Huang Y, Li X, **"Viral IL-10 Down-Regulates the "MHC-1 Antigen Processing Operon" through the NF-κB Signalling Pathway in Nasopharyngeal Carcinoma Cells"**, Cytotechnology. 2016 Dec;68(6):2625-2636.

(203) Vanikar AV, Trivedi HL, **"T-Regulatory Cells: the Recently Recognised Players of Immunomodulation"**, J Stem Cell Res Ther. 2014;4:241.

(204) Serebrennikova OB, Tsatsanis C, Mao C, Gounaris E, Ren W, Siracusa LD, Elipoulose AG, Khazaie K, Tsichlis PN, **"Tpl2 Ablation Promotes Intestinal Inflammation and Tumorgenesis In *Apc$^{min}$* Mice by Inhibiting IL-10 Secretion and Regulatory T-Cell Generation"**, *Proc Natl Acad Sci USA. 2012 May 1;109(18):E1082-E1091.*

(205) O'Garra A, Vieira P, Goldfield AE, **"IL-10-Producing and Naturally Occurring CD4+ Tregs: Limiting Collateral Damage"**, J Clin Invest. 2004 Nov;114(10):1372-1378.

(206) Viera PL, Christensen JR, Minaee S, O'Neill EJ, Barrat FJ, Boonstra A, Barthlott T, Stockinger B, Wraith DC, O'Gaara A, **"IL-10-Secreting Regulatory T Cells Do Not Express Foxp3 but Have Comparable Regulatory Functions to Naturally Occurring CD4+ CD25+ Regulatory T Cells"**, J Immunol. 2004 May 15;172(10):5986-5993.

(207) Vincenz L, Szegezdi E, Jager R, Holohan C, O'Brien T, Samali A, **"Cytokine-Induced β-Cell Stress and Death in Type 1 Diabetes Mellitus, Type 1 Diabetes - Complications, Pathogenesis, and Alternative Treatments, Prof. Chih-Pin Liu (Ed.)"**, InTech; 2011. Available from: http://www.intechopen.com/books/type-1-diabetes-complications-pathogenesis-and-alternative-treatments/cytokine-induced-946-cell-stress-and-death-in-type-1-diabetes-mellitus

(208) Atkinson MA, Wilson SB, **"Fatal Attraction: Chemokines and Type 1 Diabetes"**, J Clin Invest. 2002 Dec 1;110(11):1611-1613.

(209) Ishizuka K, Sugimura K, Homma T, Matsuzawa J, Mochizuki T, Kobayashi M, Suzuki K, Otsuka K, Tashiro K, Yamaguchi O, Asakura H, **"Influence of Interleukin-10 on the Interleukin-1 Receptor Antagonist/Interleukin 1-Beta Ratio in the Colonic Mucosa of Ulcerative Colitis"**, Digestion. 2001;63 Suppl 1:22-27.

(210) Mortitani M, Yoshomoto K, LI S, Kondo M, Iwahana H, Yamaoka T, Sano T, Nakano N, Kikutani H, Itakura M, **"Transgenic Expression of IL-10 in Pancreatic Islet A Cells Accelerates Autoimmune Insulitis and Diabetes in Non-Obese Diabetic Mice"**, Int Immunol. 1994 Dec;6(12):1927-1936.

(211) Zhang ZL, Shen SX, Lin B, Yu LY, Zhu LH, Wang WP, Luo FH, Guo LH, **"Intramuscular Injection of Interleukin-10 Plasmid DNA Prevented Autoimmune Diabetes in Mice"**, Acta Pharmacol Sin. 2003 Aug;24(8):751-756.

(212) Balasa B, La Cava A, Van Gunsk K, Mocnik L, Balakrshna D, Nguyen N, Tucker L, Sarvetnick N, **"A Mechanism for IL-10 Mediated Diabetes in the Nonobese Diabetic (NOD) Mouse: ICAM-1 Deficiency Blocks Accelerated Diabetes"**, J Immunol. 2000 Dec 15;165(12):7330-7337.

(213) Kawamoto S, Nitta Y, Tashiro F, Nakato A, Yamato E, Tahara H, Tabayashi K, Miyazaki J, **"Suppression of Th1 Cell Activation and Prevention of Autoimmune Diabetes in NOD Mice by Local Expression of Viral IL-10"**, Int Immunol. 2001 May;13(5):685-694.

(214) Z Yang, Chen M, Wu R,Fialkow LB, Bromberg JS, Mc Duffle M, Naji A, Nadler JL, **"Suppression of Autoimmune Diabetes by Viral IL-10 Gene Transfer"**, J Immunol. 2002 Jun 15;168(12):6479-6485.

(215) Lee MS, Mueller R, Wicker LS, Peterson LB, Sarvetnick N, **"IL-10 is Necessary and Sufficient for Autoimmune Diabetes in Conjunction with NOD MHC Homozygosity"**, J Exp Med. 1996 Jun 1;183(6):2663-2668.

(216) Groux H, Bigler M, de Vries JE, Roncarolo MG, **"Inhibitory and Stimulatory Effects of IL-10 on Human CD8+ T Cells"**, J Immunol. 1998 Apr 1;160(7):3188-3193.

(217) Al Azzawi B*, Merkan MM, Kelly C, Forsyth N*, **"Mesenchymal Stem Cell Derived Products Attenuate Cytokine-Induced Apoptosis in Pancreatic Beta Cells"**, Diabetic Medicine. 2016 Mar;33:41.

(218) Russel MA, Morgan NG, **"The Impact of Anti-Inflammatory Cytokines on the Pancreatic Beta Cell"**, Islets. 2014;6(3):e950547.

(219) Cnop M, Welsh N, Jonas J, Jorns A, Lenzen S, Eizirik DL, **"Mechanisms of the Pancreatic Beta Cell Death in Type 1 and Type 2 Diabetes"**, Diabetes. 2005 Dec;54 Suppl 2:S97-S107.

(220) Poitout V, Olsen LK, Robertson RP, **"Glucose Toxicity And Paradoxical Decrease in Insulin Gene Transcription in β-TC6 Cells"**, J Investig Med. 1996 Jan 1;44(1):A112.

(221) McClenaghan NH, Barnett CR, Ah-Sing E, Abdel-Wahab YH, O'Harte FP, Yoon TW, Swanston-latt PR, **"Characterisation of a Novel Glucose-Responsive Insulin-Secreting Line, BRIN-BD11, Produced by Electrofusion"**, Diabetes. 1996 Aug;45(8):1132-1140.

(222) Poitout V, Stout LE, Armstrong MB, Walseth TF, Sorenson RL, Robertson RP, **"Morphological and Functional Characterisation of Beta TC-6 Cells—An**

**Insulin-Secreting Cell Line Derived from Transgenic Mice"**, Diabetes. 1995 Mar;44(3):306-313.

(223) **"Microscope Use in Brewing"**, Braukaiser, 7 Oct 2012, http://braukaiser.com/wiki/index.php?title=Microscope_use_in_brewing Accessed on 19th Feb 2017

(224) Wagner W, Horn P, Castoldi M, Diehlmann A, Bork S, Saffrich R, Benes Vladimir, Blake J, Pfister S, Eckstein V, Ho AD, **"Replicative Senescence of Mesenchymal Stem Cells: A Continuous and Organised Process"**, PLoS One. 2008 May 21;3(5):e2213.

(225) Turinetto V, Vitale E, Giachino C, **"Senescence in Human Mesenchymal Stem Cells: Functional Changes and Implications in Stem Cell-Based Therapy"**, Int J Mol Sci. 2016 Jul 19;17(7):1164.

(226) Sepulveda JC, Tome M, Fernandez ME, Delgado M, Campisi J, Bernard A, Gonzalez MA, **"Cell Senescence Abrogates the Therapeutic Potential of Human Mesenchymal Stem Cells in the Lethal Endotoxemia Model"**, Stem Cells. 2014 Jul;32(7):1865-1877.

(227) Faten AM, Aziza A, Zaki AA, **"Confluence-Associated Proliferation and Osteogenic Differentiation of Bone Marrow Mesenchymal Stem Cells (BMMSCs)"**, Int Res J Biological Sci. 2016 May;5(5):44-56.

(228) Sittampalam GS, Coussens NP, Brimacombe K, *Grossman A, Arkin M, Auld D, Austin C, Baell J, Bejcek B, Chung TDY, Dahlin JL, Devanaryan V, Foley TL, Glicksman M, Hall MD, Hass JV, Inglese J, Iversen PW, Kahl SD, Kales SC, Lal-Nag M, Li Z, McGee J, McManus O, Riss T, Trask OJ, Weidner JR, Xia M, Xu X* ,**"Assay Guidance Manual"**. Bethesda (MD): Eli Lilly & Company and the National Center for Advancing Translational Sciences; 2004. Available from: https://www.ncbi.nlm.nih.gov/books/NBK144065/

(229) **"MTT-Cell Based Proliferation/Toxicity Assay Kit."** FineTest, Wuhan Fine Biotech Co., Ltd, 26 May 2016, www.fn-test.com/reagents/mtt-cell-based-proliferationtoxicity-assay-kit/. Accessed on: 20th March 2017.

(230) **"Thermo Scientific™ 0.2 ML Strip Tubes."** Fisher Scientific, Thermo Fischer Scientific, 2017, www.fishersci.com/shop/products/0-2-ml-strip-tubes/p-4526084. Accessed on: 5th January 2016.

(231) Hulspas R, O'Gorman MRG, Wood BL, Gratama JW, Sutherland RD, **"Considerations for the Control of Background Fluorescence in Clinical Flow Cytometry"**, Cytometry B Clinical Cytom. 2009 Nov;76B(6):355-364.

(232) Monici M, **"Cell and Tissue Autofluorescence Research and Diagnostic Applications"**, Biotechnol Annu Rev. 2005;11:227-256.

(233) **"Exposure Times."** Molecular Probes School of Fluorescence, Thermo Fisher Scientific, 2017, www.thermofisher.com/uk/en/home/life-science/cell-analysis/cell-analysis-learning-center/molecular-probes-school-of-fluorescence/capturing-analyzing-your-samples/exposure-times.html. Acessed on: 15th April 2017.

(234) Deeds MC, Anderson JM, Armstrong AS, Gastineau DA, Hiddinga HJ, Jahangir A, Eberhardt NL, Kudva YC, **"Single Dose Streptozocin Induced Diabetes: Considerations for Study Design in Islet Transplantation Models"**, Lab Anim. 2011 Jul;45(3):131-140.

(235) Eleazu CO, Eleazu KC, Chukwuma S, Essien UN, **"Review of the Mechanism of Cell Death Resulting from Streptozocin Challenge in Experimental Animals, its Practical Use and Potential Risk to Humans"**, J Diabetes Metab Disord. 2013 Dec 23;12(1):60.

(236) Van Belle TL, Taylor P, von Herrath MG, **"Mouse Models for Type 1 Diabetes"**, Drug Discov Today Dis Models. 2009 Summer;6(2):41-45.

(237) Graham ML, Janecek JL, Kittredge JA, Hering BJ, Schuurman H, **"The Streptozocin-Induced Diabetic Nude Mouse Model: Differences between Animals from Different Sources"**, Comp Med. 2011 Aug; 61(4):356-360.

(238) Yeung TY, Seeberger KL, Kin T, Adesida A, Jomha N, Shapiro AM, Korbutt GS, **"Human Mesenchymal Stem Cells Protect Human Islets from Pro-Inflammatory Cytokines"**, PLoS One. 2012;7(5):e38189.

(239) Kyrylkova K, Kyryachenko S, Leid M, Kioussi C, **"Detection of apoptosis by TUNEL assay"**, Methods Mol Biol. 2012;887:41-47.

(240) Zhou Y, Hu Q, Chen F, Zhang J, Guo J, Wang H, Gu J, Ma L, Ho G, **"Human Umbilical Cord Matrix-Derived Stem Cells Exert Trophic Effects On β-Cell Survival in Diabetic Rats and Isolated Islets"**, Dis Model Mech. 2015 Dec;8(12):1625-1633.

(241) Khan M, Ali F, Moshin S, Akhtar S, Mehmood A, Choudhery MS, Khan SN, Riazzudin S, **"Preconditioning Diabetic Mesenchymal Stem Cells with Myogenic Medium Increases their Ability to Repair Diabetic Heart"**, Stem Cell Res Ther. 2013 May 24;4(3):58.

(242) Shibata T, Karuse K, Kamiya H, Kozakae M, Kondo M, Yasuda Y, Nakamura N, Ota K, Tosaki T, Matsuki T, Nakashima E, Hamada Y, Oiso Y, Nakamura J, **"Transplantation of Bone-Marrow Derived Mesenchymal Stem Cells Improves Diabetic Polyneuropathy in Rats."**, Diabetes. 2008 Nov;57(11):3099-3107.

(243) Gao X, Song L, Shen K, Wang H, Qian M, Niu W, Qin X, **"Bone Marrow Stem Cells Promote the Repair of Islets from Diabetic Mice through Paracrine Actions"**, Mol Cell Endocrinol. 2014 May 5;388(1-2):41-50.

(244) Li M, Zhao Y, Hao H, Dai H, Han Q, Tong C, Liu J, Han W, Fu X, **"Mesenchymal Stem Cell-Conditioned Medium Improves the Proliferation and Migration of Keratinocytes in a Diabetes-Like Microenvironment"**, Int J Low Extrem Wounds. 2015 Mar;14(1):73-86.

(245) Di G, Liu Y, Liu J, Wu C, Duan H, **"Il-6 Secreted from Senescent Mesenchymal Stem Cells Promotes Proliferation and Migration of Breast Cancer Cells"**, PLoS One. 2014 Nov 24;9(11):e113572.

(246) Li Y, Xu X, Wang L, Liu G, Li Y, Wu X, Jing Y, Li H, Wang G, "**Senescent Mesenchymal Stem Cells Promote Colorectal Cancer Cells Growth via Gelectin-3 Expression"**, Cell Biosci. 2015 May 6;5:21.

(247) Croce CM, **"Oncogenes and Cancer"**, N Engl J Med. 2008 Jan 31;358(5):502-511.

(248) Howarth FC, Jacobson M, Shafiullah M, Adeghate E, **"Long-Term Effects of Streptozocin-Induced Diabetes on the Electrocardiogram, Physical Activity and Body Temperature in Rats"**, Exp Physiol. 2005 Nov;90(6):827-835.

(249) Cheng SK, Park EY, Pehar A, Rooney AC, Gallicano GI, **"Current Progress of Human Trials Using Stem Cell Therapy as a Treatment for Diabetes Mellitus"**, Am J Stem Cells. 2016 Oct 20;5(3):74-86.

(250) Hokenson MA, Wang Y, Hawwa RL, Huang Z, Sharma S, Sanchez-Estaban J, **"Reduced IL-10 Production in Fetal Type II Epithelial Cells Exposed to Mechanical Stretch is Mediated via Activation of IL-6SOC3 Signalling Pathway"**, PLoS One. 2013;8(3):e59598.

(251) Denning TL, Campbell NA, Song F, Garoalo RP, Klimpel GR, Reyes VE, Ernst PB, **"Expression of IL-10 Receptors on Epithelial Cells from the Murine Small and Large Intestine"**, Int Immunol. 2000 Feb;12(2):133-139.

(252) Bonifacio E, **"Predicting Type 1 Diabetes Using Biomarkers"**, Diabetes Care. 2015 Jun;38(6):989-996.